1-1-2006

Low oxidation state Group 15 cations: Synthesis, reactivity and computational studies.

Bobby Dean Ellis
University of Windsor

Low Oxidation State Group 15 Cations:

Synthesis, Reactivity and Computational Studies

By

Bobby Dean Ellis

A Dissertation
Submitted to the Faculty of Graduate Studies and Research
Through Chemistry and Biochemistry
in Partial Fulfillment of the Requirements for
the Degree of Doctor of Philosophy at the
University of Windsor

Windsor, Ontario, Canada
2006

Your file Votre référence
ISBN: 978-0-494-35972-3
Our file Notre référence
ISBN: 978-0-494-35972-3

Abstract

The area of low oxidation state Group 15 chemistry has emerged from its humble beginnings into a field of increasing interest for many researchers. One of the largest limitations when investigating the chemistry of cations containing phosphorus(I) centres is the isolation of salts without the by-products generated concomitantly. We have developed a new method for the synthesis of phosphine-stabilized P^I cations using the disproportionation of PI_3 in the presence of chelating diphosphines. These iodide salts are ideal candidates for metathesis reactions to generate P^I salts containing non-reactive anions amenable to reactivity studies. We have used the resultant "triphosphenium" tetraphenylborate salts to generate a variety of new carbene-stabilized P^I (phosphamethine cyanines) salts through N-heterocyclic carbene (NHC) for phosphine ligand exchange. Halide salts of these same cations are also accessible from the direct reaction of NHCs and phosphorus(III) halides. Both classes of cations have also been examined using computational chemistry to further elucidate the electronic structure of these stable species.

Phosphine-stabilized P^I tetraphenylborate salts have also been used to probe the coordination chemistry of these reagents, which have the potential to form adducts using either one or both of the available "lone pairs" of electrons on the P^I centre. Whereas reported complexes for related compounds appear to be stable, coordination complexes with both Main Group and Transition Metal electron acceptors tends to dissociate upon remaining in solution.

Recently there has been interest in the use of diimines to trap Pn^{I} cations (Pn = P, As), which depending on the nature of the diimine, may be oxidized to Pn^{III}. Several experimental examples of such trapped cations containing either phosphorus or arsenic have been synthesized and computational chemistry has been used to help explain the experimental observations.

There have been significantly fewer examples of As^{I} cations and we have determined that the disproportionation pathway for phosphorus is also amenable to phosphine-stabilized As^{I} formation. The resultant iodide salts can undergo selective oxidation of the chelating phosphine to release "As-I" fragments for the formation of clusters.

Co-Authorship Statement

The majority of the material contained within this document has been previously published in peer-reviewed journals. In accordance with regulations defined by the Faculty of Graduate Studies and Research, this dissertation is presented in manuscript format. I was the principal investigator for all publications and I had a significant role in the preparation of the manuscripts. I acknowledge my supervisor Dr. Charles Macdonald as a co-author in this work as he also made a significant contribution to the writing of manuscripts and the acquisition of some of the computational data. Other listed authors on manuscripts contributed through raw data acquisition. The dissertation is based on the following publications:

Chapter 1

Ellis, B.D. and Macdonald, C.L.B., Stable Compounds Containing Heavier Group 15 Elements in the +1 Oxidation State, *Coord. Chem. Rev.*, **2006**, in press.

Chapter 2

Ellis, B.D., Carlesimo, M. and Macdonald, C.L.B., Stabilised Phosphorus(I) and Arsenic(I) Iodide: Readily-Synthesised Reagents for Low Oxidation State Main Group Chemistry, *Chem. Commun.*, **2003**, 1946-1947. DOI: 10.1039/b302292g.

Ellis, B.D. and Macdonald, C.L.B., Phosphorus(I) Iodide: A Versatile Metathesis Reagent for the Synthesis of Low Oxidation State Phosphorus Compounds, *Inorg. Chem.*, **2006**, *45*, 6864-6874. DOI: 10.1021/ic060186o.

Chapter 3

Ellis, B.D., Dyker, C.A., Decken, A. and Macdonald, C.L.B., The Synthesis, Characterisation and Electronic Structure of *N*-Heterocyclic Carbene Adducts of P^{I} Cations, *Chem. Commun.*, **2005**, 1965-1967. DOI: 10.1039/b500692a.

Chapter 5

Ellis, B.D. and Macdonald, C.L.B., Cycloaddition and Electron Transfer: On A Synthetically-Useful Aspect of Pnictogen(I) Reactivity, *Inorg. Chim. Acta*, **2006**, in press.

Chapter 6

Ellis, B.D., Carlesimo, M. and Macdonald, C.L.B., Stabilised Phosphorus(I) and Arsenic(I) Iodide: Readily-Synthesised Reagents for Low Oxidation State Main Group Chemistry, *Chem. Commun.*, **2003**, 1946-1947. DOI: 10.1039/b302292g.

Ellis, B.D. and Macdonald, C.L.B., Low Oxidation State Group 15 Elements as Pnicta-Wittig Reagents, *Phosphorus, Sulfur Silicon Relat. Elem.*, **2004**, *179*, 775-778. DOI: 10.1080/10426500490427015.

Ellis, B.D. and Macdonald, C.L.B., Stabilized Arsenic(I) Iodide: A Ready Source of Arsenic Iodide Fragments and a Useful Reagent for the Generation of Clusters, *Inorg. Chem.*, **2004**, *43*, 5981-5986. DOI: 10.1021/ic049281s.

For Tracy

Acknowledgements

I would like to begin by thanking my supervisor Dr. Chuck Macdonald. He took a chance on accepting me as his first and only graduate student five years ago and I have been so fortunate for the opportunities that his decision to accept me has provided. I'm sure it will be many years from now until I will be able to totally grasp the sheer amount of information that he has taught me. I can not thank him enough for all his time, teaching, patience and putting up with me over these past years.

I would like to thank my committee members Dr. Rob Schurko and Dr. Doug Stephan for their help and guidance over the past years. Also, I wish to thank Dr. Derek Northwood for agreeing to be my Outside Department reader and of course Dr. François Gabbaï for agreeing to be my External Examiner.

Thank you to Dr. Shuangquan Zhang who was very helpful with obtaining mass spectrometry data and Mike Fuerth for all his assistance with NMR spectrometry.

I have also been very fortunate to work with a number of Undergraduate researchers during my time as a graduate student at Windsor. I know they taught me more than I taught them, and I will be forever grateful for my time with them in and out of the laboratory. Direct contributions to my dissertation have been made by Erica Morasset, Deyzi Gueorguieva, Kevin Renaud and Michelle Carlesimo through their various research projects. I would also like to thank the other members (past and present) of the Macdonald group who have helped me during my time here, in particular the other graduate students: Erin Norton, Benjamin Cooper & Chris Andrews. The Johnson group (Alana, Jill, Ritu, Han & Meghan), which has shared the office have helped make the

time in Windsor almost fun at times, particularly on ice cream days. Their "encouragement" for me to finish has definitely kept me on pace to finish, if for no other reason than my safety.

I may not have even went to graduate school if not for the advice my graduate student advisor, so long ago. Thanks to Denise Walsh for all of her encouragement and direction early on, as well as convincing me to stay and complete a Ph.D. Sometimes I think that if not for her, office mate Joe DiMartino, and fellow Grad student Lourisa Cabrera I would have never made it through, at least not with my sanity.

Sam and Nora have definitely helped me along the way and always waited up for me to come home on those late nights. Finally, I wish to thank my wife Tracy for her never ending support, even on the many late nights. Her encouragement and unwavering confidence in me has helped me through both undergraduate and graduate degrees. I could have never done it without her!

Statement of Originality

I certify that this thesis, and the research to which it refers, are the product of my own work and that any ideas from the work of other people, published or otherwise, are fully acknowledged in accordance with the standard referencing practices of the discipline. I acknowledge the helpful guidance and support of my supervisor Dr. C.L.B. Macdonald.

Table of Contents

List of Tables

List of Figures

List of Abbreviations, Symbols, Nomenclature

Å	Angstrom
Abs. coef.	absorption coefficient
Ad	1-adamantyl, $C_{10}H_{15}$
Ad-NHC	1,3-bis(1-adamantyl)imidazol-2-ylidene
Ar	aryl
Ar-BIAN	bis(arylimino)acenaphthene
Bipy	2,2'-bipyridine
Bu	butyl, $(CH_2)_3CH_3$
calc'd	calculated
cod	1,5-cyclooctadiene, C_8H_{12}
CSD	Cambridge Structural Database
δ	chemical shift (NMR)
D	doublet (NMR)
DBU	1,8-diazabicyclo[5.4.0]undec-7-ene
DFT	density functional theory
dhpe	1,2-bis(hosphine)ethane, $H_2P(CH_2)_2PH_2$
Dimpy	α,α'-diiminopyridine
Dipp	2,6-diisopropylphenyl, $(CH(CH_3)_2)_2C_6H_2$
Dipp-DAB	*N*,*N*'-Bis-(2,6-diisopropylphenyl)butane-2,3-diimine
dmadppe	1-(dimethylamino)-2-(diphenylphosphino)ethane, $Me_2N(CH_2)_2PPh_2$
dme	dimethoxyethane, $MeO(CH_2)_2Ome$
Dmp	2,6-dimesitylphenyl, 1,6-$Mes_2C_6H_3$
dmpe	1,2-bis(dimethylphosphino)ethane, $Me_2P(CH_2)_2Pme_2$
DMSO	dimetylsulfoxide
dp	decomposition point
dppe	1,2-bis(diphenylphosphino)ethane, $Ph_2P(CH_2)_2PPh_2$
dppp	1,3-bis(diphenlyphosphino)propane, $Ph_2P(CH_2)_3PPh_2$
Dtp	2,6-bis(triisopropylphenyl)phenyl), 2,6-$Tripp_2C_6H_3$
E	energy (DFT)
en	ethylenediamine, $H_2N(CH_2)_2NH_2$
Et	ethyl, CH_2CH_3
Et-NHC	1,3-diethyl-4,5-dimethylimidazol-2-ylidene
G	any substituent
HR-ESI-MS	high resolution electrospray ionization mass spectrometry
Hz	hertz
^{i}Pr	iso-propyl, $CH(CH_3)_2$
^{i}Pr-NHC	1,3-diisopropyl-4,5-dimethylimidazol-2-ylidene

IR	infrared spectroscopy
$^{n}J_{XY}$	n-bond coupling constant between nuclei x and y
L	neutral ligand
Me	methyl, CH_3
Me-NHC	1,3,4,5-tetramethylimidazole-2-ylidene
MeOH	methanol
Mes	mesityl, 2,4,6-trimethylphenyl, $Me_3C_6H_2$
Mes-NHC	1,3-bis(2,4,6-trimethylphenyl)imidazol-2-ylidene
Mes*	supermesityl, 2,4,6-tri-*tert*-butylphenyl, $^{t}Bu_3C_6H_2$
mmol	millimole
mp	melting point
NacNac	β-diketiminate, $[ArNC(Me)C(H)C(Me)NAr]^-$
NBO	natural bond orbital
NBS	*N*-bromosuccinimide, $C_4H_4BrNO_2$
NHC	*N*-heterocyclic carbene
NMR	nuclear magnetic resonance
OTf	trifluoromethane sulfonate (triflate), OSO_2CF_3
Ph	phenyl, C_6H_5
Ph-N_3HC	2,4,5-triphenyl-1,2,4-triazol-3-ylidene
Pn	pnictogen, Group 15 element: N, P, As, Sb, Bi
ppm	parts per million
q	quartet (NMR)
R	any organic substituent
RedOx	reduction-oxidation
s	singlet (NMR)
t	triplet (NMR)
^{t}Bu	tert-butyl, $C(CH_3)_3$
thf	tetrahydrofuran
tmeda	tetramethylethylenediamine, $Me_2N(CH_2)_2NMe_2$
TMS	trimethylsilyl, $SiMe_3$
Tripp	triisopropylphenyl, $^{i}Pr_3C_6H_2$
xs	excess

Chapter 1 – Introduction

1.1 General Introduction

The elements of Group 15 (nitrogen, phosphorus, arsenic, antimony and bismuth) are often collectively referred to as pnictogens.[1] The term pnictogen is derived from the Greek word pniktos (πνικτός), which is often referenced incorrectly as the infinitive "to suffocate" rather than the more accurate past participle "strangled".[2,3] The term pnictogen is not officially accepted by the International Union of Pure and Applied Chemistry (IUPAC); however the term is commonly used by chemists who routinely use Group 15 elements.[4-7] "Pentel" is another term occasionally employed when referring to Group 15 elements.[8] The term "pnictogens" or "Pn" will be used throughout this thesis to refer to Group 15 elements. The elements of Group 15 are diverse in their nature, both physically and chemically. Nitrogen and phosphorus are non-metals, arsenic and antimony are metalloids and bismuth is a metal. Elemental nitrogen is a diatomic gas, while the heavier pnictogens are all solids at standard temperature and pressure. One of the many allotropes of phosphorus is also diatomic, however it is only observed at high temperatures and low pressure.[9] The most common form of elemental phosphorus is cubic, white α-P_4; red and black allotropes feature polymeric structures with three coordinate phosphorus atoms.[9] The elemental forms of arsenic, antimony and bismuth are all similar to that of black phosphorus.[9]

The reactivity of the pnictogens is influenced, in the same way as all of the elements, by fundamental properties such as effective nuclear charge, ionization energy, electron affinity, atomic radii (covalent and ionic) and electronegativities. The goal of

this thesis is to examine the heavier pnictogens, in particular phosphorus and arsenic, in the atypical +1 oxidation state in order to better understand the synthesis and properties of such compounds. These low oxidation state compounds offer a promising route to new materials and an improved understanding of their structure, bonding and reactivity is necessary in order to pursue such avenues.

1.2 Oxidation States

The concept of an atom existing in a particular oxidation state (or oxidation number) is one of the fundamental ideas that may be used to rationalize the structural features, bonding and reactivity of a molecule. The utility of the oxidation state model derives from the understanding that the oxidation state of a particular atom in a molecule provides insight into the number of electrons directly associated with, and hence the chemistry of, the atom in question. Oxidation state is defined as "*the actual charge of the atom if it exists as a monoatomic ion, or a hypothetical charge assigned to the atom in the substance by simple rules*".[10] Using such rules (e.g. H is always in the +1 oxidation state, O is always in the -2 oxidation state), the Group 15 elements are assigned formal oxidation states ranging from -3 to +5 under normal conditions.[9,11,12]

The idea of elements having formal oxidation states or oxidation numbers is certainly useful in the context of balancing reduction-oxidation (RedOx) reactions, however, the rules used to assign such formal oxidation states sometimes yield results that are not chemically intuitive. For example, whereas the formal oxidation state of the phosphorus center in PH_3 is -3, the formal oxidation state of the phosphorus center in PMe_3 may be either +3 or -3 (depending on the electronegativity scale that is used) and

the formal oxidation state of the phosphorus center in $P(NMe_2)_3$ is +3 in spite of the similar chemical behaviors and electronic structures of the three Lewis bases.

Also from the perspective of chemical reactivity, such counting rules suggest that while the coordination of the "lone pair" of electrons on a molecule such as PH_3 to H^+ does not change the oxidation state of the phosphorus center, the identical Lewis acid-base reaction between PH_3 and CH_3^+ might change the oxidation state of P, and the related reaction of PH_3 with an O atom will certainly change the oxidation state of the phosphorus center. Such conclusions are seemingly absurd in the context that each of the three reactions produces a tetrahedral-shaped molecule with no remaining "lone pair" of electrons on the phosphorus atom and each of the reactions involves the formation of a new bond between phosphorus and an isolobal fragment. Given the foregoing, it is necessary to remember that the formal oxidation states obtained from the use of such counting methods are simply models that are useful in many instances but they should not be overly-interpreted.

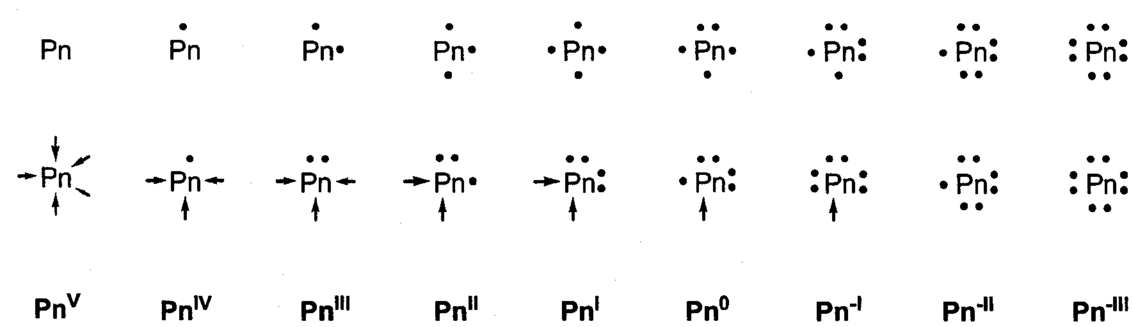

Figure 1.1 - Oxidation states of pnictogens; the arrows suggest a typical number of covalent bonds that may be made to an element in each oxidation state.

An alternative model one can use to define the oxidation state of an atom in a molecule is based on the number of non-bonding electrons associated with that particular atom. Such an approach corresponds perhaps more closely with the less-commonly used

concept of a "valence state"[13] and is also more compatible with the use of the isolobal analogy[14] to understanding chemical structure and reactivity. This model, illustrated in Figure 1.1, is advantageous in that it more obviously emphasizes the similarities in the electronic structures, geometrical features and perhaps chemical behaviors of compounds containing elements in a given "oxidation state". The implicit assumption in the model presented in Figure 1.1 is that the Pn atom is less electronegative than all of the elements to which it may be bonded. While this assumption may be unrealistic when Pn = N, the model eliminates many of the ambiguities and oddities in the chemistry of compounds containing an element in a given oxidation state. For example, whereas the counting rules might suggest that the phosphorus atom in PMe_2H is +1, the phosphine has more structural and chemical similarities to $AsMe_2H$, containing As^{III}, than to a phosphinidene that contains P^{I}. Using the method outlined in Figure 1.1, both $PnMe_2H$ compounds are considered to contain Pn^{III} and both are expected to have different structural properties and chemistry than the compound containing Pn^{I}.

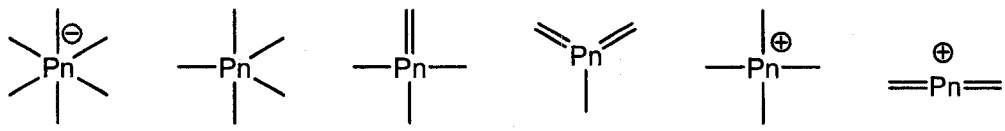

Figure 1.2 - Selected bonding environments observed for compounds containing Pn^{V} centers.

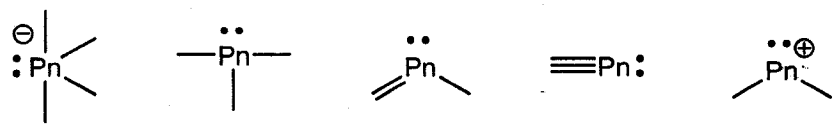

Figure 1.3 - Selected bonding environments for compounds containing Pn^{III} centers.

When pnictogens are in the +5 oxidation state, Pn^{V}, there are no valence electrons that are not associated with a bond, i.e. there are no "lone pair" electrons, as illustrated in

Figure 1.2. The +3 oxidation state, Pn^{III}, corresponds to an environment in which there is a single "lone pair" of electrons as depicted in Figure 1.3.

Finally, a comment about the chemical drawings used in this dissertation is warranted. Because a given molecule can be depicted in various manners, the oxidation state of the Pn atom contained therein might seem ambiguous, as illustrated in Figure 1.4. Such chemical drawings are often made using rules (e.g. minimize the number of formal charges) that suggest that one drawing is superior to another drawing on the basis of formalisms that have no relationship to the actual electronic structure of the molecule depicted. Again, one must remember that such Lewis-type structures are simple models that should not be accorded too much significance. More accurate models of the actual electronic structures of such molecules are obtained from computational investigations or inferred from structural and reactivity studies. The depictions of chemical structures are in a manner that conforms to the drawings that have appeared in the literature (for example, many structures are often drawn in the manner of either of the Pn^{III} forms shown in Figure 1.4). As a final note, for general structural types "R" represents a formally anionic ligand, such as an alkyl group, and "Do" represents a formally neutral ligand, such as a phosphine.

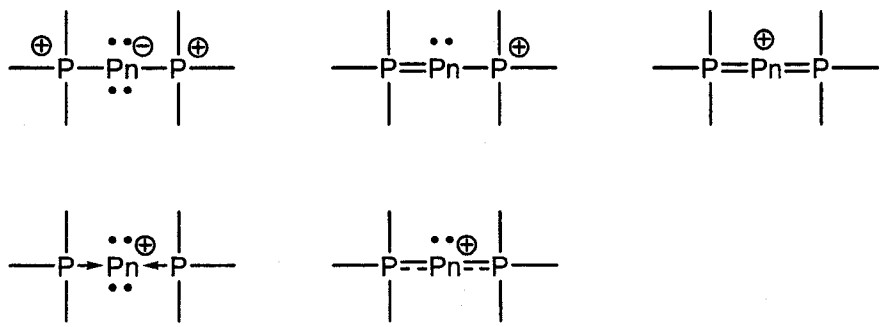

Figure 1.4 - Ambiguity in Lewis-type chemical structure drawings of a single cation having the formula $[Pn(PR_3)_2]^+$.

1.3 Low Oxidation State Pnictogen Compounds

Pnictogens are commonly found in either the +3 or +5 oxidation state, with either one "lone pair" of electrons or no non-bonding electrons. As with the other groups in the periodic table, Group 15 follows the same trend that low oxidation state are favoured by the heavier elements. Using the definition above, pnictogen atoms in the +2 oxidation state are radicals.[15] Elemental pnictogens are often used in reactions, in particular white phosphorus,[16] which is an example of pnictogen atoms in the 0 oxidation state. Examples of other compounds containing Pn elements in lower oxidation states typically involve "naked" (substituent-free) Pn atoms bound to transition metals.[17] The most common of the lower oxidation state for pnictogens in organo-pnictogen compounds is +1, in which the pnictogen atom bears four non-bonding electrons. There are several different structural types that may be envisioned for Pn^{I} depicted in Figure 1.5. The potential compounds include neutral, cationic and anionic species that contain either mono- or di-coordinate phosphorus centers however, in practice, only compounds containing the di-coordinate environments are found to be adequately stable to allow for their isolation under typical laboratory conditions.

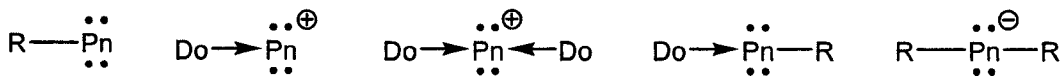

Figure 1.5 - General structural drawings for compounds containing Pn^{I} centres.

In spite of their instability under standard laboratory conditions, one of the most widely studied families of Pn^{I} compounds are the neutral phosphinidenes having the general form R-P, which are a heavier analogue nitrenes.[18] Free phosphinidenes exist only as coordinatively-unsaturated and highly-reactive intermediates with either a triplet

or, more rarely, a singlet ground state. In the absence of other reagents, phosphinidenes are prone to oligomerization to give either double-bonded diphosphenes or the more familiar cyclic polyphosphines of the form $(R\text{-}P)_n$, as pictured in Figure 1.6, depending on the size of the R substituent. Although all of the compounds in Figure 1.6 are formally considered to contain P^I centers, their structural features and reactivity is more typical of that expected by P^{III} centers; the utility of such oligomers for the generation of Pn^I species is examined later in this chapter.

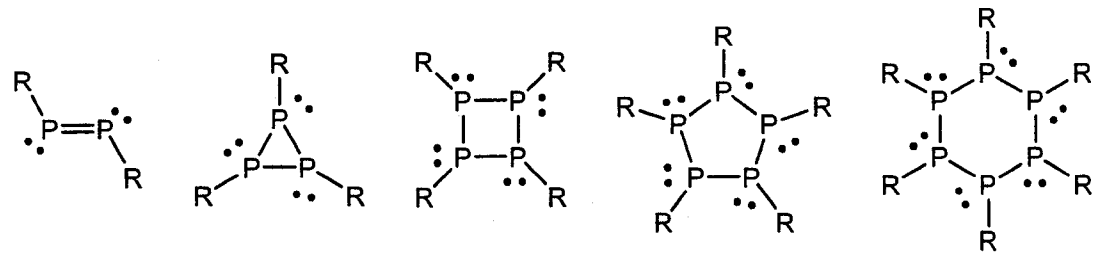

Figure 1.6 - Phosphinidene oligomerization products.

Work involving transient phosphinidenes has been extensively reviewed.[19-21] In many instances, monomers of the transient species can be stabilized through coordination with either Lewis bases or metal centers. Such stabilized phosphinidenes, which have proven to be useful phospha-Wittig reagents for the formation of new carbon-phosphorus bonds that may otherwise be very difficult to produce,[22] are examined in the section below covering the stable, di-coordinate neutral P^I species.

There is one class of molecule that has been described as being equivalent to a stabilized singlet phosphinidene, namely the so-called "10-P-3" (meaning a total of 10 electrons around a phosphorus center which is connected to 3 other atoms) hypervalent molecules initially described by Arduengo and co-workers.[23] As shown in Figure 1.7, such molecules consist of a phosphorus atom ligated by a substituted diketoamido (R-

DKA) ligand. When the molecule has a planar bicyclic arrangement, the phosphorus atom is described as 10-P-3; this description implies a pseudo-trigonal bipyramidal (ψ-tbp) arrangement with two lone pairs of electrons in equatorial sites and thus merits classification as a P^I compound by the convention outlined in Figure 1.1. Alternatively, such compounds can possible adopt a folded bicyclic arrangement in which the phosphorus atom is described as 8-P-3; this would thus be classified as a P^{III} center.

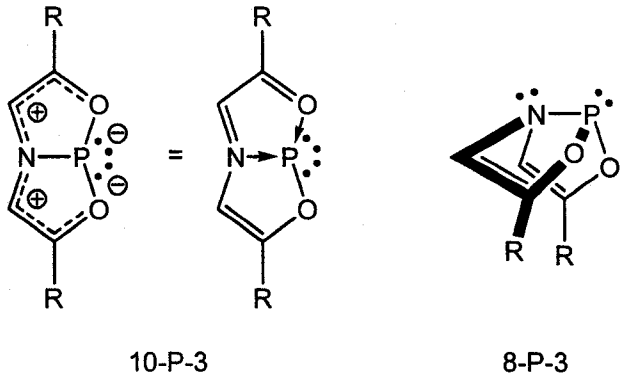

Figure 1.7 - Drawings of (R-DKA)P molecules illustrating difference between the planar 10-P-3 P^I arrangement and the folded 8-P-3 P^{III} arrangement.

The focus of this thesis is pnictogen atoms in the +1 oxidation state that contain two "lone pairs" of electrons and are bound to two groups. Examples of these types of compounds are presented in the following sections of this chapter.

1.3.1 Cationic P^I Compounds

1.3.1.1 Phosphine-Stabilized P^I Cations

In the early 1980's, Schmidpeter began initial work on the synthesis of cations that contain phosphorus in the +1 oxidation state.[24] For the next fifteen years there was very little work in the area, with examples being reported sporadically. More recently there has been an increasing interest in the investigation of not only the synthesis of such

species but also of the unique reactivity and utility of compounds containing phosphorus and its heavier congeners in the +1 oxidation state stabilized by phosphines.

Syntheses Employing SnX_2 Oxidation

In 1982, Schmidpeter published the first example of what he would later call a "triphosphenium" cation.[25,26] The reduction of phosphorus(III) chloride with tin(II) chloride in the presence of a chelating phosphine, namely bis(diphenylphosphino)ethane (dppe), generated the hexachlorostannate salt of the P^I cation $[(dppe)P]^+$, **1.1** (Equation 1.1).

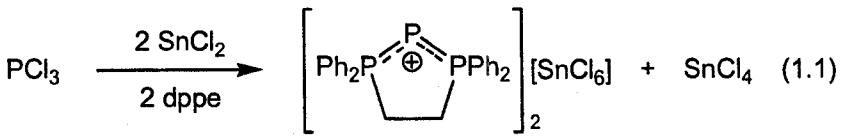

1.1$_2$[$SnCl_6$]

Schmidpeter characterized the salt of **1.1** using both ^{31}P NMR and X-ray crystallography, in addition to microanalysis. In solution, the composition of the cation was readily confirmed by its ^{31}P NMR spectrum, which consists of a doublet at 64 ppm (2 P atoms) and a triplet at –232 ppm (1 P atom). Symmetrical triphosphenium cations of the general form $[(R_3P)_2P]^+$ display the easily identifiable spectrum of an AX_2 spin system with very large $^1J_{P\text{-}P}$ coupling constants that typically exceed 400 Hz. The ligating phosphorus centres exhibit ^{31}P NMR signals from the nuclei that are usually deshielded relative to phosphoric acid, and that resonate between δ = +30 to +90 ppm depending on the nature of the R substituents. In contrast, the dicoordinate P^I centre is significantly shielded and exhibits signals in the ^{31}P NMR spectrum that resonate in the range of δ = –175 to –235 ppm.[27]

The solid state structure of **1.1** reveals short P–P bonds, 2.122(1) and 2.128(2) Å, which are intermediate between what is considered typical single (2.217(1) Å in Ph_2P-PPh_2[27]) and double (2.034(2) Å in Mes*P=PMes*[28]) bonds. The very small P-P-P angle of 88.9(1)° is largely a consequence of the constraints imposed of the chelating diphosphine. However, the strongly-bent geometry is typical of all structurally-characterized triphosphenium cations.

Related cyclic compounds have been synthesized by other groups using variations of Schmidpeter's approach using either different chelating diphosphines or using tin(II) bromide as the reducing agent. Whereas the salts $\mathbf{1.7}_2[SnCl_6]$, $\mathbf{1.10}_2[SnCl_6]$ and $\mathbf{1.10}[AlCl_4]$ were also structurally characterized and show similar P-P bond lengths to **1.1**, the presence of the other cations was inferred primarily on the basis of characteristic ^{31}P NMR data.[29-32]

1.1 R = Ph
1.2 R = Et
1.3 R = Me
1.4 R = Cy
1.5 R = Ph,Et

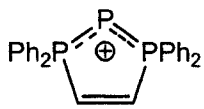

1.6

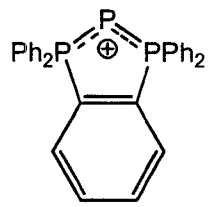

1.7

1.8 R = Me
1.9 R = Cy

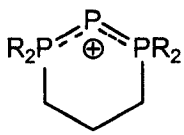

1.10 R = Ph
1.11 R = Et

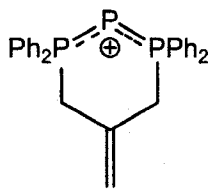

1.12

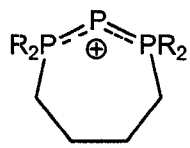

1.13 R = Ph
1.14 R = Cy

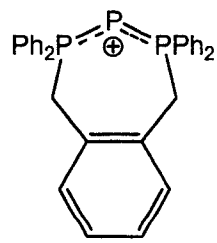

1.15

It is worthy of note that certain diimines (bis-nitrogen donors) have also been used recently to trap P^I centres generated using the $PCl_3/SnCl_2$ protocol. In the case of

the readily-reduced BIAN system, the P^{I} centre is oxidized to P^{III} and the diimine is reduced in the course of the reaction (Equation 1.2) as evidenced by both the metrical parameters in the solid-state structure and the high frequency ^{31}P NMR chemical shift of 232 ppm, which is in the range characteristic of dicoordinate P^{III} phosphenium cations.[33]

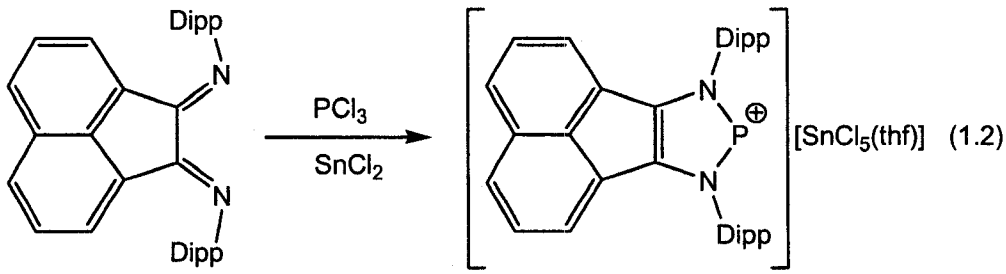

(1.2)

1.16[$SnCl_5$(thf)]

Syntheses Employing Ligand Oxidation

Examples of salts containing acyclic cations were reported by Schmidpeter shortly after his initial report of the cyclic compounds. The synthetic approach to the acyclic species involved reduction of phosphorus(III) chloride by an additional equivalent of the ligating phosphine (PPh_3 or $P(NMe_2)_3$), which is oxidized from P^{III} to P^{V} in the process (Equations 1.3 & 1.4).[26,34,35] The tetrachloroaluminate salt of the PPh_3 stabilized cation **1.17** was characterized using X-ray crystallography and ^{31}P NMR spectroscopy, in addition to microanalysis. The solid state structure again exhibits P-P bond lengths that are intermediate between single and double bonds. Importantly, the cation contains a strongly-bent P-P-P arrangement even in the absence of the constraints imposed by the chelating ligands in the cyclic systems outlined above. The ^{31}P NMR chemical shift of the P^{I} centre is to lower feequency than those found in the cyclic analogues.

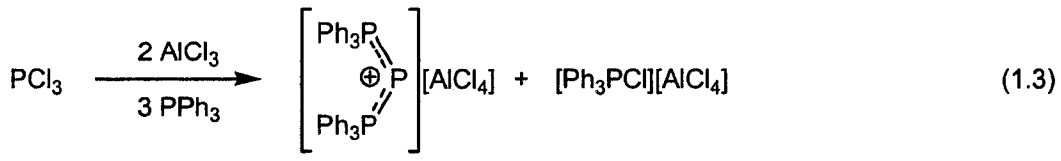

1.17[$AlCl_4$]

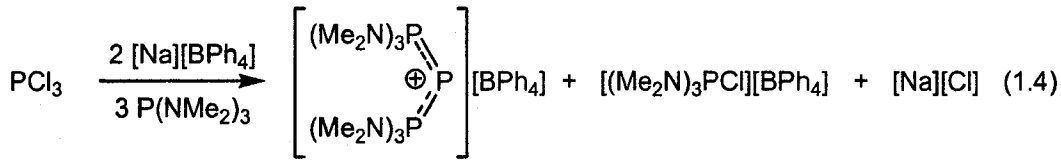

1.18[BPh_4]

In a similar manner, many of the cyclic cations that have been isolated with hexahalostannate counter ions have also been prepared with halide anions (Cl^-, Br^-, I^-) using the ligand oxidation protocol.[30,31] A significant complication to using this approach on a preparative scale, for salts containing either acyclic or cyclic cations, is the similar solubilities of the halo-phosphonium salt by-products and the desired P^I salts. As a result, many of the cations prepared using this method have been characterized only by ^{31}P NMR.

Ligand Exchange Reactions

Other triphosphenium P^I salts are accessible through various exchange reactions employing the salts obtained using the syntheses outlined above. The acyclic cation **1.17**[$AlCl_4$] can undergo sequential substitution by more basic phosphines to generate both symmetric and asymmetric acyclic cations or cyclic P^I cations (Equation 1.5).[34] Such reactivity is in keeping with the idea of cations such as **1.17** as being a "P^+" cation coordinated by two neutral phosphine ligands. Similarly, unsymmetrical cyclic cations may also be obtained through the use of an asymmetric chelating diphosphine.[31] While

this type of ligand exchange reactivity has been verified extensively by ^{31}P NMR, side reactions often preclude the bulk isolation of pure products using this method.[36,37]

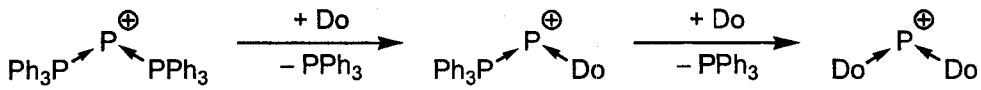

(1.5)

Do = $PMePh_2$, PMe_2Ph, PBu_3, $P(NMe_2)_3$, $P(OEt)_3$

Reactivity

Although they are positively charged, cations containing P^I centres can behave as electron donors. For example, acyclic P^I cations, $[(R_3P)_2P]^+$ (R = Ph, NMe_2), have been shown to coordinate to aluminium trichloride in typical Lewis base/Lewis acid fashion (Equation 1.6). In the presence of hydrochloric acid, protonation (which is equivalent to oxidation in terms of the model described in Figure 1.1) rapidly occurs at P^I to give dications of the form $[(R_3P)_2PH][AlCl_4]_2$.[35,36] Oxidation by a variety of alkyl chlorides readily occurs for acyclic cations (Equation 1.7);[36] however, cyclic P^I cations are more resistant and typically require stronger oxidizing agents such as methyl triflate.[32,38] Cyclic cations can also be protonated/oxidized by H^+ from HCl, HOTf or $^tBuCl/AlCl_3$.[36,38] Oxidized triphosphenium cations exhibit only minor changes in their chemical shifts in ^{31}P NMR spectra of the stabilizing phosphines, although that of the P^I centre shifts by 50 to more than 100 ppm to higher frequency upon oxidation and the magnitude of the $^1J_{PP}$ coupling constant decreases by approximately 150 Hz.

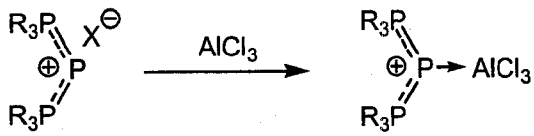

(1.6)

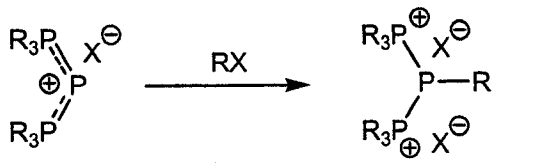

(1.7)

The only structurally characterized oxidation product that retains the original P-P-P framework is $[(Ph_3P)_2PH][AlCl_4]_2$ **1.19**$[AlCl_4]_2$.[36] In comparison to $[(Ph_3P)_2P][AlCl_4]$ **1.17**, the solid-state structure shows a lengthening of the P-P bonds by 0.077 and 0.087 Å and a slight PPP angle increase from 102.2° to 106.4°. Of particular importance is the distinctly pyramidal arrangement of the substituents around the central phosphorus atom (the sum of the angles around P is 288.25°); this is consistent with the presence of a single "lone pair" of electrons on the phosphorus atom and thus it may be classified as a P^{III} centre using the convention outlined above.

A rare well-characterized reduction of a P^{I} centre occurs when the acyclic cation **1.18**$[BPh_4]$ is treated with Schwartz's reagent, $Cp_2Zr(H)Cl$. In conjunction with the destruction of the P-P-P framework and oxidation of the $P(NMe_2)_3$ ligands to $[(Me_2N)_3PCl][BPh_4]$, the P^{I} centre is reduced to P^{-III} and trapped in an eight-membered ring composed of hydride-bridged zirconocene fragments **1.20** (Equation 1.8).[39-41] The four coordinate "phosphonium cation" is bound to the zirconium centres in an unusual square-planar arrangement and exhibits a ^{31}P NMR chemical shift of 254 ppm; such an unprecedented product demonstrates some of the unique chemistry of triphosphenium reagents.

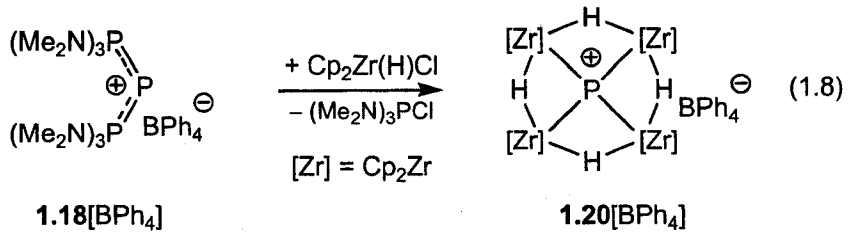

(1.8)

1.18[BPh_4] **1.20**[BPh_4]

1.3.1.2 Carbon-based donor-stabilized P^I Cations

Phosphamethine cyanines, which are the phosphorus analogues of methine cyanine dyes,[42] are among the oldest class of compounds that may be considered to contain P^I centres in many cases. Although such compounds are traditionally regarded as special cases of 2-phosphaallylic cations, which contain P^{III} centres, many examples exhibit structural features and reactivities that are more consistent with their being understood as carbene-stabilized P^I cations (Figure 1.5).

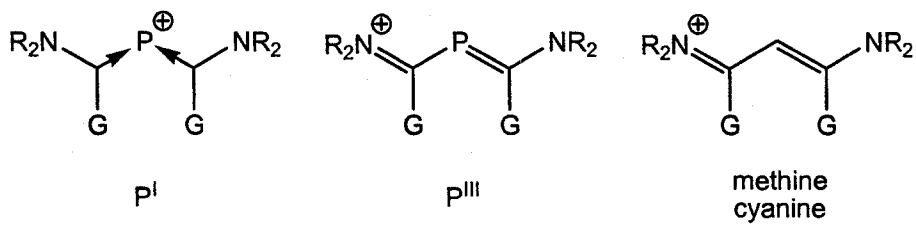

Figure 1.8 - Phosphamethine cyanines.

In a similar manner to the situation illustrated for triphosphenium-like cations in Figure 1.4, different canonical forms may be used to depict the electronic structure of phosphamethine cyanine cations, as shown in Figure 1.6. Although they are well-known for nitrogen analogues, linear structures which can be considered to contain P^V, have not been observed for phosphorus. Conversely, structural types containing P^{III} and P^I both predict bent geometries at the phosphorus centre and both are thus more apt depictions of observed structures. Whereas the P^{III} structure could explain the presence of relatively

short P-C bonds, the required planar structure is not observed in almost any of the examples that have been studied crystallographically. In this light, the pronounced twisting of the carbene fragments away from C-P-C plane, which diminishes the potential for π-overlap, suggests that the P^I drawing is generally the most realistic depiction of such species.

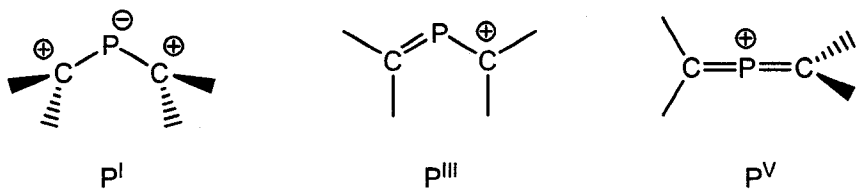

Figure 1.9 - Canonical structures of 2-phosphaallylic cations.

Syntheses

These P^I compounds were originally prepared by the elimination of acid from the product of cyclic imidoyl-type precursors and $P(CH_2OH)_3$ to provide salts containing cations of the type **1.21** (G = S, $(CH)_2$, NR_2) (Equation 1.9).[43-45] Similarly, the reaction of $P(SiMe_3)_3$ with similar precursors produced salts of cations containing either cyclic or acyclic carbenic ligands **1.22** (G = H, R, Ar, NR_2, SR) (Equation 1.10).[46,47]

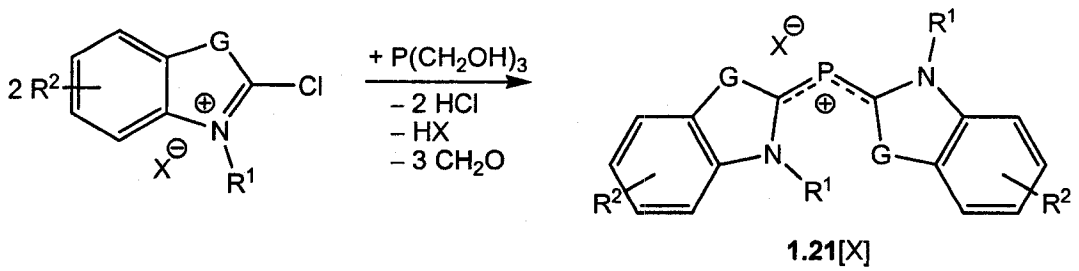

(1.9)

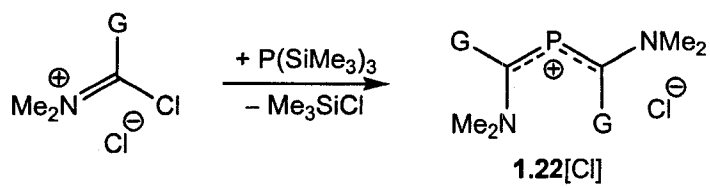

(1.10)

An alternative synthetic route to phosphamethinecyanine cations discovered by Schmidpeter et al. involved the insertion of a P^I centre from the triphosphenium cation **1.18** into certain electron-rich olefins (Equation 1.11).[48,49] Cyclic four-membered cationic rings can be synthesized by treatment of phosphaalkynes with methylating reagents, which undergo cyclization to give cations such as **1.24** (Equation 1.12).[50]

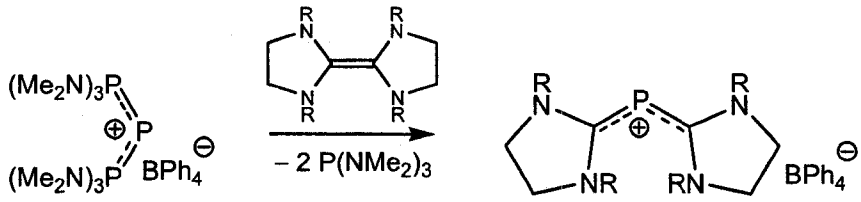

(1.11)

1.18[BPh_4] **1.23**[BPh_4]

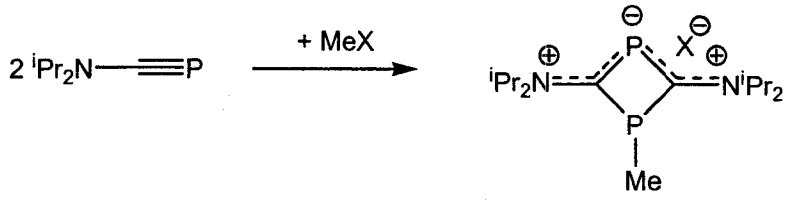

(1.12)

1.24[X]

Although the chemical shifts of carbon-based donor-stabilized P^I cations are often found to lower frequency than that of phosphoric acid, the actual shifts change markedly according to the nature of the G fragment. It should be noted that many phosphamethine cyanine cations, particularly those containing extended π-systems in the carbenic fragment, exhibit absorptions in the visible region. These absorptions result in intensely coloured compounds and these compounds have been investigated for their dye-like properties.

In spite of the large number of phosphamethine cyanine salts that have been synthesized, only a handful of examples have been structurally characterized. The P-C

bond lengths are all approximately 1.80 Å,[51,52] which are typical of P-C_{aryl} single bonds, except for **1.21** when G = S, which are shorter at around 1.75 Å.[53,54]

Reactivity

The chemistry of phosphamethine cyanines has not been examined in great detail. However, the oxidation chemistry of such species support their inclusion as P^I cations. For example, the oxidation of the 2-phosphaallyl cations **1.22** with MeI (Equation 1.13) does not lead to a planar structure, but rather to a pyramidal product consistent with oxidation of the P^I centre to a P^{III} centre.[52] Oxidation of the same cation with ozone, hydrogen peroxide or dimethyl sulfoxide (Equation 1.14) results in a complete oxidation of P^I to P^V.[55] The oxidation of other phosphamethine cyanines with hydrogen peroxide results in the oxidation of the carbon donors to generate the corresponding ketones and also in the complete oxidation of the P^I centre to PO_4^{-3}.[44] Treatment of the cations with H_2O or protic acids also decomposes the cation to form H_3PO_4 and imidazolium-type cations.[44,45]

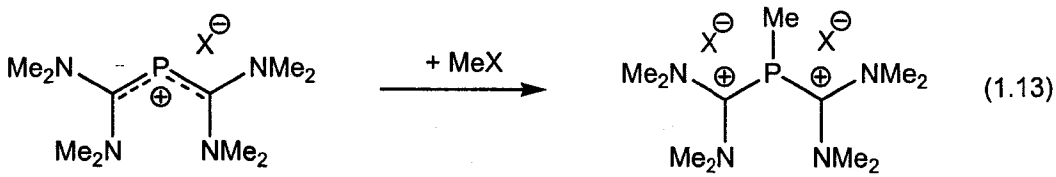

1.22[X] **1.25**[$X]_2$ (1.13)

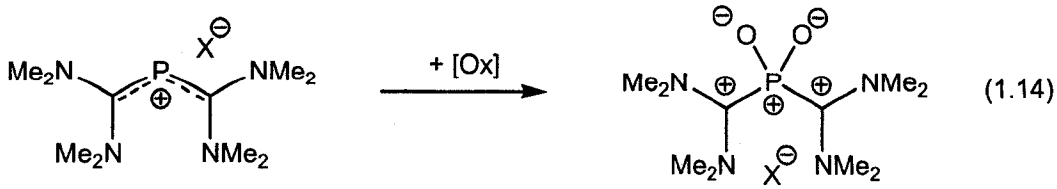

1.22[X] **1.26**[X] (1.14)

1.3.2 Anionic P^I Compounds

Syntheses

Anionic P^I compounds are P^I ions stabilized by two anionic donor molecules. The most well-known examples of anionic P^I compounds are phosphide (phosphanide) anions, PR_2^-, which are typically formed by reduction/deprotonation of the corresponding secondary phosphines (Equation 1.15).[11] Stable phosphides are known for a variety of carbon-based donor groups (R = Ph, CF_3, Ar) and are useful reagents for the synthesis of phosphorus-containing compounds. All known organophosphides exhibit a strongly-bent C-P-C fragment and P-C distances that are "typical" of single bonds. Organic phosphides are used extensively for the generation of element-phosphorus bonds through salt metathesis reactions.

$$R_2PH \xrightarrow[-\ H_2 \text{ or } HR]{+\ M,\ [M][H] \text{ or } [M][R]} [M][PR_2] \qquad (1.15)$$

A series of anionic P^I compounds stabilized by carbon donors that has been examined extensively is the salts containing dicyanophosphide anions, $[P(CN)_2]^-$ **1.27**. These anions are formed by either the addition of alkali metal cyanides to white phosphorus (Equation 1.16) or by the reduction of phosphorus(III) cyanide (Equation 1.17), however, the resultant salts are only stable in solution when the Group 1 cations are ligated by crown ethers.[56-58] The potassium salt of $[P(CN)_2^-]$ can also be obtained through the reaction of $P(CN)_3$ with KF in the presence of a crown ether[57] or by double

substitution of triphosphenium cations by cyanide anions (Equation 1.18).[37] The structure of the anion exhibits the bent C-P-C geometry.

$$P_4 + 8\,[M][CN] \longrightarrow [M][P(CN)_2] \quad (1.16)$$
[M]1.27

$$P(CN)_3 + [M][PO(OR)_2] \xrightarrow[-\,PO(CN)(OR)_2]{} [M][P(CN)_2] \quad (1.17)$$
[M]1.27

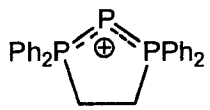

$$+ \; 2\,[M][CN] \xrightarrow[-\,dppe]{} [M][P(CN)_2] \quad (1.18)$$
[M]1.27

The oxidation chemistry of dicyanophosphide anions has provided some interesting results. The oxidation of **1.27** anions with MeI occurs exclusively at the P^I centre, which is more nucleophilic than the nitrogen atoms in the cyanide substituents, to yield $MeP(CN)_2$;[56] this chemical behaviour is analogous to that which was described above for the methylation of cationic P^I compounds. Likewise, the P^I anions can also be oxidized by elemental chalcogens (O_2, S_8, Se) to either P^{III} or P^V through sequential oxidations.[59] Perhaps the most interesting oxidation chemistry is observed in the reaction of dicyanophosphide salts with halogens or pseudohalogens. For example, the reaction of **1.27** with Br_2 (Equation 1.19) results in the two-electron oxidation of the anion to produce a salt containing the $[P(CN)_2Br_2]$ anion, which exhibits the disphenoidal shape expected for an anionic P^{III} centre.[60]

$$P(CN)_2^{\ominus} + Br{-}X \xrightarrow[X = Br,\ CN]{} Br{-}P^{\ominus}(NC){-}X(CN) \quad (1.19)$$
1.27

Asymmetric anionic P^I compounds of the type $RPCN^-$ are available synthetically through the degradation of the cyclic $(PhP)_5$ species by cyanide salts (Equation 1.20), or

through treatment of $P(CN)_2^-$ with alkyl or aryl lithium salts (Equation 1.21).[61] Substitution of $P(CN)_2^-$ with a variety of phosphinite-type donors (PR_2E^-) leads to either asymmetric or symmetric P^I anions based on reaction stoichiometry (Equation 1.22). In a similar vein, the reaction of white phosphorus with a chelating diphosphide dianion also results in the trapping of P^I between to the two anionic donors.[62]

$$(PhP)_5 + 5\,[M][CN] \longrightarrow [M][PhPCN] \qquad (1.20)$$

$$[M][P(CN)_2] + [Li][R] \xrightarrow[-\,[Li][CN]]{} [M][RPCN] \qquad (1.21)$$

[M]1.27

$$[M][P(CN)_2] + [M][PR_2E] \longrightarrow [M][(ER_2P)PCN] \qquad (1.22)$$

[M]1.27

R = Ph, OEt, NMe_2
E = O, S, NPh, lone pair

Symmetric anionic P^I compounds stabilized by phosphorus donors may also be generated directly from the reaction of white phosphorus with phosphinite anions (Equation 1.23).[62,63] Reaction stoichiometry is very important in such preparations, because either "P^+" or "P_2^+" fragments are ligated by the two phosphinite anions when two and two fifths or four equivalents are used, respectively. An alternative route to such anions is provided by the reaction of tris(dialkylphosphoryl)phosphines, $P(P(O)(OR)_2)_3$, with two equivalents of a secondary amines (NH_3, Et_2NH, $(CH_2)_4NH$, $(CH_2)_5NH$), wherein one equivalent of the amine extracts a $P(O)(OR)_2$ moiety in exchange for a proton and the second equivalent deprotonates the resultant molecule to produce the anionic species **1.31** or **1.32** (Equation 1.24).[64,65] The crystal structures of the anionic P-P-P species are, predictably, very similar to those of the triphosphenium cations described above.

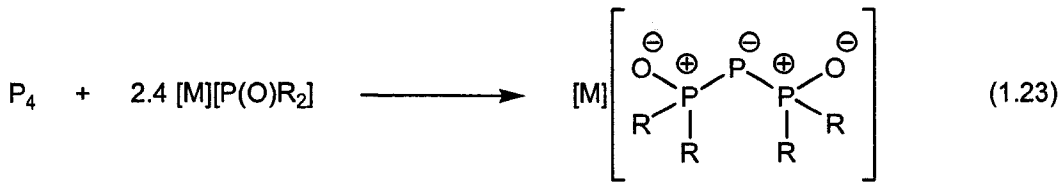

(1.23)

[M]**1.28** R = Et
[M]**1.29** R = Ph
[M]**1.30** R = NMe_2

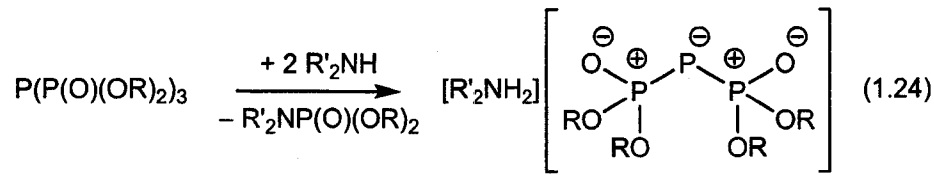

(1.24)

$[R'_2NH_2]$**1.31** R = Et
$[R'_2NH_2]$**1.32** R = ^iPr

Like the cyanide-stabilized species, these anions can also be oxidized at P^I by methyl cations or elemental sulphur, although they are resistant to both oxygen and moisture.[62] And as with many other phosphides, these anions may be used as ligands for transition metal complexes.[66-68]

An alternative approach to such triphosphorus anions involves the elimination of Me_3SiBu following the treatment of the appropriate phosphorus-silyl compound with BuLi (Equation 1.25).[69] These anionic P^I compounds can be used in the generation of related neutral low oxidation state phosphorus compounds, which are discussed below.

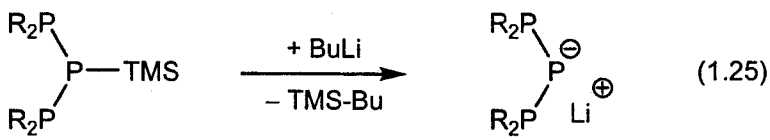

(1.25)

1.3.3 Neutral P^I Compounds

Neutral P^I compounds may be divided into two general categories: cyclic species with an anionic chelating ligand and acyclic species stabilized by one neutral donor and one anionic donor (Figure 1.7).

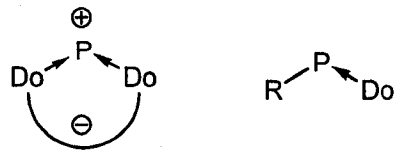

Figure 1.10 - General structural arrangements of neutral P^I compounds.

Syntheses

Lithium salts of the diphosphinomethanide carbanions, [Li][$C(PR_2)_2TMS$] react with phosphorus trichloride to give P^I rings of various sizes depending on the carbanion substituents and reaction conditions (Equations 1.26 and 1.27). In such reactions, the presence of bulkier substituent groups (such as when R = Ph) on the phosphine fragments appears to favour the formation of primarily four-membered rings exhibiting very acute P-P-P angles; such rings can be generated through reactions with either PCl_3 or P_4.[70] The presence of smaller substituents (R = Me) on the phosphine fragments tends to result in the formation of larger non-planar rings; for instance, either eight-membered or six-membered rings are obtained from the reaction of PCl_3 with three equivalents of the lithium diphosphinomethanide.[71-73] Somewhat in contrast to the case of the carbanion, the addition of two equivalents of the diphosphinoamide salt [Li][$N(PPh_2)_2$] to P_4 does not produce a four-membered ring but yields instead a symmetric, non-planar eight-membered ring, in which two P^I centres are bridged by the diphosphinoamide anions.[74,75] The product is obtained via an acyclic anionic P^I intermediate that was identified by ^{31}P NMR spectroscopy (Equation 1.29).[76] Treatment of PCl_3 with three equivalents of the same amide generates an identical eight-membered ring, with the extra amide being oxidized in the process.[77] This neutral P^I compound **1.37** is able to coordinate to Pd^{II} complexes through donation from both P^I centres.[78]

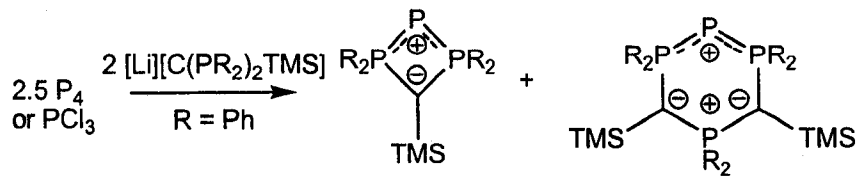

1.33 **1.34** (1.26)

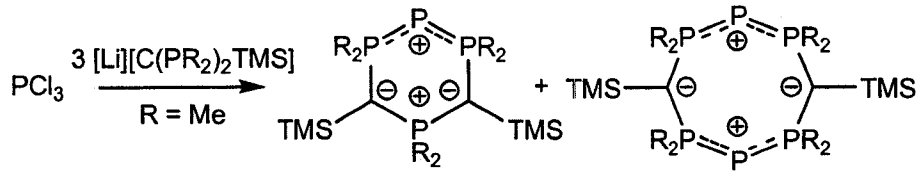

1.35 **1.36** (1.27)

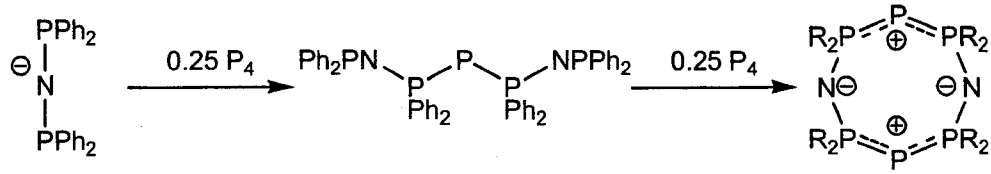

1.37 (1.28)

The lithium phosphide [Li]**1.38** or its parent secondary phosphine $(2\text{-Py})_2PH$ can be converted to a variety of zwitterions containing P^I centres, through reaction with group 13 Lewis acids. The product results from the loss of either a halide of alkyl substituent from aluminum or gallium during reaction with either the lithium phosphide or phosphines (Equations 1.29 and 1.30).[79-82]

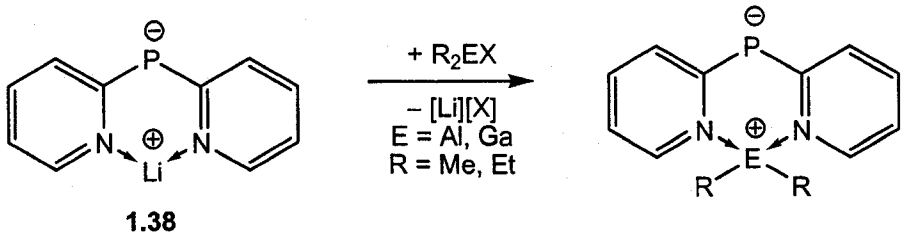

1.38 (1.29)

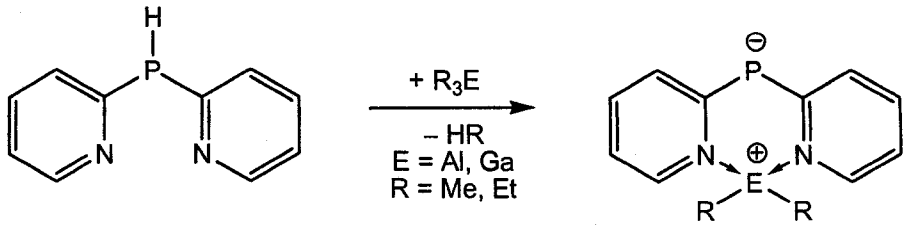

(1.30)

Whereas the addition of alkyl halides to amino-substituted phosphaalkynes was shown above to generate P^I cations, treatment with elemental chalcogens (O_2, S_8, Se) or CS_2 yields the analogous neutral species where one of the P atoms has undergone complete oxidation to P^V (Equation 1.31).[83,84]

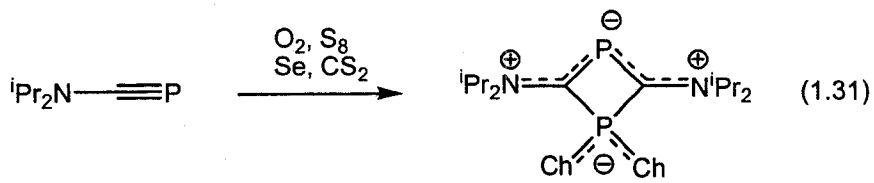

(1.31)

As outlined above, cyclic phosphinidenes contain P^I centres on the basis of formal counting rules but have structural and electronic features that are more consistent with P^{III} centres. Such rings can, however, be broken apart by suitable strong donors (phosphines, *N*-heterocyclic carbenes) to produce neutral compounds that may be more accurately described as containing P^I; in appropriate cases, such compounds can be considered reasonably as being base-stabilized phosphinidenes (Equation 1.32).[85-87] The first report of this approach was the reaction of four equivalents of PMe_3 with $(PCF_3)_4$, to yield the P^I compound Me_3PPCF_3 **1.39**.[88]

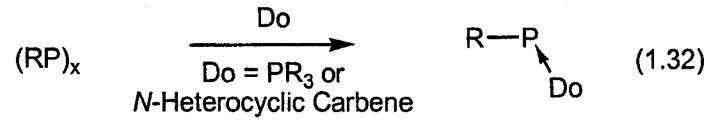

(1.32)

Whereas carbene-stabilized phosphindenes are often considered to be a type of phosphaalkene, which contain P^{III} centres,[89,90] the structural features of the NHC-stabilized phosphinidenes are more consistent with the presence of a P^I centre.[91] In particular, the structural features exhibited by NHC-stabilized phosphinidenes are, predictably, virtually identical to those found in the corresponding NHC-stabilized cations and dialkylphosphides described above. Of particular note is the observation that

neither of the groups attached to the phosphorus atom are co-planar with the C-P-C framework.

Compounds that can be considered as intramolecularly carbene-stabilized phosphinidenes can also be isolated from the treatment of amino-substituted phosphaalkynes with *N*-heterocyclic carbenes (Equation 1.33).[92]

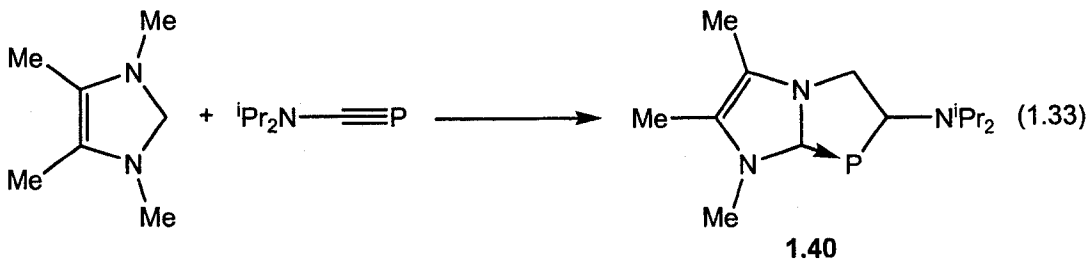

(1.33)

1.40

Analogous phosphine stabilized phosphinidenes can also be isolated when an aryldichlorophosphine, $ArPCl_2$, is reduced in the presence of PMe_3 (Equation 1.34).[93] This method has only produced monomeric products when sterically-demanding groups are affixed to the P^I centre (Ar = 2,4,6-$^{t}Bu_3C_6H_2$, *Mes**; Ar = 2,6-$Mes_2C_6H_3$, *Dmp*, Mes = 2,4,6-$Me_3C_6H_2$). When this synthetic approach is attempted with less bulky substituents on the phosphorus atom the only products that are isolated result from phosphinidene oligiomerization to give the corresponding cyclic polyphosphine. In contrast, the synthetic approach employing the Lewis-base phosphinidene extraction from cyclic polyphosphines allows for much smaller groups on the P^I centre such as $-CF_3$.[87]

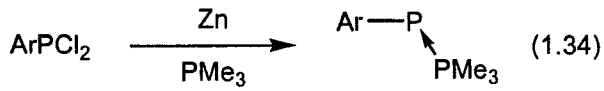

(1.34)

Reactivity

Phosphine-stabilized phosphinidenes can undergo exchange of PMe_3 with other non-hindered trialkylphosphines, such as PBu_3,[94] and have proven useful as phospha-Wittig reagents and can be employed for the formation of new P-C bonds (Equation

1.35)[94] and were the subject of a recent review.[22] Phosphine- and NHC-stabilized phosphinidenes have been shown to coordinate to two equivalents of BH_3 (Equations 1.36 and 1.37).[95] Bulkier substituents on the phosphinidene fragment seem to prevent the coordination of two borane molecules (Equation 1.38).[93] Similar bis-adducts are also observed with the intramolecularly carbene-stabilized molecule **1.40** (Equation 1.39).

(1.35)

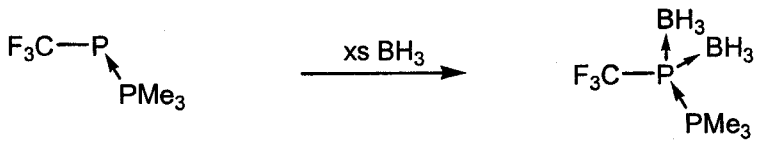

(1.36)

1.39 **1.41**

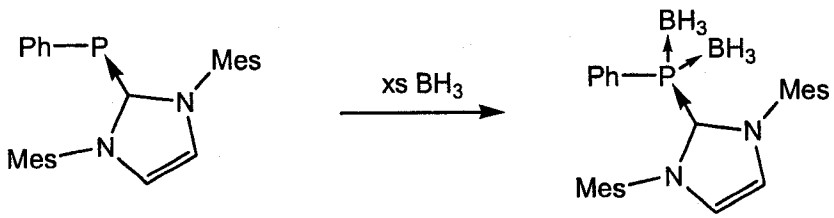

(1.37)

1.42 **1.43**

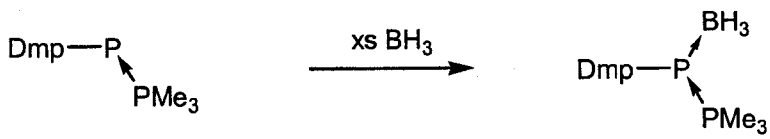

(1.38)

1.44 **1.45**

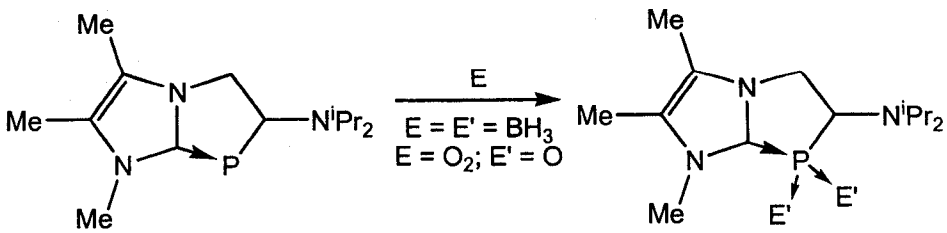

(1.39)

1.40

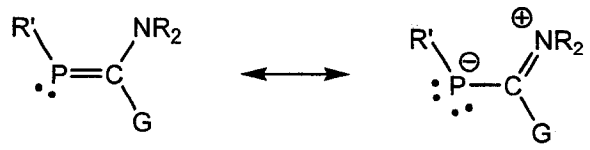

Figure 1.11 - "Inverse electron density" phosphaalkenes.

As outlined by Weber,[96] "inverse electron density" phosphaalkenes can be considered to contain P^I centres in that the canonical structure containing the phosphide-like fragment is an important resonance contributor to the actual electronic structure (Figure 1.8). When G is an NR_2 fragment, such compounds are clearly analogous to the NHC-stabilized phosphinidenes described above. It must be noted, however, that the description of such compounds as containing P^I centres is only justified when the R' group is not able to form a P=C or (P=E) multiple bond. For example, whereas $(TMS)P=C(NMe_2)_2$ **1.46** can reasonably be considered to contain a P^I centre, the corresponding P-acyl phosphaalkenes (obtained through the reaction of **1.46** with organic acid chlorides[97]) are more aptly described as containing P^{III} centres; this description is a consequence of the enolate form of the RC(O)P fragment as depicted in Figure 1.9. While the structures of free P-acyl phosphaalkenes of the type $RC(O)P=C(NMe_2)_2$ are not known, the structure of the $B(C_6F_5)_3$ adduct clearly shows that the acyl group is co-planar with the C-P-C moiety and is thus consistent with the presence of a P^{III} environment. In spite of this observation, the coordination chemistry of the P atom in such molecules is very similar to that which is observed for the other P^I compounds described above.[98]

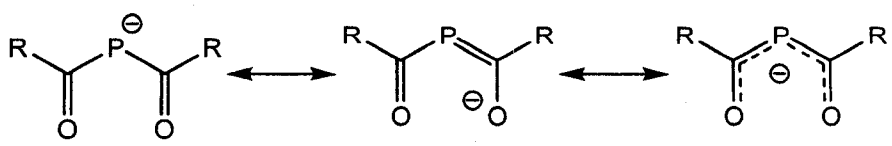

Figure 1.12 - Canonical structures of 2-phospha-dionato anions.

Finally, it should be noted that neutral P^I compounds can also be generated from existing P^I anions and cations. For example, displacement of cyanide from $P(CN)_2^-$ **1.27** by $(Ph_2P)_2CCN^-$ generates related ring structures related to **1.37** where each N atom has been replaced by a CCN fragment (Equation 1.40). Similarly, equimolar mixtures of carbene stabilized P^I cations and cyanide stabilized P^I anions leads to ligand scrambling, resulting in overall neutral P^I compounds with both carbene and cyanide donors (Equation 1.41).[99] Lastly, some cyclic P^I cations can be deprotonated by DBU (1,8-diazabicyclo[5.4.0]undec-7-ene)[100] to yield zwitterionic compounds as shown in Equation 1.42.[29]

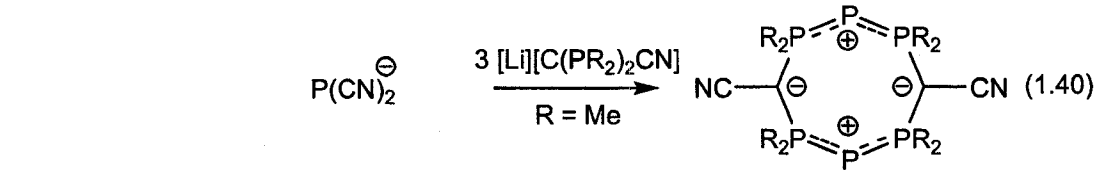

1.27 **1.47**

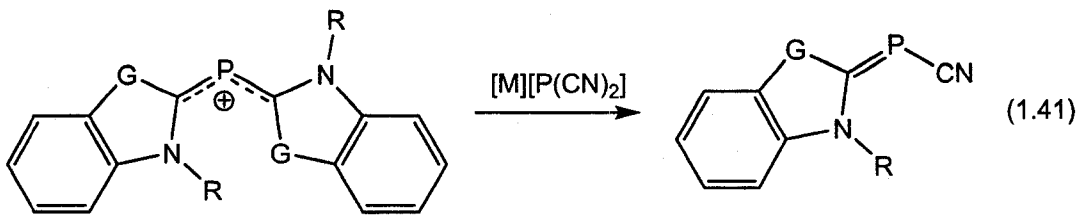

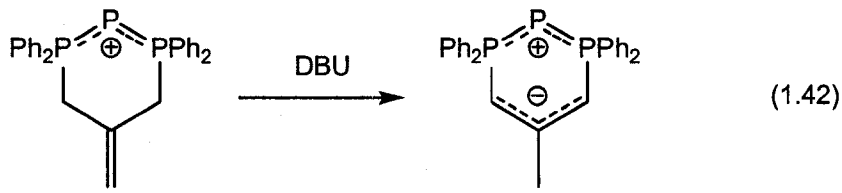

1.12 **1.48**

The reaction of the anionic bis-phosphide stabilized P^I salt $[Li][P(P^tBu_2)_2]$ [Li]**1.49** with 1,2-dibromoethane generates an oxidized phosphorus compound of the type $(R_2P)_2PBr$, which then undergoes a tautomerization involving the transfer of Br from the

central phosphorus atom (providing a P^I-like centre) to one of the phosphide fragments (producing a P^V-like centre) leads to the product $^tBu_2P$–P=P(Br)$^tBu_2$ (Equation 1.43).[101]

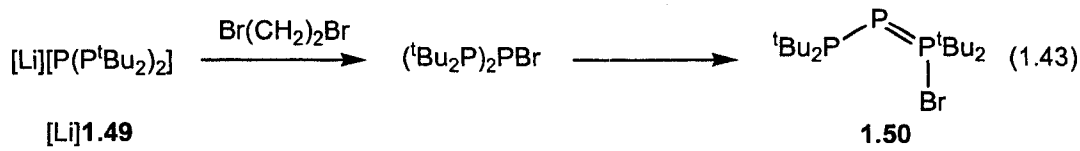

(1.43)

[Li]**1.49** **1.50**

In a similar vein, the treatment of $(^tBu_2P)_2P$–TMS with various halogenating agents (X_2G = Br_2, I_2, NBS, CCl_4, CBr_4, CI_4 or C_2Cl_6) also results in the formation of other halogen derivatives of **1.50** (Equation 1.44).[102] The methylated analogue is accessible through the reaction of [Li][$P(P^tBu_2)_2$] with either Me_2SO_4 or MeCl (Equation 1.45).[103] Other analogous neutral P^I compounds, such as ^tBu(TMS)P–P=P(Me)$^tBu_2$ **1.52**, are accessible using the same synthetic approach by altering the initial lithium diphosphinophosphide reagent (Equation 1.46).[103] Such species can likewise be converted to the related halogenated species through treatment with halogenating reagents and concomitant loss of TMS–X (Equation 1.47).[104]

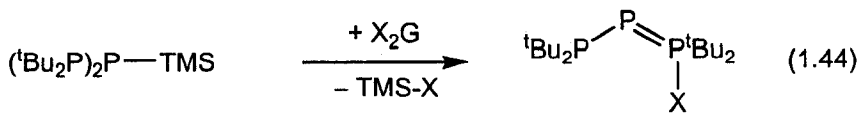

(1.44)

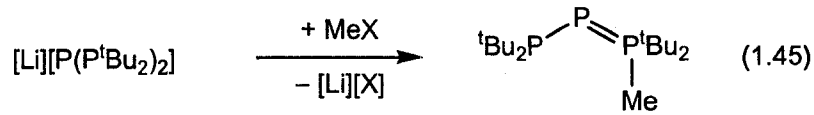

(1.45)

[Li]**1.49** **1.51**

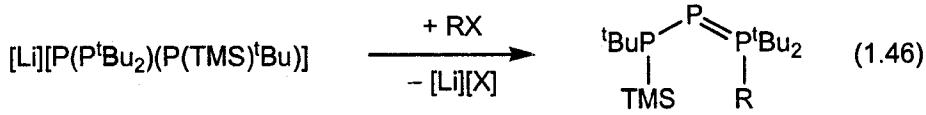

(1.46)

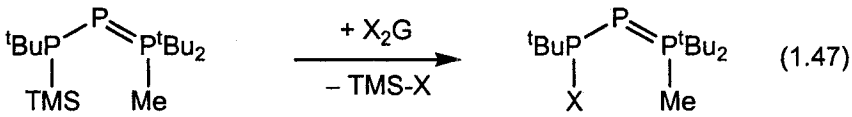

(1.47)

1.52

The reaction of $^tBu_2P–P=P(Br)^tBu_2$ **1.50** with lithium phosphides produce diphosphines and result in the oxidation of the P^I centre to yield $P(PR_2)(P^tBu_2)_2$ (Equation 1.48).[105] Treatment of **1.50** with alkyl lithium reagents results in both the exchange of Br for R and the oxidation of the P^I centre to give a phosphine of the form $PR(P^tBu_2)_2$ as the major project and some P^I species (Equation 1.49).[105] The reaction of $R^tBuP–P=P(Me)^tBu_2$ with $Ni(CO)_4$ results in the cyclization of the $P\text{-}P^tBu_2$ phosphinidene-like units into a three-membered ring and coordination to nickel via the pendant P^tBu_2 fragments.[106]

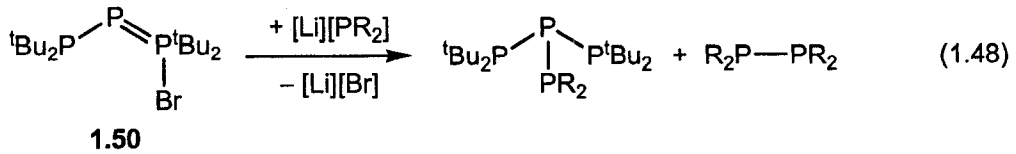

1.50 (1.48)

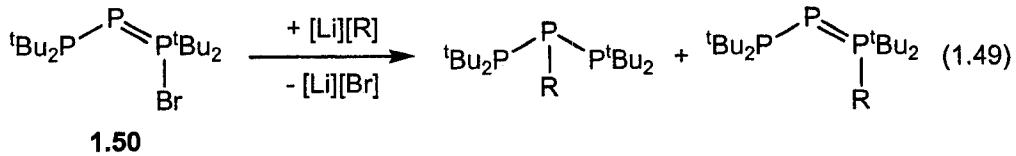

1.50 (1.49)

1.3.4 As^{I} Compounds

As is the case for phosphorus, the traditional classes of compounds that are formally considered to contain As^{I} centres are exemplified by the molecules composed of oligomers of unstable arsinidene fragments pictured in Figure 1.10.

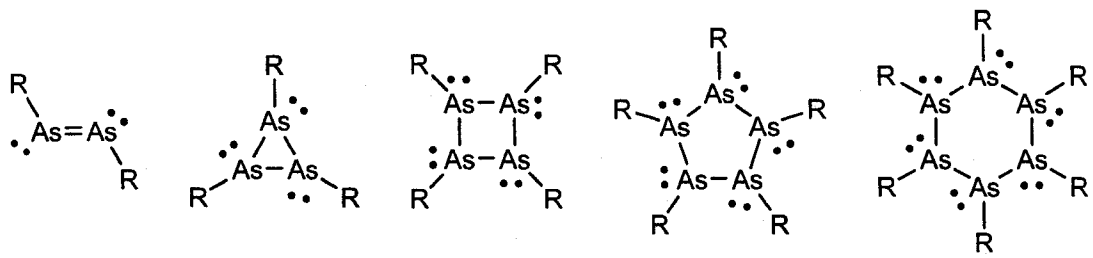

Figure 1.13 - Oligomeric organo-arsinidene structures.

Perhaps the most well-known example of such a compound is the drug "Salvarsan",[107] which has been shown to consist of primarily 3- and 5-membered rings. Despite their classification as As^{I} compounds on the basis of counting rules, all of the cyclo-polyarsines[108] contain exclusively pyramidal environments around arsenic that are consistent with the As^{III} centres, as outlined above for the phosphorus analogues. In this light, the types of compounds that contain As^{I} centres as outlined in Figure 1.1 are similar to the dicoordinate examples described above for phosphorus.

Cationic As^I Compounds

While there are fewer examples of As^I compounds, they tend to be synthesized by synthetic routes that have been used to obtain the analogous P^I compounds. For example, cationic phosphine-stabilized As^I compounds may be synthesized by the reduction of $AsCl_3$ by $SnCl_2$ in the presence of a chelating phosphines (Equation 1.50).[29,31] Several compounds that have been obtained using this synthetic approach have also been characterized crystallographically with examples of cations containing saturated and unsaturated backbones. In every case the compounds exhibit As-P bonds that are intermediate in length between those of As-P single bonds (CSD[109] average 2.34 Å) and As=P double bonds (2.124(4) Å in Mes*P=AsDis[110]). The angles of the P-As-P fragments in all of the cyclic cations are acute, with the angles being, expectedly, smaller than those of the corresponding phosphorus analogues. The ^{31}P NMR spectra chemical shifts for the stabilizing-phosphines are similar to those observed for the phosphorus analogues.

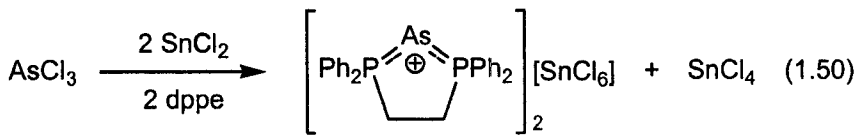

1.53$_2SnCl_6$

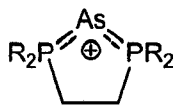

1.53 R = Ph
1.54 R = Et
1.55 R = Ph,Et

1.56

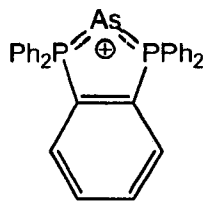

1.57

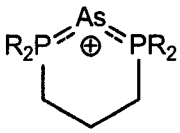

1.58

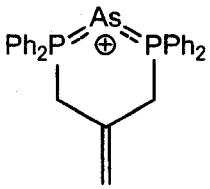

1.59

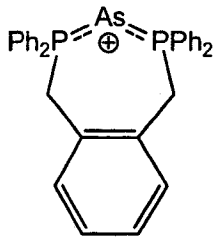

1.60

As demonstrated for the phosphorus analogues, diimines have recently been used to trap As^{I} centres generated using the $AsCl_3/SnCl_2$ protocol. The metrical parameters of the cation in the [(BIAN)As][$SnCl_5$(thf)] clearly demonstrate that the As^{I} centre is oxidized to As^{III} (Equation 1.51) and the diimine is reduced to the corresponding diamide in the process.[33] More recently, Cowley *et al.* have shown if a diimine that is not easily reduced is used in analogous trapping reactions, the product obtained does indeed contain an As^{I} centre (Equation 1.52).[111] The structure is perhaps best described as containing a 10-As-3 centre[112] with a ψ-tbp geometry; in this light, the compound can be considered to be equivalent to a base-stabilized arsidene in the same manner as the R-DKA molecules of Arduengo (see Figure 1.7). In this context, the As-N distances are reported to be consistent with dative As-N bonds and the metrical parameters of the diimine fragment are almost identical to those of the free diimine ligand and thus are not indicative of ligand reduction.

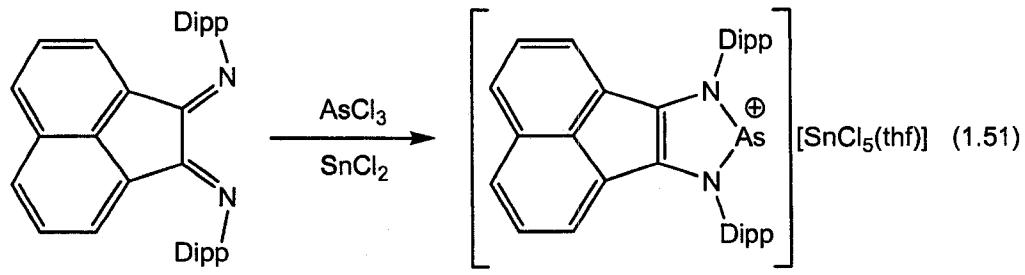

1.61[$SnCl_5$(thf)]

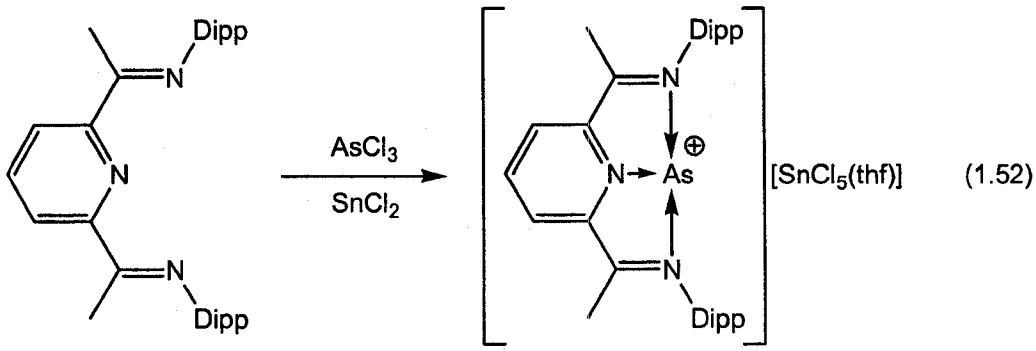

1.62[$SnCl_5$(thf)]

In a similar manner to that described above for the phosphorus derivatives, an additional equivalent of ligating phosphine can also be used to reduce As^{III} to As^{I} to generate acyclic and cyclic cations (Equation 1.53).[31,40,41] The molecular structure of the acyclic As^{I} cation **1.63** displays the expected bent P-As-P fragment containing short P-As bonds.

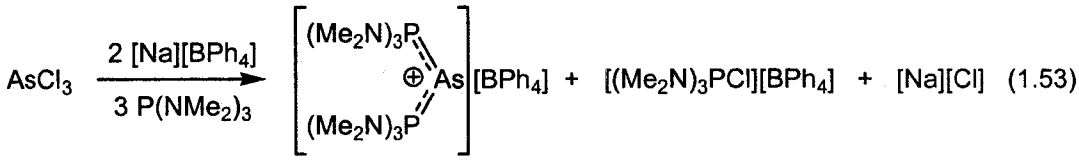

1.63[BPh_4]

When the acyclic As^{I} compound **1.63** is treated with a large excess of the Schwartz reagent ($Cp_2Zr(H)Cl$) the triaminophosphine ligands are cleaved and oxidized to produce [$(Me_2N)_3PCl$] cations and the arsenic centre is reduced to As^{-III} and trapped in a Zr_4H_4 ring **1.64** (Equation 1.54) in a manner analogous that described above for the

phosphorus congener.[40,41] A complication in the synthesis is the unexpected production of the P analogue during the reaction; thus the product crystallizes as the [BPh_4] salt containing a mixture of P and As atoms at the centre of the Zr_4H_4 ring.

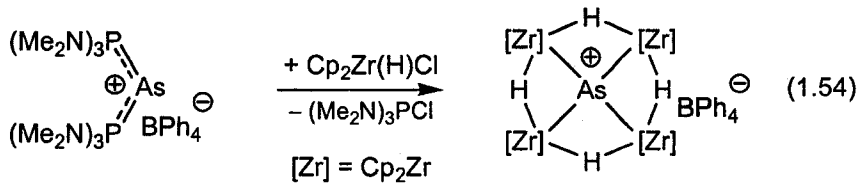

(1.54)

1.63[BPh_4] **1.64**[BPh_4]

The arsenic analogues of phosphamethine cyanines, which are known as arsamethine cyanines and may also be considered as carbene-stabilized As^I centres, can be isolated from the reaction of 2-chlorobenzothiazolium and tris(trimethylsily)arsine, driven by the loss of Me_3SiCl (Equation 1.55).[46] While the arsenic analogues also exhibit transitions in the visible region, no examples have been characterized by X-ray crystallography to date and the chemistry of such compounds has not been investigated in detail.

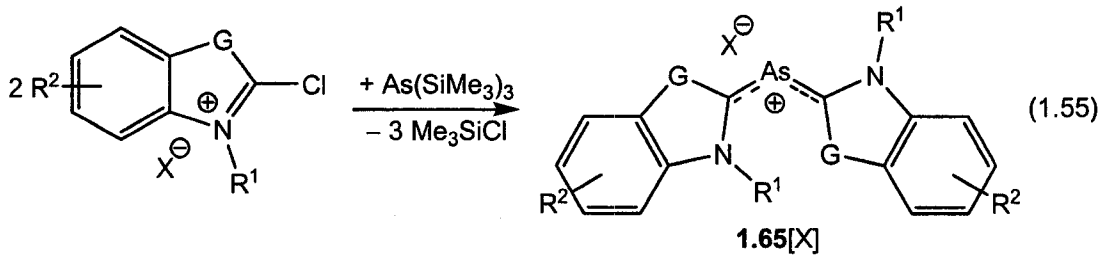

(1.55)

1.65[X]

Anionic As^I Compounds

As with phosphorus, some of the most well known As^I-containing species are the diorgano arsenide salts that contain anions of the type R_2As^-. Such species are useful reagents for the generation of other organoarsenic compounds through nucleophilic substitution or metathesis reactions.[113-115] In comparison with the phosphorus congeners there are considerably fewer examples of stable arsenides that do not feature coordination

of the arsenic atom to the counter cations. One family of such salts are those that contain the diphenylarsenide anion, Ph_2As^-. These anionic As^I compounds may be generated through the reduction of diphenylarsine with ^nBuLi. Coordination of the lithium cation with oxygen donors (crown ethers, dioxanes) allows for the collection of crystals suitable for examination by X-ray crystallography.[116,117] The molecular structure of $AsPh_2^-$ shows that the As-C bond distances are all greater than 1.93 Å and are thus consistent with typical single As-Ar distances found in the CSD and are certainly much larger than the distances reported for As=C double bonds (*ca.* 1.80 Å or smaller). Cyclic, anionic As^I compounds of the type $[(RP)_nAs^-]$ are accessible through the reaction of $As(NMe_2)_3$ with lithium salts of primary phosphines (Equation 1.56).[118,119]

$$AsCl_3 \xrightarrow[\text{tmeda}]{\text{[Li][RPH]}} \text{[(tmeda)Li][(RP)}_n\text{As]} \quad (1.56)$$

Another class of anionic compounds that may be considered to contain As^I centres are the 2-arsadionates, which are isovalent with β-diketonate anions. These arsenic compounds are readily available from the reaction [Li][$As(SiMe_3)_2$] [Li]**1.66** and two equivalents of acid chloride, which results in the elimination of TMS-Cl and the desired salt (Equation 1.57).[120] Compounds of this type have the ability to coordinate to transition metal complexes through either the arsenic centre or the oxygen atoms.[121-123] Coordination is not limited to the d-block, complexes with both the s- and p-blocks have also been reported.[124] For example, reaction of three equivalents of [Li]**1.67** or [Li]**1.68** with phosphorus(III) chloride results in loss of lithium chloride and formation of tris(diacylarsinido)phosphines (Equation 1.58).[125] 2-Arsadionate anions invariably exhibit planar O-C-As-C-O fragments, which suggest that such molecules contain an As^{III} centre. While the planar structure is likely a consequence of π-delocalization, it should

be noted that As-C bond distances in such complexes are relatively long and the structures are often constrained to be planar by the chelation of the anion to a single metal centre. Regardless, the structures of the Main Group and Transition Metal complexes obtained through the formation of As-E bonds have pyramidal environments about the As atoms and are thus more consistent with those obtained from arsenide anions than those from normal arsaalkene ligands.

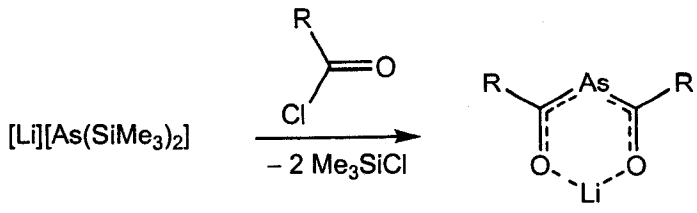

[Li]**1.66** [Li]**1.67** R = Ph [Li]**1.68** R = ^{t}Bu (1.57)

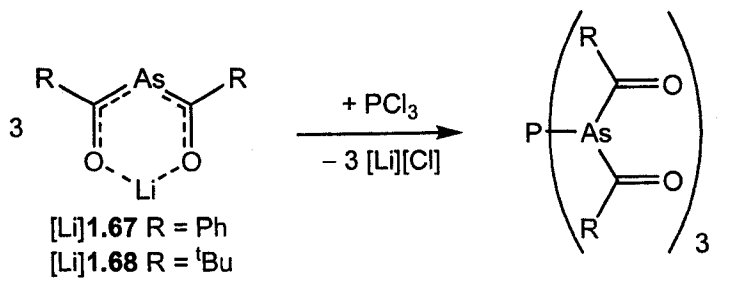

[Li]**1.67** R = Ph [Li]**1.68** R = ^{t}Bu (1.58)

Neutral As^I Compounds

In contrast to the phosphorus congener, the As^I cation **1.59** cannot be deprotonated to produce the corresponding neutral species.[29] However, in an analogous manner to the phosphorus derivatives, bis(pyridyl)arsenides **1.69** react with Group 13 compounds to give zwitterions, such as when complexed with $AlMe_2$ cations **1.70**.[80]

Most of the neutral As^I compounds that have been reported are generated through the reaction of arsenic trihalides with lithium diphosphinomethanide salts in a manner similar to that observed for phosphorus. For example, the reaction of arsenic(III) chloride with [Li][CR_2TMS], where R = PPh_2 results in the formation of the four-

membered ring compound **1.71** and involves the oxidation of the additional equivalent of the carbanion (Equation 1.59).[70] In contrast, when R = PMe_2, the eight-membered ring is not observed; instead, four arsenic centres with an average oxidation state of 0.5 are trapped between two carbanions and oxidation of the extra carbanion (Equation 1.60).[73,126] The treatment of arsenic(III) iodide with either two or three equivalents of the lithium amide $[Li][N(PPh_2)_2]$ results in the formation of either a seven-membered As^I cation **1.73** with an iodide anion (Equation 1.61) or an eight-membered ring with two As^I centres (Equation 1.62).[127] Application of heat drives the reduction to elemental arsenic and further oxidation of the remaining amides.

$$AsCl_3 \xrightarrow[R = Ph]{2\ [Li][C(PR_2)_2TMS]} \text{1.71} \qquad (1.59)$$

$$AsCl_3 \xrightarrow[R = Me]{3\ [Li][C(PR_2)_2TMS]} \text{1.72} \qquad (1.60)$$

$$AsI_3 \xrightarrow{2\ [Li][N(PPh_2)_2]} \text{1.73[I]} \qquad (1.61)$$

$$AsI_3 \xrightarrow{3\ [Li][N(PPh_2)_2]} \text{1.74} \qquad (1.62)$$

In a manner similar to that which is observed for cyclo-polyphosphines, strong nucleophiles such as *N*-heterocyclic carbenes are able to break apart cyclic-polyarsines of the type $(R\text{-}As)_x$, to give neutral stabilized As^I centres.[87] The structures of the molecules produced using this method exhibit As-C distances of roughly 1.90 Å that fall in the range of single As-C bonds. Furthermore, the twisting of substituents from the C-As-C plane reduces the possibility of As-C multiple bonding.

Reduction of sterically-demanding arylarsine dichlorides (aryl = 2,6-bis(2,4,6-triisopropylphenyl)phenyl) by zinc in the presence of PMe_3 stabilizes the arsinidene generated.[128] The structure of **1.75** is reminiscent of the phosphorus analogue described above. These As-P bonds are anticipated to undergo arsa-Wittig reactions in a manner similar to the phosphorus analogues, although this has only been shown so far by indirect evidence. The loss of the PMe_3 ligand from the molecule results in the formation of the corresponding diarsene R-As=As-R, as one would expect for an arsinidene bearing such a large R substituent.

1.3.5 Antimony and Bismuth

There are significantly fewer examples of organo-element compounds that contain antimony or bismuth in Pn^I environments and, because the structural and chemical properties of these compounds is similar in many cases, the compounds containing Sb and Bi are treated together in this section.

As with the lighter congeners, whereas the free stibinidenes (R-Sb) or bismuthinidenes (R-Bi) are unstable, the cyclic-polypnictines formally derived from such fragments are well-known for both elements.[129,130] In every such case, the geometry

about each pnictogen atom is pyramidal and thus the molecules are best described as containing Pn^{III} centres.

Unlike all of the lighter pnictogen analogues, there are no examples of cationic or neutral antimony(I) or bismuth(I) compounds. The absence of such species is often a consequence of the tendency of antimony and bismuth compounds to be completely reduced to Sb^0 and Bi^0 under most of the reduction conditions that have been used to synthesize the lighter congeners. For example, the syntheses employing lithium amides used to generate the neutral As^I zwitterions described above result in the deposition of either elemental Sb or Bi.[127] Conversely, the synthetic approaches involving the reaction of SbX_3 or BiX_3 with donors such as phosphines or *N*-heterocyclic carbenes do not result in the formation Pn^I species but instead generate donor-acceptor complexes that retain the Pn^{III} centres (Equation 1.63 illustrates a typical result).[131-137]

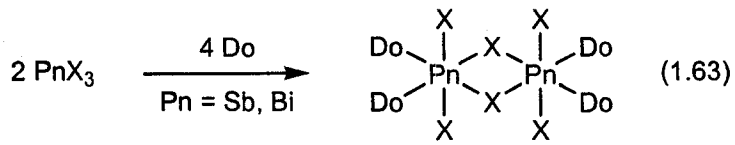

(1.63)

Anionic Sb^I and Bi^I compounds are known, although there are relatively few examples in comparison to those of phosphorus and arsenic. Diphenylstibinide, Ph_2Sb^- **1.76**, can be generated by the treatment of diphenylstibine with ^{n}BuLi, in a manner similar to that which is observed for the lighter Group 15 elements.[117]

The reduction of $SbPh_3$ with lithium yields the lithium salt of an anion that consists of a Sb^I centre ligated by two Ph_2Sb moieties (Equation 1.64).[117] The ^{t}Bu analogue, $[(Sb^tBu_2)_2Sb]^-$ **1.78** is obtained from the reduction of $(^tBuSb)_4$ with excess potassium[138,139] and the Li and Na analogues are prepared analogously (Equation 1.65).[138,140] The reaction of $Sb(SiMe_3)_3$ with MeLi yields a salt containing the anion

$[(Me_3Si)_2Sb]^-$ **1.79** in which the lithium cation is coordinated by dme molecules (Equation 1.66).[141] The bismuth analogue, $[(Me_3Si)_2Bi]^-$ **1.80**, is accessible through the related procedure,[142] and exhibits contacts with the counter cation. The only structurally characterized example of such an anion for Bi in which there are no obvious cation-anion contacts is found in the lithium salt of the extremely bulky anion $[((Me_3Si)_3Si)_2Bi]^-$ **1.81**.[143]

$$SbPh_3 \xrightarrow[tmeda]{Li} [(tmeda)Li][(Ph_2Sb)_2Sb] \quad (1.64)$$

1.77

$$(^tBuSb)_4 \xrightarrow[L]{M} [(L)M][(^tBu_2Sb)_2Sb] \quad (1.65)$$

1.78

$$Sb(SiMe_3)_3 \xrightarrow[-\ SiMe_4]{+\ MeLi,\ dme} [(dme)Li][(Me_3Si)_2Sb] \quad (1.66)$$

1.79

Finally, it is also worth noting that the only cyclic compound that contains either an Sb^I or Bi^I centre is the anion $[Sb(PCy)_4]^-$ **1.82**, which crystallizes as a bis-Na-bridged dimer. As with its arsenic analogue mentioned above, it is also prepared through the addition of primary phosphido alkali metal complexes to $Sb(NMe_2)_3$.[118,119]

1.4 Dissertation Overview

This dissertation contains six additional chapters that describe synthesis and reactivity of compounds containing low oxidation state pnictogen atoms. Chapter 2 details the synthesis of cyclic P^I iodide salts, which have been isolated in the absence of by-products, and a variety of other P^I salts that have been obtained through anion

metathesis. Computational studies probe the electronic structure of phosphine-stabilized P^I cations and their nitrogen-stabilized analogues. Chapter 3 describes the synthesis of new P^I compounds through the exchange of phosphines with *N*-heterocyclic carbenes. The coordination chemistry of cyclic P^I cations is explored in Chapter 4 with reactions involving both Main Group and Transition Metal electron acceptors. Computational chemistry is used to help explain some experimental observations. Trapping of Pn^I cations generated through two different protocols by diimines is presented in Chapter 5, along with computational results to help rationalize the electronic structure in these cations as well as in examples from recent literature reports. Chapter 6 examines the synthesis of heavier Pn^I cations and the use of iodide salts of As^I cations as reagents for the generation of arsenic-iodide clusters. Finally Chapter 7 summarizes the various chapters in this dissertation and connects the individual studies together. Suggestions for additional research are given at the end of each chapter and the experimental details of the research reported are found within each chapter.

1.5 References

1. Arduengo, A.J., III, Stewart, C.A., Davidson, F., Dixon, D.A., Becker, J.Y., Culley, S.A. and Mizen, M.B., *J. Am. Chem. Soc.*, **1987**, *109*, 627-647.
2. Brown, R.W. in *Composition of Scientific Words*, 1956, Baltimore: Reese Press, p. 620.
3. Liddell, H.G. and Scott, R. in *A Greek-English Lexicon, 9th Edition*, 1968, Oxford: Clarendon Press, p. 1425.

4. Leon-Escamilla, E.A., Hurng, W.-M., Peterson, E.S. and Corbett, J.D., *Inorg. Chem.*, **1997**, *36*, 703-710.

5. Briand, G.G. and Burford, N., *Adv. Inorg. Chem.*, **2000**, *50*, 285-357.

6. Mitsumoto, Y. and Nitta, M., *Bull. Chem. Soc. Jpn.*, **2003**, *76*, 1029-1034.

7. Fish, C., Green, M., Jeffery, J.C., Kilby, R.J., Lynam, J.M., McGrady, J.E., Pantazis, D.A., Russell, C.A. and Willans, C.E., *Chem. Commun.*, **2006**, 1375-1377.

8. Thomas, F., Schulz, S. and Nieger, M., *Z. Anorg. Allg. Chem.*, **2002**, *628*, 235-242.

9. Greenwood, N.N. and Earnshaw, A., *Chemistry of the Elements, 2nd Edition*, 1997, Oxford: Elsevier Butterworth-Heinemann, pp. 1341.

10. Ebbing, D.D., *General Chemistry, 5th Edition*, 1996, Boston: Houghton Mifflin Company, pp. 1087.

11. Corbridge, D.E.C., *Studies in Inorganic Chemistry, Vol. 2: Phosphorus: An Outline of its Chemistry, Biochemistry and Technology, 2nd Edition*, 1980, Amsterdam: Elsevier Scientific Publishing Company, pp. 560.

12. Cotton, F.A., Wilkinson, G., Bochmann, M. and Murillo, C., *Advanced Inorganic Chemistry, 6th Edition*, 1998, New York: John Wiley & Sons, Inc., pp. 1355.

13. Coulson, C.A., *Valence, 2nd Edition*, 1961, London: Oxford University Press, pp. 417.

14. Hoffmann, R., *Angew. Chem., Int. Ed. Engl.*, **1982**, *21*, 711-724.

15. Power, P.P., *Chem. Rev.*, **2003**, *103*, 789-809.

16. Milyukov, V.A., Budnikova, Y.H. and Sinyashin, O.G., *Russ. Chem. Rev.*, **2005**, *74*, 781-805.

17. Scherer, O.J., *Acc. Chem. Res.*, **1999**, *32*, 751-762.

18. Platz, M.S. in *Nitrenes*, 2004, Hoboken, N.J.: John Wiley & Sons, Inc., p. 501-559.

19. Mathey, F., *Angew. Chem., Int. Ed. Engl.*, **1987**, *26*, 275-286.

20. Lammertsma, K. and Vlaar, M.J.M., *Eur. J. Org. Chem.*, **2002**, 1127-1138.

21. Lammertsma, K., *Top. Curr. Chem.*, **2003**, *229*, 95-119.

22. Shah, S. and Protasiewicz, J.D., *Coord. Chem. Rev.*, **2000**, *210*, 181-201.

23. Culley, S.A. and Arduengo, A.J., III, *J. Am. Chem. Soc.*, **1984**, *106*, 1164-1165.

24. Schmidpeter, A., *Heteroat. Chem.*, **1999**, *10*, 529-537.

25. Schmidpeter, A., Lochschmidt, S. and Sheldrick, W.S., *Angew. Chem., Int. Ed. Engl.*, **1982**, *21*, 63-64.

26. Schmidpeter, A. and Lochschmidt, S., *Inorg. Synth.*, **1990**, *27*, 253-258.

27. Lochschmidt, S. and Schmidpeter, A., *Phosphorus Sulfur Relat. Elem.*, **1987**, *29*, 73-109.

28. Yoshifuji, M., Shima, I., Inamoto, N., Hirotsu, K. and Higuchi, T., *J. Am. Chem. Soc.*, **1981**, *103*, 4587-4589.

29. Gamper, S.F. and Schmidbaur, H., *Chem. Ber.*, **1993**, *126*, 601-604.

30. Boon, J.A., Byers, H.L., Dillon, K.B., Goeta, A.E. and Longbottom, D.A., *Heteroat. Chem.*, **2000**, *11*, 226-231.

31. Barnham, R.J., Deng, R.M.K., Dillon, K.B., Goeta, A.E., Howard, J.A.K. and Puschmann, H., *Heteroat. Chem.*, **2001**, *12*, 501-510.

32. Dillon, K.B., Monks, P.K., Olivey, R.J. and Karsch, H.H., *Heteroat. Chem.*, **2004**, *15*, 464-467.

33. Reeske, G., Hoberg, C.R., Hill, N.J. and Cowley, A.H., *J. Am. Chem. Soc.*, **2006**, *128*, 2800-2801.

34. Schmidpeter, A., Lochschmidt, S. and Sheldrick, W.S., *Angew. Chem., Int. Ed. Engl.*, **1985**, *24*, 226-227.

35. Schmidpeter, A. and Lochschmidt, S., *Angew. Chem., Int. Ed. Engl.*, **1986**, *25*, 253-254.

36. Schmidpeter, A., Lochschmidt, S., Karaghiosoff, K. and Sheldrick, W.S., *J. Chem. Soc., Chem. Commun.*, **1985**, 1447-1448.

37. Lochschmidt, S. and Schmidpeter, A., *Z. Naturforsch., B: Anorg. Chem., Org. Chem.*, **1985**, *40B*, 765-773.

38. Dillon, K.B. and Olivey, R.J., *Heteroat. Chem.*, **2004**, *15*, 150-154.

39. Driess, M., Aust, J., Merz, K. and Van Wullen, C., *Angew. Chem. Int. Ed.*, **1999**, *38*, 3677-3680.

40. Ackermann, H., Aust, J., Driess, M., Merz, K., Monse, C. and Van Wullen, C., *Phosphorus, Sulfur Silicon Relat. Elem.*, **2002**, *177*, 1613-1616.

41. Driess, M., Ackermann, H., Aust, J., Merz, K. and Von Wullen, C., *Angew. Chem. Int. Ed.*, **2002**, *41*, 450-453.

42. Koraiem, A.I.M., Hassan, K.M. and Abd el All, R.M., *Dyes Pigm.*, **1990**, *13*, 269-280.

43. Dimroth, K. and Hoffmann, P., *Angew. Chem., Int. Ed. Engl.*, **1964**, *3*, 384.

44. Dimroth, K. and Hoffmann, P., *Chem. Ber.*, **1966**, *99*, 1325-1331.

45. Dimroth, K., *Fortschr. Chem. Forsch.*, **1973**, *38*, 1-147.

46. Maerkl, G. and Lieb, F., *Tetrahedron Lett.*, **1967**, 3489-3493.

47. Schmidpeter, A. and Willhalm, A., *Angew. Chem., Int. Ed. Engl.*, **1984**, *23*, 903-904.

48. Schmidpeter, A., Lochschmidt, S. and Willhalm, A., *Angew. Chem., Int. Ed. Engl.*, **1983**, *22*, 545-546.

49. Schmidpeter, A., Lochschmidt, S. and Willhalm, A., *Angew. Chem. Suppl.*, **1983**, 710-717.

50. Grobe, J., Le Van, D., Hegemann, M., Krebs, B. and Laege, M., *Heteroat. Chem.*, **1994**, *5*, 337-341.

51. Kawada, I. and Allmann, R., *Angew. Chem., Int. Ed. Engl.*, **1968**, *7*, 69.

52. Day, R.O., Willhalm, A., Holmes, J.M., Holmes, R.R. and Schmidpeter, A., *Angew. Chem., Int. Ed. Engl.*, **1985**, *24*, 764-765.

53. Allmann, R., *Angew. Chem., Int. Ed. Engl.*, **1965**, *4*, 150.

54. Allmann, R., *Chem. Ber.*, **1966**, *99*, 1332-1340.

55. Schmidpeter, A., Zirzow, K.H., Willhalm, A., Holmes, J.M., Day, R.O. and Holmes, R.R., *Angew. Chem., Int. Ed. Engl.*, **1986**, *25*, 457-458.

56. Schmidpeter, A. and Zwaschka, F., *Angew. Chem., Int. Ed. Engl.*, **1977**, *16*, 704-705.

57. Schmidpeter, A., Burget, G., Zwaschka, F. and Sheldrick, W.S., *Z. Anorg. Allg. Chem.*, **1985**, *527*, 17-32.

58. Schmidpeter, A. and Burget, G., *Inorg. Synth.*, **1989**, *25*, 126-129.

59. Schmidpeter, A. and Burget, G., *Z. Naturforsch., B: Anorg. Chem., Org. Chem.*, **1985**, *40B*, 1306-1313.

60. Sheldrick, W.S., Schmidpeter, A., Zwaschka, F., Dillon, K.B., Platt, A.W.G. and Waddington, T.C., *J. Chem. Soc., Dalton Trans.*, **1981**, 413-418.

61. Schmidpeter, A., Zirzow, K.H., Burget, G., Huttner, G. and Jibril, I., *Chem. Ber.*, **1984**, *117*, 1695-1706.

62. Schmidpeter, A., Lochschmidt, S., Burget, G. and Sheldrick, W.S., *Phosphorus Sulfur Relat. Elem.*, **1983**, *18*, 23-26.

63. Schmidpeter, A., Burget, G., Von Schnering, H.G. and Weber, D., *Angew. Chem., Int. Ed. Engl.*, **1984**, *23*, 816-817.

64. Weber, D., Heckmann, G. and Fluck, E., *Z. Naturforsch., B: Anorg. Chem., Org. Chem.*, **1976**, *31B*, 81-84.

65. Weber, D. and Fluck, E., *Inorg. Nucl. Chem. Lett.*, **1976**, *12*, 515-518.

66. Peters, K. and Weber, D., *Cryst. Struct. Commun.*, **1981**, *10*, 1259-1262.

67. Weber, D., Fluck, E., Von Schnering, H.G. and Peters, K., *Z. Naturforsch., B: Anorg. Chem., Org. Chem.*, **1982**, *37B*, 594-600.

68. Roesky, H.W., Djarrah, H., Noltemeyer, M. and Sheldrick, G.M., *Z. Naturforsch., B: Anorg. Chem., Org. Chem.*, **1982**, *37B*, 1580-1583.

69. Kovacs, I., Krautscheid, H., Matern, E., Sattler, E., Fritz, G., Hoenle, W., Borrmann, H. and von Schnering, H.G., *Z. Anorg. Allg. Chem.*, **1996**, *622*, 1564-1572.

70. Karsch, H.H., Witt, E. and Hahn, F.E., *Angew. Chem., Int. Ed. Engl.*, **1996**, *35*, 2242-2244.

71. Karsch, H.H., Witt, E., Schneider, A., Herdtweck, E. and Heckel, M., *Angew. Chem., Int. Ed. Engl.*, **1995**, *34*, 557-560.

72. Karsch, H.H., Richter, R. and Witt, E., *Phosphorus, Sulfur Silicon Relat. Elem.*, **1996**, *109-110*, 165-168.

73. Karsch, H.H. and Witt, E., *J. Organomet. Chem.*, **1997**, *529*, 151-169.

74. Fei, Z. and Dyson, P.J., *Coord. Chem. Rev.*, **2005**, *249*, 2056-2074.

75. Appleby, T. and Derek Woollins, J., *Coord. Chem. Rev.*, **2002**, *235*, 121-140.

76. Schmidpeter, A. and Burget, G., *Angew. Chem., Int. Ed. Engl.*, **1985**, *24*, 580-581.

77. Braunstein, P., Hasselbring, R., Tiripicchio, A. and Ugozzoli, F., *J. Chem. Soc., Chem. Commun.*, **1995**, 37-38.

78. Schmidpeter, A., Steinmueller, F. and Sheldrick, W.S., *Z. Anorg. Allg. Chem.*, **1989**, *579*, 158-172.

79. Steiner, A. and Stalke, D., *J. Chem. Soc., Chem. Commun.*, **1993**, 444-446.

80. Steiner, A. and Stalke, D., *Organometallics*, **1995**, *14*, 2422-2429.

81. Pfeiffer, M., Stey, T., Jehle, H., Klupfel, B., Malisch, W., Stalke, D. and Chandrasekhar, V., *Chem. Commun.*, **2001**, 337-338.

82. Pfeiffer, M., Baier, F., Stey, T., Leusser, D., Stalke, D., Engels, B., Moigno, D. and Kiefer, W., *J. Mol. Model.*, **2000**, *6*, 299-311.

83. Grobe, J., Le Van, D., Immel, F., Hegemann, M., Krebs, B. and Laege, M., *Z. Anorg. Allg. Chem.*, **1996**, *622*, 24-34.

84. Grobe, J., Le Van, D., Pohlmeyer, T., Immel, F., Pucknat, H., Krebs, B., Kuchinke, J. and Lage, M., *Tetrahedron*, **2000**, *56*, 27-33.

85. Cowley, A.H. and Cushner, M.C., *Inorg. Chem.*, **1980**, *19*, 515-518.

86. Arduengo, A.J., III, Dias, H.V.R. and Calabrese, J.C., *Chem. Lett.*, **1997**, 143-144.

87. Arduengo, A.J., III, Calabrese, J.C., Cowley, A.H., Dias, H.V.R., Goerlich, J.R., Marshall, W.J. and Riegel, B., *Inorg. Chem.*, **1997**, *36*, 2151-2158.

88. Burg, A.B. and Mahler, W., *J. Am. Chem. Soc.*, **1961**, *83*, 2388-2389.

89. Le Floch, P., *Coord. Chem. Rev.*, **2006**, *250*, 627-681.

90. Weber, L., *Coord. Chem. Rev.*, **2005**, *249*, 741-763.

91. Cowley, A.H., *Acc. Chem. Res.*, **1997**, *30*, 445-451.

92. Hahn, F.E., Le Van, D., Moyes, M.C., Von Fehren, T., Frohlich, R. and Wurthwein, E.-U., *Angew. Chem. Int. Ed.*, **2001**, *40*, 3144-3148.

93. Shah, S., Yap, G.P.A. and Protasiewicz, J.D., *J. Organomet. Chem.*, **2000**, *608*, 12-20.

94. Shah, S. and Protasiewicz, J.D., *Chem. Commun.*, **1998**, 1585-1586.

95. Arduengo, A.J., III, Carmalt, C.J., Clyburne, J.A.C., Cowley, A.H. and Pyati, R., *Chem. Commun.*, **1997**, 981-982.

96. Weber, L., *Eur. J. Inorg. Chem.*, **2000**, 2425-2441.

97. Weber, L., Uthmann, S., Boegge, H., Mueller, A., Stammler, H.-G. and Neumann, B., *Organometallics*, **1998**, *17*, 3593-3598.

98. Weber, L., Uthmann, S., Stammler, H.-G., Neumann, B., Schoeller, W.W., Boese, R. and Blaser, D., *Eur. J. Inorg. Chem.*, **1999**, 2369-2381.

99. Schmidpeter, A., Gebler, W., Zwaschka, F. and Sheldrick, W.S., *Angew. Chem., Int. Ed. Engl.*, **1980**, *19*, 722-723.

100. Oediger, H., Moeller, F. and Eiter, K., *Synthesis*, **1972**, 591-598.

101. Kovacs, I. and Fritz, G., *Z. Anorg. Allg. Chem.*, **1994**, *620*, 1-3.

102. Kovacs, I. and Fritz, G., *Z. Anorg. Allg. Chem.*, **1994**, *620*, 1364-1366.

103. Kovacs, I., Balema, V., Bassowa, A., Matern, E., Sattler, E., Fritz, G., Borrmann, H., Bauernschmitt, R. and Ahlrichs, R., *Z. Anorg. Allg. Chem.*, **1994**, *620*, 2033-2040.

104. Sattler, E., Krautscheid, H., Matern, E., Fritz, G. and Kovacs, I., *Z. Anorg. Allg. Chem.*, **2001**, *627*, 186-193.

105. Kovacs, I. and Fritz, G., *Z. Anorg. Allg. Chem.*, **1994**, *620*, 4-7.

106. Krautscheid, H., Matern, E., Olkowska-Oetzel, J., Pikies, J. and Fritz, G., *Z. Anorg. Allg. Chem.*, **2001**, *627*, 999-1002.

107. Lloyd, N.C., Morgan, H.W., Nicholson, B.K. and Ronimus, R.S., *Angew. Chem. Int. Ed.*, **2005**, *44*, 941-944.

108. Breunig, H.J. in *The Chemistry of Organic Arsenic, Antimony and Bismuth Compounds (Chemistry of Functional Groups)*, 1994, S. Patai (Ed), John Wiley & Sons, Inc., Organoarsenic and organoantimony homocycles, pp. 563-577.

109. Allen, F.H., *Acta Crystallogr., Sect. B: Struct. Sci.*, **2002**, *B58*, 380-388.

110. Cowley, A.H., Lasch, J.G., Norman, N.C., Pakulski, M. and Whittlesey, B.R., *J. Chem. Soc., Chem. Commun.*, **1983**, 881-882.

111. Reeske, G. and Cowley, A.H., *Chem. Commun.*, **2006**, 1784-1786.

112. Arduengo, A.J., III and Stewart, C.A., *Chem. Rev.*, **1994**, *94*, 1215-1237.

113. Gustafsson, M., Bergqvist, K.-E. and Frejd, T., *J. Chem. Soc., Perkin Trans. 1*, **2001**, 1452-1457.

114. Gillespie, D.G. and Walker, B.J., *J. Chem. Soc., Perkin Trans. 1*, **1983**, 1689-1695.

115. Gillespie, D.G., Walker, B.J., Stevens, D. and McAuliffe, C.A., *J. Chem. Soc., Perkin Trans. 1*, **1983**, 1697-1703.

116. Hope, H., Olmstead, M.M., Power, P.P. and Xiaojie, X., *J. Am. Chem. Soc.*, **1984**, *106*, 819-821.

117. Bartlett, R.A., Rasika Dias, H.V., Hope, H., Murray, B.D., Olmstead, M.M. and Power, P.P., *J. Am. Chem. Soc.*, **1986**, *108*, 6921-6926.

118. Beswick, M.A., Hopkins, A.D., Mosquera, M.E.G., Raithby, P.R., Rothenberger, A., Wheatley, A.J., Wright, D.S., Choi, N., McPartlin, M. and Stalke, D., *Chem. Commun.*, **1998**, 2485-2486.

119. Bashall, A., Beswick, M.A., Choi, N., Hopkins, A.D., Kidd, S.J., Lawson, Y.G., Mosquera, M.E.G., McPartlin, M., Raithby, P.R., Wheatley, A.A.E.H., Wood, J.A. and Wright, D.S., *Dalton*, **2000**, 479-486.

120. Durkin, J., Hibbs, D.E., Hitchcock, P.B., Hursthouse, M.B., Jones, C., Jones, J., Malik, K.M.A., Nixon, J.F. and Parry, G., *J. Chem. Soc., Dalton Trans.*, **1996**, 3277-3282.

121. Jones, C., Black, S.J. and Steed, J.W., *Organometallics*, **1998**, *17*, 5924-5926.

122. Jones, C., Junk, P.C., Steed, J.W., Thomas, R.C. and Williams, T.C., *J. Chem. Soc., Dalton Trans.*, **2001**, 3219-3226.

123. Jones, C. and Williams, T.C., *J. Organomet. Chem.*, **2004**, *689*, 1648-1656.

124. Bruce, S., Hibbs, D.E., Jones, C., Steed, J.W., Thomas, R.C. and Williams, T.C., *New J. Chem.*, **2003**, *27*, 466-474.

125. Jones, C., Junk, P.C. and Williams, T.C., *J. Chem. Soc., Dalton Trans.*, **2002**, 2417-2418.

126. Karsch, H.H. and Schier, A., *J. Chem. Soc., Chem. Commun.*, **1994**, 2703-2704.

127. Dotzler, M., Schmidt, A., Ellermann, J., Knoch, F.A., Moll, M. and Bauer, W., *Polyhedron*, **1996**, *15*, 4425-4433.

128. Smith, R.C., Gantzel, P., Rheingold, A.L. and Protasiewicz, J.D., *Organometallics*, **2004**, *23*, 5124-5126.

129. Ates, M., Breunig, H.J., Ebert, K., Guelec, S., Kaller, R. and Draeger, M., *Organometallics*, **1992**, *11*, 145-150.

130. Breunig, H.J., Rosler, R. and Lork, E., *Angew. Chem. Int. Ed.*, **1998**, *37*, 3175-3177.

131. Clegg, W., Elsegood, M.R.J., Graham, V., Norman, N.C. and Pickett, N.L., *J. Chem. Soc., Dalton Trans.*, **1993**, 997-998.

132. Clegg, W., Elsegood, M.R.J., Graham, V., Norman, N.C., Pickett, N.L. and Tavakkoli, K., *J. Chem. Soc., Dalton Trans.*, **1994**, 1743-1751.

133. Clegg, W., Elsegood, M.R.J., Norman, N.C. and Pickett, N.L., *J. Chem. Soc., Dalton Trans.*, **1994**, 1753-1757.

134. Genge, A.R.J., Hill, N.J., Levason, W. and Reid, G., *J. Chem. Soc., Dalton Trans.*, **2001**, 1007-1012.

135. Willey, G.R., Daly, L.T. and Drew, M.G.B., *J. Chem. Soc., Dalton Trans.*, **1996**, 1063-1067.

136. Clegg, W., Errington, R.J., Fisher, G.A., Green, M.E., Hockless, D.C.R. and Norman, N.C., *Chem. Ber.*, **1991**, *124*, 2457-2459.

137. Clegg, W., Errington, R.J., Flynn, R.J., Green, M.E., Hockless, D.C.R., Norman, N.C., Gibson, V.C. and Tavakkoli, K., *J. Chem. Soc., Dalton Trans.*, **1992**, 1753-1754.

138. Breunig, H.J., Ghesner, M.E. and Lork, E., *J. Organomet. Chem.*, **2002**, *660*, 167-172.

139. Althaus, H., Breunig, H.J., Probst, J., Rosler, R. and Lork, E., *J. Organomet. Chem.*, **1999**, *585*, 285-289.

140. Breunig, H.J., Ghesner, M.E. and Lork, E., *Z. Anorg. Allg. Chem.*, **2005**, *631*, 851-856.

141. Becker, G., Muench, A. and Witthauer, C., *Z. Anorg. Allg. Chem.*, **1982**, *492*, 15-27.

142. Mundt, O., Becker, G., Roessler, M. and Witthauer, C., *Z. Anorg. Allg. Chem.*, **1983**, *506*, 42-58.

143. Linti, G., Kostler, W. and Pritzkow, H., *Eur. J. Inorg. Chem.*, **2002**, 2643-2647.

Chapter 2 – Low Oxidation State P^I Salts: Synthetic and Computational Investigations

2.1 Introduction

The synthesis and examination of compounds containing phosphorus in low coordinate bonding environments has been a focus of Main Group chemistry for more than two decades.[1,2] The observations and conclusions derived from such investigations, in conjunction with the realization of the close relationship between the behaviour of phosphorus and carbon, have provided for an incredible advancement in the understanding of structure, bonding and reactivity of phosphorus compounds in particular and those of the p-block elements more generally.[3] The preceding studies of phosphorus compounds have typically concentrated on compounds containing the element in either of the common oxidation states (+3 or +5).[4] Excluding metal phosphide minerals, the chemistry of compounds containing phosphorus in lower oxidation states has been largely limited to investigations of transient phosphinidenes, their transition metal or Lewis-base adducts, their cyclic polyphosphine oligomers, other catenated polyphosphines and elemental phosphorus.[1,2,5-8] The related chemistry of the heavier pnictogen (Pn) derivatives has been largely ignored.[9-11]

As a preliminary milestone of our investigation of low oxidation state p-block chemistry, we required readily accessible and functionalizable low oxidation state Group 15 reagents; because of their relative stability in comparison to other phosphorus(I) compounds, salts containing "triphosphenium" cations of the type first described by Schmidpeter presented an ideal starting point.[12-15] These cations are related to phospha-Wittig reagents and earlier work by Schmidpeter on dicyanophosphides, in which either

one or both phosphines are replaced by anionic groups.[16-18] Furthermore, triphosphenium cations **2.1** are the heavier analogues of the ubiquitous and inert bis(triphosphoranylidene)ammonium ("PNP") cations **2.2** that are used as non-coordinating cations in numerous salts. Such cations are also isovalent with carbodiphosphoranes **2.3**, which are interesting ligands for transition metal complexes[19] and are potential di-Wittig reagents for organic synthesis.[20]

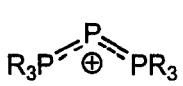

2.1

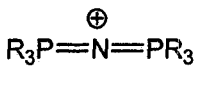

2.2

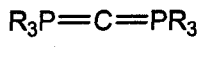

2.3

The unique reactivity of P^I and As^I compounds is exemplified by Driess' synthesis of the first square planar phosphonium and arsonium salts through the action of P^I and As^I sources on Schwartz's reagent.[9,21] In spite of such unprecedented and impressive results, apart from the investigation of phospha-Wittig chemistry,[16] the behaviour and utility of compounds such as **1** have not been explored or exploited to any significant extent. To successfully investigate many types of reactivity that may be exhibited by such salts, the presence of a robust and non-reactive counter anion is of critical importance. In this light, we required a suitable source for Pn^I ions in which we could readily change the counter anion. Herein we detail the facile synthesis of the iodide salts of two stable P^I sources, $[(1,2\text{-bis(diphenylphosphino)ethane})P]^+$ **2.4** and $[(1,3\text{-bis(diphenylphosphino)propane})P]^+$ **2.5**, and describe the metathesis reactivity of these reagents. In addition, the structural features, reactivities and remarkable stabilities of selected examples of such compounds are explained using density functional theory (DFT) calculations.

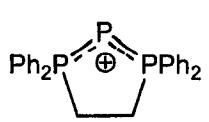

2.4

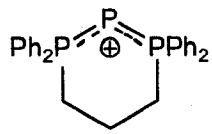

2.5

2.2 Experimental

Reagents and General Procedures. All manipulations were carried out using standard inert-atmosphere techniques. Phosphorus(III) iodide, 1,2-bis(diphenylphosphino)ethane (dppe), 1,3-bis(diphenylphosphino)propane (dppp), silver trifluoromethanesulfonate (silver triflate, [Ag][OTf]) and potassium hexafluorophosphate were purchased from Strem Chemicals Inc. and all other chemicals and reagents were obtained from Aldrich; all reagents were used without further purification. MeOH was dried over magnesium turnings, CD_2Cl_2 was dried over calcium hydride and all other solvents were dried on a series of Grubbs' type columns[22] and were degassed prior to use. Silver salts are sensitive to light and precautions were taken to minimize light exposure in reactions involving such salts. The ligand $Me_2N(CH_2)_2PPh_2$ was prepared by a literature procedure.[23] The compound $dppeI_4$ **2.6** was synthesized by the slight modification of a literature procedure.[24] The relatively low yields of the iodide salts **2.4**[I] and **2.5**[I] are a consequence of the extensive washing with thf used to remove the I_2; such treatment dissolves some of the iodide salt and also promotes the formation of an insoluble orange by-product, which must be removed by filtration.

Instrumentation. NMR spectra were recorded at room temperature in CD_2Cl_2 solutions on a Bruker Avance 300 MHz spectrometer. Chemical shifts are reported in ppm, relative to external standards ($SiMe_4$ for ^1H and ^{13}C, 85% aq. H_3PO_4 for ^{31}P,

$BF_3{\cdot}OEt_2$ for ^{11}B, $CFCl_3$ for ^{19}F, $Ga(NO_3)_3$ for ^{71}Ga). Coupling constant magnitudes, $|J|$, are given in Hz. Melting points (mp) or decomposition points (dp) were obtained on samples sealed in glass capillaries under dry nitrogen using an Electrothermal® Melting Point Apparatus. Elemental analysis was performed in-house using a PerkinElmer 2400 C, H, N analyzer in the Centre for Catalysis and Materials Research, Department of Chemistry and Biochemistry, University of Windsor.

Theoretical Methods. Calculations were preformed with the Gaussian 98 suite of programs.[25] Geometry optimizations have been calculated using density functional theory (DFT), specifically implementing the B3PW91 method [containing Becke's three-parameter hybrid functional for exchange (B3, including ca. 20% Hartree-Fock exchange)[26] combined with the generalized gradient approximation for correlation of Perdew and Wang (PW91)[27]] in conjunction with the 6-31+G(d) basis set. The geometries were restricted to the highest reasonable symmetry and each stationary point was confirmed to be a minimum by having zero imaginary vibrational frequencies. The electronic energies of the molecules have been corrected by the unscaled, zero-point vibrational energy (ZPVE). Single point energies have been calculated at the B3PW91/6-311+G(3df,2p)//B3PW91/6-31G(d) level of theory. Population analyses were conducted using the Natural Bond Orbital (NBO)[28] method implemented in Gaussian98.

X-ray Crystallography. Crystals were coated in Nujol, mounted on a glass fibre and placed in the 173 K N_2 boil-off stream of the Kryoflex low-temperature apparatus. Reflection data were integrated from frame data obtained using hemisphere scans with the SMART[29] software on a Bruker APEX CCD diffractometer using a graphite monochromator with MoKα radiation (λ = 0.71073Å). Diffraction data and unit-cell

parameters were consistent with assigned space groups. Lorentz and polarization corrections and empirical absorption corrections, based on redundant data at varying effective azimuthal angles, were applied to the data sets using SAINTPlus[30] and SADABS[31] software. The structures were solved by direct methods using SHELXS[32] or Sir97[33] (as implemented in the WinGX software package[34]), completed by subsequent Fourier syntheses and refined with full-matrix least-squares methods against F^2 data using SHELXL.[35] All non-hydrogen atoms were refined anisotropically and all hydrogen atoms were placed in appropriate geometrically-calculated positions. Thermal ellipsoid plots of the molecular structures were generated using SHELXTL.[36] The experimental details for each of the diffraction experiments are listed in Table 2-1 and Table 2-2.

Preparation of [(dppe)P][I], 2.4[I] from PI_3

A colourless solution of dppe (5.071 g; 12.728 mmol) in CH_2Cl_2 (75 mL) was added to a red solution of PI_3 (5.240 g; 12.728 mmol) in CH_2Cl_2 (100 mL), which resulted in the formation of a burgundy solution and an orange precipitate. The mixture was left to stir for 1 hour. Volatile components were removed under reduced pressure and the crude residue was washed with thf (3 × 30 mL). The solid was redissolved in CH_2Cl_2 (75 mL) and filtered through Celite to remove the orange precipitate. Volatile Components were again removed under reduced pressure. Following dissolution in MeCN and slow evaporation of the solvent, colourless crystalline material was obtained. Yield: 52% (3.680 g; 6.615 mmol). $^{31}P\{^1H\}$ NMR: -231.4 (t, $^1J_{PP}$ = 453, 1P), 64.4 (d, $^1J_{PP}$ = 453, 1P) (Lit.[37] -232.7 (t, $^1J_{PP}$ = 453), 62.9 (d, $^1J_{PP}$ = 453)). $^{13}C\{^1H\}$ NMR: 30.3

(d, $^1J_{CP}$ = 42), 126.2 (d of d, $^1J_{CP}$ = 75, $^2J_{CP}$ = 8), 130.2 (s), 133.0 (s), 134.0 (s). ^{1}H NMR: 3.54 (d, $^2J_{HP}$ = 16, 4H), 7.58 (m, 12H), 7.87 (m, 8H). dp: 149-150 °C. Anal. Calcd. For $C_{26}H_{24}IP_3$ (556.295): C 56.14, H 4.35. Found: C 54.92, H 4.32%.

Preparation of [(dppe)P][I], 2.4[I] from P_2I_4

[(dppe)P][I] can also be prepared from P_2I_4 (0.796 g; 1.398 mmol) and dppe (1.114 g; 2.795 mmol) in a 1:2 ratio in a similar manner to the preparation from PI_3. Yield: 39 % (0.603 g; 1.084 mmol). Identical spectroscopic data are observed as when **4**[I] is prepared from PI_3.

Preparation of [(dppp)P][I], 2.5[I] from PI_3

A colourless solution of dppp (3.247 g; 7.872 mmol) in CH_2Cl_2 (75 mL) was added to a red solution of PI_3 (3.241 g; 7.872 mmol) in CH_2Cl_2 (100 mL), which produced a reddish-orange solution and an orange precipitate. The mixture was left to stir for 1 hour. The volatile components were removed under reduced pressure and the crude residue was washed with thf (3 × 30 mL). The solid was redissolved in CH_2Cl_2 (75 mL) and filtered through Celite to remove the orange precipitate. Volatile components were again removed under reduced pressure. Following dissolution in MeCN and slow evaporation of the solvent, colourless crystalline material was obtained. Yield: 56% (2.531 g; 4.438 mmol). ^{31}P{^{1}H} NMR: -209.5 (t, $^1J_{PP}$ = 423, 1P), 22.4 (d, $^1J_{PP}$ = 423, 2P) (Lit.[37] -208.9 (t, $^1J_{PP}$ = 423), 23.5 (d, $^1J_{PP}$ = 453)). ^{13}C{^{1}H} NMR: 19.5 (s), 25.0 (d, $^1J_{CP}$ = 47), 125.7 (d of d, $^1J_{CP}$ = 77, $^2J_{CP}$ = 12), 130.2 (s), 132.4 (s), 134.0 (s). ^{1}H NMR: 2.56

(m, 2H), 3.05 (m, 4H), 7.44 (m, 8H), 7.65 (m, 12H). dp: 96-97 °C. Anal. Calcd. For $C_{27}H_{26}IP_3$ (570.321): C 56.86, H 4.60. Found: C 56.32, H 4.99%.

Preparation of [(dppp)P][I], 2.5 [I] from P_2I_4

[(dppp)P][I] can also be prepared from P_2I_4 (0.454 g; 0.797 mmol) and dppp (0.658 g; 1.594 mmol) in a 1:2 ratio in a similar manner to the preparation from PI_3. Yield: 17 % (0.156 g; 0.274 mmol). Identical spectroscopic data are observed as when **5**[I] is prepared from PI_3.

Preparation of [(dppe)P][BPh_4], 2.4[BPh_4]

To a colourless solution of **2.4**[I] (0.625 g; 1.124 mmol) in MeOH (10 mL) was added a colourless solution of [Na][BPh_4] (0.384 g; 1.124 mmol) in MeOH (10 mL), and a white precipitate formed instantly. The precipitate was collected by filtration and washed with MeOH (5 mL). The crude product was dissolved in MeCN and upon slow evaporation of the solvent colourless crystalline material was deposited. Yield: 98% (0.824 g; 1.100 mmol). $^{31}P\{^1H\}$ NMR: -235.5 (t, $^1J_{PP}$ = 456, 1P), 64.4 (d, $^1J_{PP}$ = 456, 2P). $^{11}B\{^1H\}$ NMR: -6.9 (s). $^{13}C\{^1H\}$ NMR: 29.0 (d, $^1J_{CP}$ = 46), 122.4 (s), 125.9 (d of d, $^1J_{CP}$ = 75, $^2J_{CP}$ = 9), 126.2 (s), 130.2 (s), 132.8 (s), 134.2 (s), 136.4 (s), 164.4 (q, $^1J_{CB}$ = 49). ^1H NMR: 2.48 (d, $^2J_{HP}$ = 16, 4H), 6.80 (m, 4H), 6.93 (m, 8H), 7.33 (m, 8H), 7.60 (m, 20H). mp: 174-175 °C. Anal. Calcd. For $C_{50}H_{44}BP_3$ (748.617): C 80.22, H 5.92. Found: C 77.83, H 6.68%.

Preparation of [(dppp)P][BPh_4], 2.5[BPh_4]

To a colourless solution of **2.5**[I] (0.225 g; 0.395 mmol) in MeOH (10 mL) was added a colourless solution of [Na][BPh_4] (0.135 g; 0.395 mmol) in MeOH (10 mL), and a white precipitate formed instantly. The precipitate was collected by filtration and washed with MeOH (5 mL). The crude product was dissolved in MeCN and upon slow evaporation of the solvent colourless crystalline material formed. Yield: 71% (0.214 g; 0.281 mmol). $^{31}P\{^1H\}$ NMR: -210.2 (t, $^1J_{PP}$ = 424, 1P), 22.7 (d, $^1J_{PP}$ = 424, 2P). $^{11}B\{^1H\}$ NMR: -6.9 (s). $^{13}C\{^1H\}$ NMR: 19.1 (s), 25.2 (d, $^1J_{CP}$ = 47), 122.4 (s), 125.6 (d of d, $^1J_{CP}$ = 75, $^2J_{CP}$ = 9), 126.2 (s), 130.2 (s), 132.3 (s), 134.0 (s), 136.5 (s), 164.6 (q, $^1J_{CB}$ = 49). ^1H NMR: 2.06 (m, 2H), 2.44 (m, 4H), 6.89 (m, 4H), 7.02 (m, 8H), 7.36 (m, 8H), 7.52 (m, 20H). mp: 168-169 °C. Anal. Calcd. For $C_{51}H_{46}BP_3$ (762.643): C 80.32, H 6.08. Found: C 79.66, H 6.39%.

Preparation of [(dppp)P][$GaCl_4$], 2.5[$GaCl_4$]

To a colourless solution of **2.5**[I] (0.369 g; 0.647 mmol) in MeOH (10 mL) was added a colourless solution of [Li][$GaCl_4$] (0.141 g; 0.647 mmol) in MeOH (10 mL), and the mixture became slightly cloudy white. The mixture was stirred for 30 minutes. The volatile components were removed under reduced pressure and the product was extracted from the crude reaction mixture using CH_2Cl_2 (15 mL) followed by filtration through Celite. Slow evaporation of the solvent yielded colourless crystalline material. Yield: 31% (0.130 g; 0.198 mmol). $^{31}P\{^1H\}$ NMR: -209.9 (t, $^1J_{PP}$ = 425, 1P), 22.6 (d, $^1J_{PP}$ = 425, 2P). ^{71}Ga NMR: 249 (s). $^{13}C\{^1H\}$ NMR: 19.6 (s), 25.9 (d, $^1J_{CP}$ = 47), 125.6 (d of d, $^1J_{CP}$ = 76, $^2J_{CP}$ = 11), 130.3 (s), 132.5 (s), 134.1 (s). ^1H NMR: 2.60 (m, 2H), 2.98 (m,

4H), 7.50 (m, 8H), 7.64 (m, 12H). mp: 195-196 °C. Anal. Calcd. For $C_{27}H_{26}Cl_4GaP_3$ (654.950): C 49.51, H 4.00. Found: C 49.56, H 4.22%.

Preparation of [(dppp)P][PF_6], 2.5[PF_6]

To a colourless solution of **2.5**[I] (0.509 g; 0.892 mmol) in MeOH (10 mL) was added a colourless solution of [K][PF_6] (0.164 g; 0.892 mmol) in MeOH (10 mL), and the mixture became slightly cloudy white. The mixture was stirred for 30 minutes. The volatile components were removed under reduced pressure and the product was extracted from the crude reaction mixture using CH_2Cl_2 (15 mL) followed by filtration through Celite. Slow evaporation of the solvent produced colourless crystalline material. Yield: 53 % (0.277 g; 0.471 mmol). $^{31}P\{^1H\}$ NMR: -210.2 (t, $^1J_{PP}$ = 424, 1P), -143.8 (septet, $^1J_{PF}$ = 711, 1P), 22.6 (d, $^1J_{PP}$ = 424, 2P). $^{19}F\{^1H\}$ NMR: -73.4 (d, $^1J_{FP}$ = 711). $^{13}C\{^1H\}$ NMR: 19.4 (s), 25.6 (d, $^1J_{CP}$ = 48), 125.8 (d of d, $^1J_{CP}$ = 76, $^2J_{CP}$ = 11), 130.2 (s), 132.5 (s), 134.0 (s). ^1H NMR: 2.60 (m, 2H), 2.99 (m, 4H), 7.49 (m, 8H), 7.67 (m, 12H). mp: 185-186 °C. Anal. Calcd. For $C_{27}H_{26}F_6P_4$ (588.381): C 55.12, H 4.45. Found: C 54.96, H 4.71%.

Preparation of [(dppp)P][OTf], 2.5[OTf]

To a colourless solution of **2.5**[I] (0.176 g; 0.309 mmol) in MeOH (10 mL) was added a colourless solution of [Ag][OTf] (0.079 g; 0.309 mmol) in MeOH (10 mL), and a yellow precipitate formed instantly. The volatile components were removed under reduced pressure and the product was extracted from the crude reaction mixture using CH_2Cl_2 (15 mL) followed by filtration through Celite. Slow evaporation of the solvent

afforded colourless crystalline material. Yield: 69% (0.126 g; 0.213 mmol). $^{31}P\{^{1}H\}$ NMR: -210.0 (t, $^{1}J_{PP}$ = 424, 1P), 22.7 (d, $^{1}J_{PP}$ = 424, 2P). $^{19}F\{^{1}H\}$ NMR: -79.1 (s). $^{13}C\{^{1}H\}$ NMR: 19.4 (s), 25.5 (d, $^{1}J_{CP}$ = 48), 121.7 (q, $^{1}J_{CF}$ = 321), 126.0 (d of d, $^{1}J_{CP}$ = 76, $^{2}J_{CP}$ = 11), 130.2 (s), 132.6 (s), 133.9 (s). ^{1}H NMR: 2.57 (m, 2H), 3.04 (m, 4H), 7.47 (m, 8H), 7.65 (m, 12H). dp: 177-178 °C. Anal. Calcd. For $C_{28}H_{26}F_3O_3P_3S{\cdot}CH_2Cl_2$ (677.419): C 51.42, H 4.17. Found: C 52.23, H 4.54%.

Preparation of [(dppp)P][BF_4], 2.5[BF_4]

To a colourless solution of **2.5**[I] (0.183 g; 0.321 mmol) in MeOH (10 mL) was added a colourless solution of [Na][BF_4] (0.035 g; 0.321 mmol) in MeOH (10 mL), with no noticeable colour change. The mixture was stirred for 30 minutes. The volatile components were removed under reduced pressure and the product was extracted from the crude reaction mixture using CH_2Cl_2 (15 mL) followed by filtration through Celite. Slow evaporation of the solvent afforded colourless crystalline material. Yield: 66% (0.113 g; 0.213 mmol). $^{31}P\{^{1}H\}$ NMR: -209.7 (t, $^{1}J_{PP}$ = 423, 1P), 22.7 (d, $^{1}J_{PP}$ = 423), 2P). $^{11}B\{^{1}H\}$ NMR: -1.3 (s). $^{19}F\{^{1}H\}$ NMR: -152.9 (s). $^{13}C\{^{1}H\}$ NMR: 19.6 (s), 25.4 (d, $^{1}J_{CP}$ = 48), 125.9 (d of d, $^{1}J_{CP}$ = 77, $^{2}J_{CP}$ = 10), 130.1 (s), 132.6 (s), 133.8 (s). ^{1}H NMR: 2.59 (m, 2H), 3.14 (m, 4H), 7.47 (m, 8H), 7.65 (m, 12H). The results of several single crystal diffraction experiments suggest that the crystals contain a mixture of [BF_4] and [I] anions thus microanalysis experiments were not undertaken.

Preparation of $[(Me_2N(CH_2)_2PPh_2)_2P]_2[SnCl_6]$, 2.7

A colourless solution of $Me_2N(CH_2)_2PPh_2$ (0.300 g; 1.166 mmol) in CH_2Cl_2 (10 mL) was added to a $SnCl_2$ (0.221 g; 1.166 mmol) slurry in CH_2Cl_2 (10 mL). Following stirring for ten minutes, white precipitate had formed. A colourless solution of PCl_3 (0.160 g; 1.166 mmol) in CH_2Cl_2 (10 mL) was slowly added and the mixture became a bright yellow solution. The volatile components were removed under reduced pressure to produce a bright yellow solid. Yield: 0.213 g (mixture of **2.7** and $(Me_2N(CH_2)_2PPh_2)SnCl_4$ **2.8**). $^{31}P\{^1H\}$ NMR: -197.5 (t, $^1J_{PP}$ = 493, **2.7**), -22.4 (s, **2.8**), 27.1 (d, $^1J_{PP}$ = 493, **2.7**). HR-ESI-MS Calcd. For $C_{64}H_{80}Cl_6N_4P_6Sn$ $[½M - SnCl_6]^+$: *m/z* = 545.2404. Found 545.2443 (7.2 ppm).

Table 2-1 - Summary of X-ray Crystallographic Data for compounds 2.4[I], 2.5[I], 2.4[BPh_4] and 2.5[BPh_4].

Compound	**2.4[I]**	**2.5[I]**	**2.4[BPh_4]**	**2.5[BPh_4]**
Empirical formula	$C_{26}H_{24}IP_3$	$C_{27}H_{26}IP_3$	$C_{50}H_{44}BP_3$	$C_{51}H_{46}BP_3$
Formula weight	556.26	570.29	748.22	762.60
Crystal system	Triclinic	Monoclinic	Monoclinic	Monoclinic
Space group	*P-1*	$P2_1/c$	$P2_1/n$	$P2_1/c$
Unit cell dimensions:				
a (Å)	10.1179(13)	10.9315(10)	12.0031(8)	12.244(3)
b (Å)	13.5649(17)	19.2143(18)	17.5742(12)	17.883(3)
c (Å)	19.688(3)	12.9085(12)	19.6302(13)	21.258(4)
α (°)	71.970(1)	90	90	90
β (°)	81.280(1)	110.931(2)	100.893(1)	114.957(10)
γ (°)	68.866(1)	90	90	90
Volume ($Å^3$)	2394.2(5)	2532.4(4)	4066.3(5)	4220.0(15)
Z	4	4	4	4
Density (calc'd) ($g\ cm^{-3}$)	1.543	1.496	1.223	1.200
Abs. coef. (mm^{-1})	1.549	1.467	0.181	0.176
F(000)	1112	1144	1576	1608
θ range for data collection (°)	1.09 to 27.50	1.99 to 27.49	1.57 to 27.50	1.55 to 27.50
Limiting indices	$-13 \le h \le 13$ $-17 \le k \le 17$ $-25 \le l \le 25$	$-13 \le h \le 14$ $-24 \le k \le 24$ $-16 \le l \le 16$	$-15 \le h \le 15$ $-22 \le k \le 22$ $-25 \le l \le 25$	$-15 \le h \le 14$ $-20 \le k \le 23$ $-27 \le l \le 27$
Reflections collected	26843	24349	39288	29565
Independent reflections	10586	5809	9355	9692
R_{int}	0.0330	0.0229	0.0350	0.1148
Data / restraints / parameters	10586 / 0 / 585	5809 / 0 / 280	9355 / 0 / 529	9692 / 0 / 496
Goodness-of-fit on F^2	1.299	1.033	1.011	0.962
Final *R* indices[a] [I>2s(I)]	*R*1 = 0.0596 *wR*2 = 0.1177	*R*1 = 0.0206 *wR*2 = 0.0507	*R*1 = 0.0435 *wR*2 = 0.1121	*R*1 = 0.0626 *wR*2 = 0.1008
R indices (all data)	*R*1 = 0.0694 *wR*2 = 0.1240	*R*1 = 0.0241 *wR*2 = 0.0522	*R*1 = 0.0578 *wR*2 = 0.1238	*R*1 = 0.2144 *wR*2 = 0.1460
Largest difference map peak and hole ($e\ Å^{-3}$)	1.348 and -0.914	0.653 and -0.253	0.402 and -0.260	0.263 and -0.202

Table 2-2 - Summary of X-ray Crystallographic Data for compounds 2.5[$GaCl_4$], 2.5[PF_6], 2.5[OTf] and 2.6.

Compound	2.5[$GaCl_4$]	2.5[PF_6]	2.5[OTf]	2.6
Empirical formula	$C_{27}H_{26}Cl_4GaP_3$	$C_{27}H_{26}F_6P_4$	$C_{29}H_{28}Cl_2F_3O_3P_3S$	$C_{26}H_{24}I_4P_2$
Formula weight	654.91	588.36	677.38	905.99
Crystal system	Monoclinic	Monoclinic	Monoclinic	Orthorhombic
Space group	$P2_1/c$	$P2_1/c$	$P2_1/m$	*Aba2*
Unit cell dimensions:				
a (Å)	9.7274(16)	12.690(8)	9.303(3)	15.2158(8)
b (Å)	14.815(3)	15.736(9)	15.661(5)	15.2876(8)
c (Å)	21.255(3)	17.815(8)	11.127(3)	12.3342(6)
α (°)	90	90	90	90
β (°)	106.894(6)	131.57(3)	109.605(3)	90
γ (°)	90	90	90	90
Volume (Å^3)	2930.9(9)	2662(3)	1527.2(8)	2869.1(3)
Z	4	4	2	4
Density (calc'd) (g cm^{-3})	1.484	1.468	1.473	2.097
Abs. coef. (mm^{-1})	1.483	0.342	0.487	4.469
F(000)	1328	1208	696	1688
θ range for data collection (°)	1.70 to 27.50	2.00 to 27.50	2.32 to 27.50	2.51 to 27.49
Limiting indices	$-12 \le h \le 12$ $-19 \le k \le 19$ $-26 \le l \le 26$	$-16 \le h \le 16$ $-20 \le k \le 19$ $-22 \le l \le 21$	$-11 \le h \le 12$ $-20 \le k \le 20$ $-14 \le l \le 14$	$-19 \le h \le 19$ $-19 \le k \le 19$ $-15 \le l \le 15$
Reflections collected	40601	21301	15971	13423
Independent reflections	6663	5693	3549	3294
R_{int}	0.0442	0.0654	0.1442	0.0245
Data / restraints / parameters	6663 / 0 / 316	5693 / 0 / 334	3549 / 0 / 230	3294 / 1 / 163
Goodness-of-fit on F^2	1.148	1.199	1.089	1.055
Final *R* indices[a] [I>2s(I)]	$R1 = 0.0505$ $wR2 = 0.1010$	$R1 = 0.0938$ $wR2 = 0.2195$	$R1 = 0.1213$ $wR2 = 0.2778$	$R1 = 0.0195$ $wR2 = 0.0469$
R indices (all data)	$R1 = 0.0691$ $wR2 = 0.1115$	$R1 = 0.1231$ $wR2 = 0.2299$	$R1 = 0.1901$ $wR2 = 0.3162$	$R1 = 0.0202$ $wR2 = 0.0473$
Largest difference map peak and hole (e Å^{-3})	0.588 and -0.294	0.629 and -0.563	1.509 and -0.593	0.857 and -0.360

Table 2-3 - Summary of X-ray Crystallographic Data for compounds 2.5[$(BF_4)_{0.26}I_{0.74}$], 2.8 · CH_2Cl_2 and 2.8

Compound	**2.5[$(BF_4)_{0.26}I_{0.74}$]**	**2.8 · CH_2Cl_2**	**2.8**
Empirical formula	$C_{27}H_{26}B_{0.26}F_{1.03}I_{0.74}P_3$	$C_{17}H_{22}Cl_6NPSn$	$C_{48}H_{60}Cl_{12}N_3P_3Sn_3$
Formula weight	559.71	602.74	1553.37
Crystal system	Monoclinic	Monoclinic	Orthorhombic
Space group	$P2_1/c$	$P2_1/n$	$P2_12_12_1$
Unit cell dimensions:			
a (Å)	12.741(5)	11.1908(12)	15.0140(19)
b (Å)	15.580(5)	14.9321(17)	15.919(2)
c (Å)	17.640(5)	14.2858(16)	24.679(3)
α (°)	90	90	90
β (°)	133.479(17)	104.9920(10)	90
γ (°)	90	90	90
Volume (Å^3)	2540.9(15)	2305.9(4)	5898.4(13)
Z	4	4	4
Density (calc'd) (g cm^{-3})	1.464	1.736	1.749
Abs. coef. (mm^{-1})	1.166	1.876	1.922
F(000)	1132	1192	3072
θ range for data collection (°)	2.06 to 27.50	2.01 to 27.50	1.52 to 27.50
Limiting indices	$-16 \le h \le 16$ $-20 \le k \le 20$ $-22 \le l \le 22$	$-14 \le h \le 14$ $-19 \le k \le 19$ $-18 \le l \le 18$	$-19 \le h \le 19$ $-20 \le k \le 20$ $-32 \le l \le 31$
Reflections collected	27908	25493	66521
Independent reflections	5780	5245	13428
R_{int}	0.0864	0.0289	0.0494
Data / restraints / parameters	5780 / 21 / 319	5245 / 0 / 237	13428 / 8 / 639
Goodness-of-fit on F^2	1.265	1.168	1.035
Final R indices[a] [I>2s(I)]	$R1 = 0.1094$ $wR2 = 0.1893$	$R1 = 0.0269$ $wR2 = 0.0671$	$R1 = 0.0335$ $wR2 = 0.0625$
R indices (all data)	$R1 = 0.1317$ $wR2 = 0.1983$	$R1 = 0.0345$ $wR2 = 0.0773$	$R1 = 0.0432$ $wR2 = 0.0676$
Largest difference map peak and hole (e Å^{-3})	1.125 and -0.895	1.242 and -0.418	1.144 and -0.464

Table 2-4 - Selected Metrical Parameters for Compounds 2.4[I], 2.5[I], 2.4[BPh_4], 2.5[BPh_4].

Parameter	2.4[I]	2.5[I]	2.4[BPh_4]	2.5[BPh_4]
	Distances (Å)			
P1-P2	2.1263(17) [2.1223(18)]	2.1318(6)	2.1166(6)	2.1224(13)
P2-P3	2.1315(18) [2.1240(18)]	2.1203(6)	2.1293(6)	2.1326(14)
P1-C5 (or -C6)	1.821(5) [1.820(5)]	1.8068(16)	1.8164(17)	1.807(3)
P3-C4	1.826(5) [1.837(5)]	1.8112(16)	1.8430(16)	1.804(3)
C4-C5	1.520(7) [1.500(7)]	1.533(2)	1.521(2)	1.523(4)
C5-C6		1.531(2)		1.523(4)
	Angles (°)			
P1-P2-P3	88.37(7) [89.46(7)]	97.77(2)	86.52(2)	93.98(5)

Table 2-5 - Selected Metrical Parameters for Compounds 2.5[$GaCl_4$], 2.5[PF_6], 2.5[OTf] and 2.5[$(BF_4)_{0.26}I_{0.74}$]

Paramater	2.5[$GaCl_4$]	2.5[PF_6]	2.5[OTf]	2.5[$(BF_4)_{0.26}I_{0.74}$]
		Distances (Å)		
P1-P2	2.1276(12)	2.122(2)	2.119(3)	2.109(3)
P2-P3	2.1211(12)	2.113(2)	2.119(3)	2.125(3)
P1-C5 (or –C6)	1.815(3)	1.811(6)	1.813(8)	1.803(7)
P3-C4	1.816(3)	1.815(6)	1.813(8)	1.813(7)
C4-C5	1.532(5)	1.521(9)	1.531(9)	1.537(10)
C5-C6	1.530(4)	1.526(9)	1.531(9)	1.527(10)
		Angles (°)		
P1-P2-P3	93.76(5)	97.19(9)	95.11(15)	97.60(10)

Table 2-6 - Selected Metrical Parameters for Compounds 2.8 · CH_2Cl_2 and 2.8.

Parameter	2.8 · CH_2Cl_2	2.8
	Distances (Å)	
Sn(1)-P(1)	2.6000(7)	2.6191(11), 2.5968(12), 2.6155(11)
Sn(1)-N(1)	2.392(2)	2.390(3), 2.388(4), 2.393(4)
P(1)-C(1)	1.811(3)	1.816(4), 1.827(18), 1.838(11), 1.813(4)
N(1)-C(2)	1.494(3)	1.488(5), 1.537(10), 1.493(5)
C(1)-C(2)	1.526(4)	1.521(6), 1.512(13), 1.521(9), 1.528(6)
	Angles (°)	
N(1)-Sn(1)-P(1)	79.81(6)	79.49(9), 79.63(9), 79.73(9)

2.3 Results and Discussion

Synthesis of [(dppe)P][I] and [(dppp)P][I]

In the 1980's, Schmidpeter and co-workers reported the synthesis of a variety of triphosphenium salts **2.1** through the reduction of PCl_3 in the presence of trihydrocarbylphosphines or trisamidophosphines. The reducing agents used in these reactions were either $SnCl_2$ or an excess amount of the phosphine ligands (vide infra) and the resultant salts, containing anions such as $[SnCl_6]^{-2}$, $[AlCl_4]^-$, $[BPh_4]^-$, were separated by fractional crystallization from the by-products.[12,38,39] Some of the by-products, such as $[(Me_2N)_3PCl][BPh_4]$, have very similar solubility characteristics to the desired salts; thus, the isolation of high-purity triphosphenium salts is difficult and the yields are relatively small using this approach.

While the triphosphenium cations appear to be a reasonable source of phosphorus(I) centres, some of the anions obtained using Schmidpeter's original methods are not suitable for many of the reactivity studies that we wish to pursue. For example, salts containing tetrachloroaluminate anions may be susceptible to degradation by nucleophiles, the salts containing such metallate anions may also be air- or moisture-sensitive, and the insolubility of certain triphosphenium salts could hinder our investigations. For this reason, we sought a convenient and relatively high-yield synthesis of Pn^I halides with the hope that such compounds would be useful reagents for the metathetical preparation of salts with any desired counter anion.

The room temperature reaction of PI_3 with dppe in dichloromethane (Equation 2.1) produces a burgundy solution. *It is important to note that the use of the non-nucleophilic solvent is necessary to avoid the excessive formation of by-products.* After 2

hours of stirring, the volatile components were removed under reduced pressure and the solid was washed rapidly with thf to remove the resultant I_2.[40] It must be noted that while the formation of the cation is quantitative according to ^{31}P NMR spectra of the reaction mixture (Figure 2.1), the concentration of the reaction mixture and, particularly, the washing of the crude solid with thf to remove the iodine results in the formation of an orange by-product and reduces the isolated yield. Redissolution of the crude solid in dichloromethane and filtration to remove any of the insoluble orange by-product affords pale yellow solutions that deposit colourless solid upon concentration. Multinuclear NMR spectra of the solid exhibit signals that are attributable to the cation $[(dppe)P]^+$ **2.4**. Negative-ion electrospray mass spectrometry experiments and micro-analytical data for the product are consistent with the proposed composition as an iodide salt and not a triiodide salt. It should be noted that **2.4**[I] is stable in air and can be washed with water in the open atmosphere.

$$PI_3 \xrightarrow[-I_2]{\text{+ dppe or dppp}} \underset{\textbf{2.4}[I]}{[(dppe)P][I]} \text{ or } \underset{\textbf{2.5}[I]}{[(dppp)P][I]} \qquad (2.1)$$

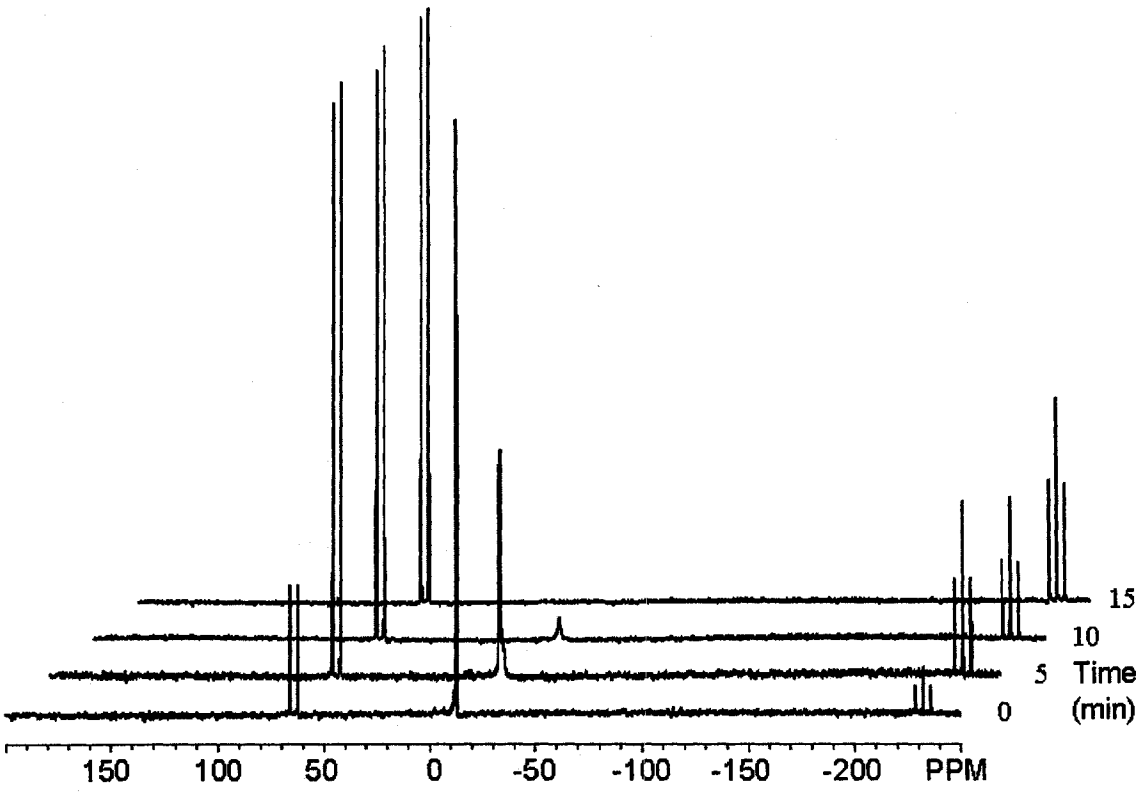

Figure 2.1 - ^{31}P NMR spectra of the reaction of PI_3 with dppe in CH_2Cl_2. Relevant chemical shifts in ppm: PI_3 173, dppe -12, $dppeI_4$ 51, [(dppe)P][I] 64(d) and -231(t).

The proposed composition of the salt is also supported by the results of an X-ray crystallographic investigation. Whereas the precipitated iodide salt of **2.4** are generally microcrystalline materials that are unsuitable for single crystal diffraction studies, larger crystals of **2.4**[I] may be obtained by recrystallization from MeCN. The salt crystallizes in the space group *P-1* with two independent ion pairs in the asymmetric unit, as illustrated in Figure 2.2. One notable feature of the structure is the lack of any close interactions between the cations and the anions; the shortest P-I distance is 4.702(3) Å and the closest contacts to the iodide anions are, in fact, from various H atoms on the dppe ligands; these contacts are all in excess of 3.055(2) Å. The metrical parameters of the cation, listed in Table 2-4, are similar to those that have been observed in Schmidpeter's original hexachlorostannate salt of the $[(dppe)P]^+$ cation, $\mathbf{2.4}_2[SnCl_6]$.[12,41]

For the cation containing P(11), the P-P distances of 2.1305(17) and 2.1260(17) Å (the corresponding values for the cation containing P(21) are 2.1328(17) and 2.1286(16) Å) compare well with the average distance of 2.133 Å found between dicoordinate and tetracoordinate phosphorus atoms in organo-phosphorus compounds reported in the Cambridge Structural Database (CSD).[42] It is noteworthy that these distances are significantly shorter than typical P-P single bond lengths such as those found in Me_2P-PMe_2 (2.212(1) Å)[43] or Ph_2P-PPh_2 (2.217(1) Å)[44] and they are likewise considerably shorter than the average distance of 2.215 Å between tricoordinate and tetracoordinate phosphorus atoms for organo-phosphorus compounds in the CSD.[42] The unusual shortness of the P-P bonds in cations such as **2.4**, even when differences in the covalent radii and coordination number are taken into account, is generally attributed to the presence of partial multiple bonding; the nature of the bonding in such cations is discussed in more detail in the *Theoretical Results* section below. The angle at the dicoordinate P atom 89.35(6)° [88.45(6)°] is notably small because of the geometric constraints of the dppe chelate.

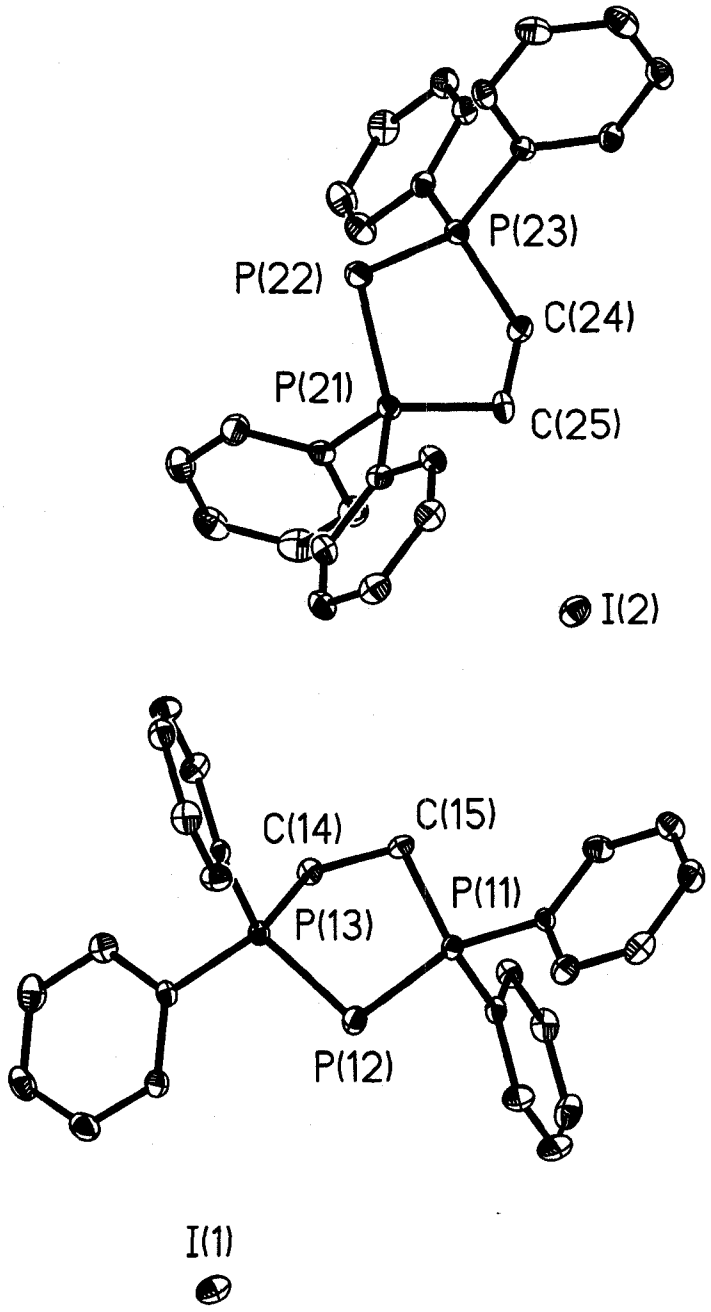

Figure 2.2 - Thermal ellipsoid plot (30% probability surface) of 2.4[I]. Hydrogen atoms are omitted for clarity.

In a similar manner, the room temperature reaction of PI_3 with dppp in dichloromethane also produces a reddish-orange solution with orange precipitate. Following stirring for 2 hours and removal of the solvent, the crude product can be rinsed with thf to remove I_2. Extraction in dichloromethane affords colourless solutions that yield colourless solid upon concentration. Signals in the multinuclear NMR spectra of the solid are attributable to the cation $[(dppp)P]^+$ **2.5**. The microcrystalline solid is air- and moisture-stable and can be recrystallized from MeCN to obtain material suitable for single crystal X-ray diffraction. The salt crystallizes in the space group $P2_1/c$, the molecular structure is shown in Figure 2.3 and relevant metrical parameters are listed in Table 2-4. As observed in **2.4**[I] the P-P bond distances in **2.5**[I] are shorter than typical single bonds and are similar to those observed in the only two other salts containing cations of this type, namely $\mathbf{2.5}_2[SnCl_6]$ and **2.5**$[AlCl_4]$.[37,45] The P-P-P angle of 97.77(2) is wider than the corresponding angle in **2.4**[I] as one would expect for the 6-membered ring produced by the larger and more flexible dppp chelate.

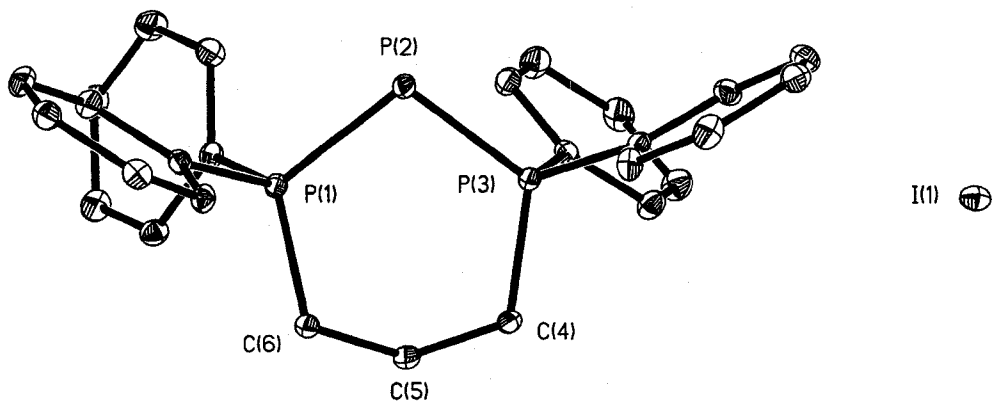

Figure 2.3 - Thermal ellipsoid plot (30% probability surface) of a 2.5[I]. Hydrogen atoms are omitted for clarity.

While the production of P^I derivatives from the direct reaction of phosphorus trihalides with various phosphine donors has been demonstrated unambiguously using ^{31}P NMR methods,[37] the fact that these reactions proceed in such a manner is surprising both in terms of known phosphorus chemistry and that of its heavier congeners. For example, the reaction of equimolar amounts of PMe_3 and PBr_3 results in the formation of the Lewis acid-base adduct $Me_3P \rightarrow PBr_3$,[44] which is perhaps a more predictable result.[46] Similarly, the reaction of arsenic trihalides with mono- and bi-dentate phosphine or arsine donors also results in the formation of acid-base adducts in certain cases,[47] or in the formation of the arsenic analogues of **2.1** in other instances.[10,48] In this light, the rapid and spontaneous nature of the reactions of PI_3 with the chelating donors outlined above is perhaps unexpected and is certainly dependent on the stoichiometries and conditions used for the reaction.

In 1985, Schmidpeter and associates demonstrated that the acyclic triphosphenium salt $[(Ph_3P)_2P][AlCl_4]$ is obtained by the reaction of PCl_3 with three equivalents of PPh_3 in the presence of $AlCl_3$; the by-product isolated from the reaction was $[Ph_3PCl][AlCl_4]$, which indicates that one equivalent of PPh_3 is oxidized during the course of the reaction.[38] Likewise, in 1986, the same researchers showed that reaction of PCl_3 with three equivalents of $P(NMe_2)_3$ in the presence of $[Na][BPh_4]$ proceeds in a similar manner to yield $[((Me_2N)_3P)_2P][BPh_4]$ and $[(Me_2N)_3PCl][BPh_4]$. More recently, the spectroscopic investigations of Dillon and associates illustrated the spontaneous nature of the reduction of PX_3 (X = Cl, Br, I) to P^I cations in the absence of auxiliary reducing agents.[37] In each of these cases, the completely reasonable suggestion has

been that a phosphine ligand acts as the RedOx couple for the reduction of the P^{III} to P^{I} in that it is oxidized to the corresponding halo-phosphonium halide (P^{III} to P^{V}).

While a P^{III} to P^{V} RedOx couple is certainly plausible, the ^{31}P NMR spectra of the reaction mixtures described in this work do not show signals attributable to the iodo-phosphonium salt during the reaction of PI_3 with either of the chelating ligands *when the reactions are conducted in dichloromethane.* Under such conditions, the potential iodo-phosphonium iodide by-product is only observed if the initial reaction mixtures are allowed to stir for extended periods. In contrast, significant amounts of the iodo-phosphonium by-product are generated when the reactions are performed in donor solvents such as thf or Et_2O. Given the foregoing, we believe that the experimental observations suggest that the iodo-phosphonium iodide by-product is attributable to the reaction of two equivalents of I_2 and dppe.[49] In this vein, we have verified that the reaction of two equivalents of iodine with dppe occurs in dichloromethane and produces colour changes that are consistent with those observed after the formation of **2.4**[I] in reactions containing excess dppe. To confirm the NMR assignment, a mixture of dppe and 2 equivalents of iodine was concentrated to obtain yellow crystals that were suitable for analysis by single crystal X-ray diffraction; the molecular structure of (dppe)·I_4 **2.6** is depicted in Figure 2.4.

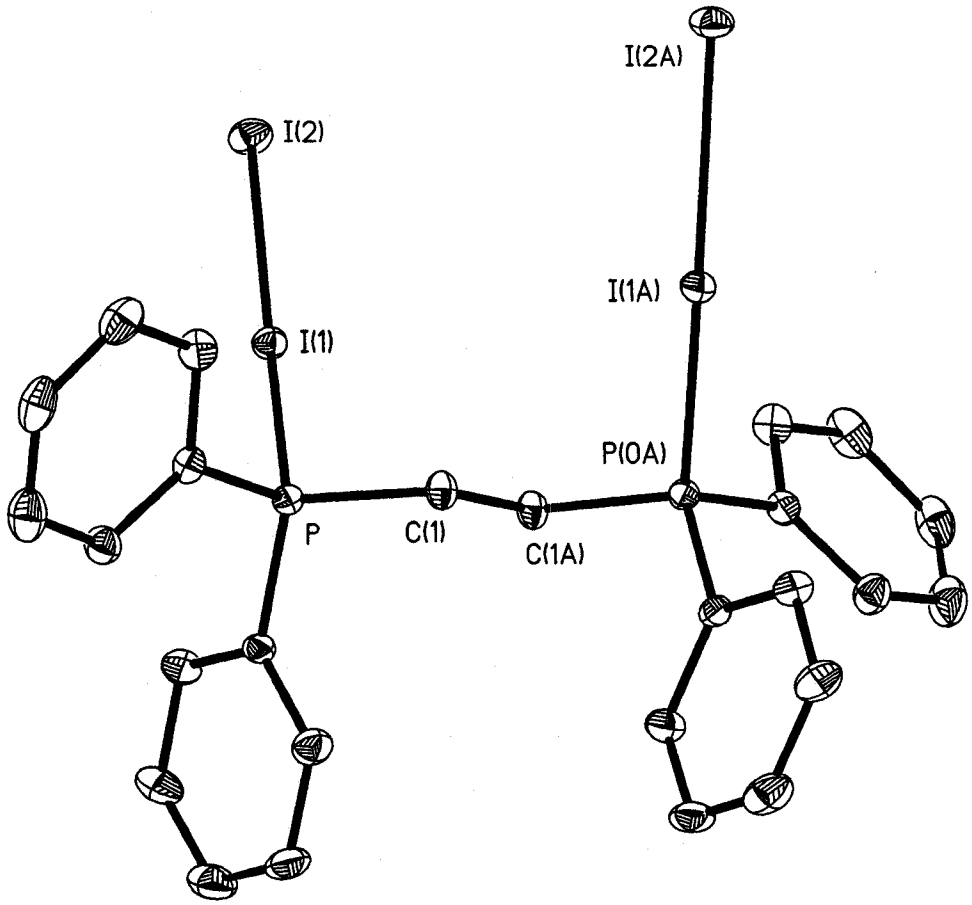

Figure 2.4 - Thermal ellipsoid plot (30% probability surface) of 2.6. Hydrogen atoms are omitted for clarity.

The iodine-dppe complex crystallizes in the space group *Aba2* and the individual molecules are linked to one another through a series of long (> 3.0 Å) H-I intermolecular hydrogen bonds. The metrical parameters of the individual adducts are similar to those of other phosphine-iodine adducts. For example, the P-I bond length of 2.4712(1) Å and the I-I distance of 3.1482(4) Å in **2.6** are comparable to the corresponding P-I (2.481(4) Å) and I-I (3.16(2) Å) distances found for Ph_3P-I_2.[49] While the structural features of the new adduct are unexceptional, the crystallographic investigation confirms the

composition of **2.6**, which is a material that is soluble in dichloromethane and that produces a signal at 51 ppm in the $^{31}P\{^{1}H\}$ NMR spectrum. Most importantly, this result confirms that **2.6** is not formed in the preparations of **2.4**[I] or **2.5**[I] using the procedure described above.

Given the preceding observations and arguments, it is possible that the experimental observation of by-products of the form $[X\text{-}PR_3]^+$ (X = Cl, Br) in the reduction of PX_3 result from the transient in situ formation of X_2. However, since chlorine and bromine are much more potent oxidizing agents than iodine and will react more rapidly with PR_3 to form cations with stronger P-X bonds, it is unlikely that the intermediate formation of X_2 would be observed experimentally under conditions similar to those used for the synthesis of **2.4**[I]. In any event, in terms of being able to separate the P^I salt from the by-products, the use of PI_3 as the phosphorus source in such preparative experiments allows one to obtain both greater yields and products of higher purity.

It is worthy of note that insight into the mechanism of the formation of P^I iodide in the process outlined in Equation 2.1 is provided by the solution behaviour of the phosphorus triiodide starting material itself. Variable-temperature ^{31}P NMR experiments reveal that, in solution, PI_3 is in equilibrium with P_2I_4 and I_2. We postulate that a further disproportionation to oligomeric $(P\text{-}I)_n$ may occur to provide the "P-I" fragments that are complexed by the dppe or dppp chelates. In accord with the results of previous investigations of the interaction of Lewis bases with halophosphines, this additional disproportionation is undoubtedly facilitated or enabled by the presence of the chelating ligands.[50] While we have, as yet, only obtained circumstantial evidence for the

formation of $(P\text{-}I)_n$,[51] the existence of $(P\text{-}Cl)_6$ and $(P\text{-}Br)_6$ at low temperature has been reported,[52] and our investigations of the arsenic analogue of **2.4**[I] reveal that the oxidative cleavage of the dppe ligand produces an ion containing an $(As\text{-}I)_6$ ring from the formal release of "As-I" fragments (Chapter 6). Regardless of the intermediacy of $(P\text{-}I)_n$, we have verified that the reaction of P_2I_4 with appropriate amounts of either dppe or dppp yields **2.4**[I] or **2.5**[I] with the concomitant elimination of I_2.

Anion Exchange

As anticipated, the iodide anion in **2.4**[I] or **2.5**[I] is readily replaced using metathesis reactions with a variety of alkali metal or silver salts. As depicted in Equation 2.2, the reactions of **2.4**[I] or **2.5**[I] with $[Na][BPh_4]$, [Ag][OTf], $[K][PF_6]$, $[Li][GaCl_4]$, or other suitable salts in methanol proceed rapidly at room temperature to produce the desired tetraphenylborate, triflate, hexafluorophosphate or tetrachlorogallate salts, respectively. It must be noted that the use of solvents other than methanol for such reactions generally gives products in significantly lower yield and of lower purity. Following extraction into dichloromethane, the colourless solution of the desired salt is filtered from the metal iodide by-product and subsequent removal of all volatile compounds under reduced pressure provides colourless solid salts in high yield.

$$\begin{matrix}\textbf{2.4}[I] \\ \text{or} \\ \textbf{2.5}[I]\end{matrix} \xrightarrow[-\,[M][I]]{+\,[M][A]} \begin{matrix}\textbf{2.4}[A] \\ \text{or} \\ \textbf{2.5}[A]\end{matrix} \qquad (2.2)$$

[M][A] = $[Na][BPh_4]$, [Ag][OTf], $[K][PF_6]$, $[Li][GaCl_4]$, $[Na][BF_4]$, etc.

NMR studies of the salts demonstrate the integrity of either the $[(dppe)P]^+$ or the $[(dppp)P]^+$ cation in every case and suggest that there is little interaction between the anions and the cations in solution. Although, in some instances, there are minor changes

in the chemical shift of the P^I centre depending on the identity of the anion in the salt, the differences from the chemical shift observed for the iodide salt are small in any case. Interestingly, salts containing air-stable counter anions such as tetraphenylborate or triflate appear to be stable for at least several hours upon exposure to air either as solids or as solutions in CD_2Cl_2. It should be emphasized that this behaviour is in stark contrast to other P^I compounds (e.g. phosphinidenes) or dicoordinate P^{III} compounds (e.g. phosphaalkenes, iminophosphines, phosphenium salts). Examples of reactions that illustrate the need for robust and non-reactive counter anions for the systematic study of the chemistry of P^I cations, such as ligand replacement chemistry are discussed in Chapter 3.

Each of the salts formed by the anion exchange reactions was characterized completely by multinuclear NMR and other suitable analytical methods; in the cases of the tetraphenylborate, triflate, hexafluorophosphate and tetrachlorogallate salts, crystals suitable for examination using X-ray crystallography were also obtained by recrystallization from either acetonitrile or dichloromethane. The tetrafluroroborate salt crystallizes as a mixture of BF_4^- and I^- counter anions.

The tetraphenylborate salt **2.4**[BPh_4] crystallizes in the space group $P2_1/c$; the molecular structure is depicted in Figure 2.5 and pertinent metrical parameters are assembled in Table 2-4. The solid-state arrangement of the salt consists of discrete cations and anions and there are no unusually short contacts between any of the ions. The metrical parameters for the anion correspond to those anticipated for an undistorted tetraphenylborate anion and the metrical parameters for the cation are entirely consistent with those found in **2.4**[I].

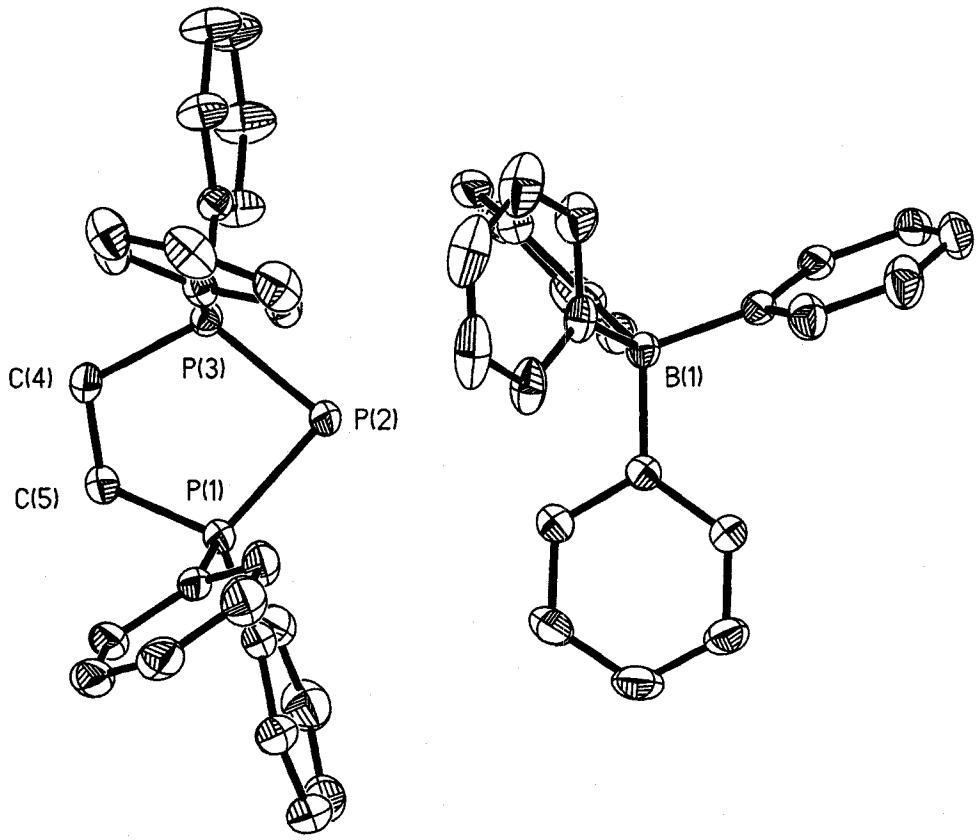

Figure 2.5 - Thermal ellipsoid plot (30% probability surface) of a 2.4[BPh_4]. Hydrogen atoms are omitted for clarity.

Crystals of suitable quality for analysis by single crystal X-ray diffraction were likewise obtained for the tetraphenylborate salt **2.5**[BPh_4], which crystallizes in the space group $P2_1/c$. The molecular structure is depicted in Figure 2.6 and relevant metrical parameters are compiled in Table 2-4. Once again there are no unusually close contacts between the cation and anion. The metrical parameters of the tetraphenylborate anion are consistent with those expected and those of the cation are similar to those observed in the structure of **2.5**[I].

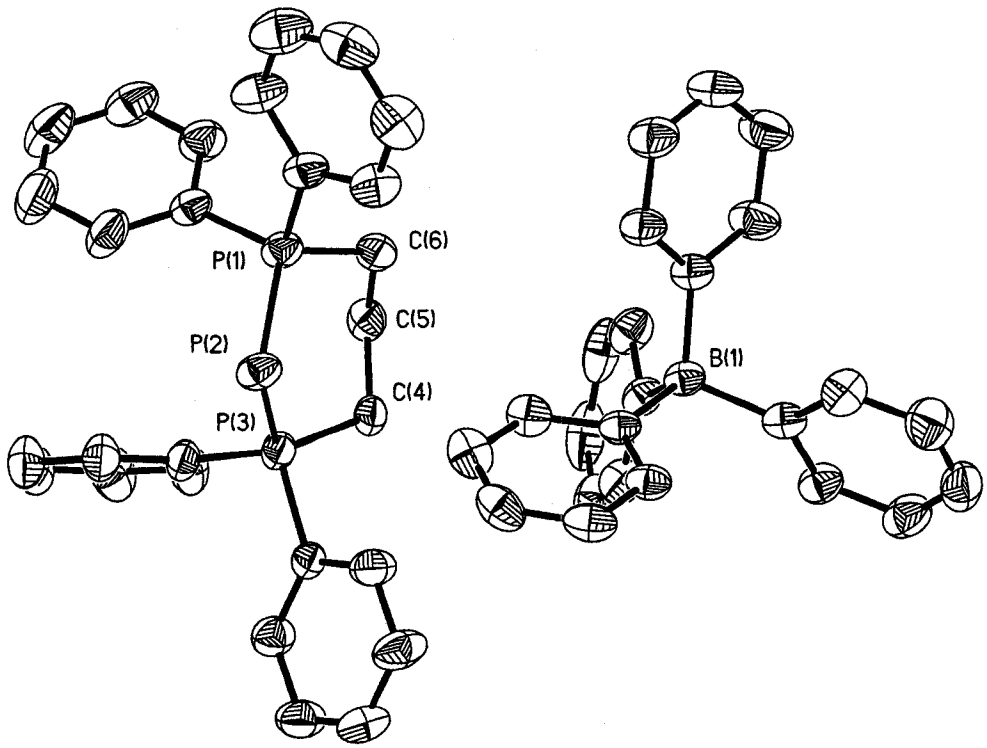

Figure 2.6 - Thermal ellipsoid plot (30% probability surface) of a 2.5[BPh_4]. Hydrogen atoms are omitted for clarity.

In a similar manner, the tetrachlorogallate and hexafluorophosphate salts of **2.5**, **2.5**[$GaCl_4$] and **2.5**[PF_6], also gave crystals suitable for crystallographic analysis. Both salts crystallized in the monoclinic space group $P2_1/c$. Figure 2.7 and Figure 2.8 show the molecular structures and pertinent metrical parameters are summarized in Table 2-5. The anions in both salts exhibit metrical parameters that are unexceptional and that do not suggest any strong interactions with the cations; the cations are again consistent with those observed in the iodide and tetraphenylborate salts described above. The salt **2.5**[PF_6] is also interesting in that it is an example of a single compound containing phosphorus atoms in di-, tetra- and hexa-coordinate environments; the $^{31}P\{^1H\}$ NMR

spectrum in Figure 2.9 emphasizes the differences in the shielding associated with the three different environments.

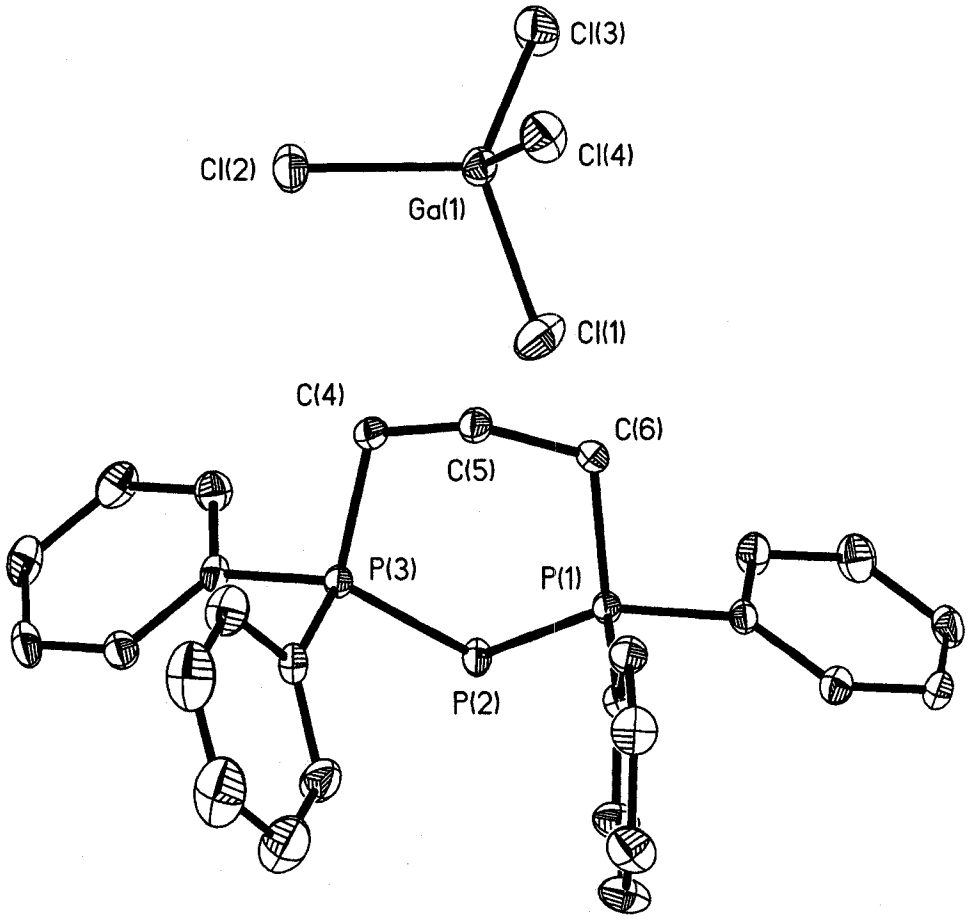

Figure 2.7 - Thermal ellipsoid plot (30% probability surface) of a 2.5[$GaCl_4$]. Hydrogen atoms are omitted for clarity.

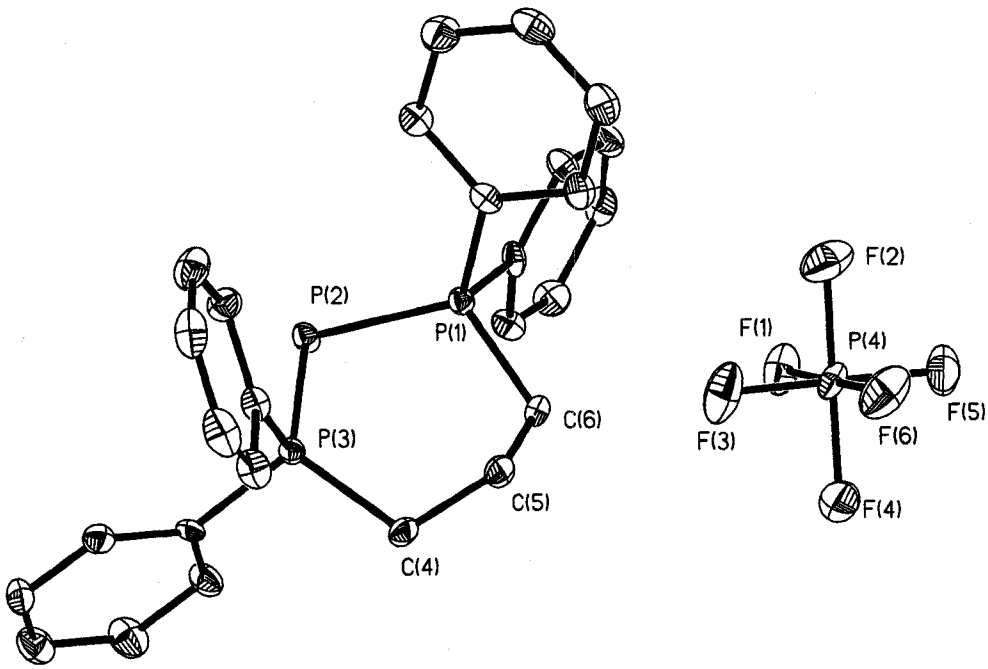

Figure 2.8 - Thermal ellipsoid plot (30% probability surface) of a 2.5[PF_6]. Hydrogen atoms are omitted for clarity.

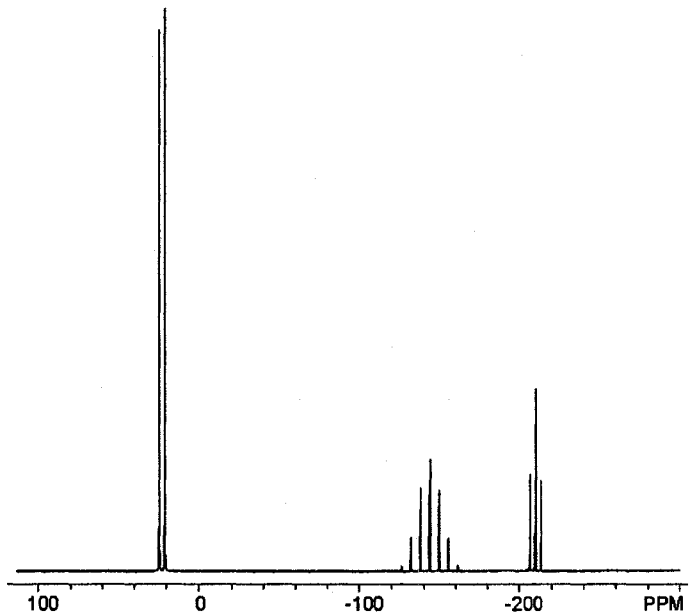

Figure 2.9 - $^{31}P\{^{1}H\}$ NMR Spectrum of 2.5[PF_6].

The triflate salt of the six-membered ring cation, **2.5**[OTf], yielded crystals of relatively low quality that were used to obtain the molecular structure shown in Figure 2.10. The salt crystallizes in the space group $P2_1/m$ and contains one molecule of dichloromethane solvent for each cation. Only half of each cation, anion and solvent molecule is found in the asymmetric unit and the anion is oriented in such a manner that it is distributed equally over two positions that are related by the mirror plane. While the crystallographic investigation identifies the nature and connectivity of the components unambiguously, the relatively poor quality of the crystals diminishes the reliability of the metrical parameters. It is noteworthy that the distances and angles observed for both the cation and the anion fall within the ranges expected for each component.

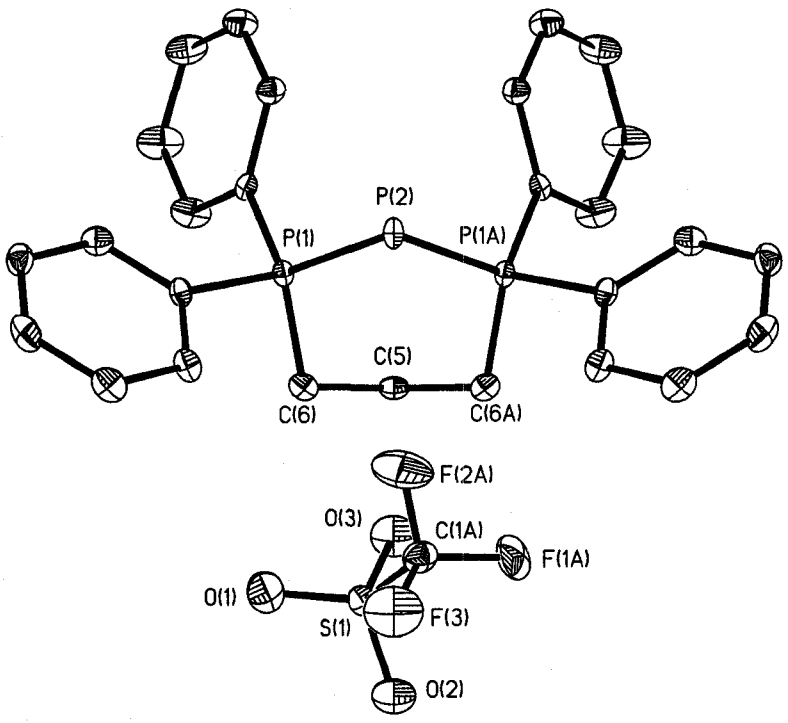

Figure 2.10 - Thermal ellipsoid plot (30% probability surface) of a 2.5[OTf]. Hydrogen atoms and a molecule of dichloromethane are omitted for clarity. Only one of the disordered triflate anion positions is depicted.

The tetrafluoroborate salt crystallized in approximately a 1:3 mixture with the iodide salt. Attempts at purifying the mixture were unsuccessful due to the similar solubilities of the salts. The mixture crystallizes in the space group $P2_1/c$. Figure 2.11 shows the molecular structure of the mixture of salts and relevant metrical data is presented in Table 2-5. The six-membered cation is similar to those observed for the previous salts and does not require further discussion.

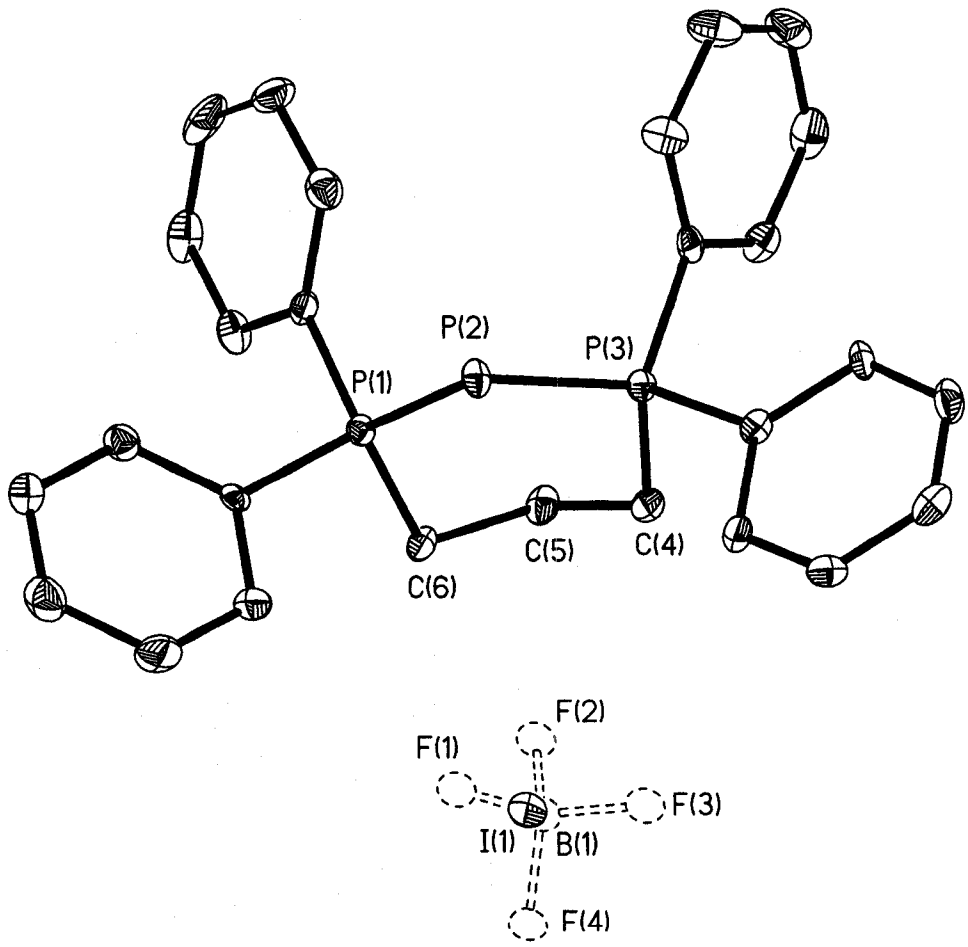

Figure 2.11 - Thermal ellipsoid plot (30% probability surface) of a 2.5[$(BF_4)_{0.26}I_{0.74}$]. Hydrogen atoms are omitted for clarity.

Synthesis of an Acyclic P^I cation Using $SnCl_2$ Protocols

Schmidpeter's synthetic procedures for the generation of the first triphosphenium cation involving the reduction of phosphorus(III) chloride and oxidation of tin(II) chloride,[12] have been used to generate a wide variety of other cyclic cations containing chelating diphosphine ligands.[10,37] We attempted to generate a cyclic P^I cation stabilized by both a phosphine and an amine using the ligand $Me_2N(CH_2)_2PPh_2$ and Schmidpeter's $SnCl_2$ reduction protocol of PCl_3 (Equation 2.3).

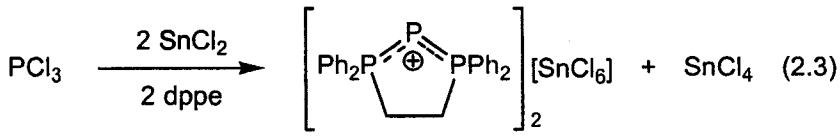

2.4$_2$[$SnCl_6$]

The reaction proceeds with the expected colour changes and precipitate formation, however the ^{31}P NMR spectrum of the product shows a coupling pattern indicative of a symmetrical triphosphenium cation, that we have characterized as $[(Me_2N(CH_2)_2PPh_3)_2P][SnCl_6]$ **2.7**. High resolution mass spectrometry confirms the presence of a species with a phosphorus atom coordinated by two 1-amino-2-phosphinoethane ligands. Attempts at recrystallizing the reaction mixture from a dichloromethane solution, however, consistently results in the isolation of an expected by-product: the ligand coordinated to the oxidized tin centre, $(Me_2N(CH_2)_2PPh_2)SnCl_4$ **2.8**. Although the ligand has been shown to coordinate to various transition metal fragments, this is the first example of its chelation to a Main Group element. Compound **2.8** along with one molecule of dichloromethane crystallizes in the space group $P2_1/n$. The molecular structure is shown in Figure 2.12 and important metrical parameters are summarized in Table 2-6. The metrical parameters all exhibit expected values. For

example, the Sn-N bond length of 2.392(2) Å is typical of Sn-N bonds in chelating complexes [*cf.* 2.388(7) Å in $(Me_2N(CH_2)_2S)SnEt_2Cl$[53]] and the Sn-P distance of 2.6000(7) Å is also consistent with related chelating complexes [cf. 2.679(46) and 2.654(24) in $(dppe)SnCl_4$[54]].

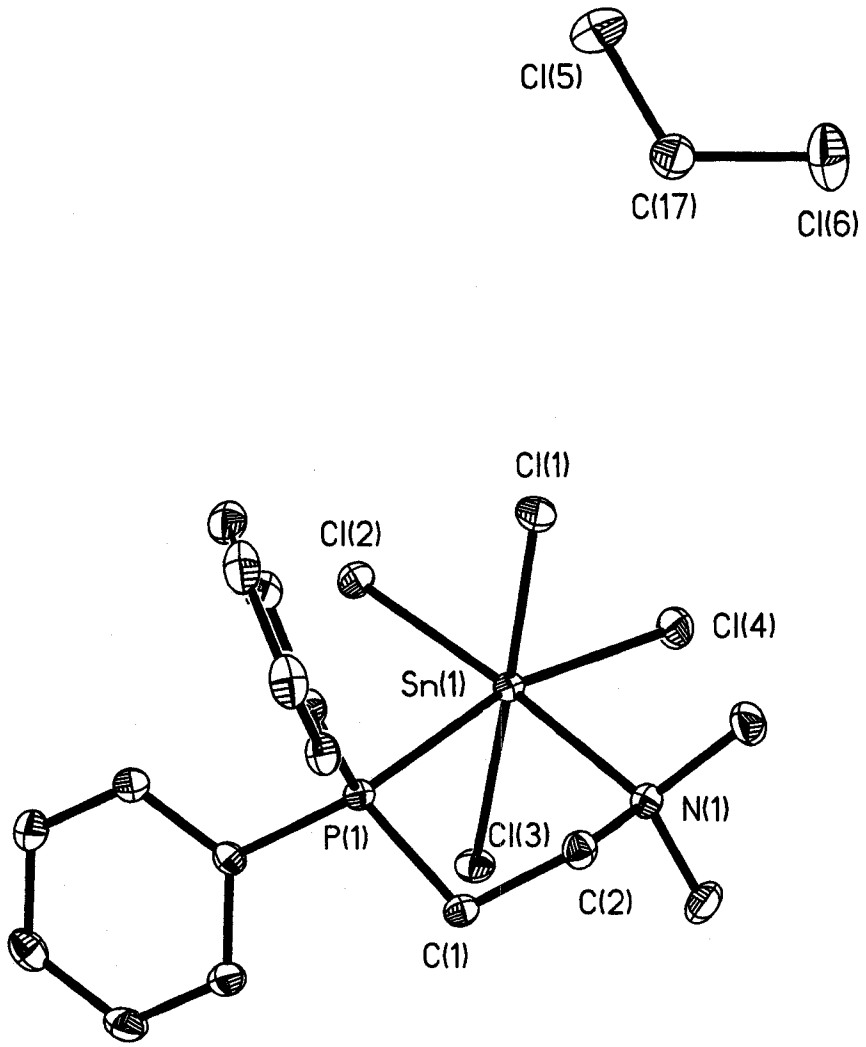

Figure 2.12 - Thermal ellipsoid plot (30% probability surface) of a 2.8 · CH_2Cl_2. Hydrogen atoms are omitted for clarity.

Further attempts at acquiring X-ray quality single crystals of the triphosphenium cation **2.7** by varying the solvent to acetonitrile resulted in the crystallization of the non-solvated structure of **2.8**. The solvent-free compound **2.8** crystallizes with 3 crystallographically independent molecules in the asymmetric unit, depicted in Figure 2.13. The metrical parameters of the compound, listed in Table 2-6, are similar to those found in the solvent structure and do not require further comment.

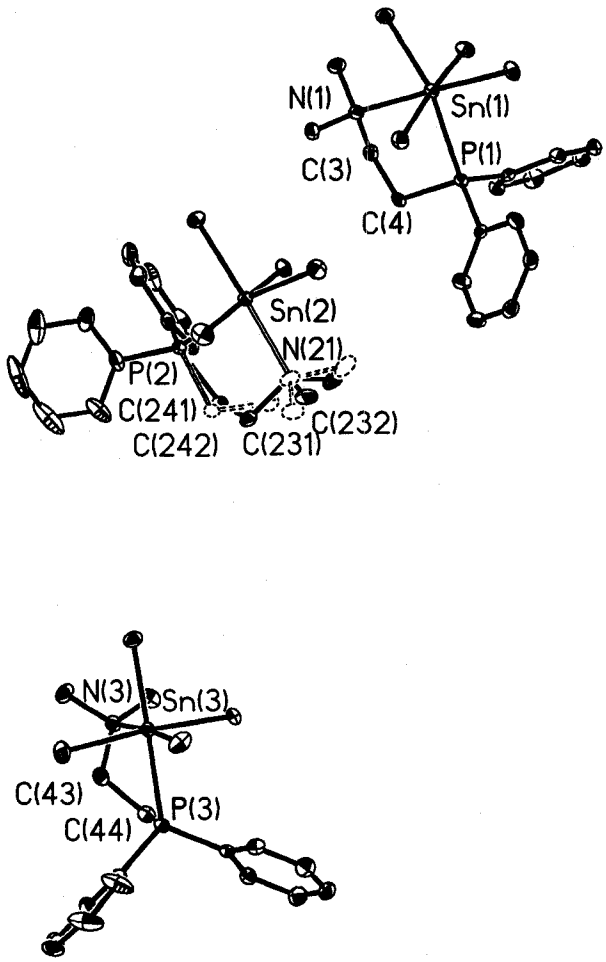

Figure 2.13 - Thermal ellipsoid plot (30% probability surface) of 2.8. Hydrogen atoms are omitted for clarity.

Computational Results and Predictions

In an effort to explain the remarkable stability of the univalent phosphorus cations that we have examined experimentally, we performed a series of DFT calculations. In order to assess the importance of the nature of the donor ligands on the stabilities of the complexes, the model compounds were chosen to contain either phosphine (PH_3 **2.9**, PMe_3 **2.10**, dhpe = 1,2-bis(phosphinoethane) **2.11**, dmpe = 1,2-bis(dimethylphosphino)ethane **2.12**), amine (NH_3 **2.13**, NMe_3 **2.14**, en = ethylenediamine **2.15**, tmeda = tetramethylethylenediamine **2.16**) or both phosphine and amine (PH_3/NH_3 **2.17**, PMe_3/NMe_3 **2.18**, $H_2P(CH_2)_2NH_2$ **2.19**, $Me_2P(CH_2)_2NMe_2$ **2.20**) donor groups to the P^I centre. For completeness, these model compounds include both acyclic and cyclic examples and are depicted in Figure 2.14. A summary of important calculated values is presented in Table 2-7 and Table 2-8.

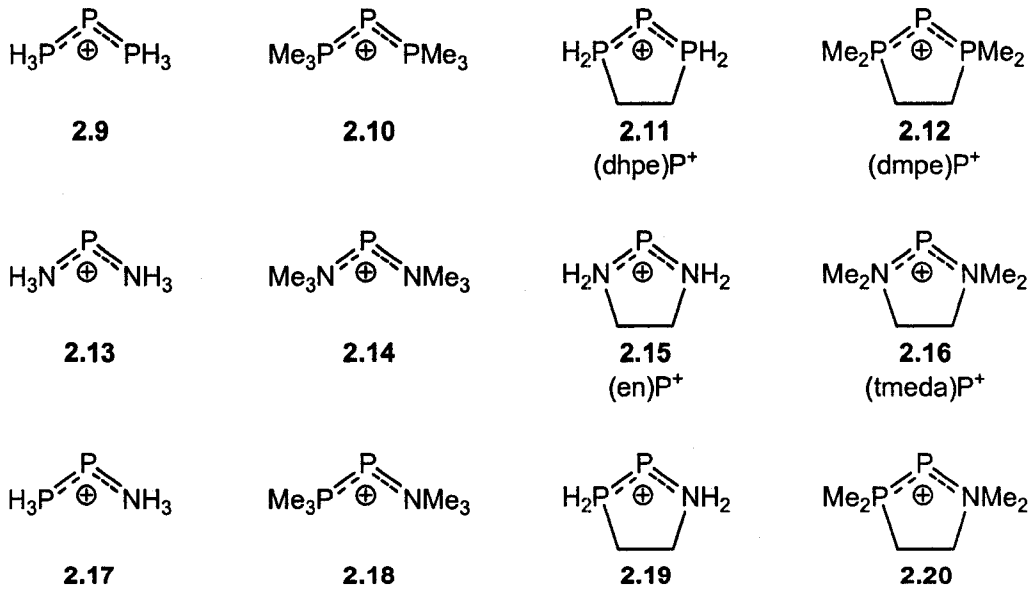

Figure 2.14 - Model cation systems 2.9 – 2.20 investigated using DFT methods.

Table 2-7 - Summary of Computational Results for Compounds 2.9 – 2.20, Part I.

Model	Sym	Corrected energy, E_{total}[a] (au)	E_{HOMO} (eV)	E_{LUMO} (eV)	P-P (Å)	P-N (Å)	E-P-E (°)
2.9	C_{2v}	-1027.15994	-10.852	-5.919	2.153		97.0
2.10	C_{2v}	-1262.91180	-9.342	-4.126	2.150		105.0
2.11	C_2	-1104.55033	-10.405	-5.775	2.152		87.8
2.12	C_2	-1261.72364	-9.406	-4.207	2.149		90.2
2.13	C_{2v}	-454.01314	-9.700	-5.787		1.925	93.9
2.14	C_2	-689.62546	-8.746	-4.231		1.944	107.3
2.15	C_2	-531.37169	-9.352	-5.530		1.931	86.3
2.16	C_2	-688.45028	-8.748	-4.809		1.926	90.6
2.17	C_s	-740.58620	-10.404	-6.376	2.142	1.934	97.2
2.18	C_1	-976.26798	-9.097	-4.837	2.151	1.930	105.9
2.19	C_1	-817.95986	-10.014	-5.894	2.142	1.934	87.1
2.20	C_1	-975.08467	-9.160	-4.968	2.144	1.935	90.2

[a] $E_{total} = E_{calculated} + ZPVE$.

Table 2-8 - Summary of Computational Results for Compounds 2.9 – 2.20, Part II.

Model	Occ P[b] (3p)	q(P)[c] (au)	P-P WBI[d]	P-N WBI[d]	P-P BO[e]	P-N BO[e]	P(3p) %[f]
2.9	1.721	-0.22	1.0979		0.8328		86.398
2.10	1.729	-0.32	1.0971		0.8166		85.976
2.11	1.673	-0.22	1.1014		0.8579		83.949
2.12	1.664	-0.27	1.1070		0.9031		83.328
2.13	1.947	0.31		0.6274		0.4947	97.535
2.14	1.938	0.30		0.5836		0.4483	96.993
2.15	1.948	0.30		0.6106		0.4760	97.578
2.16	1.924	0.33		0.5877		0.4693	96.318
2.17	1.789	0.08	1.1438	0.6433	0.8556	0.4878	89.736
2.18	1.800	0.02	1.1311	0.6027	0.8034	0.4855	90.046
2.19	1.725	0.08	1.1296	0.6330	0.8601	0.4770	88.740
2.20	1.764	0.06	1.1339	0.6041	0.9032	0.4660	87.596

[b] Natural Bond Orbital (NBO) population of the $3p_x$ orbital on the dicoordinate P atom. [c] NBO charge on the dicoordinate P atom. [d] NBO Wiberg bond indices for the specified bonds. [e] NBO atom-atom overlap-weighted Natural Atomic Orbital bond order for the specified bonds. [f] NBO Natural Localized Molecular Orbital percentage contribution of the $3p_x$ orbital on the dicoordinate P atom to the "lone pair" or delocalized "lone pair" orbital.

The calculated metrical parameters in models **2.9** – **2.12** are in reasonably good agreement with those that have been determined experimentally given the simplified

nature of the models and attest to the viability of the chosen models. Although the calculated P-P distances tend to be slightly longer than those observed in the crystallographic experiments outlined above, the values are still much shorter than those of typical single P-P bonds.[55] In contrast, the models employing amine substituents (**2.13** – **2.16**) have computed bond lengths that are much longer than typical P-N single bonds (*cf.* 1.696(3) Å for $PhHN\text{-}PPh_2$[56]). Although such long P-N distances may appear odd, it must be emphasized that the covalent radius of P^I will be significantly larger than those of P^{III} or P^V which are contained in the compounds containing the "typical" bonds. The model compounds containing both phosphine and amine donors (**2.17** – **2.20**) exhibit calculated P-P and P-N bond lengths that are comparable to those of the corresponding homoleptic models. The calculated P-P-P angles for the cyclic models **2.11** and **2.12** correlate well with those observed experimentally for salts of **2.4**. Similarly, the calculated angles for the acyclic triphosphenium cations **2.9** and **2.10** are also in good agreement with reported experimental values.[38]

The potentially ambiguous nature of the electronic structure of triphosphenium cations (Chapter 1.2) is emphasized by the possible canonical drawings that may be used to depict such compounds, as illustrated by structures **2.1a** – **2.1d**. Drawing **2.1a** suggests the presence of a P^V centre bearing no "lone pairs" of electrons and exhibiting a linear, allene-like P=P=P geometry. Because every structurally-characterized triphosphenium compound has a bent P-P-P moiety, drawing **2.1a** is not an instructive or reasonable depiction of such cations. Accordingly, if computational models such as **2.9** are constrained to D_{3d} symmetry, they exhibit several imaginary frequencies and are thus not true minima on their potential energy surfaces. In the literature, triphosphenium

cations are most-typically depicted using drawings such as **2.1b** in which the dicoordinate phosphorus atom has one "lone pair" of electrons and is thus a P^{III} centre. Model **2.1b** also suggests the presence of one double bond delocalized between the dicoordinate P centre and the P atoms of the phosphine substituents and could thus account for the short P-P distances observed experimentally. A third Lewis-type structure that is sometimes used to depict triphosphenium cations is a bis-ylidic model illustrated by **2.1c** in which the dicoordinate P atom bears two "lone pairs" of electrons and is thus able to be described a P^{I} centre. An alternative but equivalent depiction of **2.1c** is **2.1d**, which may be used to emphasize that such molecules can be considered as coordination compounds of P^{I} cations.

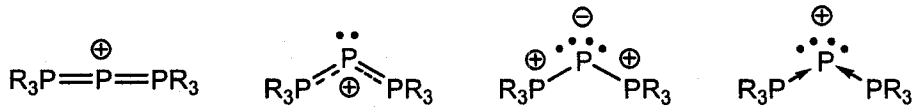

2.1a **2.1b** **2.1c** **2.1d**

While Lewis-type drawings should certainly not be over-interpreted, such simple models can provide insight into the structural properties and potential reactivity of compounds such as **2.1**. In this vein, we examined the frontier orbitals of model compounds **2.9** – **2.20** in an effort to gain insight into the real electronic structure of triphosphenium cations and to assess the appropriateness of models such as **2.1b** and **2.1c**. Drawings of the relevant frontier orbitals for the most realistic cyclic models **2.12**, **2.16** and **2.20** are presented in Figure 2.15 and pertinent details of the NBO analysis are listed in Table 2-8.

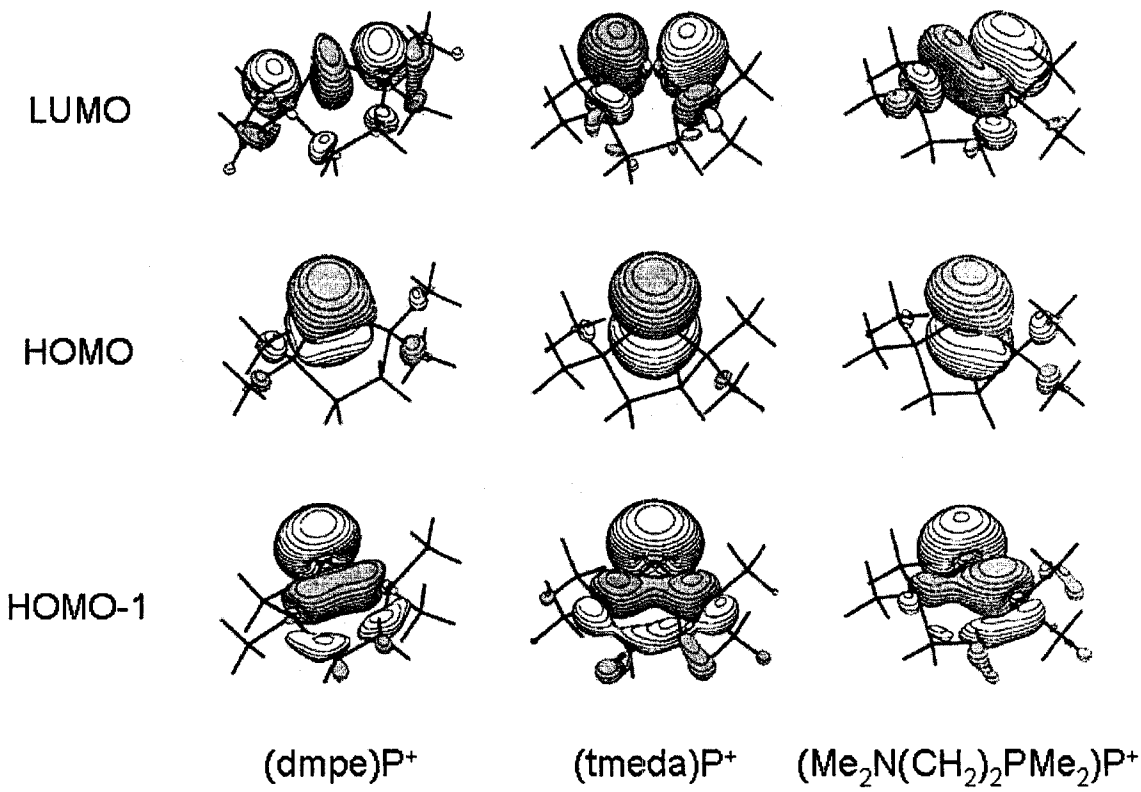

Figure 2.15 - MOLDEN depictions of the highest-occupied and lowest-unoccupied molecular orbitals for the model cations $(dmpe)P^+$ 2.12, $(tmeda)P^+$ 2.16 and $(Me_2N(CH_2)_2PMe_2)P^+$ 2.20.

Perhaps the most important overall feature that is apparent in Figure 2.15 is the general similarity of the appearance of two highest-occupied molecular orbitals (HOMO-1 and HOMO) in each model regardless of the composition of the stabilizing ligand. In every case, the HOMO-1 orbital is of *a*-type symmetry and is consistent with a "lone pair" orbital on the dicoordinate P atom in the E-P-E plane (where E = N or P depending on the model). Similarly, the HOMO in each of the models is a *b*-symmetry (for the C_2 models) orbital that is almost exclusively composed of the atomic $3p_x$ orbital on the dicoordinate P atom. The highest occupied molecular orbitals thus appear almost identical to those of water and suggest that the ylidic model **2.1c** (or **2.1d**) is the most appropriate drawing in terms of the overall electronic structure.

In spite of the general similarity in the appearance of the occupied orbitals of the model compounds depicted in Figure 2.15 and those of the other model compounds listed in Table 2-7, there are significant differences between them in terms of their energies. In particular, whereas the energy of the LUMO remains roughly similar in the corresponding models regardless of whether they contain amine or phosphine ligands, the energies of the HOMO's are considerably lower for models containing phosphine ligands. For example, in the series of models **2.11**, **2.15** and **2.19**, the energies of the LUMO's are similar: -5.775, -5.530, and -5.894 eV, respectively. In sharp contrast, the energies of the corresponding HOMO's are significantly different, the value being: -10.405, -9.352 and -10.014, respectively. Thus it is apparent that the presence of phosphine donor ligands on the dicoordinate P centre stabilizes the HOMO and increases the HOMO-LUMO separation in comparison to when amine donors are used.

Given the foregoing, an explanation for the remarkable stability of triphosphenium cations is almost certainly related to the stabilization of the HOMO. An explanation is provided by the understanding that, in contrast to amines, phosphine ligands may act as back-bond acceptors, as they are known to do in compounds containing phosphines ligated to transition metals. In phosphine ligands, the empty π-type P-R anti-bonding orbitals (these have *e* symmetry in the C_{3v} point group of the free PR_3 ligand) are of the correct symmetry and appropriate energy to accept electron density from the filled $3p_x$ orbital on the P^I centre (Figure 2.16). Such a back-bonding interaction lower the energy of the molecular orbital thus formed and stabilize the electron-rich centre. It should be noted that, in Main Group or organic compounds, back-bonding

interactions of the type depicted in Figure 2.16 are more commonly described using the term "hyperconjugation".

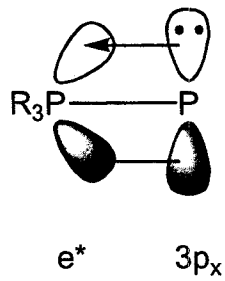

Figure 2.16 - Orbital interactions between the empty P-R anti-bonding orbitals and filled $3p_x$ orbital on P^I allow for back-bonding from the dicoordinate P^I to the phosphine substituents.

Direct evidence of back-bonding interactions is found in the results of the NBO population analysis. In the absence of a back-bonding interaction, the population of the $3p_x$ orbital on the P^I centre should be roughly 2 electrons. In all of the models containing phosphine ligands, back-bonding allows for the effective partial oxidation of the P^I centre, which is reflected in the decreased population of the $3p_x$ orbital on the dicoordinate phosphorus centre, as shown in Table 2-8. A comparable decrease in the $3p_x$ population is not observed in the case of the models containing the corresponding amine ligands in which the orbital population remains at a value of almost 2. The magnitude of the interaction is also confirmed by the results of NLMO calculations, which provide a measure of the delocalization of the "lone pair" orbitals. As listed in Table 2-8, these calculations show virtually no delocalization in the amine-substituted models and significant delocalization in the phosphine-containing models. Furthermore, the NBO analysis indicates that the back-bonding delocalization stabilizes the model compound $(H_3P)_2P^+$ **2.9** by around 187 kJ mol^{-1}, while the much-less-favourable interaction in the model $(H_3N)_2P^+$ **2.13** provides only 66 kJ mol^{-1} of stabilization. For the

cations containing both phosphine and amine substituents, there is a decrease in the orbital population, although less than that observed for models containing two phosphine donors.

In addition to the differences in orbital occupancies and energies, the presence or absence of the back-bonding interaction is clearly manifested in the shape of the HOMO for each of the model cations, as depicted in Figure 2.15. In the case of models containing phosphine ligands, there are perturbations of the lobe derived primarily from the $3p_x$ orbital on the P^I centre towards the phosphine substituents to produce orbitals that are consistent with the presence of a π-bonding interaction between the P atoms. The much smaller magnitude of the back-bonding in the amine-substituted models is further emphasized by the presence of a nearly undistorted $3p_x$ orbital on P^I in the HOMO of the model depicted in Figure 2.15.

In addition to the effects on the shape and composition of the HOMO, the greater magnitude of back-bonding in the phosphine-substituted model compound $(H_3P)_2P^+$ **2.9** is highlighted by the structural consequences of preventing the back-bonding interactions. When the important acceptor orbitals on the phosphine ligands are removed using the NBOdel method, the optimized P-P bond distance increases to 2.350 Å from the 2.149 Å distance in the unperturbed model; this is a change of more than 0.2 Å. The comparable change in the amine-substituted analogue is less than 0.1 Å (from 1.919 to 2.012 Å). For the mixed-ligand model system $(H_3P)P(NH_3)^+$ **2.17**, the P-P bond distance changes from 2.141 to 2.364 Å, while the P-N bond distance only changes from 1.926 to 2.022 Å when back-bonding interactions are prevented. Thus both structural features and energy values demonstrate that the magnitude of the back-bonding is clearly more pronounced for the

phosphine ligands, as one would expect. In this light, the Lewis-type model **2.1b** certainly provides insight into the stability of triphosphenium cations.

In addition to the effects on the occupied orbitals, it is notable that the composition of the LUMO is also highly-dependent on the nature of the ligands as shown in Figure 2.15. For model **2.12** the LUMO is localized primarily on the phosphine substituents, whereas for **2.16** the orbital is principally on the dicoordinate phosphorus atom (the MO resembles a $3p_y$ atomic orbital) and for **2.20** the orbital is mainly localized over the two P atoms. Thus the calculations suggest that the nature of the ligand not only affects the stability of the E-P-E framework but should also have a large impact on the reactivity of the coordinated P^I centre. Overall, these computational results suggest that there are many possible ways to tune the reactivity of such compounds through the judicious choice of stabilizing ligand. While there is much more experimental work to be done in this regard, we have already demonstrated that an understanding of the frontier molecular orbitals can be used to control the oxidation chemistry of some analogous As^I compounds (Chapter 6).

Overall, examinations of the electronic structure of several model compounds suggest that the two highest occupied orbitals in triphosphenium cations correspond to "lone pairs" of electrons that are primarily localized on the dicoordinate P atom; in this light, the ylidic description (**1c**) of the bonding in such molecules is the most appropriate. However, the HOMO in triphosphenium cations is rendered significantly more stable by back-bonding interactions with the adjacent phosphine ligands so, while ylidic depictions such as **2.1c** most accurately describe the electronic structure, a canonical structure such as **2.1b** provides insight into the remarkable stability of these compounds.

2.4 Conclusions

High purity iodide salts of cations containing P^I centres are readily prepared and isolated in good yield by the base-induced spontaneous elimination of I_2 from PI_3. The facile exchange of the iodide anion in **2.4**[I] or **2.5**[I] using metathesis reactions allows for the tailoring of reactivity and solubility of univalent phosphorus salts, and will allow for further investigations into the unique chemistry and potential uses for this easily accessible reagent. In contrast to most other P^I compounds, many of these salts are stable even in the presence of water and air. The remarkable stability of these phosphorus(I) salts is largely attributable to the back bonding interactions between the ligand and the P^I centre and such an understanding may be used to tune the behaviour of these reagents. Amines are unable to participate in back-bonding interactions, as exemplified in the computational studies, which explains the absence of amine-stabilized P^I compounds.

2.5 Prospective Developments

The disproportionation of PI_3 offers a clean and effective way to generate P^I cations of iodide salts and should be extended to encompass heavier Group 15 elements, which is discussed below in Chapter 6. The limitations of uses lighter PX_3 analogues lies in the enhanced RedOx capability of Cl_2 and Br_2, however the isolation of pure P^I salts of chloride or bromide anions will be accessible through the addition of a quenching reagent that is more readily oxidized than a phosphine. Schmidpeter showed that new triphosphenium cations are accessible through substitution of $(Ph_3P)_2P^+$ with more basic phosphines.[38] We have begun exploring this pathway with diphosphines that are

restricted from chelating due to geometrical design (*para-* and *meta-*diphosphinobenzenes and 1,3-diphosphino-substituted cyclopentadianides). Preliminary results indicate extended structures containing multiple P^I centres and synthetic strategies are being developed for the controlled formation of P^I oligomers.

2.6 References

1. Dillon, K.B., Mathey, F. and Nixon, J.F., *Phosphorus: The Carbon Copy: From Organophosphorus to Phospha-organic Chemistry*, 1998, Chichester: John Wiley & Sons, Inc., pp. 366.
2. Regitz, M. and Scherer, O.J., *Multiple Bonds and Low Coordination in Phosphorus Chemistry*, 1990, Stuttgart: Georg Thieme Verlag, pp. 478.
3. Bouhadir, G. and Bourissou, D., *Chem. Soc. Rev.*, **2004**, *33*, 210-217.
4. We prefer to use a simple, chemically-intuitive convention in which the oxidation state of phosphorus is indicated by the number of lone pairs associated with the atom: P(+5) has no lone pairs, P(+3) has one lone pair and P(+1) has two lone pairs, as discussed in Chapter 1.
5. Baudler, M. and Glinka, K., *Chem. Rev.*, **1993**, *93*, 1623-1667.
6. Mathey, F., *Angew. Chem., Int. Ed. Engl.*, **1987**, *26*, 275-286.
7. Lammertsma, K. and Vlaar, M.J.M., *Eur. J. Org. Chem.*, **2002**, 1127-1138.
8. Lammertsma, K., *Top. Curr. Chem.*, **2003**, *229*, 95-119.
9. Driess, M., Ackermann, H., Aust, J., Merz, K. and Von Wullen, C., *Angew. Chem. Int. Ed.*, **2002**, *41*, 450-453.

10. Barnham, R.J., Deng, R.M.K., Dillon, K.B., Goeta, A.E., Howard, J.A.K. and Puschmann, H., *Heteroat. Chem.*, **2001**, *12*, 501-510.

11. Dikarev, E.V. and Li, B., *Inorg. Chem.*, **2004**, *43*, 3461-3466.

12. Schmidpeter, A., Lochschmidt, S. and Sheldrick, W.S., *Angew. Chem., Int. Ed. Engl.*, **1982**, *21*, 63-64.

13. Schmidpeter, A. and Lochschmidt, S., *Inorg. Synth.*, **1990**, *27*, 253-258.

14. Lochschmidt, S. and Schmidpeter, A., *Z. Naturforsch., B: Anorg. Chem., Org. Chem.*, **1985**, *40B*, 765-773.

15. Schmidpeter, A., *Heteroat. Chem.*, **1999**, *10*, 529-537.

16. Shah, S. and Protasiewicz, J.D., *Coord. Chem. Rev.*, **2000**, *210*, 181-201.

17. Schmidpeter, A. and Zwaschka, F., *Angew. Chem., Int. Ed. Engl.*, **1977**, *16*, 704-705.

18. Schmidpeter, A., Burget, G., Zwaschka, F. and Sheldrick, W.S., *Z. Anorg. Allg. Chem.*, **1985**, *527*, 17-32.

19. Schmidbaur, H., *Angew. Chem., Int. Ed. Engl.*, **1983**, *22*, 907-927.

20. Schmidbaur, H., *Pure Appl. Chem.*, **1978**, *50*, 19-25.

21. Driess, M., Aust, J., Merz, K. and Van Wullen, C., *Angew. Chem. Int. Ed.*, **1999**, *38*, 3677-3680.

22. Pangborn, A.B., Giardello, M.A., Grubbs, R.H., Rosen, R.K. and Timmers, F.J., *Organometallics*, **1996**, *15*, 1518-1520.

23. Habtemariam, A., Watchman, B., Potter, B.S., Palmer, R., Parsons, S., Parkin, A. and Sadler, P.J., *J. Chem. Soc., Dalton Trans.*, **2001**, 1306-1318.

24. Schmidt, S.P. and Brooks, D.W., *Tetrahedron Lett.*, **1987**, *28*, 767-768.

25. Frisch, M.J., Trucks, G.W., Schlegel, H.B., Scuseria, G.E., Robb, M.A., Cheeseman, J.R., Zakrzewski, V.G., Montgomery, V.G., Jr., Stratmann, R.E., Burant, J.C., Dapprich, S., Millam, J.M., Daniels, A.D., Kudin, K.N., Strain, M.C., Farkas, O., Tomasi, J., Barone, V., Cossi, M., Cammi, R., Mennucci, B., Pomelli, C., Adamo, C., Clifford, S., Ochterski, J., Petersson, G.A., Ayala, P.Y., Cui, Q., Morokuma, K., Salvador, P., Dannenberg, J.J., Malick, D.K., Rabuck, A.D., Raghavachari, K., Foresman, J.B., Cioslowski, J., Ortiz, J.V., Baboul, A.G., Stefanov, B.B., Liu, G., Liashenko, A., Piskorz, P., Komaromi, I., Gomperts, R., Martin, R.L., Fox, D.J., Keith, T., Al-Laham, M.A., Peng, C.Y., Nanayakkara, A., Challacombe, M., Gill, P.M.W., Johnson, B., Chen, W., Wong, M.W., Andres, J.L., Gonzalez, C., Head-Gordon, M., Replogle, E.S. and Pople, J.A., *Gaussian98*, Revision A.11.1, 2001, Pittsburgh, PA: Gaussian, Inc.

26. Becke, A.D., *J. Chem. Phys.*, **1993**, *98*, 5648-5652.

27. Perdew, J.P. and Wang, Y., *Phys. Rev. B: Condens. Matter*, **1992**, *45*, 13244-13249.

28. Reed, A.E., Curtiss, L.A. and Weinhold, F., *Chem. Rev.*, **1988**, *88*, 899-926.

29. *SMART, Molecular Analysis Research Tool*, 2001, Madison, WI: Bruker AXS, Inc.

30. *SAINTPlus, Data Reduction and Correction Program*, 2001, Madison, WI: Bruker AXS, Inc.

31. *SADABS, An Empirical Absorption Correction Program*, 2001, Madison, WI: Bruker AXS, Inc.

32. Sheldrick, G.M., *SHELXS-97*, 1997, Gottingen: Universitat Gottingen.

33. Altomare, A., Burla, M.C., Camalli, M., Cascarano, G.L., Giacovazzo, C., Guagliardi, A., Moliterni, A.G.G., Polidori, G. and Spagna, R., *J. Appl. Crystallogr.*, **1999**, *32*, 115-119.

34. Farrugia, L.J., *J. Appl. Crystallogr.*, **1999**, *32*, 837-838.

35. Sheldrick, G.M., *SHELXL-97*, 1997, Gottingen: Universitat Gottingen.

36. Sheldrick, G.M., *SHELXTL*, 2001, Madison, WI: Bruker AXS, Inc.

37. Boon, J.A., Byers, H.L., Dillon, K.B., Goeta, A.E. and Longbottom, D.A., *Heteroat. Chem.*, **2000**, *11*, 226-231.

38. Schmidpeter, A., Lochschmidt, S. and Sheldrick, W.S., *Angew. Chem., Int. Ed. Engl.*, **1985**, *24*, 226-227.

39. Schmidpeter, A. and Lochschmidt, S., *Angew. Chem., Int. Ed. Engl.*, **1986**, *25*, 253-254.

40. EI-MS: calcd. for I2 [M]+ m/z = 253.81, found 253.61.

41. Ellis, B.D. and Macdonald, C.L.B., *Acta Crystallogr., Sect. E: Struct. Rep. Online*, **2006**, *E62*, m1235-m1236.

42. Allen, F.H., *Acta Crystallogr., Sect. B: Struct. Sci.*, **2002**, *B58*, 380-388.

43. Mundt, O., Riffel, H., Becker, G. and Simon, A., *Z. Naturforsch., B: Chem. Sci.*, **1988**, *43*, 952-958.

44. Dashti-Mommertz, A. and Neumuller, B., *Z. Anorg. Allg. Chem.*, **1999**, *625*, 954-960.

45. Deng, R.M.K., Goeta, A.E., Dillon, K.B. and Thompson, A.L., *Acta Crystallogr., Sect. E: Struct. Rep. Online*, **2005**, *E61*, m296-m298.

46. Burford, N. and Ragogna, P.J., *J. Chem. Soc., Dalton Trans.*, **2002**, 4307-4315.

47. Hill, N.J., Levason, W. and Reid, G., *J. Chem. Soc., Dalton Trans.*, **2002**, 1188-1192.

48. Gamper, S.F. and Schmidbaur, H., *Chem. Ber.*, **1993**, *126*, 601-604.

49. Godfrey, S.M., Kelly, D.G., McAuliffe, C.A., Mackie, A.G., Pritchard, R.G. and Watson, S.M., *J. Chem. Soc., Chem. Commun.*, **1991**, 1163-1164.

50. Kirsanov, A.V., Gorbatenko, Z.K. and Feshchenko, N.G., *Pure Appl. Chem.*, **1975**, *44*, 125-139.

51. Preliminary results suggest that (PI)n is the primary component of the insoluble orange precipitate formed in these reactions – further investigations to elucidate the structure and reactivity of this material are currently underway.

52. Baudler, M., Grenz, D., Arndt, U., Budzikiewicz, H. and Feher, M., *Chem. Ber.*, **1988**, *121*, 1707-1709.

53. Couce, D., Valle, G., Casellato, U., Graziani, R. and Russo, U., *Z. Kristallogr. - New Cryst. Struct.*, **2000**, *215*, 285-286.

54. Kunkel, F., Dehnicke, K., Goesmann, H. and Fenske, D., *Z. Naturforsch., B: Chem. Sci.*, **1995**, *50*, 848-850.

55. Hinchley, S.L., Morrison, C.A., Rankin, D.W., Macdonald, C.L.B., Wiacek, R.J., Voigt, A., Cowley, A.H., Lappert, M.F., Gundersen, G., Clyburne, J.A. and Power, P.P., *J. Am. Chem. Soc.*, **2001**, *123*, 9045-9053.

56. Wetzel, T.G., Dehnen, S. and Roesky, P.W., *Angew. Chem. Int. Ed.*, **1999**, *38*, 1086-1088.

57. Schaftenaar, G. and Noordik, J.H., *J. Comput.-Aided Mol. Des.*, **2000**, *14*, 123-134.

Chapter 3 – *N*-Heterocyclic Carbene Adducts of P^I Cations

3.1 Introduction

The chemistry of phosphamethine cyanine cations, $[P(CZNR_2)_2]^+$ (Z = CR_3, NR_2, SR, etc.), and other phospha-allylic compounds occupies an important position in the history of phosphorus chemistry.[1] These dyes comprised one of the first families of phosphorus compounds reported that contained unambiguous di-coordinate P centres.[2-4] Such compounds are typically made through the reaction of suitable chloro-carbon precursors with explosive or pyrophoric reagents such as $P(CH_2OH)_3$ or $P(SiMe_3)_3$, respectively. In 1983, Schmidpeter *et al.* reported that the triphosphenium salt $[((Me_2N)_3P)_2][BPh_4]$ reacts with particular electron rich olefins at elevated temperatures to produce phosphamethine cyanine salts and they proposed that the reaction proceeds in the manner shown in Equation 3.1.[5,6]

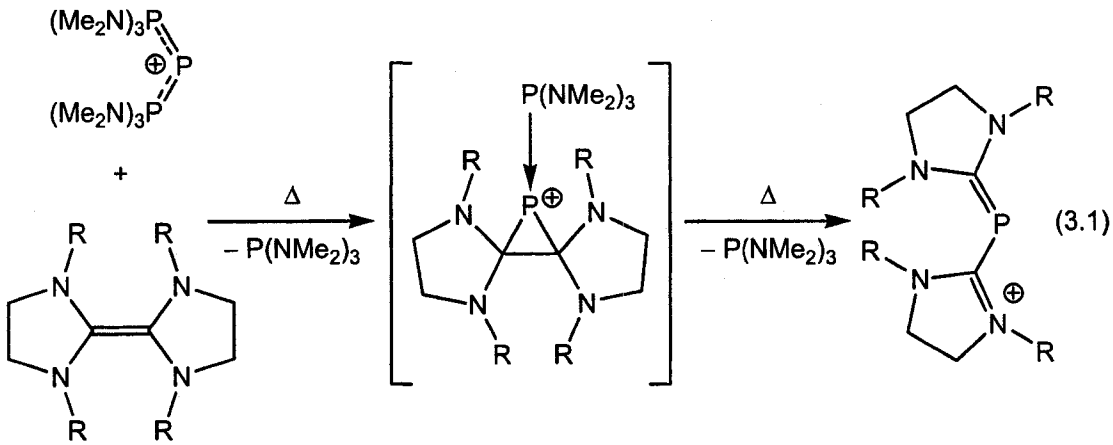

Since Arduengo's report of stable *N*-heterocyclic carbenes (NHCs) in 1991,[7] the analogy between phosphines and NHCs has been well documented.[8,9] In the interim, a large number of stable NHCs and related carbenes have been synthesised and characterised. In light of the relationship between phosphines and NHCs, and the facile

synthesis of diphosphine-stabilized P^I and As^I salts (Chapters 2 and 6), we have commenced an investigation of carbene-stabilized P^I salts. Herein we present two new synthetic approaches to phosphamethine cyanine salts, which appear to be more accurately considered as NHC-stabilized P^I salts.

3.2 Experimental

Reagents and General Procedures. All manipulations were carried out using standard inert-atmosphere techniques. Phosphorus(III) iodide, 1,2-bis(diphenylphosphino)ethane (dppe), 1,3-bis(diphenylphosphino)propane (dppp), silver trifluoromethanesulfonate (silver triflate, [Ag][OTf]) and potassium hexafluorophosphate were purchased from Strem Chemicals Inc. and all other chemicals and reagents were obtained from Aldrich; all reagents were used without further purification. MeOH was dried over magnesium turnings, CD_2Cl_2 was dried over calcium hydride and all other solvents were dried on a series of Grubbs' type columns[10] and were degassed prior to use. Silver salts are sensitive to light and precautions were taken to minimize light exposure in reactions involving such salts. 1,3,4,5-Tetramethylimidazol-2-ylidene (Me-NHC),[11] 1,3-diethyl-4,5-dimethylimidazol-2-ylidene (Et-NHC),[11] 1,3-diisopropyl-4,5-dimethylimidazol-2-ylidene (^{i}Pr-NHC),[11] 2,4,5-triphenyl-1,2,4-triazol-3-ylidene (Ph-N_3HC)[12], 1,3-bis(2,4,6-trimethylphenyl)imidazol-2-ylidene (Mes-NHC),[13] and [(dppe)P][BPh_4] (Chapter 2)[14] were synthesized by literature procedures. Yields of the chloride salts are calculated in conjunction with integration of ^{1}H NMR spectra of the product mixture containing both the P^I chloride salt and the oxidized *N*-heterocyclic carbene NHC-Cl_2, which is difficult to separate due to similar solubilities. Analogous

bromide and iodide salts are obtained in the reactions of PBr_3 and PI_3 with *N*-heterocyclic carbenes, as described below for PCl_3, with nearly indistinguishable multi-nuclear NMR chemical shifts, and as such are not presented in detail below. All reactions are quantitative by ^{31}P NMR spectra.

Instrumentation. NMR spectra were recorded at room temperature in CD_2Cl_2 solutions on a Bruker Avance 300 MHz spectrometer. Chemical shifts are reported in ppm, relative to external standards ($SiMe_4$ for ^{1}H and ^{13}C, 85% aq. H_3PO_4 for ^{31}P, $BF_3{\cdot}OEt_2$ for ^{11}B). Coupling constant magnitudes, $|J|$, are given in Hz. Melting points (mp) or decomposition points (dp) were obtained on samples sealed in glass capillaries under dry nitrogen using an Electrothermal® Melting Point Apparatus. Elemental analysis was performed in-house using a PerkinElmer 2400 C, H, N analyzer in the Centre for Catalysis and Materials Research, Department of Chemistry and Biochemistry, University of Windsor.

Theoretical Methods. Calculations were preformed with the Gaussian 98 suite of programs.[15] Geometry optimizations have been calculated using density functional theory (DFT), specifically implementing the B3PW91 method [containing Becke's three-parameter hybrid functional for exchange (B3, including ca. 20% Hartree-Fock exchange)[16] combined with the generalized gradient approximation for correlation of Perdew and Wang (PW91)[17]] in conjunction with the 6-31+G(d) basis set. The geometries were restricted to the highest reasonable symmetry and each stationary point was confirmed to be a minimum by having zero imaginary vibrational frequencies. The electronic energies of the molecules have been corrected by the unscaled, zero-point vibrational energy (ZPVE). Single Point Energies have been calculated at the

B3PW91/6-311+G(3df,2p)//B3PW91/6-31G(d) level of theory. Population analyses were conducted using the Natural Bond Orbital (NBO) method implemented in Gaussian98.[18]

X-ray Crystallography. Crystals were coated in Nujol, mounted on a glass fibre and placed in the 173 K N_2 boil-off stream of the Kryoflex low-temperature apparatus. Reflection data were integrated from frame data obtained using hemisphere scans with the SMART[19] software on a Bruker APEX CCD diffractometer using a graphite monochromator with MoKα radiation (λ = 0.71073Å). Diffraction data and unit-cell parameters were consistent with assigned space groups. Lorentz and polarization corrections and empirical absorption corrections, based on redundant data at varying effective azimuthal angles, were applied to the data sets using SAINTPlus[20] and SADABS[21] software. The structures were solved by direct methods using SHELXS[22] or Sir97[23] (as implemented in the WinGX software package[24]), completed by subsequent Fourier syntheses and refined with full-matrix least-squares methods against F^2 data using SHELXL.[25] All non-hydrogen atoms were refined anisotropically and all hydrogen atoms were placed in appropriate geometrically-calculated positions or refined isotropically when bound to a phosphorus atom. Thermal ellipsoid plots of the molecular structures were generated using SHELXTL.[26] The experimental details for each of the diffraction experiments are listed in Table 3-1.

Preparation of [(Me-NHC)$_2$P][Cl], 3.2a[Cl]

A colourless solution of Me-NHC (0.193 g; 1.554 mmol) in thf (10 mL) was added to a colourless solution of PCl_3 (0.071 g; 0.518 mmol) in thf (10 mL), which resulted in the rapid formation of a yellow precipitate. The mixture was left to stir for 16 hours. Volatile components were removed under reduced pressure to produce a yellow powder. Yield: 58% (0.094 g; 0.300 mmol). $^{31}P\{^1H\}$ NMR: -114.8 (s). $^{13}C\{^1H\}$ NMR: 9.3 (s), 34.0 (s), 124.6 (s). ^1H NMR: 2.22 (s, 12H), 3.48 (s, 12H). HR-ESI-MS Calcd. For $C_{14}H_{24}ClN_4P$ $[M - Cl]^+$: m/z = 279.1738. Found 279.1631 (38.3 ppm).

Preparation of [(Et-NHC)$_2$P][Cl], 3.2b[Cl]

An orange solution of Et-NHC (0.468 g; 3.074 mmol) in thf (10 mL) was added to a colourless solution of PCl_3 (0.141 g; 1.025 mmol) in thf (10 mL), which resulted in the rapid formation of a tan precipitate. The mixture was left to stir for 16 hours. Volatile components were removed under reduced pressure to produce a tan powder. Yield: 76% (0.287 g; 0.774 mmol). $^{31}P\{^1H\}$ NMR: -127.4 (s). $^{13}C\{^1H\}$ NMR: 8.6 (s), 15.7 (s), 42.2 (s), 127.2 (s). ^1H NMR: 0.866 (m, 6H), 1.70 (s, 6H), 4.04 (m, 4H). HR-ESI-MS Calcd. For $C_{18}H_{24}ClN_4P$ $[M - Cl]^+$: m/z = 335.2364. Found 335.2290 (22.1 ppm).

Preparation of [(^{i}Pr-NHC)$_2$P][Cl], 3.2c[Cl]

A colourless solution of ^{i}Pr-NHC (0.282 g; 1.564 mmol) in thf (10 mL) was added to a colourless solution of PCl_3 (0.072 g; 0.521 mmol) in thf (10 mL), which resulted in the rapid formation of a yellow precipitate. The mixture was left to stir for 16

hours. Volatile components were removed under reduced pressure to produce a pale yellow powder. Yield: 55% (0.123 g; 0.289 mmol). $^{31}P\{^{1}H\}$ NMR: -124.2 (s). $^{13}C\{^{1}H\}$ NMR: 11.0 (s), 21.2 (s), 51.5 (s), 128.1 (s). ^{1}H NMR: 1.66 (d, $^{3}J_{HH}$ = 6.7, 24H), 2.25 (s, 12H), 4.50 (septet, $^{3}J_{HH}$ = 6.8, 4H). HR-ESI-MS Calcd. For $C_{22}H_{40}ClN_4P$ $[M - Cl]^+$: *m/z* = 391.2990. Found 391.2986 (1.0 ppm).

Preparation of [(Me-NHC)$_2$P][BPh$_4$], 3.2a[BPh$_4$]

A colourless solution of Me-NHC (0.034 g; 0.274 mmol) in thf (10 mL) was added to a colourless solution of [(dppe)P][BPh$_4$] (0.102 g; 0.137 mmol) in thf (10 mL), which resulted in the formation of a dark yellow solution. The mixture was left to stir for 16 hours. Volatile components were removed under reduced pressure to produce a yellow powder, which was washed with toluene to remove the free dppe. Yield: 76% (0.062 g; 0.104 mmol). $^{31}P\{^{1}H\}$ NMR: -112.8 (s). $^{11}B\{^{1}H\}$ NMR: 6.8 (s). $^{13}C\{^{1}H\}$ NMR: 9.1 (s), 34.0 (s), 122.2 (s), 126.1 (s), 126.7 (s), 136.4 (s), 164.6 (q $^{1}J_{CB}$ = 49). ^{1}H NMR: 2.20 (s, 12H), 3.40 (s, 12H), 7.34 (m, 20H). HR-ESI-MS Calcd. For $C_{38}H_{44}BN_4P$ $[M - BPh_4]^+$: *m/z* = 279.1738. Found 279.1617 (43.3 ppm).

Preparation of [(Et-NHC)$_2$P][BPh$_4$], 3.2b[BPh$_4$]

An orange solution of Et-NHC (0.049 g; 0.321 mmol) in thf (10 mL) was added to a colourless solution of [(dppe)P][BPh$_4$] (0.120 g; 0.160 mmol) in thf (10 mL), which resulted in the formation of a yellow solution. The mixture was left to stir for 16 hours. Volatile components were removed under reduced pressure to produce a yellow powder, which was washed with toluene to remove the free dppe. Yield: 67% (0.070 g; 0.107

mmol). $^{31}P\{^1H\}$ NMR: -126.5 (s). $^{11}B\{^1H\}$ NMR: -6.9 (s). $^{13}C\{^1H\}$ NMR: 8.2 (s), 15.3 (s), 42.3 (s), 121.9 (s), 125.7 (s), 126.3 (s), 135.5 (s), 164.2 (q, $^1J_{BC}$ = 49). ^1H NMR: 0.829 (m, 6H), 1.70 (s, 6H), 4.09 (m, 4H), 7.28 (m, 20H). HR-ESI-MS Calcd. For $C_{42}H_{52}BN_4P$ $[M - BPh_4]^+$: *m/z* = 335.2364. Found 335.2349 (4.5 ppm).

Preparation of [(^{i}Pr-NHC)$_2$P][BPh$_4$], 3.2c[BPh$_4$]

A colourless solution of ^{i}Pr-NHC (0.069 g; 0.383 mmol) in thf (10 mL) was added to a colourless solution of [(dppe)P][BPh$_4$] (0.143 g; 0.191 mmol) in thf (10 mL), which resulted in the formation of a yellow solution. The mixture was left to stir for 16 hours. Volatile components were removed under reduced pressure to produce a yellow powder, which was washed with toluene to remove the free dppe. Yield: 72% (0.098 g; 0.138 mmol). $^{31}P\{^1H\}$ NMR: -126.1 (s). $^{11}B\{^1H\}$ NMR: -6.9 (s). $^{13}C\{^1H\}$ NMR: 11.0 (s), 21.2 (s), 51.6 (s), 122.2 (s), 127.2 (s), 127.9 (s), 136.5 (s), 164.6 (q, $^1J_{CB}$ = 49). ^1H NMR: 1.58 (d, $^3J_{HH}$ = 6.6, 24H), 2.12 (s, 12H), 4.41 (m, 4H), 7.33 (m, 20H). HR-ESI-MS Calcd. For $C_{46}H_{60}BN_4P$ $[M - BPh_4]^+$: *m/z* = 391.2990. Found 391.2978 (3.1 ppm).

Preparation of [(Ph-N$_3$HC)$_2$P][BPh$_4$], 3.2g[BPh$_4$]

A colourless solution of Ph-N$_3$HC (0.142 g; 0.480 mmol) in thf (10 mL) was added to a colourless solution of [(dppe)P][BPh$_4$] (0.180 g; 0.240 mmol) in thf (10 mL), which resulted in the formation of an orange solution. The mixture was left to stir for 16 hours. Volatile components were removed under reduced pressure to produce a bright orange powder, which was washed with toluene to remove the free dppe. Yield: 88% (0.198 g; 0.210 mmol). $^{31}P\{^1H\}$ NMR: -96.8 (s). $^{11}B\{^1H\}$ NMR: -6.8 (s). $^{13}C\{^1H\}$

NMR: 121.9 (s), 122.9 (s), 125.8 (s), 128.7 (s), 128.9 (s), 129.4 (s), 129.7 (s), 130.8 (s), 131.8 (s), 132.3 (s), 132.9 (s), 136.2 (s), 136.8 (s), 138.7 (s), 153.7 (s), 164.4 (q, $^1J_{BC}$ = 49). ^{1}H NMR: 6.92 (m, 3H), 7.05 (m, 3H), 7.17 (m, 6H), 7.38 (m, 26 H), 7.61 (m, 6H), 7.73 (m, 6H). HR-ESI-MS Calcd. For $C_{64}H_{50}BN_6P$ $[M - BPh_4]^+$: m/z = 625.2270. Found 625.2208 (9.9 ppm).

Table 3-1 - Summary of X-ray Crystallographic Data for Compounds 3.2c[Cl] and 3.4a[Cl]$_3$.

Compound	**3.2c[Cl]**	**3.4a[Cl]$_3$**
Empirical formula	$C_{29}H_{48}ClN_4P$	$C_{14}H_{26}Cl_3N_4P$
Formula weight	519.13	387.71
Crystal system	Triclinic	Monoclinic
Space group	*P-1*	$P2_1/c$
Unit cell dimensions:		
a (Å)	10.134(3)	8.107(3)
b (Å)	12.243(3)	13.353(4)
c (Å)	13.037(3)	17.997(6)
α (°)	103.358(4)	90
β (°)	99.906(5)	101.669(4)
γ (°)	100.772(4)	90
Volume (Å^3)	1506.3(7)	1908.0(11)
Z	2	4
Density (calc'd) (g cm^{-3})	1.145	1.350
Abs. coef. (mm^{-1})	0.203	0.566
F(000)	564	816
θ range for data collection (°)	1.65 to 27.49	1.91 to 27.49
Limiting indices	$-13 \le h \le 12$ $-15 \le k \le 15$ $-16 \le l \le 16$	$-10 \le h \le 10$ $-17 \le k \le 17$ $-23 \le l \le 22$
Reflections collected	10360	20987
Independent reflections	6428	4336
R_{int}	0.0180	0.0833
Data / restraints / parameters	6428 / 0 / 477	4336 / 0 / 215
Goodness-of-fit on F^2	1.094	1.022
Final *R* indices[a] [I>2s(I)]	$R1 = 0.0524$ $wR2 = 0.1425$	$R1 = 0.0729$ $wR2 = 0.1787$
R indices (all data)	$R1 = 0.0754$ $wR2 = 0.1560$	$R1 = 0.1307$ $wR2 = 0.2113$
Largest difference map peak and hole (e Å^{-3})	0.788 and -0.509	1.160 and -0.628

Table 3-2 - Selected Metrical Parameters for Compounds 3.2[Cl] and 3.4a[Cl]$_3$.

Parameter	3.2c[Cl]	3.4a[Cl]$_3$
Distances (Å)		
P(1)-C(12)	1.824(2)	1.824(4)
P(1)-C(22)	1.823(2)	1.850(4)
P(1)-H(1)		1.33(3)
P(1)-H(2)		1.23(4)
C(12)-N(11)	1.359(2)	1.338(5)
C(12)-N(13)	1.361(3)	1.338(5)
C(22)-N(21)	1.368(3)	1.336(5)
C(22)-N(23)	1.357(3)	1.338(5)
Angles (°)		
C(12)-P(1)-C(22)	97.35(9)	95.85(19)
C(22)-P(1)-C(12)-N(11)	-61.6(2)	-111.0(4)
C(12)-P(1)-C(22)-N(21)	131.2(2)	-116.0(4)

3.3 Results and Discussion

Synthesis Employing PCl_3 Reduction

As illustrated in Equation 3.2, the reaction of phosphorus trichloride with three equivalents of NHCs produces salts of the type $[(NHC)_2P][Cl]$, **3.2**[Cl], in essentially quantitative yield. The additional equivalent of NHC is required to sequester the reactive Cl_2 by-product that is generated during the reduction of the P^{III} centre. As outlined in Table 3-3, this method works for a variety of NHCs bearing relatively small (R^1 = Et, ^{i}Pr) and certain larger (R^1 = Mes) substituents at the nitrogen centres. In contrast, the reactions of NHCs bearing considerably bulkier substituents (R^1 = ^{t}Bu, Ad) on nitrogen do not produce the desired products. The progress of these reactions is readily monitored by multinuclear (^{1}H, ^{13}C and ^{31}P) NMR spectroscopy given the distinctive signals of the starting materials and products. For example, the ^{31}P chemical shift of **3.2b**, **3.2c** and **3.2f** are all around -125 ppm. It should be noted that the formation of **3.2** by such a

coordination chemistry approach is perhaps surprising given the more typical formation of carbene-phosphenium adducts (i.e. [NHC-PR_2][X]) from the reaction of an NHC with halophosphines.[27]

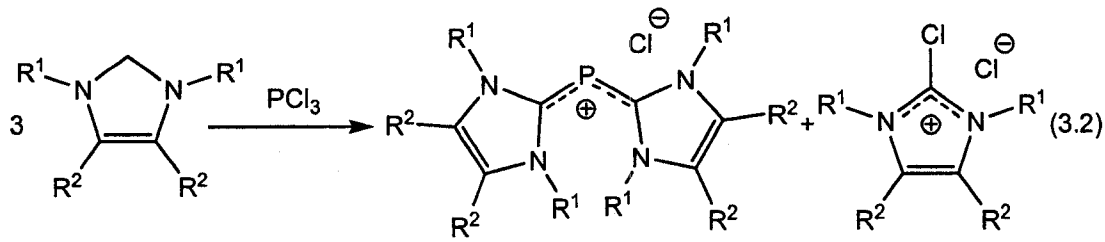

3.1a-f **3.2a-f**

Table 3-3 - ^{31}P NMR data from reactions outlined in Equation 3.2.

NHC label	R^1	R^2	δ^a
3.1a	Me	Me	-114.8
3.1b	Et	Me	-127.4
3.1c	^{i}Pr	Me	-124.2
3.1d	^{t}Bu	H	N
3.1e	Ad	H	N
3.1f	Mes	H	-124.2

[a] ^{31}P NMR chemical shift in ppm;
N = reaction does proceed as depicted in Equation 3.2.

Synthesis Employing Substitution of [(dppe)P][BPh_4]

An alternative synthetic method, illustrated in Equation 3.3, that can be used to obtain salts of **3.2** is the NHC replacement of bis(diphenylphosphino)ethane (dppe) from the P^I sources such as [(dppe)P][BPh_4], **3.3**[BPh_4] (Chapter 2). Thus the treatment of salts of **3.3** with at least two equivalents of various NHCs results in the formation of salts **3.2**[BPh_4] and the concomitant liberation of dppe. This approach is conceptually similar that used by Arduengo, Cowley and co-workers for the synthesis of NHC-phosphinidene adducts.[28,29] The major advantages of this method over the one outlined in Equation 3.2 are reduced amount of NHC required and that the dppe by-product may be readily

removed by washing with non-polar solvents. Furthermore, this method can also be used with salts of **3.3** with a variety of anions, under the condition that they are non-reactive towards NHCs.

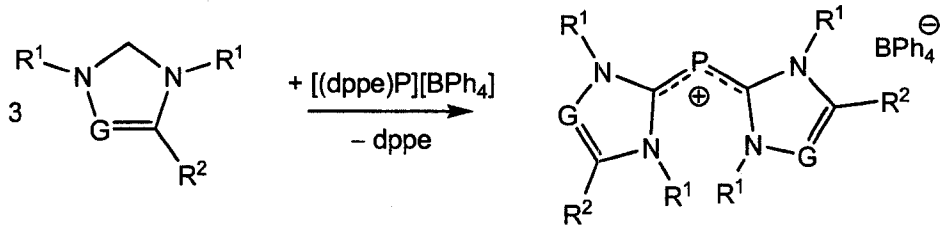

3.1a-g **3.2a-g** (3.3)

Table 3-4 - ^{31}P NMR data from reactions outlined in Equation 3.3.

NHC label	R^1	R^2	G	δ^a
3.1a	Me	Me	CMe	-112.8
3.1b	Et	Me	CMe	-126.5
3.1c	^{i}Pr	Me	CMe	-126.1
3.1d	^{t}Bu	H	CH	BP
3.1e	Ad	H	CH	BP
3.1f	Mes	H	CH	BP
3.1g	Ph	Ph	N	-96.8

[a] ^{31}P NMR chemical shift in ppm; BP = the expected free dppe by-product is observed, however **3.2** is not detected by ^{31}P NMR.

X-ray Crystallography Studies

A depiction of the molecular structure of the salt **3.2c**[Cl] · toluene is presented in Figure 3.1. The salt crystallizes in the space group *P-1* and the metrical parameters of the cation, summarized in Table 3-2, in this salt provide insight into the nature of the bonding in such species. Importantly, there are no unusually short interionic contacts. In regard to the P^I cation, the C-P bonds of 1.824(2) and 1.823(2) Å are typical of P-C_{aryl} single bonds and are significantly longer than those reported previously (1.746(4) Å to 1.794(2) Å) for NHC-phoshinidene adducts.[28,29] The bond distances and angles within the heterocycles are consistent with those of related NHC-P adducts found in the Cambridge

Structural Database.[30] The C-P-C angle of 97.35(9)° is much smaller than the angles observed in the only three somewhat comparable cations that have been structurally characterised.13,14,15 Perhaps the most notable feature in the structure of the cation is the twisting (*ca.* 50° to 60°) of the NHC heterocycles from the C-P-C plane. Such twisting should diminish or preclude the interaction of the π-system on the NHC rings with the filled 3p orbital on the P atom, which is discussed below in the computational studies.

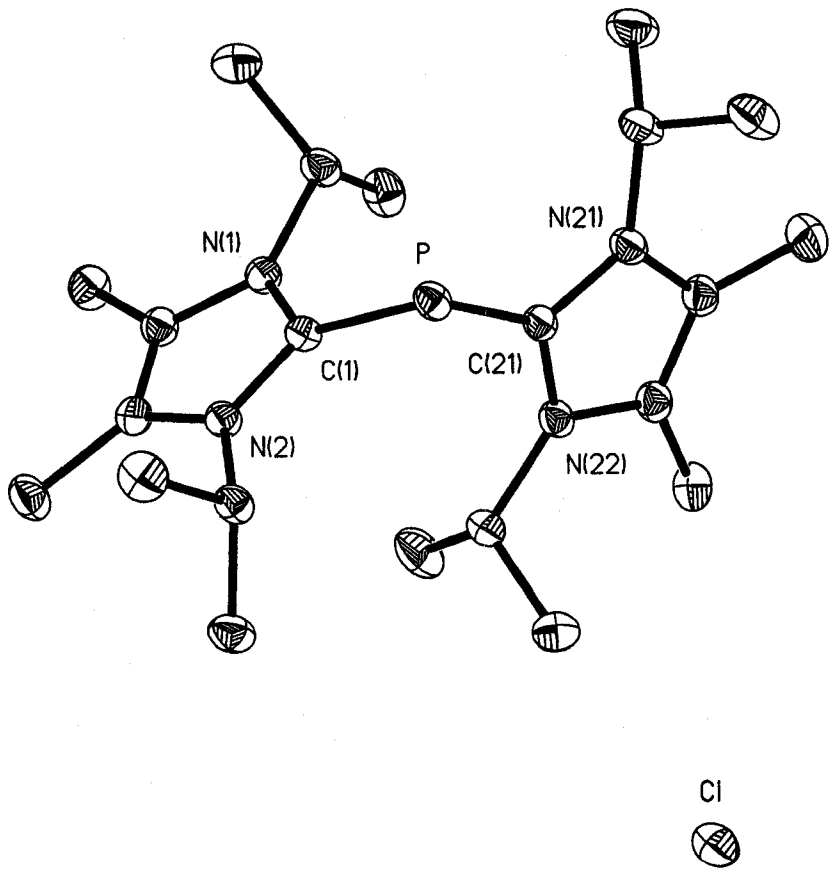

Figure 3.1 - Thermal ellipsoid plot (30% probability surface) of a cation and anion of 3.2c[Cl]. Hydrogen atoms and a molecule of toluene are omitted for clarity.

In an attempt to obtain suitable crystals of **3.2a**[Cl], the crude product was dissolved in dichloromethane. Following slow evaporation of the solvent at ambient temperature in a glove box, crystals amenable to single crystal X-ray diffraction were deposited in the solution. The resulting molecular structure was not that of **3.2a**[Cl], but rather the product of the oxidation (see Chapter 1) of **3.2a**[Cl] by two equivalents of hydrochloric acid, **3.4a**$[Cl]_3$ (Equation 3.4). The molecular structure is shown in Figure 3.1 and selected metrical parameters are compiled in Table 3-2.

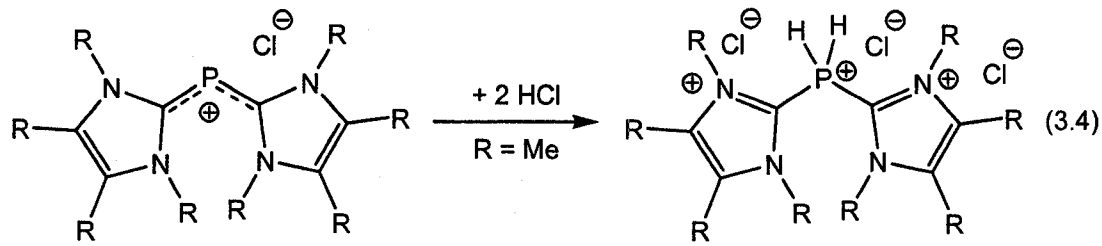

(3.4)

3.2a[Cl] **3.4a**$[Cl]_3$

The salt **3.4a**$[Cl]_3$ crystallizes in the space group $P2_1/c$ with the complete trication and the three anions in the asymmetric unit. There are no unusually close contacts between the trication and anions; the shortest distance of 2.688(4) Å is between Cl(1) and a hydrogen atom on one of the methyl groups. The distances between the phosphorus atom and the carbon centres of the carbenes (1.824(4) and 1.850(4) Å) do not lengthen significantly upon oxidation, as compared with **3.2c**[Cl] (1.823(2) and 1.824(2) Å).[31] This is unexpected in light of the short P-P distances observed in the phosphine analogues attributed to partial multiple bonding (Chapter 2) and is further discussed below. The C-P-C of 95.85(19)° is more acute than those observed in other dihydrophosphnium cations (cf. 110.87(16)°)[32] in the Cambridge Structural Database (CSD).[30] The *N*-heterocyclic carbene rings are twisted away from the C-P-C plane (-111.0(4) and -116.0(4)°), as

would be expected with no available orbitals on phosphorus to interact with the "empty" $2p_x$ orbital on the carbenic centres.

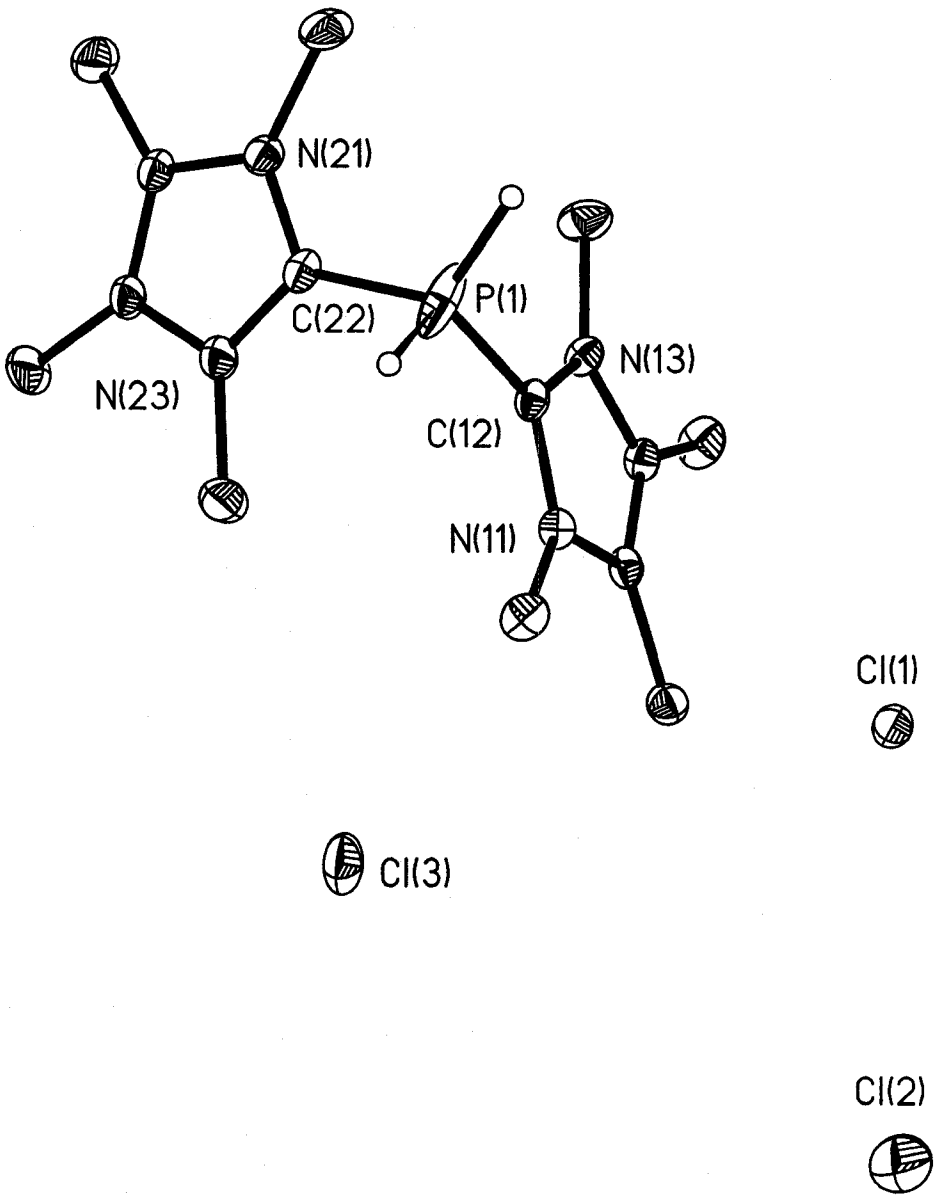

Figure 3.2 - Thermal ellipsoid plot (30% probability surface) of a cation and anion of 3.4a[Cl]$_3$. Most of the hydrogen atoms have been removed for clarity.

Computational Studies

Since the elongated P-C bonds and the twisting of NHC heterocycles from the C-P-C plane in the molecular structure of **3.2c** are not consistent with the presence of multiple-bonding, we elected to perform a series of Density Functional Theory (DFT) calculations to elucidate the nature of the electronic structure in cations such as **3.2** using the model **3.2h** (R_1,R_2 = H). The bending at the P atom in **3.2c** is inconsistent with a classical allene-type "P^V" bonding model (**A** in Figure 3.2) thus some more probable bonding models for such cations are shown in Figure 3.2.

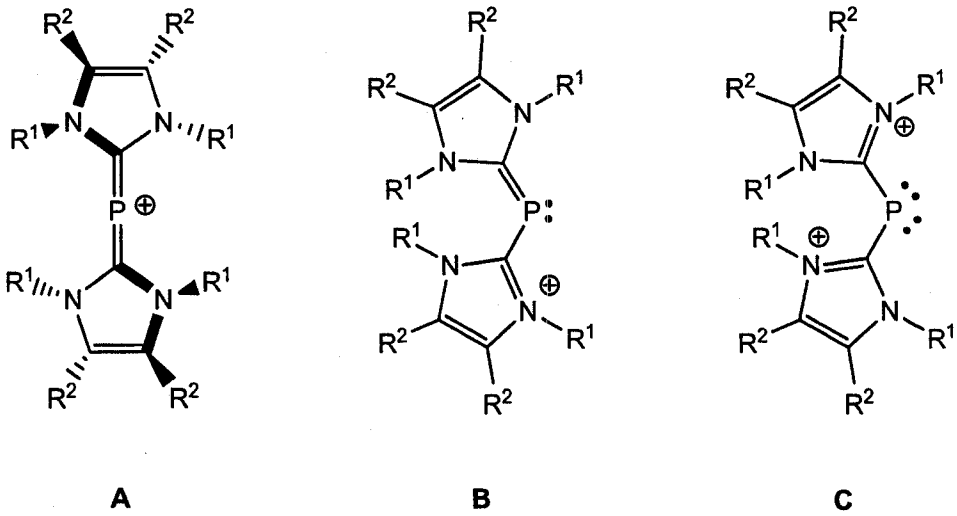

Figure 3.3 - Some possible Lewis-type depictions of 3.2.

The twisting of the NHC heterocycles is accurately predicted by the calculations (the C_2 symmetry isomer being the only true minimum on the potential energy surface) and such distortions diminish the effective overlap of the π-systems on the NHC fragments with the 3p orbital on P. Thus the twisting of the NHC fragments and the long P-C distances (1.799 Å calculated for **3.2h**) would suggest that the "P^I" model **C** in Figure 3.2 is the best representations of the electronic structure in such cations. It must

be noted that, however, in spite of the calculated ca. 36° C-P-C-N torsion angle, there is clear evidence for some interaction between the π systems on the NHC ligands and the 3p orbital on P in both the appearance of the HOMO-2 orbital in **3.2h** (Figure 3.3) and in the results of the electron population analyses. The presence of π-delocalization is also evident in the distinctive bright yellow colours exhibited by the real ions thus it appears that a "P^{III}" canonical structure of the type **B** is not completely prevented by the distortion of the cation from planarity.

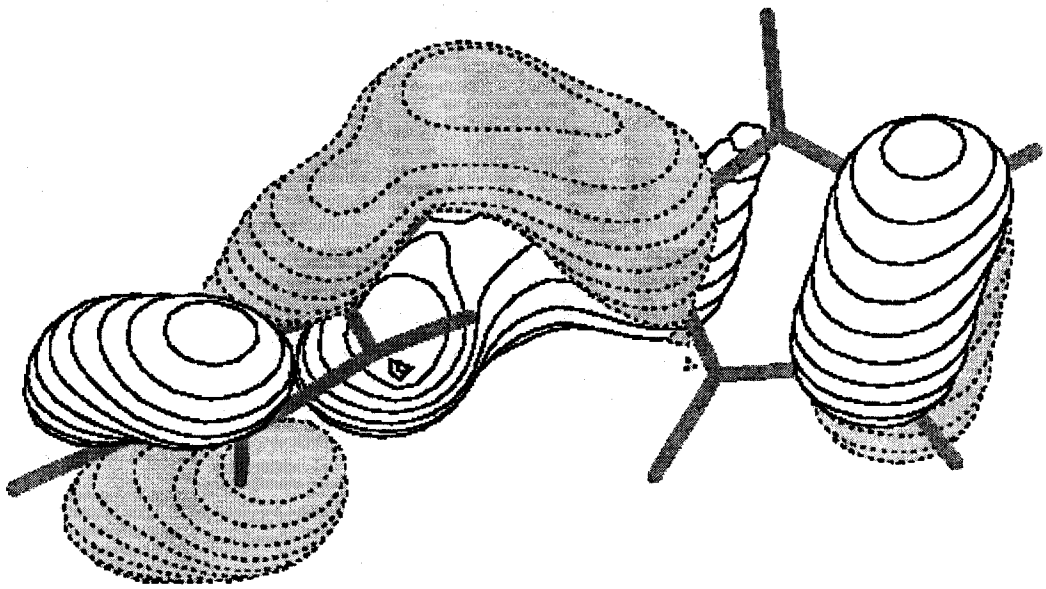

Figure 3.4 - MOLDEN depiction of the third highest occupied molecular orbital (HOMO-2).

The apparent relative unfavourability of the cations **3.2d** and **3.2e** may be rationalized using the results of semi-empirical calculations that were performed with Fujitsu's CAChe 6.0 suite of programs.[34] The optimization of complete model cations at

the PM3 level of theory suggests that bulky substituents on N result in much longer P-C distances (>1.9Å) and C-P-C angles (>111°). Single-point DFT calculations on appropriate models derived from the semi-empirical results reveal that such distortions in the metrical parameters destabilize the cations and thus may render them more amenable to decomposition.

The experimental results outlined above suggest that an alternative mechanism to that outlined in Equation 3.1 is conceivable for the formation of phosphamethine cyanine salts from the reaction of electron rich olefins with P^I sources such as **3.3**. It appears possible that the reaction may occur by way of NHCs generated in situ by the thermolysis of the electron rich olefins.[35]

3.5 Conclusions

In conclusion, we have shown that NHCs can be used as effective ligands for P^I cations and that a number of new, convenient and safe synthetic approaches can be used to obtain salts of such species. We are currently proving the generality of these synthetic approaches with other stable carbenes and other Group 15 elements. We have also presented structural and computational evidence for an improved understanding of the nature of the bonding in this historically important type of phosphorus cation.

3.6 Prospective Developments

Experiments have shown that carbene-stabilized cations discussed above may also be also generated from a variety of existing P^I sources including acyclic cations $(Ph_3P)_2P^+$ and $((Me_2N)_3P)_2P^+$. The application of *N*-heterocyclic carbenes to stabilize P^I centres

opens a wide range of potential new cations, both acyclic and cyclic, given the scope of available stable carbenes. Preliminary investigations involving anionic carbenes have successfully resulted in the generation of anionic P^I molecules, however thus far the reactions are not clean, producing multiple by-products. The existing methodologies should prove amenable to synthesizing the As^I analogues (historically called arsamethine cyanine cations[36]), of which there are significantly fewer examples. Initial reactions have also begun towards extending the methodology to neutral low oxidation state Group 14 (E) compounds. Compounds of the type NHC-E-NHC are related to carbodiphosphoranes[37] as well as allenes and their heavier analogues.[38,39] Initial strategies involve the reduction of Group 14 halide compounds in the presence of carbenes (Equation 3.5). Substitution of the phosphines in carbodiphosphoranes by carbenes presents an alternative pathway to the carbene-stabilized C^0 species.

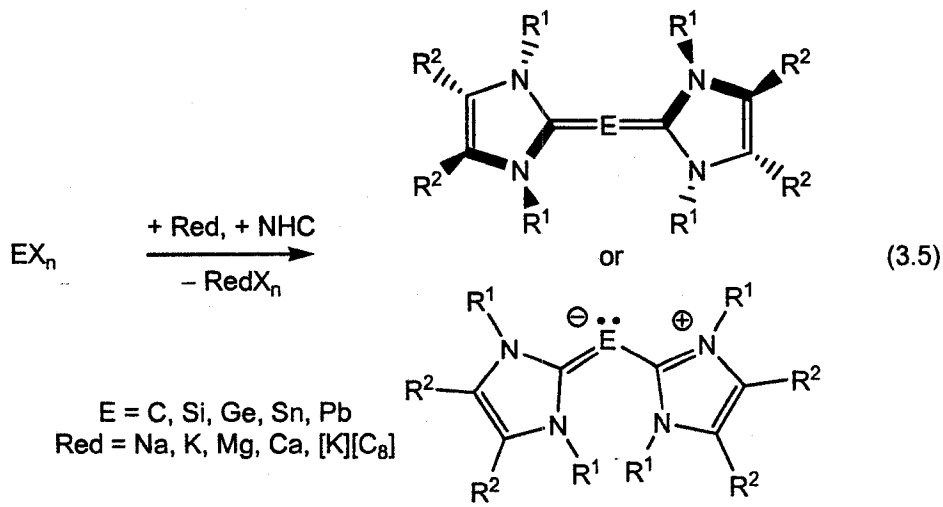

(3.5)

3.7 References

1. Schmidpeter, A. in *Multiple Bonds and Low Coordination in Phosphorus Chemistry*, 1990, M. Regitz and O. J. Scherer (Ed), Stuttgart: Georg Thieme Verlag, 2-Phosphaallylic Cations, pp. 149-154.
2. Dimroth, K., *Fortschr. Chem. Forsch.*, **1973**, *38*, 1-147.
3. Dimroth, K. and Hoffmann, P., *Angew. Chem., Int. Ed. Engl.*, **1964**, *3*, 384.
4. Dimroth, K. and Hoffmann, P., *Chem. Ber.*, **1966**, *99*, 1325-1331.
5. Schmidpeter, A., Lochschmidt, S. and Willhalm, A., *Angew. Chem., Int. Ed. Engl.*, **1983**, *22*, 545-546.
6. Schmidpeter, A., Lochschmidt, S. and Willhalm, A., *Angew. Chem. Suppl.*, **1983**, 710-717.
7. Arduengo, A.J., III, Harlow, R.L. and Kline, M., *J. Am. Chem. Soc.*, **1991**, *113*, 361-363.
8. Arduengo, A.J., III, *Acc. Chem. Res.*, **1999**, *32*, 913-921.
9. Bourissou, D., Guerret, O., Gabbaie, F.P. and Bertrand, G., *Chem. Rev.*, **2000**, *100*, 39-91.
10. Pangborn, A.B., Giardello, M.A., Grubbs, R.H., Rosen, R.K. and Timmers, F.J., *Organometallics*, **1996**, *15*, 1518-1520.
11. Kuhn, N. and Kratz, T., *Synthesis*, **1993**, 561-562.
12. Enders, D., Breuer, K., Kallfass, U. and Balensiefer, T., *Synthesis*, **2003**, 1292-1295.

13. Arduengo, A.J., III, Krafczyk, R., Schmutzler, R., Craig, H.A., Goerlich, J.R., Marshall, W.J. and Unverzagt, M., *Tetrahedron*, **1999**, *55*, 14523-14534.

14. Ellis, B.D. and Macdonald, C.L.B., *Inorg. Chem.*, **2006**, *45*, 6864-6874.

15. Frisch, M.J., Trucks, G.W., Schlegel, H.B., Scuseria, G.E., Robb, M.A., Cheeseman, J.R., Zakrzewski, V.G., Montgomery, V.G., Jr., Stratmann, R.E., Burant, J.C., Dapprich, S., Millam, J.M., Daniels, A.D., Kudin, K.N., Strain, M.C., Farkas, O., Tomasi, J., Barone, V., Cossi, M., Cammi, R., Mennucci, B., Pomelli, C., Adamo, C., Clifford, S., Ochterski, J., Petersson, G.A., Ayala, P.Y., Cui, Q., Morokuma, K., Salvador, P., Dannenberg, J.J., Malick, D.K., Rabuck, A.D., Raghavachari, K., Foresman, J.B., Cioslowski, J., Ortiz, J.V., Baboul, A.G., Stefanov, B.B., Liu, G., Liashenko, A., Piskorz, P., Komaromi, I., Gomperts, R., Martin, R.L., Fox, D.J., Keith, T., Al-Laham, M.A., Peng, C.Y., Nanayakkara, A., Challacombe, M., Gill, P.M.W., Johnson, B., Chen, W., Wong, M.W., Andres, J.L., Gonzalez, C., Head-Gordon, M., Replogle, E.S. and Pople, J.A., *Gaussian98*, Revision A.11.1, 2001, Pittsburgh, PA: Gaussian, Inc.

16. Becke, A.D., *J. Chem. Phys.*, **1993**, *98*, 5648-5652.

17. Perdew, J.P. and Wang, Y., *Phys. Rev. B: Condens. Matter*, **1992**, *45*, 13244-13249.

18. Reed, A.E., Curtiss, L.A. and Weinhold, F., *Chem. Rev.*, **1988**, *88*, 899-926.

19. *SMART, Molecular Analysis Research Tool*, 2001, Madison, WI: Bruker AXS, Inc.

20. *SAINTPlus, Data Reduction and Correction Program*, 2001, Madison, WI: Bruker AXS, Inc.

21. *SADABS, An Empirical Absorption Correction Program*, 2001, Madison, WI: Bruker AXS, Inc.

22. Sheldrick, G.M., *SHELXS-97*, 1997, Gottingen: Universitat Gottingen.

23. Altomare, A., Burla, M.C., Camalli, M., Cascarano, G.L., Giacovazzo, C., Guagliardi, A., Moliterni, A.G.G., Polidori, G. and Spagna, R., *J. Appl. Crystallogr.*, **1999**, *32*, 115-119.

24. Farrugia, L.J., *J. Appl. Crystallogr.*, **1999**, *32*, 837-838.

25. Sheldrick, G.M., *SHELXL-97*, 1997, Gottingen: Universitat Gottingen.

26. Sheldrick, G.M., *SHELXTL*, 2001, Madison, WI: Bruker AXS, Inc.

27. Burford, N. and Ragogna, P.J., *J. Chem. Soc., Dalton Trans.*, **2002**, 4307-4315.

28. Arduengo, A.J., III, Carmalt, C.J., Clyburne, J.A.C., Cowley, A.H. and Pyati, R., *Chem. Commun.*, **1997**, 981-982.

29. Arduengo, A.J., III, Calabrese, J.C., Cowley, A.H., Dias, H.V.R., Goerlich, J.R., Marshall, W.J. and Riegel, B., *Inorg. Chem.*, **1997**, *36*, 2151-2158.

30. Allen, F.H., *Acta Crystallogr., Sect. B: Struct. Sci.*, **2002**, *B58*, 380-388.

31. Ellis, B.D., Dyker, C.A., Decken, A. and Macdonald, C.L.B., *Chem. Commun.*, **2005**, 1965-1967.

32. Dornhaus, F., Lerner, H.W. and Bolte, M., *Acta Crystallogr., Sect. E: Struct. Rep. Online*, **2005**, *E61*, o448-o449.

33. Schaftenaar, G. and Noordik, J.H., *J. Comput.-Aided Mol. Des.*, **2000**, *14*, 123-134.

34. *CAChe WorkSystem Pro*, Version 6.1.12.33, 2004, Fujitsu Limited.

35. Denk, M.K., Hatano, K. and Ma, M., *Tetrahedron Lett.*, **1999**, *40*, 2057-2060.

36. Maerkl, G. and Lieb, F., *Tetrahedron Lett.*, **1967**, 3489-3493.

37. Ramirez, F., Desai, N.B., Hansen, B. and McKelvie, N., *J. Am. Chem. Soc.*, **1961**, *83*, 3539-3540.

38. Ishida, S., Iwamoto, T., Kabuto, C. and Kira, M., *Nature*, **2003**, *421*, 725-727.

39. Iwamoto, T., Abe, T., Kabuto, C. and Kira, M., *Chem. Commun.*, **2005**, 5190-5192.

Chapter 4 – Coordination of P^I Cations to Main Group and Transition Metal Acceptors

4.1 Introduction

The chemistry of low coordinate phosphorus compounds has been of an increasing interest over the past two decades.[1-3] The information gained from studying the synthesis and reactivity of the compounds has lead to an improved understanding of their structure and bonding and subsequently guided further investigations. These studies typically involve phosphorus in either of its common oxidation states: +3 or +5.[4] Whereas in recent years there has been increased attention in the synthesis of cations containing phosphorus in lower oxidations,[5-7] the successive investigations into their reactivity has been limited.

Schmidpeter *et al.*, who synthesized the first "triphosphenium" cation,[8] showed that acyclic P^I cations are readily oxidized from to P^{III} dications by mild oxidizing agents such as alkyl halides.[9] Conversely, cyclic cations are more resistant to oxidation and require harsher conditions such as halide extraction from CH_2Cl_2 by $AlCl_3$ to afford the oxidized dications.[10,11] Although reactions with methyl iodide showed no evidence of oxidation in the ^{31}P NMR data, the stronger oxidizing agent methyl triflate partially converts a variety of cyclic cations to dications, however the addition of even four equivalents of MeOTf to the P^I cations did not result in complete conversion to the methylated P^{III} species.[12] Protonation of the acyclic cation $P(PPh_3)_2^+$ can be achieved by HCl,[9] whereas again the cyclic derivatives require stronger conditions such as triflic acid or a 1:1 mixture of $AlCl_3$ and ^tBuCl, which is reported to generate H^+ *in situ*.[11]

Coordination of triphosphenium cations to $AlCl_3$ to form mono-adducts has only been reported to occur for the acyclic cations $P(P(NMe_2)_3)_2^+$ **4.1** and $P(P(NMe_2)_3)(PPh_3)^+$ **4.2**, although this is solely on the basis of ^{31}P NMR data.[13,14] The only examples of the coordination of triphosphenium-like species to Transition Metal fragments come from the related anionic P^I species $P(P(OR)_2O)_2^-$, in which the P^I centres have been shown to coordinate with either one or two Group 6 carbonyl complexes, many of which have been confirmed through crystallographic investigations.[15-18]

We have sought to further investigate the coordination chemistry of cyclic triphosphenium cations **4.3** and **4.4**, with non-coordinating anions, with both Main Group and Transition Metal acceptors. The availability of two "lone pairs" of electrons afforded by the low oxidation state of phosphorus could allow for either mono- or di-coordination of traditional Lewis acids such as $AlCl_3$ as well as coordination to transition metal fragments.

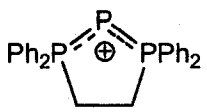

4.3

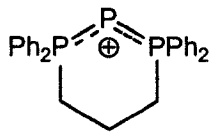

4.4

4.2 Experimental

Reagents and General Procedures. All manipulations were carried out using standard inert-atmosphere techniques. Chromium carbonyl, molybdenum carbonyl, tungsten carbonyl and iron nonacarbonyl were purchased from Strem Chemicals Inc. and all other chemicals and reagents were obtained from Aldrich; gallium(III) chloride was sublimed prior to use and all other reagents were used without further purification.

CD_2Cl_2 was dried over calcium hydride and all other solvents were dried on a series of Grubbs' type columns[19] and were degassed prior to use. The compounds [(dppe)P][BPh_4] **4.3** and [(dppp)P][BPh_4] **4.4** were synthesized by following literature procedures.[20] Obtaining pure products has proved difficult as multiple equivalents of a given Lewis acid are needed to yield even the mono-adducts, which often appear concurrently with the bis-adducts under such conditions. Only $^{31}P\{^1H\}$ NMR data is presented below which is highly diagnostic of the coordination environment of the P^I centre.

Instrumentation. NMR spectra were recorded at room temperature in CD_2Cl_2 solutions on a Bruker Avance 300 MHz spectrometer. Chemical shifts are reported in ppm, relative to external standards (85% aq. H_3PO_4 for ^{31}P). Coupling constant magnitudes, $|J|$, are given in Hz. High resolution electrospray ionization (ESI) mass spectra were recorded on a Micromass LCT time-of-flight spectrometer from dichloromethane solutions in lockmass mode.

Theoretical Methods. Calculations were preformed with the Gaussian 98 suite of programs.[21] Geometry optimizations have been calculated using density functional theory (DFT), specifically implementing the B3PW91 method [containing Becke's three-parameter hybrid functional for exchange (B3, including ca. 20% Hartree-Fock exchange)[22] combined with the generalized gradient approximation for correlation of Perdew and Wang (PW91)[23]] in conjunction with the 6-31+G(d) basis set. The geometries were restricted to the highest reasonable symmetry and each stationary point was confirmed to be a minimum by having zero imaginary vibrational frequencies. The electronic energies of the molecules have been corrected by the unscaled, zero-point

vibrational energy (ZPVE). Single Point Energies have been calculated at the B3PW91/6-311+G(3df,2p)//B3PW91/6-31G(d) level of theory. Population analyses were conducted using the Natural Bond Orbital (NBO)[24] method implemented in Gaussian98.

Reaction of [(dppe)P][BPh_4] (4.3[BPh_4]) with $AlCl_3$

A colourless solution of [(dppe)P][BPh_4] (0.167 g; 0.223 mmol, **4.3**) in CH_2Cl_2 (10 mL) was added to a white slurry of $AlCl_3$ (0.089 g; 0.669 mmol) in CH_2Cl_2 (10 mL), which resulted in the formation of a cloudy white mixture. The mixture was left to stir for 16 hours. The solution had become pale yellow and very little insoluble material remained. Volatile components were removed under reduced pressure to produce a pale brown film on the bottom of the flask. A yield could not be determined. $^{31}P\{^1H\}$ NMR: -233.9 (t, $^1J_{PP}$ = 454, **4.3**), -77.7 (t, $^1J_{PP}$ = 283, **4.3**-$AlCl_3$), 52.3 (d, $^1J_{PP}$ = 283, **4.3**-$AlCl_3$), 64.3 (d, $^1J_{PP}$ = 454, **4.3**).

Reaction of [(dppe)P][BPh_4] (4.3[BPh_4]) with a Large Excess of $AlCl_3$

A colourless solution of [(dppe)P][BPh_4] (0.229 g; 0.306 mmol, **4.3**) in CH_2Cl_2 (10 mL) was added to a white slurry of $AlCl_3$ (0.408 g; 3.059 mmol) in CH_2Cl_2 (15 mL), which resulted in the formation of a cloudy pale red mixture. The mixture was left to stir for 16 hours. The solution had become darker red and some insoluble red material had formed. Volatile components were removed under reduced pressure to produce a dark brown oil on the bottom of the flask. A yield could not be determined. $^{31}P\{^1H\}$ NMR: -153.7 (t, $^1J_{PP}$ = 238, **4.3**-$(AlCl_3)_2$), 53.1 (d, $^1J_{PP}$ = 238, **4.3**-$(AlCl_3)_2$).

Reaction of [(dppe)P][BPh_4] (4.3[BPh_4]) with $GaCl_3$

A colourless solution of [(dppe)P][BPh_4] (0.146 g; 0.195 mmol, **4.3**) in CH_2Cl_2 (10 mL) was added to a colourless solution of $GaCl_3$ (0.069 g; 0.390 mmol) in CH_2Cl_2 (10 mL), which resulted in a colourless solution. The mixture was left to stir for 16 hours. The solution had no noticeable colour change. Volatile components were removed under reduced pressure to produce a white powder. Yield: 0.149 g (mixture of **4.3**-$GaCl_3$ and free $GaCl_3$). $^{31}P\{^1H\}$ NMR: -96.1 (t, $^1J_{PP}$ = 289, **4.3**-$GaCl_3$), 53.1 (d, $^1J_{PP}$ = 289, **4.3**-$GaCl_3$).

Reaction of [(dppe)P][BPh_4] (4.3[BPh_4]) with a Large Excess of $GaCl_3$

A colourless solution of [(dppe)P][BPh_4] (0.218 g; 0.291 mmol, **4.3**) in CH_2Cl_2 (10 mL) was added to a colourless solution of $GaCl_3$ (0.513 g; 2.912 mmol) in CH_2Cl_2 (15 mL), which resulted in a red solution. The mixture was left to stir for 16 hours. The solution had become darker red and no precipitate had formed. Volatile components were removed under reduced pressure to produce a dark brown oil on the bottom of the flask. A yield could not be determined. $^{31}P\{^1H\}$ NMR: -153.8 (t, $^1J_{PP}$ = 238, **4.3**-$(GaCl_3)_2$), 53.0 (d, $^1J_{PP}$ = 289, **4.3**-$(GaCl_3)_2$).

Reaction of [(dppp)P][BPh_4] (4.4[BPh_4]) with $Cr(CO)_5$(thf)

A slurry of $Cr(CO)_6$ (0.216 g; 0.776 mmol) in thf (15 mL) was irradiated for 1 hour and it was then sparged with nitrogen for fifteen minutes to generate a yellow solution of $Cr(CO)_5$(thf). The $Cr(CO)_5$(thf) solution was added to a colourless solution of [(dppp)P][BPh_4] (0.296 g; 0.388 mmol, **4.4**) in thf (10 mL) to give a yellow solution.

The mixture was left to stir for 16 hours. The solution had changed to an orange colour. Volatile components were removed under reduced pressure and the crude residue was extracted into CH_2Cl_2 (20 mL). The resulting mixture was filtered through Celite. Volatiles were again removed under reduced pressure to produce a yellow solid. Yield: 0.431 g (mixture of **4.4**-$Cr(CO)_5$ and **4.4**). $^{31}P\{^1H\}$ NMR: -210.7 (t, $^1J_{PP}$ = 424, **4.4**), -87.9 (t, $^1J_{PP}$ = 386, **4.4**-$Cr(CO)_5$), 22.3 (d, $^1J_{PP}$ = 424, **4.4**), 26.8 (d, $^1J_{PP}$ = 386, **4.4**-$Cr(CO)_5$).

Reaction of [(dppp)P][BPh_4] (4.4[BPh_4]) with $Mo(CO)_5$(thf)

A slurry of $Mo(CO)_6$ (0.137 g; 0.519 mmol) in thf (15 mL) was irradiated for 1 hour and it was then sparged with nitrogen for fifteen minutes to generate a yellow solution of $Mo(CO)_5$(thf). The $Mo(CO)_5$(thf) solution was added to a colourless solution of [(dppp)P][BPh_4] (0.198 g; 0.260 mmol, **4.4**) in thf (10 mL) to give a yellow solution. The mixture was left to stir for 16 hours. The solution had changed to an orange colour. Volatile components were removed under reduced pressure and the crude residue was extracted into CH_2Cl_2 (20 mL). The resulting mixture was filtered through Celite. Volatiles were again removed under reduced pressure to produce a brown powder. Yield: 0.198 g (mixture of **4.4**-$Mo(CO)_5$ and **4.4**). $^{31}P\{^1H\}$ NMR: -210.6 (t, $^1J_{PP}$ = 425, **4.4**), -116.4 (t, $^1J_{PP}$ = 373, **4.4**-$Mo(CO)_5$), 22.4 (d, $^1J_{PP}$ = 425, **4.4**), 24.3 (d, $^1J_{PP}$ = 373, **4.4**-$Mo(CO)_5$).

Reaction of [(dppp)P][BPh_4] (4.4[BPh_4]) with $W(CO)_5$(thf)

A slurry of $W(CO)_6$ (0.515 g; 1.465 mmol) in thf (15 mL) was irradiated for 1 hour and it was then sparged with nitrogen for fifteen minutes to generate a red solution of $W(CO)_5$(thf). The $W(CO)_5$(thf) solution was added to a colourless solution of [(dppp)P][BPh_4] (0.233 g; 0.732 mmol, **4.4**) in thf (10 mL) to give a dark red solution. The mixture was left to stir for 16 hours. No further colour change was observed. Volatile components were removed under reduced pressure and the crude residue was extracted into CH_2Cl_2 (20 mL). The resulting mixture was filtered through Celite. Volatiles were again removed under reduced pressure to produce a brown solid. Yield: 0.198 g (mixture of **4.4**-$W(CO)_5$, **4.4**-$(W(CO)_5)_2$ and **4.4**). $^{31}P\{^1H\}$ NMR: -210.3 (t, $^1J_{PP}$ = 425, **4.4**), -129.6 (t, $^1J_{PP}$ = 371, $^1J_{PW}$ = 135, **4.4**-$W(CO)_5$), -96.9.3 (t, $^1J_{PP}$ = 350, signal-to-noise too low to observe $^1J_{PW}$, **4.4**-$(W(CO)_5)_2$), 20.9 (d, $^1J_{PP}$ = 350, **4.4**-$(W(CO)_5)_2$), 21.8 (d, $^1J_{PP}$ = 371, **4.4**-$W(CO)_5$), 22.4 (d, $^1J_{PP}$ = 425, **4.4**).

Reaction of [(dppe)P][BPh_4] (4.3[BPh_4]) with $Fe_2(CO)_9$

A colourless solution of [(dppe)P][BPh_4] (0.115 g; 0.154 mmol, **4.3**) in CH_2Cl_2 (10 mL) was added to an orange slurry of $Fe_2(CO)_9$ (0.168 g; 0.461 mmol) in CH_2Cl_2 (10 mL), which resulted in the slow formation of a dark red solution. The mixture was left to stir for 16 hours. No further colour change was observed. Volatile components were removed under reduced pressure to produce a brown powder. Yield: 0.082 g (mixture of **4.3**-$Fe(CO)_4$ and other unidentified products). $^{31}P\{^1H\}$ NMR: -78.2 (t, $^1J_{PP}$ = 411, **4.3**-$Fe(CO)_4$), 50.9 (d, $^1J_{PP}$ = 411, **4.3**-$Fe(CO)_4$).

Reaction of [(dppp)P][BPh_4] (4.4[BPh_4]) with $Fe_2(CO)_9$

A colourless solution of [(dppp)P][BPh_4] (0.210 g; 0.275 mmol, **4.4**) in thf (10 mL) was added to a red solution of $Fe_2(CO)_9$ (0.200 g; 0.551 mmol) in thf (10 mL), which resulted in the formation of a dark red solution. The mixture was left to stir for 16 hours. No further colour change was observed. Volatile components were removed under reduced pressure to produce a dark red powder. Yield: 0.131 g (mixture of **4.4**-$Fe(CO)_4$ and **4.4**). $^{31}P\{^1H\}$ NMR: -210.6 (t, $^1J_{PP}$ = 424, **4.4**), -54.0 (t, $^1J_{PP}$ = 392, **4.4**-$Fe(CO)_4$), 17.8 (d, $^1J_{PP}$ = 392, **4.4**-$Fe(CO)_4$), 22.2 (d, $^1J_{PP}$ = 424, **4.4**).

Reaction of [(dppp)P][BPh_4] (4.4[BPh_4]) with a Large Excess of $Fe_2(CO)_9$

A colourless solution of [(dppp)P][BPh_4] (0.342 g; 0.448 mmol) in thf (20 mL) was added to an orange slurry of $Fe_2(CO)_9$ (1.631 g; 4.484 mmol) in thf (30 mL), which resulted in the formation of a dark red solution. The mixture was left to stir for 16 hours. No further colour change was observed. Volatile components were removed under reduced pressure to produce a dark brown oil on the bottom of the flask. A yield could not be determined. $^{31}P\{^1H\}$ NMR: -49.3 (t, $^1J_{PP}$ = 391, **4.4**-$(Fe(CO)_4)_2$), 19.5 (d, $^1J_{PP}$ = 391, **4.4**-$(Fe(CO)_4)_2$).

4.3 Results and Discussion

Coordination with Main Group Lewis Acids

Since Schmidpeter's synthesis of the first triphosphenium cation, there has been very little attention directed towards the chemistry of these species, aside from the substitution of the stabilizing phosphines to generate new cations.[25] As demonstrated in Chapter 2, triphosphenium cations have two "lone pairs" of electrons potentially available for reactivity, and thus should respond similarly to other P^I compounds in the presence of traditional Lewis Acids. For example, the neutral P^I compounds where phosphinidene (R–P) moieties are stabilized by either *N*-heterocyclic carbenes or phosphines have been shown to coordinate to either one or two BH_3 molecules through the non-bonding electrons on P^I.[26-28] In contrast, the treatment of the P^I cations **4.3** or **4.4** with similar conditions, even with a ten-fold excess of the borane-thf complex, does not result in adduct formation, as evidenced by ^{31}P NMR spectra.

Aluminum(III) chloride was shown by Schmidpeter *et al.* to react rapidly with acyclic triphosphenium cations to yield mono-adducts (Equation 4.1).[13,14] These complexes were identified by their ^{31}P NMR spectra, which in both cases show a slight shift of the phosphine P^{III} signals to lower frequency and a more pronounced chnage of the P^I signal to higher frequency by an average of 50 ppm. In addition, a substantial decrease of 200 Hz in the $^1J_{PP}$ coupling constant magnitude was observed. In our lab, treatment of the cyclic triphosphenium cation **4.3** with one equivalent of $AlCl_3$ resulted in no noticeable shift in the characteristic peaks observed in the ^{31}P NMR spectrum even after a prolonged exposure of 24 hours. Further addition of the Lewis acid only produced a change upon reaching 3 equivalents, when a new doublet/triplet coupling pattern was

visible in the ^{31}P NMR spectrum, although free **4.3** was always present. Following the addition of a total of ten equivalents of $AlCl_3$, only peaks corresponding to the bis-adduct were present in the ^{31}P NMR spectrum. A similar requirement for additional equivalents of reagent was noted by Dillon and co-workers in their attempts to oxidize cyclic P^I cations with MeOTf.[12] The changes observed in the ^{31}P NMR spectrum of the solution of the $AlCl_3$/**4.3** mixture were similar to those observed for the acyclic analogues. The $^1J_{PP}$ coupling constant decreased in magnitude by 170 Hz after the first adduct formation and an additional 50 Hz upon bis-coordination. The chemical shift for the bis-adduct is more shielded than the mono-adduct, which may appear counter-intuitive, although the observations are completely consistent with the reaction stoichiometries. The ^{31}P NMR data are summarized in Table 4-1. The $AlCl_3$ adducts are unstable and prone to dissociation upon standing in solution, which limits the utility of purification through crystallization. Furthermore, the complex is unstable within the mass spectrometer, as the only peaks present are attributable to the uncoordinated **4.3** cation.

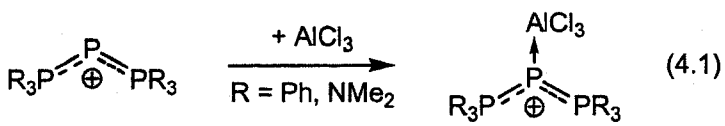

(4.1)

Similar reactivity is observed during reactions between **4.3** and gallium(III) chloride. Upon the addition of one equivalent, no reaction is observed in the ^{31}P NMR spectrum of the mixture. Following the addition of 2 equivalents of $GaCl_3$ peaks are present in the ^{31}P NMR spectrum attributable to the mono-adduct, and following the addition of five or more equivalents of the Lewis acid, only peaks attributable to the bis-adduct are visible. A summary of the ^{31}P NMR data is presented in Table 4-1.

Table 4-1 - Summary of ^{31}P NMR data for Reactions of P^I cations with $AlCl_3$ and $GaCl_3$.

Cation	δP^I	δP^{III}	$^1J_{PP}$	$\Delta\ ^1J_{PP}$	Ref.
4.1	-194	85	513		[13]
4.2	-180	29, 84	493, 523		[14]
4.3	-235	64.4	456		[20]
4.1-$AlCl_3$	-142	70	290	223	[14]
4.2-$AlCl_3$	-135	27,69	297, 378	145, 196	[14]
4.3-$AlCl_3$	-77.7	52.3	283	173	
4.3-$(AlCl_3)_2$	-153.7	53.1	238	218	
4.3-$GaCl_3$	-96.1	53.1	289	167	
4.3-$(GaCl_3)_2$	-153.8	53.0	238	218	

Coordination to Transition Metal Fragments

There are no examples in the literature of triphosphenium cations coordinating to transition metal fragments. Related anionic P^I compounds of the type $P(P(OR)_2O)_2^-$, **4.5** R = Et, have been shown to coordinate to Group 6 carbonyl complexes through either one or both of the available "lone pairs" of electrons (Equation 4.2).[16] Control over the type of adduct formed is provided by the stoichiometry of the reaction.[18] Upon coordination of one $TM(CO)_5$ fragment (TM = Cr, Mo, W) to **4.5**, a small shift of around 10 ppm to lower frequency for the P^{III} centres and a much larger shift of 40 ppm to higher frequency for the P^I centres are observed, in an analogous manner to the changes observed upon coordination to Group 13 Lewis acids. The coordination of a second transition metal fragment further shifts the peak corresponding to the P^I centre by 70 ppm and produces another small change to the P^{III} chemical shifts in the ^{31}P NMR spectrum. It is noteworthy that coordination of the anionic P^I compound to the metals also results in a decrease in the magnitude of the $^1J_{PP}$ coupling constant by approximately 100 Hz for each metal fragment coordinated. A summary of the ^{31}P NMR data is presented in Table

4-2. It should be further noted that the number of coordinated metal fragments has been verified by single crystal X-ray crystallography in many of the examples.[16-18]

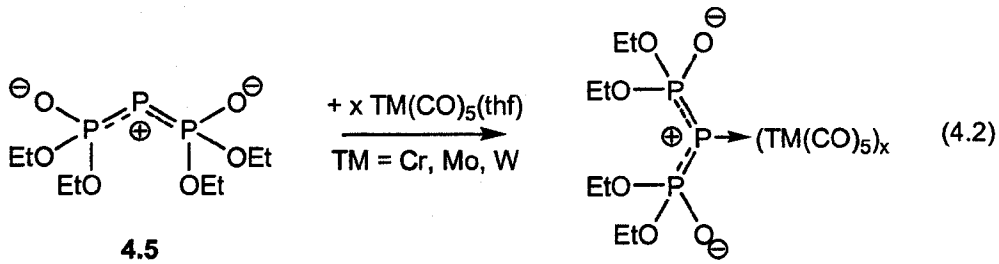

4.5 $\qquad$ 4.5-TM(CO)$_5$ $\qquad$ (4.2)

In order to assess the coordination ability of triphosphenium cations with Transition Metal fragments, reactions similar to those used to prepare the complexes above were undertaken using salts containing the cationic P^I compound **4.4**. Following the generation of the pentacarbonyl tetrahydrofuran adduct metal species using UV irradiation and sparging with purified nitrogen to remove dissolved carbon monoxide, the chromium, molybdenum or tungsten compounds were added to a thf solution of the P^I salt **4.4**[BPh_4]. The crude products were isolated from the thf solution and extracted into CH_2Cl_2 to remove any uncoordinated metal carbonyl compounds. The ^{31}P NMR chemical shifts observed for the complexes are consistent with the coordination of only one metal fragment, although there is typically evidence of significant amounts of free **4.4** in these solutions. The formation of mono-adducts in these reactions is also supported by the results of ESI-MS experiments. Surprisingly, treatment of salts of **4.4** with excess $W(CO)_5$(thf) does not result in complete conversion to the doubly coordinated complex, although the bis-adduct can be observed by their ^{31}P NMR chemical shifts if the spectrum is collected rapidly after the addition of the metal reagent. Unexpectedly, the adducts are unstable in solution and slowly de-complex, even in the presence of a ten-fold excess of the metal carbonyl reagent in solution. No solid material

precipitates from solution, however within 3 days solutions of the complexes were found to have reverted to the uncoordinated cation **4.4** by ^{31}P NMR spectroscopy. This behaviour is in stark contrast to the complexes of the anionic P^I compound **4.5**, and, unfortunately, has prevented the isolation of X-ray quality crystals.

Table 4-2 - Summary of ^{31}P NMR data for Reactions of P^I Salts with Transition Metal Carbonyl Compounds.

Cation	δP^I	δP^{III}	$^1J_{PP}$	$^1J_{PW}$[a]	$\Delta\ ^1J_{PP}$	Ref.
4.3	-235	64.4	456			[20]
4.4	-210.2	22.7	424			[20]
4.5	-187.7	67.0	411			[15]
4.5-$Cr(CO)_5$[b]	-69.4	46.5	180		231	[18]
4.5-$(Cr(CO)_5)_2$	-31.0	45.0	146		265	[18]
4.5-$Mo(CO)_5$	-134.8	55.4	305		106	[16]
4.5-$(Mo(CO)_5)_2$[b]	-69.3	45.8	158		253	[16]
4.5-$W(CO)_5$[b]	-143.7	54.6	298	NR	113	[16]
4.5-$(W(CO)_5)_2$	-75.6	45.1	152	NR	259	[16]
4.4-$Cr(CO)_5$	-87.9	26.8	386		38	
4.4-$Mo(CO)_5$	-116.4	24.3	373		51	
4.4-$W(CO)_5$	-129.6	21.8	371	135	53	
4.4-$(W(CO)_5)_2$	-96.9	20.9	350	NR	74	
4.3-$Fe(CO)_4$	-78.2	50.9	411		45	
4.4-$Fe(CO)_4$	-54.0	17.8	392		32	
4.4-$(Fe(CO)_4)_2$	-49.3	19.5	391		33	

[a] NR = not recorded. [b] Complex Structurally Characterized by X-ray Crystallography.

Treatment of tetraphenylborate salts of either P^I cation **4.3** or **4.4** with $Fe_2(CO)_9$ in either dichloromethane or thf results in the production of a dark red solution. Removal of volatile compounds and isolation of the product from the reaction with one equivalent of the iron reagent yields a material that has an identical ^{31}P NMR spectrum as that of the free cation. Peaks corresponding to the mono-adduct are visible in ^{31}P NMR spectra following the addition of two equivalents of the iron carbonyl complex and the reaction

may be driven to produce the bis-adduct using a ten-fold excess of $Fe_2(CO)_9$. In contrast to the Group 6 metal carbonyl complexes, the iron adducts appear to be stable in solution, however the isolation of crystalline material suitable for single crystal X-ray crystallography has been unsuccessful thus far.

Attempts at coordination of either **4.3** or **4.4** with a variety of non-carbonyl transition metal complexes ($RhCl(PPh_3)_3$, $(CpFe(CO)_2)_2$, $CpNiClPPh_3$, $Pt(PPh_3)_4$, $PtCl_2(cod)$, $PtCl_2(PPh_3)_2$, CuCl) consistently results in the breakdown of the P-P-P framework and coordination of the chelating diphosphine to the metal centre as indicated unambiguously by ^{31}P NMR spectroscopy. In the case of $RhCl(PPh_3)_3$, the released P^I cation is trapped by free triphenylphosphine to generate Schmidpeter's original acyclic P^I cation, $(Ph_3P)_2P^+$.[25] In a similar vein, Driess and co-workers have reported that the acyclic P^I cation $((Me_2N)_3P)_2P^+$ (and the arsenic analogue) also results in the breakdown of the triphosphenium framework upon treatment with excess Cp_2ZrHCl, however the released P^I cation is trapped within an eight-membered alternating zirconium-hydride ring instead.[29,30] It should be emphasized that the same reactivity is observed with the cyclic cation **4.3** to generate the identical product (Equation 4.3) as indicated unambiguously by ^{31}P and ^1H NMR spectra.

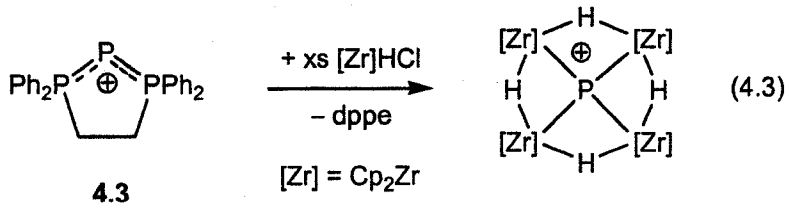

4.3 (4.3)

Computational Investigations

We sought to employ computational chemistry in order to elucidate why the anionic P^I compound **4.5** generates stable adducts with some acceptors, while cationic P^I compounds form the analogous adducts and then decomplex. We chose as our models to investigate: a cyclic triphosphenium cationic **4.6**, a neutral phosphine **4.7**, a neutral Phospha-Wittig P^I model **4.8** and anionic P^I compound **4.9**. The optimized geometry structures of the uncoordinated models are shown in Figure 4.1 and pertinent data is compiled in Table 4-3.

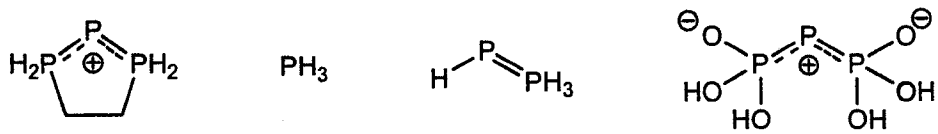

4.6 **4.7** **4.8** **4.9**

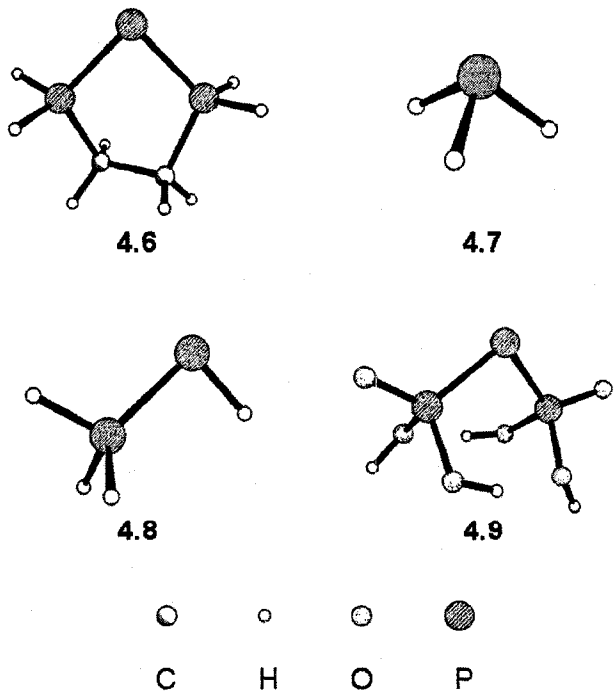

Figure 4.1 - Optimized Geometry Structures of Model Compounds 4.6 - 4.9.

Table 4-3 - Summary of Computational Results for Compounds 4.6 – 4.9.

Model	Sym.	Corrected Energy E_{total}[a] (au)	E_{HOMO} (eV)	E_{LUMO} (eV)	Occ P[b] (3p)	q(P)[c] (au)	H Affinity (kJ mol^{-1})
4.6	C_2	-1104.55033	-10.405	-5.775	1.673	-0.22	-467.0
4.7	C_{3v}	-343.06693	-7.637	0.079	1.501	-0.02	-775.0
4.8	C_s	-684.95822	-5.368	-0.904	1.725	-0.39	-925.0
4.9	C_2	-1477.66334	-1.931	2.773	1.740	-0.57	-1313.0

[a] $E_{total} = E_{calculated} + ZPVE$. [b] Natural Bond Orbital (NBO) population of the $3p_x$ orbital on the dicoordinate P atom. [c] NBO charge on the dicoordinate P atom.

Proton affinities are one simple way to rank the donor ability of the phosphorus centres in the model compounds,[31] calculated as the difference in E_{total} between the protonated species (shown in Figure 4.2) and that of the original model. It is perhaps not surprising that the ranking of proton affinities follows the trend based on the overall charge of the model, as it should be less favourable energetically to protonate a cation (-467.0 kJ mol^{-1}) than an anion (-1313.0 kJ mol^{-1}). The neutral compounds have proton affinities that fall intermediate to the charged species.

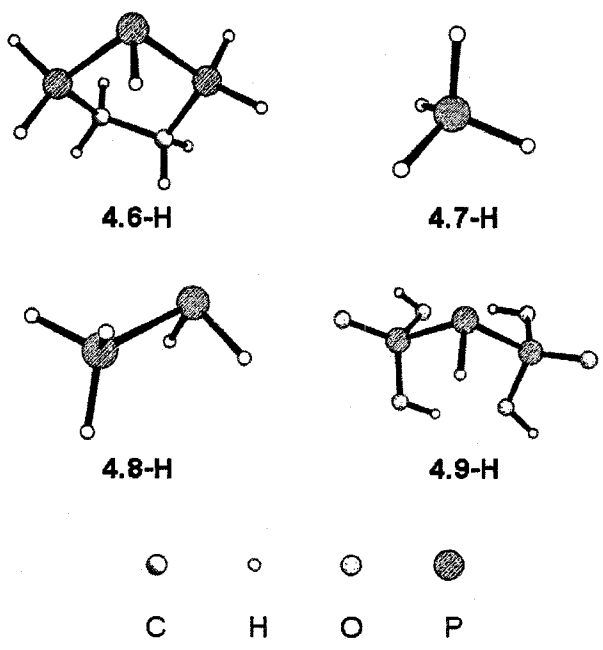

Figure 4.2 - Optimized Geometry Structures of Protonated Model Compounds 4.6 - 4.9.

A more enlightening approach to understanding the differing reactivity patterns may be to examine the reaction energies and bond energies for adducts formed between the model compounds and a Lewis acid. We have chosen aluminum(III) chloride to model the adduct formation as it displayed some degree of success experimentally. The aluminum species present with the triphosphenium cations in solution is likely to be the dimer Al_2Cl_6; thus the energies for the reactions with both $AlCl_3$ and Al_2Cl_6 are presented below and relevant data are summarized in Table 4-4.

Table 4-4 - Summary of Computational Results for Reactions Involving $AlCl_3$.

Model	Sym.	Corrected Energy E_{total} (au)	E_{rxn} with $AlCl_3$ (kJ mol^{-1})	E_{rxn} with ½ Al_2Cl_6 (kJ mol^{-1})	P-Al Bond Energy (kJ mol^{-1})	P-Al Bond Length (Å)
$AlCl_3$	D_{3h}	-1623.02102				
Al_2Cl_6	D_{2h}	-3246.08056				
4.6-$AlCl_3$	C_1	-2727.59191	-54.0	-3.4	-87.6	2.552
4.7-$AlCl_3$	C_{3v}	-1966.11559	-72.6	-22.0	-108.8	2.499
4.8-$AlCl_3$	C_1	-2307.99396	-133.7	-83.1	-195.2	2.460
4.9-$AlCl_3$	C_1	-3100.76068	-200.4	-149.8	-296.3	2.433

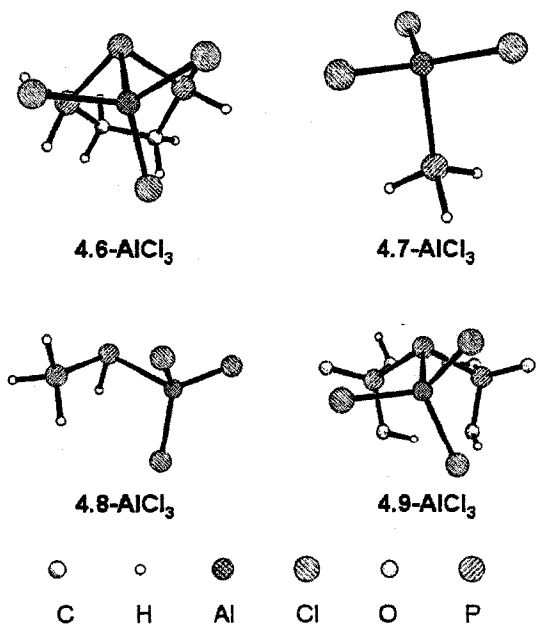

Figure 4.3 - Optimized Geometry Structures of $AlCl_3$ adducts of Model Compounds 4.6 - 4.9.

From the energies determined for the reactions of the model compounds with either $AlCl_3$ or half an equivalent of Al_2Cl_6 (optimized geometry structures are depicted in Figure 4.3), the trend follows the experimental observations. The most energetically favourable interaction involves the coordination of the anionic **4.8** with aluminum (-149.8 kJ mol^{-1}), while the reaction with the triphosphenium cation and Al_2Cl_6 is essentially energetically neutral within the errors of the calculations. This stark contrast in reaction energies highlights the differences observed experimentally: the coordination of triphosphenium cations to Lewis acids seems to be in equilibrium with the free species, whereas stable species are observed with the anionic P^I compounds. The reaction energies for the neutral phosphine and P^I compounds fall in between those involving the cationic and anionic P^I models, although, whereas the reaction involving **4.7** is only slightly exothermic, the coordination of $AlCl_3$ to **4.8** is nearly as favourable as formation of the adduct with the anionic P^I ion. The calculated exothermicity of the latter reaction gives some insight into the favourability of complexes involving base-stabilized phosphinidenes observed experimentally.[26-28]

A Ziegler-type Generalized Transition State Analysis[32] of the phosphorus-aluminum bonds was performed to determine the P-Al bond energies. This procedure involves calculating the energies of both fragments, in the geometry they possess in the complex, and subtracting it from the energy of the complex. The resultant bond energies follow the same trend as the P-Al bond lengths: the anionic P^I complex contains the strongest phosphorus-aluminum bond and the cationic P^I the weakest bond. The neutral complexes contain P-Al bonds that fall between these in terms of energies and lengths, and again **4.8** shows a stronger affinity towards electron acceptors than **4.7**.

4.4 Conclusions

While cyclic triphosphenium cations are able to coordinate to both Main Group and Transition Metal Lewis acids, as evidenced by their ^{31}P NMR spectra, the reactions are not quantitative. The complexes thus obtained are generally unstable with respect to the free donors and acceptors, and this behaviour has been attributed to an energetically neutral reaction energy for P^I cations.

4.5 Prospective Developments

Although the formation of the complexes has been identified by their ^{31}P NMR spectra, isolation of X-ray quality crystals would be helpful to confirm the number of coordinated Lewis acids. Triphosphenium cations are prone to dissociation upon attempting to coordinate to a variety of Transition Metal complexes, and this reactivity can be exploited as a means of delivering P^I ions, in the same way that oxidizing agents are used in Chapter 6 to release "As-I" fragments. Should it be desired to have the cation remain intact, the carbene-stabilized P^I cations discussed in Chapter 3 should be more strongly bound and be more amenable to remaining together upon coordination. No work has yet been reported on the coordination chemistry of arsenic(I) cations and should be explored for any similarities and differences with the phosphorus cations.

4.6 References

1. Regitz, M. and Scherer, O.J., *Multiple Bonds and Low Coordination in Phosphorus Chemistry*, 1990, Stuttgart: Georg Thieme Verlag, pp. 478.

2. Dillon, K.B., Mathey, F. and Nixon, J.F., *Phosphorus: The Carbon Copy: From Organophosphorus to Phospha-organic Chemistry*, 1998, Chichester: John Wiley & Sons, Inc., pp. 366.

3. Macdonald, C.L.B. and Ellis, B.D. in *Encyclopedia of Inorganic Chemistry, 2nd Edition*, 2005, R. B. King (Ed), Hoboken, NJ: John Wiley & Sons, Inc., Low Oxidation State Main Group, pp. 6696.

4. We prefer to use a simple, chemically-intuitive convention in which the oxidation state of phosphorus is indicated by the number of lone pairs associated with the atom: P(+5) has no lone pairs, P(+3) has one lone pair and P(+1) has two lone pairs, as discussed in Chapter 1.

5. Boon, J.A., Byers, H.L., Dillon, K.B., Goeta, A.E. and Longbottom, D.A., *Heteroat. Chem.*, **2000**, *11*, 226-231.

6. Ellis, B.D. and Macdonald, C.L.B., *ACS Symp. Ser.*, **2006**, *917*, 108-121.

7. Kilian, P., Slawin, A.M.Z. and Woollins, J.D., *Dalton Trans.*, **2006**, 2175-2183.

8. Schmidpeter, A., Lochschmidt, S. and Sheldrick, W.S., *Angew. Chem., Int. Ed. Engl.*, **1982**, *21*, 63-64.

9. Schmidpeter, A., Lochschmidt, S., Karaghiosoff, K. and Sheldrick, W.S., *J. Chem. Soc., Chem. Commun.*, **1985**, 1447-1448.

10. Lochschmidt, S. and Schmidpeter, A., *Z. Naturforsch., B: Anorg. Chem., Org. Chem.*, **1985**, *40B*, 765-773.

11. Burton, J.D., Deng, R.M.K., Dillon, K.B., Monks, P.K. and Olivey, R.J., *Heteroat. Chem.*, **2005**, *16*, 447-452.

12. Dillon, K.B. and Olivey, R.J., *Heteroat. Chem.*, **2004**, *15*, 150-154.

13. Schmidpeter, A. and Lochschmidt, S., *Angew. Chem., Int. Ed. Engl.*, **1986**, *25*, 253-254.

14. Lochschmidt, S., Mueller, G., Huber, B. and Schmidpeter, A., *Z. Naturforsch., B: Anorg. Chem., Org. Chem.*, **1986**, *41B*, 444-454.

15. Weber, D. and Fluck, E., *Inorg. Nucl. Chem. Lett.*, **1976**, *12*, 515-518.

16. Weber, D., Fluck, E., Von Schnering, H.G. and Peters, K., *Z. Naturforsch., B: Anorg. Chem., Org. Chem.*, **1982**, *37B*, 594-600.

17. Peters, K. and Weber, D., *Cryst. Struct. Commun.*, **1981**, *10*, 1259-1262.

18. Roesky, H.W., Djarrah, H., Noltemeyer, M. and Sheldrick, G.M., *Z. Naturforsch., B: Anorg. Chem., Org. Chem.*, **1982**, *37B*, 1580-1583.

19. Pangborn, A.B., Giardello, M.A., Grubbs, R.H., Rosen, R.K. and Timmers, F.J., *Organometallics*, **1996**, *15*, 1518-1520.

20. Ellis, B.D. and Macdonald, C.L.B., *Inorg. Chem.*, **2006**, *45*, 6864-6874.

21. Frisch, M.J., Trucks, G.W., Schlegel, H.B., Scuseria, G.E., Robb, M.A., Cheeseman, J.R., Zakrzewski, V.G., Montgomery, V.G., Jr., Stratmann, R.E., Burant, J.C., Dapprich, S., Millam, J.M., Daniels, A.D., Kudin, K.N., Strain, M.C., Farkas, O., Tomasi, J., Barone, V., Cossi, M., Cammi, R., Mennucci, B., Pomelli, C., Adamo, C., Clifford, S., Ochterski, J., Petersson, G.A., Ayala, P.Y., Cui, Q., Morokuma, K., Salvador, P., Dannenberg, J.J., Malick, D.K., Rabuck, A.D., Raghavachari, K., Foresman, J.B., Cioslowski, J., Ortiz, J.V., Baboul, A.G., Stefanov, B.B., Liu, G., Liashenko, A., Piskorz, P., Komaromi, I., Gomperts, R., Martin, R.L., Fox, D.J., Keith, T., Al-Laham, M.A., Peng, C.Y., Nanayakkara, A., Challacombe, M., Gill, P.M.W., Johnson, B., Chen, W., Wong, M.W., Andres,

J.L., Gonzalez, C., Head-Gordon, M., Replogle, E.S. and Pople, J.A., *Gaussian98*, Revision A.11.1, 2001, Pittsburgh, PA: Gaussian, Inc.

22. Becke, A.D., *J. Chem. Phys.*, **1993**, *98*, 5648-5652.

23. Perdew, J.P. and Wang, Y., *Phys. Rev. B: Condens. Matter*, **1992**, *45*, 13244-13249.

24. Reed, A.E., Curtiss, L.A. and Weinhold, F., *Chem. Rev.*, **1988**, *88*, 899-926.

25. Schmidpeter, A., Lochschmidt, S. and Sheldrick, W.S., *Angew. Chem., Int. Ed. Engl.*, **1985**, *24*, 226-227.

26. Arduengo, A.J., III, Carmalt, C.J., Clyburne, J.A.C., Cowley, A.H. and Pyati, R., *Chem. Commun.*, **1997**, 981-982.

27. Shah, S., Yap, G.P.A. and Protasiewicz, J.D., *J. Organomet. Chem.*, **2000**, *608*, 12-20.

28. Burg, A.B., *J. Inorg. Nucl. Chem.*, **1971**, *33*, 1575-1581.

29. Driess, M., Aust, J., Merz, K. and Van Wullen, C., *Angew. Chem. Int. Ed.*, **1999**, *38*, 3677-3680.

30. Driess, M., Ackermann, H., Aust, J., Merz, K. and Von Wullen, C., *Angew. Chem. Int. Ed.*, **2002**, *41*, 450-453.

31. Kovacevic, B. and Maksic, Z.B., *Chem. Commun.*, **2006**, 1524-1526.

32. Ziegler, T. and Rauk, A., *Theor. Chim. Acta*, **1977**, *46*, 1-10.

Chapter 5 – Trapping of Pn^I Cations with Diazabutenes

5.1 Introduction

The oxidation state of an element in a molecule can have a significant influence on the structural features, bonding and chemistry of that molecule. In recent years, many Main Group chemists have been interested in the chemistry of compounds containing Main Group elements in unusually low oxidation states because such electron-rich species often exhibit behaviour that is manifestly different than compounds containing the elements in more conventional oxidation states.[1] In regard to the heavier Group 15 elements (pnictogens; Pn = P, As, Sb, Bi) we have been particularly interested in compounds containing the elements in the +1 oxidation state.[2] While phosphinidenes and their heavier Pn^I analogues, **5.1**, are generally highly-reactive, transient species,[3-5] in the 1980's, the seminal work of Schmidpeter and co-workers demonstrated the viability of stable, di-coordinate cationic P^I compounds.[6] In particular, Schmidpeter's group showed that salts containing "triphosphenium" cations, **5.2**, which may be considered to consist of phosphine-stabilized P^I ions, can be obtained by the *in situ* reduction of PCl_3 in the presence of phosphine ligands, as depicted in Equation 5.1. Some corresponding arsenic analogues have likewise been obtained using similar preparative approaches.[7-11]

5.1 **5.2**

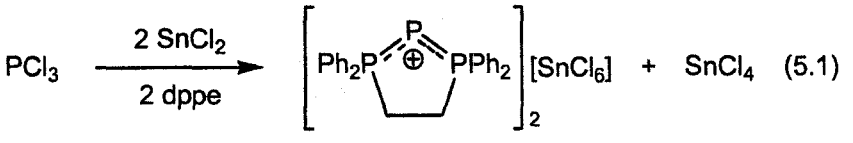

$$PCl_3 \xrightarrow[2\ dppe]{2\ SnCl_2} [Ph_2P{=}P^{\oplus}{=}PPh_2][SnCl_6] + SnCl_4 \quad (5.1)$$

In the last five years, the research groups of Dillon,[12] Woollins[13] and Macdonald (Chapters 2 and 6)[14-16] have shown that it is possible to generate and isolate halide salts of triphosphenium ions and their arsenic analogues in the absence of additional reducing agents. When appropriate conditions are employed in reactions using chelating diphosphine ligands and PI_3, it has proven possible to obtain analytically pure iodide salts of the triphosphenium cations, as illustrated in Equation 5.2. In a similar vein, it has been demonstrated that related P^I halide salts can be generated by the treatment of PX_3 (X = Cl, Br, I) with certain *N*-heterocyclic carbenes, which exhibit comparable reactivity to phosphine ligands (Chapter 3).[17]

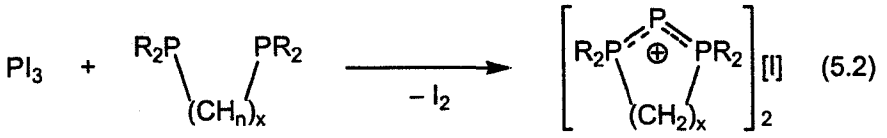

(5.2)

Recently, Cowley and co-workers have investigated the use of diimines as ligands for putative Pn^I cations generated by both of the synthetic protocols outlined above. In the case of a 1,2-bis(arylimino)acenapthene (Ar-BIAN), the reaction of $PnCl_3$ (Pn = P, As) and $SnCl_2$ in the presence of the BIAN ligand produced salts of the form [(Ar-BIAN)Pn][$SnCl_5$·thf] (Equation 5.3) and the reactions of Ar-BIAN with PnI_3 generated the corresponding triiodide salts, [(Ar-BIAN)Pn][I_3]; these reactions are illustrated in (Equation 5.4).[18] Regardless of the identity of the anion, the metrical parameters for the cations in these salts indicate that these cations are best described as phosphenium[19] or arsenium cations that contain Pn^{III} centres generated with the concomitant 2-electron reduction of the Ar-BIAN ligand. In this light, such products are analogous to those obtained when phosphinidene transfer agents are treated with α-diimines and related trapping agents.[20] Similar results are obtained from the analogous reactions of the

simpler diimine 1,4-dimesityl-1,4-diazabutadiene (Mes-DAB-H) with the $AsCl_3/SnCl_2$ mixture,[21] and it is noteworthy that **5.3** was, the perhaps surprising, result from the reaction of R-DAB-H (R = Mes or ^{t}Bu) with PCl_3 and NEt_3.[22]

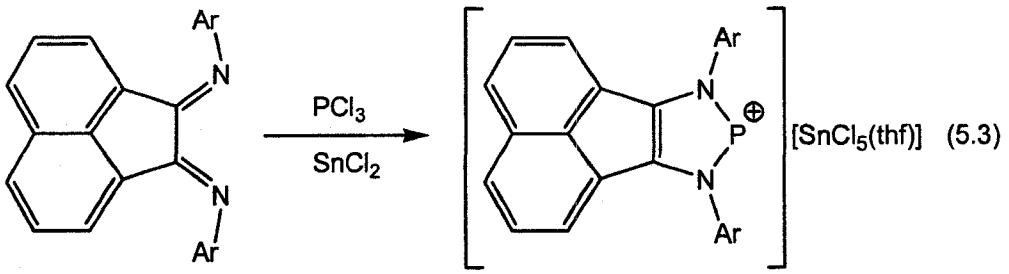

(5.3)

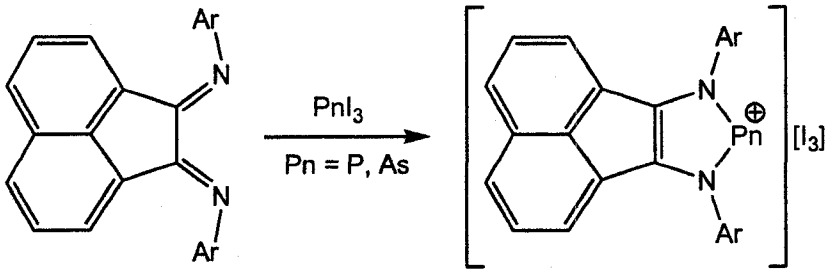

(5.4)

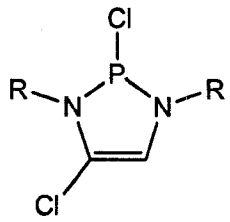

5.3

In contrast, the reaction of AsI_3 or $AsCl_3/SnCl_2$ with an α,α'-diiminopyridine (Ar-Dimpy, Equation 5.5) ligand generates salts containing the cation $[(Ar\text{-}Dimpy)As]^+$; the metrical parameters in this cation are much more consistent with the presence of an As^I cation chelated by a non-reduced Ar-Dimpy ligand. The overall T-shaped arrangement about the As centre is reminiscent of the so-called "10-As-3" centre in Arduengo's unique family of Group 15 compounds containing the diketoamido ligand.[23,24]

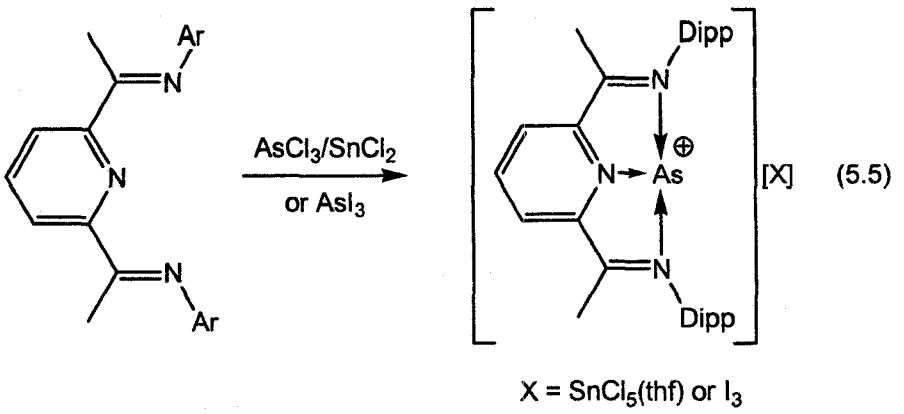

Given the importance of β-diketiminate (NacNac) ligands to Transition Metal[25] and Main Group chemistry,[26-28] several groups have attempted to coordinate such ligands to phosphorus centres. In stark contrast to the results outlined above for α-diimines, the reactions of metallated NacNac reagents with halogenated P^{III} species results in the formation of a P-C bond to the unique C_α atom instead of chelation by the nitrogen atoms.[29-31] The adoption of the monodentate binding mode and avoidance of P-N bond formation is also observed when reaction conditions are used that are analogous to those that have been employed successfully for the heterocycle syntheses described above.

In light of the range of products observed from seemingly similar reactions, we present in this chapter computational and some experimental results that elucidate important aspects of the interactions between several chelates that contain sp^2-hybridized nitrogen centers and P^I and As^I centers. It is anticipated that the insight afforded by such investigations may facilitate the design of heterocycle forming reactions involving low oxidation state reagents.

5.2 Experimental

Reagents and General Procedures. All manipulations were carried out using standard inert-atmosphere techniques. Phosphorus(III) chloride, phosphorus(III) iodide, and tin(II) chloride were obtained from Strem; all solvents were obtained from Aldrich; phosphorus(III) chloride was distilled prior to use and all other reagents were used without further purification. CD_2Cl_2 was dried over calcium hydride and all other solvents were dried on a series of Grubbs' type columns[32] and were degassed prior to use. The compounds 1,4-bis(2,6-diisopropylphenyl)-2,3-dimethyl-1,4-diazabutadiene (Dipp-DAB-Me), 1,4-bis(2,4,6-trimethylphenyl)-2,3-dimethyl-1,4-diazabutadiene (Mes-DAB-Me) and Dipp-NacNac were synthesized by literature procedures.[33,34] It should also be noted that the reactions appear to be quantitative according to all spectroscopic data recorded.

Instrumentation. NMR spectra were recorded at room temperature in CD_2Cl_2 solutions on a Bruker Avance 300 MHz spectrometer. Chemical shifts are reported in ppm, relative to external standards ($SiMe_4$ for ^1H and ^{13}C, 85% aq. H_3PO_4 for ^{31}P). Coupling constant magnitudes, $|J|$, are given in Hz. Melting points (mp) were obtained on samples sealed in glass capillaries under dry nitrogen using an Electrothermal® Melting Point Apparatus. Elemental analysis was performed in-house using a PerkinElmer 2400 C, H, N analyzer in the Centre for Catalysis and Materials Research, Department of Chemistry and Biochemistry, University of Windsor.

Theoretical Methods. Calculations were preformed with the Gaussian 98 suite of programs.[35] Geometry optimizations have been calculated using density functional theory (DFT), specifically implementing the B3PW91 method [containing Becke's three-

parameter hybrid functional for exchange (B3, including ca. 20% Hartree-Fock exchange)[36] combined with the generalized gradient approximation for correlation of Perdew and Wang (PW91)[37]] in conjunction with the 6-31+G(d) basis set. The geometries were restricted to the highest reasonable symmetry and each stationary point was confirmed to be a minimum by having zero imaginary vibrational frequencies. The electronic energies of the molecules have been corrected by the unscaled, zero-point vibrational energy (ZPVE). Single Point Energies have been calculated at the B3PW91/6-311+G(3df,2p)//B3PW91/6-31G(d) level of theory. Population analyses were conducted using the Natural Bond Orbital (NBO)[38] method implemented in Gaussian98. Drawings of the optimized structures of the model compounds were made using SHELXTL[39] and depictions of the molecular orbitals were made using Molden.[40]

X-ray Crystallography. Crystals were coated in Nujol, mounted on a glass fibre and placed in the 173 K N_2 boil-off stream of the Kryoflex low-temperature apparatus. Reflection data were integrated from frame data obtained using hemisphere scans with the SMART[41] software on a Bruker APEX CCD diffractometer using a graphite monochromator with MoKα radiation (λ = 0.71073Å). Diffraction data and unit-cell parameters were consistent with assigned space groups. Lorentz and polarization corrections and empirical absorption corrections, based on redundant data at varying effective azimuthal angles, were applied to the data sets using SAINTPlus[42] and SADABS[43] software. The structures were solved by direct methods using SHELXS[44] or Sir97[45] (as implemented in the WinGX software package[46]), completed by subsequent Fourier syntheses and refined with full-matrix least-squares methods against F^2 data using SHELXL.[47] All non-hydrogen atoms were refined anisotropically and all

hydrogen atoms were placed in appropriate geometrically-calculated positions. Thermal ellipsoid plots of the molecular structures were generated using SHELXTL.[39] The experimental details for each of the diffraction experiments are listed in Table 5-1 and Table 5-2.

Preparation of [(Dipp-DAB-Me)P][$SnCl_5$]

Solid Dipp-DAB-Me (0.433 g; 1.070 mmol) was added to a $SnCl_2$ (0.203 g; 1.070 mmol) slurry in CH_2Cl_2 (20 mL), to produce a yellow slurry. A colourless solution of PCl_3 (0.147 g; 1.070 mmol) in CH_2Cl_2 (10 mL) was slowly added and the mixture became red. The mixture was left to stir for 16 hours and then it was filtered through Celite and the volatile components were removed under reduced pressure. Dissolution of the red solid in a minimal amount of CH_2Cl_2 followed by slow evaporation produced pink crystalline material. Yield: 88% (0.692 g; 0.946 mmol). $^{31}P\{^1H\}$ NMR: 200.7 (s). $^{13}C\{^1H\}$ NMR: 13.5 (s), 23.2 (s), 26.1(s), 124.9(s), 125.8(s), 132.9(s), 144.3(s), 145.5(s). ^1H NMR: 1.21 (d, $^3J_{HH}$ = 6.9, 24H), 2.31 (s, 6H), 2.67 (septet, $^3J_{HH}$ = 6.9, 2H), 7.49 (d, $^3J_{HH}$ = 7.8, 4H), 7.69 (t, $^3J_{HH}$ = 7.8, 2H). mp: 215-216 °C. Anal. Calcd. for $C_{28}H_{40}Cl_5N_2PSn$ (731.578): C 45.97, H 5.51, N 3.83; Found C 45.78, H 5.45, 3.81 %.

Preparation of [(Dipp-DAB-Me)P][I_3]

Solid Dipp-DAB-Me (0.352 g; 0.870 mmol) was added to a solution of PI_3 (0.358 g; 0.870 mmol) in CH_2Cl_2 (15 mL), which immediately changed from reddish-orange to dark red. The solution was left to stir for 16 hours and then the volatile components were removed under reduced pressure. Dissolution of the red solid in a minimal amount of

MeCN followed by slow evaporation produced red crystalline material. Yield: 84% (0.597 g; 0.731 mmol). $^{31}P\{^{1}H\}$ NMR: 201.1 (s). $^{13}C\{^{1}H\}$ NMR: 13.9(s), 23.3 (s), 26.1(s), 125.0 (s), 125.8 (s), 132.9 (s), 144.3 (s), 145.5 (s). ^{1}H NMR: 1.22 (d, $^{3}J_{HH}$ = 7.0, 24H), 2.31 (s, 6H), 2.67 (septet, $^{3}J_{HH}$ = 7.0, 2H), 7.48 (d, $^{3}J_{HH}$ = 7.9, 4H), 7.67 (t, $^{3}J_{HH}$ = 7.9, 2H). m.p.: 290-291 °C. Anal. Calcd. for $C_{28}H_{40}I_3N_2P$ (816.318): C 41.20, H 4.94, N 3.43; Found: C 41.47, H 4.93, N 3.34 %.

Preparation of [(Mes-DAB-Me)P][I_3]

Solid Mes-DAB-Me (0.245 g; 0.765 mmol) was added to a solution of PI_3 (0.315 g; 0.765 mmol) in CH_2Cl_2 (20 mL), which immediately changed from reddish-orange to dark red. The solution was left to stir for 16 hours and then the volatile components were removed under reduced pressure. Dissolution of the red solid in a minimal amount of MeCN followed by slow evaporation produced red crystalline material. Yield: 81% (0.454 g; 0.620 mmol). $^{31}P\{^{1}H\}$ NMR: 202.0 (s). $^{13}C\{^{1}H\}$ NMR: 13.4 (s), 18.5 (s), 21.5 (s), 129.7 (s), 130.4 (s), 134.7 (s), 142.4 (s), 143.4 (s). ^{1}H NMR: 2.14 (s, 12H), 2.25 (s, 6H), 2.42 (s, 6H), 7.20 (s, 4H). mp: 210-212 °C. Anal. Calcd. for $C_{22}H_{28}I_3N_2P$ (732.158): C 36.09, H 3.85, N 3.83; Found C 37.47, H 3.93, N 4.05 %.

Preparation of [(Dipp-DAB-Me)As][I_3]

Solid Dipp-DAB-Me (0.175 g; 0.432 mmol) was added to a solution of AsI_3 (0.197 g; 0.431 mmol) in CH_2Cl_2 (25 mL), which immediately changed from gold to reddish-orange. The solution was left to stir for 16 hours and then the volatile components were removed under reduced pressure. Dissolution of the reddish-orange

solid in a minimal amount of MeCN followed by slow evaporation produced red crystalline material. Yield: 77% (0.286 g; 0.332 mmol). $^{13}C\{^{1}H\}$ NMR: 15.7 (s), 23.1 (s), 26.1 (s), 124.6 (s), 125.5, 132.1 (s), 144.3 (s), 147.4 (s). ^{1}H NMR: 1.24 (d, $^{3}J_{HH}$ = 6.8, 24 H), 2.36 (s, 6H), 2.70 (septet, $^{3}J_{HH}$ = 6.8, 2H), 7.46 (d, $^{3}J_{HH}$ = 7.8, 4H), 7.63 (t, $^{3}J_{HH}$ = 7.8, 2H). mp: 169-170 °C. Anal. Calcd. for $C_{28}H_{40}AsI_3N_2$ (860.266): C 39.09, H 4.69, N 3.26; Found C 38.68, H 4.62, N 3.41 %.

Table 5-1 - Summary of X-ray Crystallographic Data for Compounds 5.5[$SnCl_5$], 5.5[I_3] and 5.6[I_3].

Compound	**5.5[$SnCl_5$]**	**5.5[I_3]**	**5.6[I_3]**
Empirical formula	$C_{28}H_{40}Cl_5N_2PSn$	$C_{28}H_{40}I_3N_2P$	$C_{22}H_{28}I_3N_2P$
Formula weight	731.55	816.29	732.13
Crystal system	Orthorhombic	Monoclinic	Orthorhombic
Space group	*Pnma*	*C2/m*	$P2_12_12_1$
Unit cell dimensions:			
a (Å)	20.805(3)	19.044(2)	14.0163(19)
b (Å)	15.709(2)	16.745(2)	15.585(2)
c (Å)	10.7872(14)	11.6861(14)	24.023(3)
α (°)	90	90	90
β (°)	90	120.0050(10)	90
γ (°)	90	90	90
Volume (Å^3)	3525.5(8)	3227.2(6)	5247.7(12)
Z	4	4	8
Density (calc'd) (g cm^{-3})	1.378	1.680	1.853
Abs. coef. (mm^{-1})	1.168	2.973	3.645
F(000)	1488	1584	2784
θ range for data collection (°)	2.13 to 27.50	1.73 to 27.50	1.56 to 27.50
Limiting indices	$-26 \le h \le 26$	$-24 \le h \le 24$	$-17 \le h \le 17$
	$-20 \le k \le 19$	$-21 \le k \le 21$	$-20 \le k \le 19$
	$-14 \le l \le 13$	$-15 \le l \le 15$	$-31 \le l \le 31$
Reflections collected	37062	18204	58148
Independent reflections	4178	3798	11882
R_{int}	0.0492	0.0235	0.0604
Data / restraints / parameters	4178 / 0 / 185	3798 / 0 / 167	11882 / 0 / 523
Goodness-of-fit on F^2	1.205	1.031	1.157
Final *R* indices[a] [I>2s(I)]	*R*1 = 0.0421	*R*1 = 0.0418	*R*1 = 0.0724
	*wR*2 = 0.0883	*wR*2 = 0.0945	*wR*2 = 0.1630
R indices (all data)	*R*1 = 0.0712	*R*1 = 0.0539	*R*1 = 0.0995
	*wR*2 = 0.1059	*wR*2 = 0.1028	*wR*2 = 0.1840
Largest difference map peak and hole (e Å^{-3})	1.277 and -0.487	1.466 and -1.532	3.765 and -1.333

Table 5-2 - Summary of X-ray Crystallographic Data for Compounds 5.7[I_3] and [$MesNH_3$]5.8$_2$[As_3I_{12}]·2AsI_3.

Compound	5.7[I_3]	[$MesNH_3$]5.8$_2$[As_3I_{12}]·2AsI_3
Empirical formula	$C_{28}H_{40}AsI_3N_2$	$C_{53}H_{70}As_7I_{18}N_5$
Formula weight	860.24	3585.78
Crystal system	Triclinic	Orthorhombic
Space group	*P-1*	*Pnma*
Unit cell dimensions:		
a (Å)	10.3517(12)	23.789(9)
b (Å)	10.3950(12)	31.199(12)
c (Å)	16.787(2)	11.998(5)
α (°)	72.5670(10)	90
β (°)	77.6370(10)	90
γ (°)	73.3300(10)	90
Volume (Å^3)	1634.7(3)	8905(6)
Z	2	4
Density (calc'd) (g cm^{-3})	1.748	2.675
Abs. coef. (mm^{-1})	3.890	8.868
F(000)	828	6432
θ range for data collection (°)	1.28 to 27.50	1.31 to 27.50
Limiting indices	$-13 \le h \le 13$	$-30 \le h \le 30$
	$-23 \le k \le 13$	$-40 \le k \le 40$
	$-21 \le l \le 21$	$-15 \le l \le 15$
Reflections collected	18568	93126
Independent reflections	7262	10396
R_{int}	0.0214	0.0952
Data / restraints / parameters	7262 / 0 / 317	10396 / 0 / 406
Goodness-of-fit on F^2	1.060	1.346
Final *R* indices[a] [I>2s(I)]	*R*1 = 0.0310	*R*1 = 0.0769
	*wR*2 = 0.0725	*wR*2 = 0.1549
R indices (all data)	*R*1 = 0.0355	*R*1 = 0.1008
	*wR*2 = 0.0775	*wR*2 = 0.1686
Largest difference map peak and hole (e Å^{-3})	1.358 and -1.461	1.909 and -1.904

Table 5-3 - Selected Metrical Parameters for Compounds 5.5[$SnCl_5$], 5.5[I_3], and 5.6[I_3].

Parameter	5.5[$SnCl_5$]	5.5[I_3]	5.6[I_3]
P(2)-N(1)	1.667(2)	1.668(3)	1.678(8) [1.671(8)]
P(2)-N(3)			1.674(8) [1.668(8)]
N(1)-C(5)	1.377(4)	1.375(4)	1.394(11) [1.379(11)]
N(3)-C(4)			1.361(11) [1.372(11)]
C(4)-C(5)	1.373(6)	1.376(7)	1.360(12) [1.359(12)]
N(1)-P(2)-N(3)	88.87(17)	88.90(19)	89.3(4) [88.8(4)]
I(1)-I(2)-I(3)		180.000(19) [180.00(4)]	177.31(4) [179.06(3)]

Table 5-4 - Selected Metrical Parameters for Compounds 5.7[I_3] and [$MesNH_3$]5.8$_2$[As_3I_{12}]·2AsI_3.

Parameter	5.7[I_3]	[$MesNH_3$]5.8$_2$[As_3I_{12}]·2AsI_3
As(2)-N(1)	1.826(2)	1.817(10)
As(2)-N(3)	1.831(2)	1.839(9)
N(1)-C(5)	1.351(1)	1.371(13)
N(3)-C(4)	1.350(4)	1.364(14)
C(4)-C(5)	1.384(4)	1.379(16)
N(1)-As(2)-N(3)	82.95(11)	83.6(4)
I(1)-I(2)-I(3)	177.777(12)	

5.4 Results and Discussion

Cowley recently demonstrated the differing behaviour of some diimine-based ligands with P^I and As^I centres. In particular, whereas the α-diimines in Ar-BIAN or Mes-DAB-H formed phosphenium or arsenium cations that are best described as containing Pn^{III} centres, the analogous reactions with the 2,6-diimino-substituted pyridine ligand appears to contain arsenic(I) centres. Given our interest in the chemistry and the

factors affecting the stabilization of low oxidation state main group fragments, these results prompted us to elucidate the nature of the interaction between the diimine ligands and the Pn^I centres and to assess the viability of some other commonly-used ligands that contain imine-like moieties with sp^2-hybridized nitrogen centres.

NacNac as a Potential Stabilizing Ligand

In light of the apparently odd results observed when the β-diimine NacNac ligands have been ligated to phosphorus centres,[29-31] we wished to ascertain whether such diimines were suitable ligands for P^I centres, however, given the reported reactivity with halophosphines, a minor modification of the $SnCl_2$ reduction protocol was mandated.[48] In this vein, a solution of [Li][Dipp-NacNac] was added to an equimolar amount of $SnCl_2$ in THF to produce a cloudy, colourless mixture. After stirring for several minutes, a solution of an equimolar amount of PCl_3 in THF was added to the reaction mixture. The mixture rapidly produced a pale yellow precipitate and a yellow solution. The solution contains no signals in the ^{31}P NMR spectrum consistent with a neutral compound of the form (Dipp-NacNac)P **5.4**. Similarly, the reaction of [Li][Dipp-NacNac] with PI_3 in THF resulted in the immediate formation of a reddish solution and the formation of an orange precipitate. The supernatant contained no signals in the ^{31}P NMR spectrum. Likewise, the reaction of an equimolar mixture of [Dipp-NacNac]H and $SnCl_2$ in dichloromethane with a solution of PCl_3 in the same solvent did not produce the neutral compound **5.4**. In each case, the reactions produced a multitude of products that have as yet eluded separation and identification, however, there is no evidence for the formation of a neutral compound of the form (Dipp-NacNac)P.

Phosphenium Cations

To confirm that our modified synthetic approach was applicable for the preparation of P^I centres, similar reactions were undertaken with the α-diimine 1,4-bis(2,6-diisopropylphenyl)-2,3-dimethyl-1,4-diazabutadiene (Dipp-DAB-Me). Thus an equimolar mixture of Dipp-DAB-Me and $SnCl_2$ in dichloromethane was stirred for several minutes and then a solution containing an equimolar amount of PCl_3 was added to produce a red solution (Equation 5.6). Multinuclear ^1H and ^{13}C NMR experiments on the reaction mixture indicated the presence of a singular, intact ArM-DAB ligand and the single peak at 200.1 ppm in the ^{31}P NMR spectrum suggested the quantitative formation of the phosphenium cation $[(Dipp\text{-}DAB\text{-}Me)P]^+$ **5.5**. A crystalline solid was obtained by the slow concentration of a dichloromethane solution of the resultant solid and microanalysis was consistent with a salt of the form $[(Dipp\text{-}DAB\text{-}Me)P][SnCl_5]$.

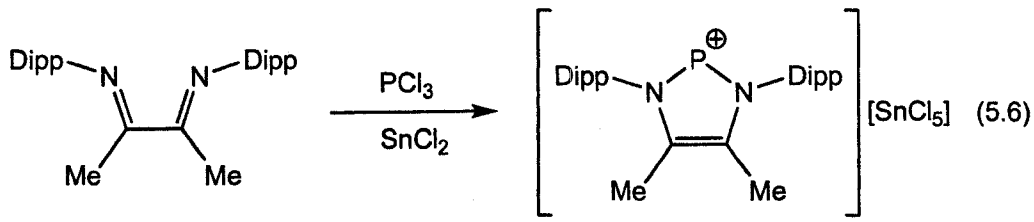

(5.6)

5.5[$SnCl_5$]

In a similar manner, the reactions of equimolar quantities of Ar-DAB-Me (Ar = Dipp, Mes) and PI_3 in dichloromethane rapidly generates red solutions (Equation 5.7). Again, multinuclear NMR experiments of the reaction mixture attest to the presence of a singular, intact Ar-DAB-Me ligand and the ^{31}P NMR spectrum contains only a single peak at 201.1 ppm (Ar = Dipp) or 202.0 ppm (Ar = Mes). The slow concentration of

acetonitrile solutions of the solid provided crystalline material having an elemental composition consistent with the formula [(Ar-DAB-Me)P][I_3].

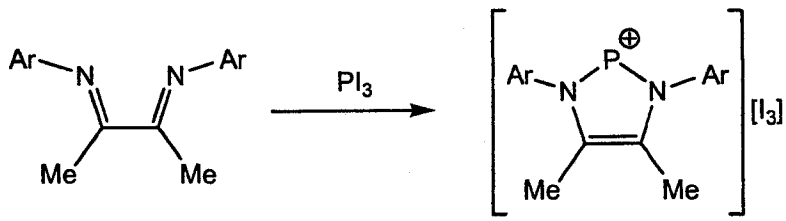

(5.7)

5.5[I_3] Ar = Dipp
5.6[I_3] Ar = Mes

In the case of each salt, the material obtained after recrystallization was suitable for analysis by single-crystal X-ray diffraction experiments. A summary of the experimental crystallographic details is compiled in Table 5-1 and selected metrical parameters are listed in Table 5-3. Depictions of the molecular structures of the salts are presented in Figure 5.1, Figure 5.2 and Figure 5.3. The pentachlorostannate salt [(Dipp-DAB-Me)P][$SnCl_5$] crystallizes in the space group *Pnma* with one half of a cation and an anion in the asymmetric unit. The phosphorus atom sits on a crystallographic mirror plane that relates the two halves of the cation and the tin atom and three of the chlorine atoms are likewise situated on the mirror plane relating the two parts of the anion. The triiodide salt [(Dipp-DAB-Me)P][I_3] crystallizes in the spacegroup *C2/m* with one half of a cation and two quarters of anions in each asymmetric unit. Again, the phosphorus atom resides on a crystallographic mirror plane that relates the two halves of the cation and all of the iodine atoms are located on special positions in the unit cell. The other triodide salt [(Mes-DAB-Me)P][I_3] crystallizes in the space group $P2_12_12_1$ with two crystallographically independent cation and anion pairs in the asymmetric unit with all atoms at general positions.

While the metrical parameters of each of the anions in these salts compare well with the average values obtained from the Cambridge Structural Database (CSD)[49] and do not warrant further discussion, the identities of the anions unambiguously demonstrate that a redox reaction has taken place: the Sn^{II} in the starting material has clearly been oxidized to Sn^{IV} in the trigonal bipyramidal $[SnCl_5]^-$ anion and the production of triiodide anions is consistent with the presence of I_2 and I^- in the other reaction mixture. It should be noted that there are no unusually short distances between the cations and the anions in either salt. The metrical parameters of the cations in each salt are important to aid in the assessment of the nature of the interaction between the diimine ligand and the pnictogen centre. Regardless of the identity of the anion, the metrical parameters of the cation are indistinguishable. For example the P-N distance in **5.5**[$SnCl_5$] is 1.667(2) Å and the distance in the triiodide salts are 1.668(3) Å for **5.5**[I_3] and 1.678(8) Å (and 1.671(8) Å) for **5.6**[I_3]. Similarly, the C-N and C-C distances within the heterocycle are 1.377(4) Å and 1.373(6) Å, respectively in **5.5**[$SnCl_5$] versus 1.375(4) Å and 1.376(7) Å for **5.5**[I_3]. Similar C-C and C-N distances are found in the salt **5.6**[I_3] (Table 5-3). The corresponding angles within the heterocyclic cations in each salt are also indistinguishable from each other: the N-P-N angles are 88.88(17)° and 88.90(19)° in **5.5**[$SnCl_5$] and **5.5**[I_3], respectively and 89.3(4)° and 88.8(4)° in **5.6**[I_3]. Overall, the metrical parameters of the cations in these salts compare excellently with the average values obtained from the CSD for the other unsaturated 5-membered ring phosphenium cations that have been reported previously,[22,50-52] thus the descriptions of these cations as containing phosphorus(III) is certainly justified.

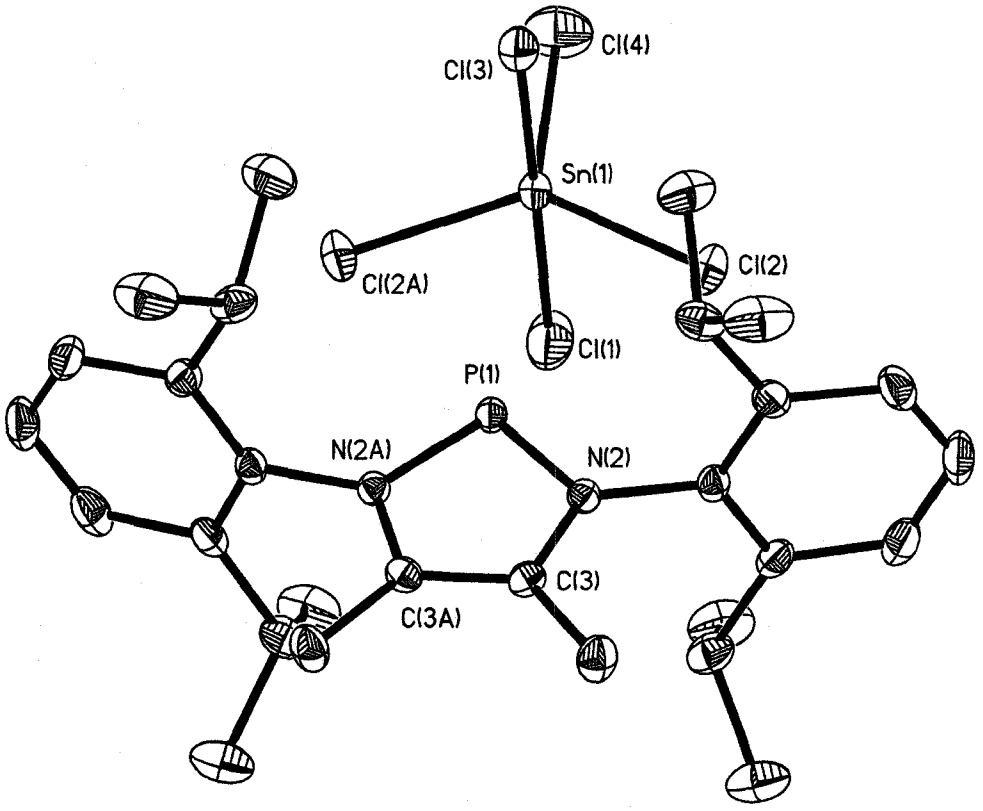

Figure 5.1 - Thermal ellipsoid plot (30% probability surface) of 5.5[$SnCl_5$]. Hydrogen atoms are omitted for clarity.

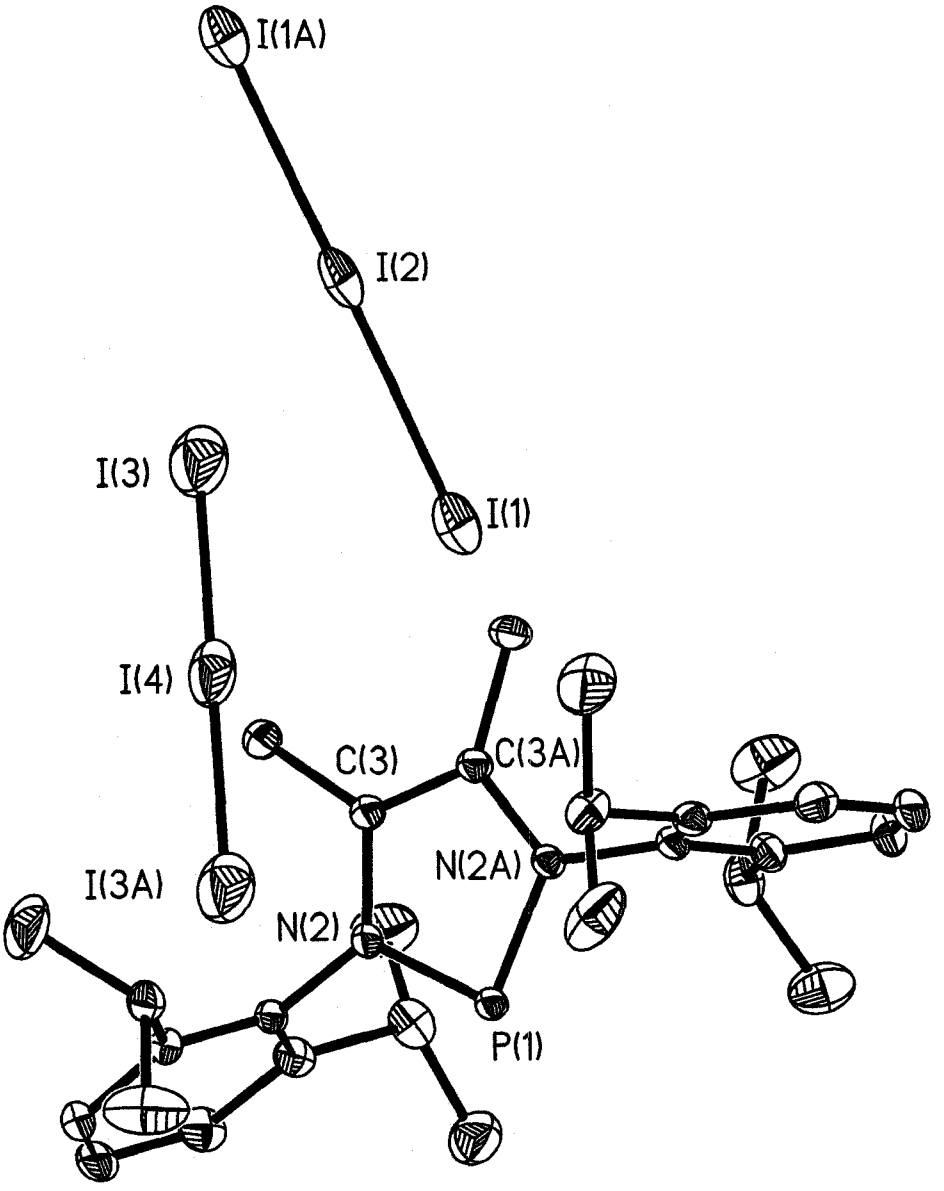

Figure 5.2 - Thermal ellipsoid plot (30% probability surface) of 5.5[I_3]. Hydrogen atoms are omitted for clarity.

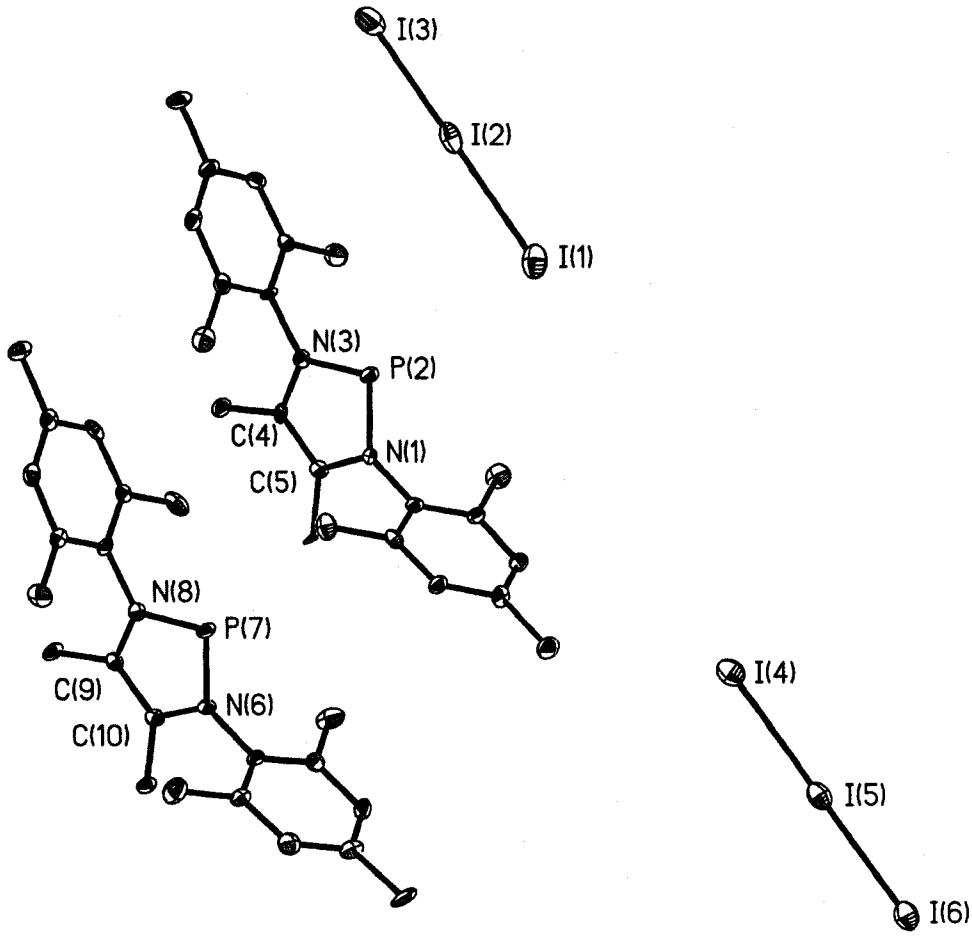

Figure 5.3 - Thermal ellipsoid plot (30% probability surface) of 5.6[I_3]. Hydrogen atoms are omitted for clarity.

Arsenium Cations

Cowley *et al.* have shown that the reduction of $AsCl_3$ with $SnCl_2$ results in the generation of As^{III} aresenium cations in the presence of easily reduced diimines (Mes-DAB-H), although AsI_3 has thus far only been used to generate As^{I} cations when the diimine is more resistant to reduction. As might be expected, AsI_3 in the presence of α-diimines does undergo an analogous process to PI_3 discussed above. The reaction

mixtures rapidly darken from a reddish-orange colour to dark red. Once again, multinuclear NMR experiments of the reaction mixture attest to the presence of a singular, intact Ar-DAB-Me ligand. In an attempt to obtain crystalline material appropriate for single crystal X-ray experiments, the crude solid from the reaction of AsI_3 with Dipp-DAB-Me was dissolved in dichloromethane and upon slow concentration suitable crystals were generated. The data obtained was of poor quality, although the connectivity of the cation could be confirmed to be $[(Dipp\text{-}DAB\text{-}Me)As]^+$, **5.7**. Interestingly, the anion was not that of $[As_2I_8]^{-2}$ reported for the As^I cation $[(Dipp\text{-}Dimpy)As]^+$ generated under similar condition, but rather $[As_3I_{11}]^{-2}$. The molecular structure of the dianion is shown in Figure 5.4 is that of an AsI_3 trimer capped by two I^- anions.

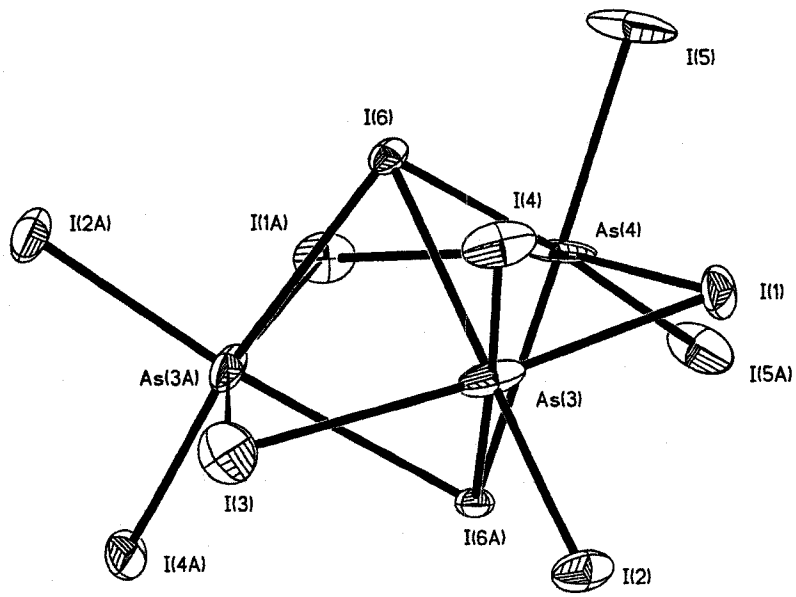

Figure 5.4 - Thermal ellipsoid plot (30% probability surface) of the dianion $[As_3I_{11}]^{-2}$.

In an attempt to obtain better quality X-ray diffraction data, the crystals of **5.7**$_2$[As_3I_{11}] were dissolved in acetonitrile. Upon slow concentration of the solution red crystals were deposited that were also suitable for single crystal X-ray diffraction, however, the molecular structure shows the anion to be triiodide, as shown in Figure 5.5. The further disproportionation of AsI_3 may be a result of the enhanced donor ability of acetonitrile, as compared with dichloromethane, as donor molecules have been shown to encourage the disproportionation of phosphorus iodides.[53] Compound **5.7**[I_3] crystallizes the space group *P-1* and selected metrical parameters are listed in Table 5-4. The metrical parameters are consistent with those reported for the three other related structures generated from different diimines.[18,21,52]

Crystals suitable for single crystal X-ray crystallography were also obtained from slow concentration of a dichloromethane solution of the product obtained from the treatment of AsI_3 with Mes-DAB-Me. Once again, the expected [(Mes-DAB-Me)As]$^+$, **5.8**, sent in the molecular structure of the product, shown in Figure 5.6, however the anion is now the trianion $[As_3I_{12}]^{-3}$, which crystallized along with free AsI_3 molecules and ammonium cations $[MesNH_3]^+$. The mixture crystallizes in the space group *Pnma* with the ammonium cation, an iodide anion and an As-I bond from the trianion lying in a crystallographic mirror plane. The asymmetric unit contains one **5.8** cation, one free AsI_3 molecule, half of the ammonium cation and half of the trianion cluster. The structure of the cluster is depicted below in Figure 5.7, shows it to be composed of a trimer of AsI_3 molecules and iodide anions. The metrical parameters (listed in Table 5-4) of the arsenic heterocycle are indistinguishable from those in **5.7**[I_3], within experimental error. The presence of the ammonium cation is more likely a result of impure solvent than of the

experimental conditions. It is interesting to note that the treatment of AsI_3 with three different imines (Dipp-Dimpy, Dipp-DAB-Me, Mes-DAB-Me) results in the generation of three different As-I anionic clusters. The conditions favouring each anion are worthy of further investigation.

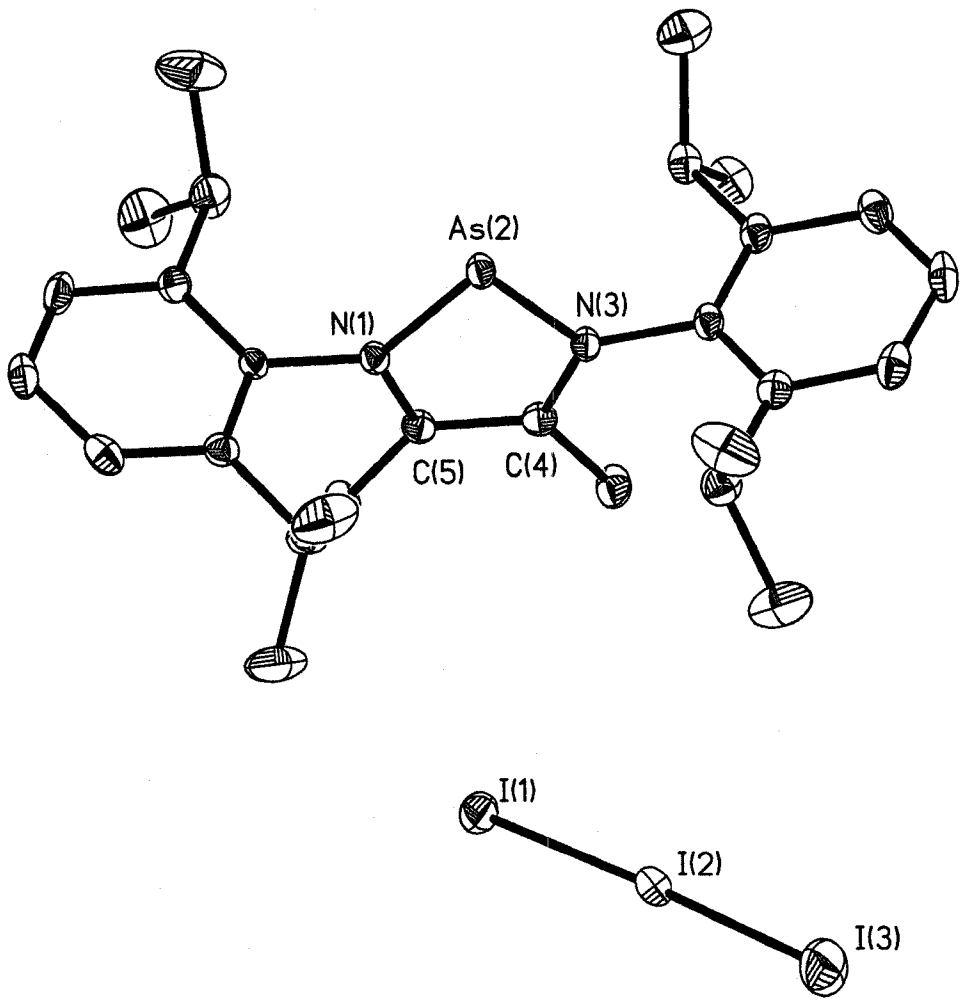

Figure 5.5 - Thermal ellipsoid plot (30% probability surface) of 5.7[I_3]. Hydrogen atoms are omitted for clarity.

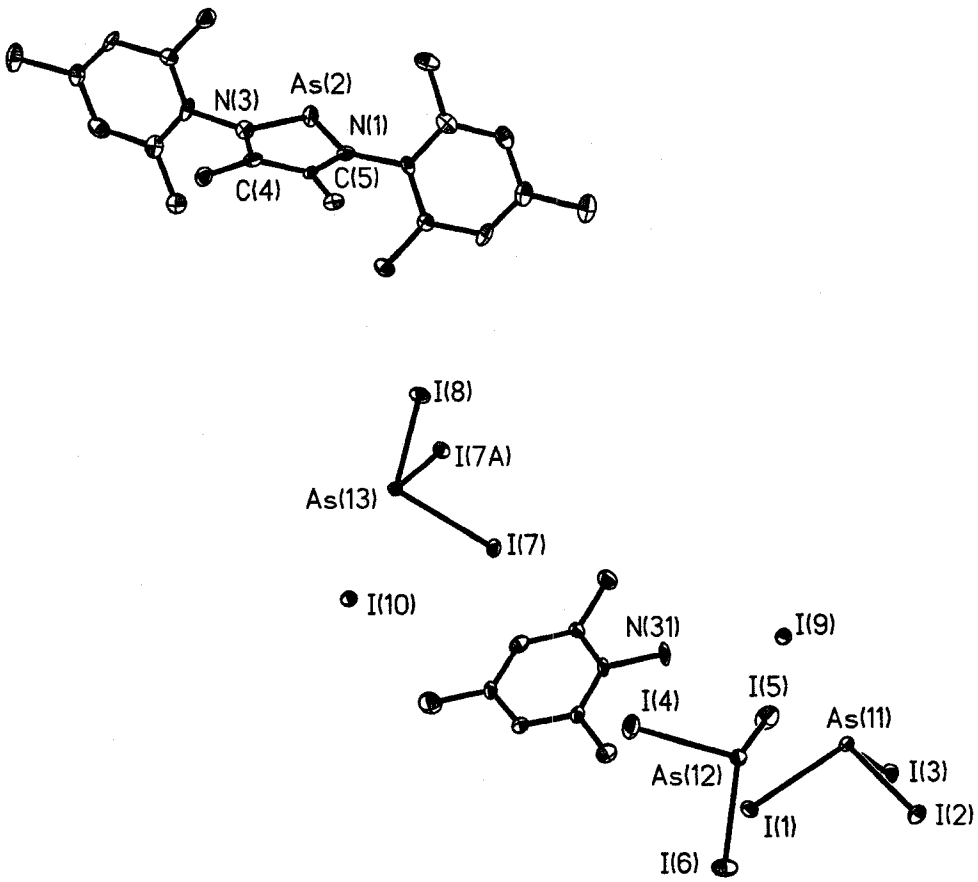

Figure 5.6 - Thermal ellipsoid plot (30% probability surface) of the asymmetric unit of $[MesNH_3]5.8_2[As_3I_{12}]\cdot 2AsI_3$. Hydrogen atoms are omitted for clarity.

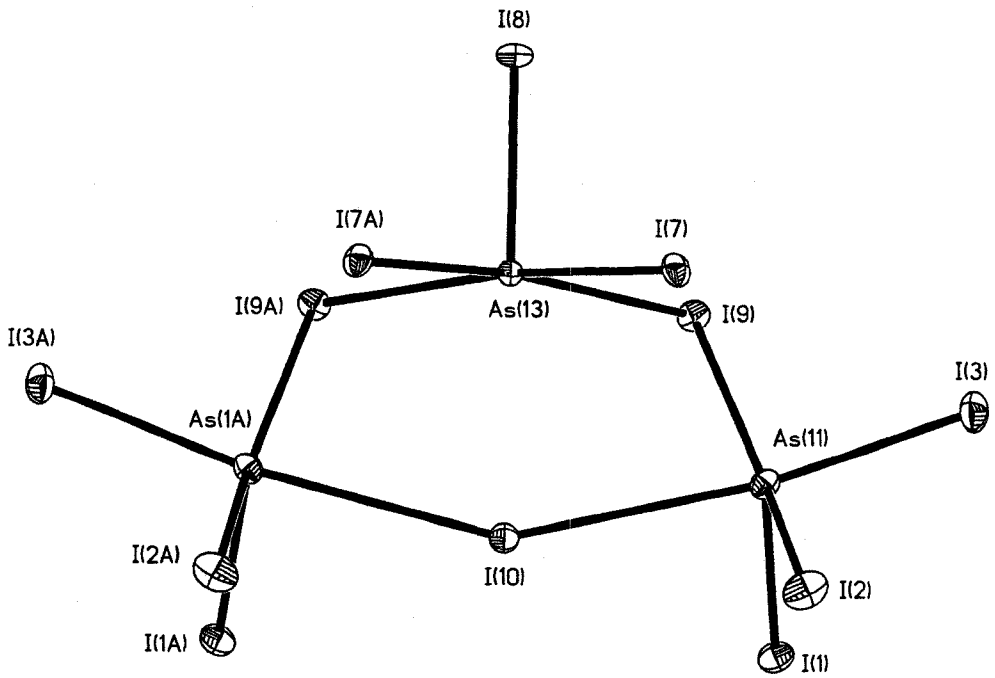

Figure 5.7 - Thermal ellipsoid plot (30% probability surface) of the trianion $[As_3I_{12}]^{-3}$.

The nature of the anions in the pnictogenium salts described above and the other salts described in the introduction indicates that RedOx processes occur in the formation of the heterocycles that are completely consistent with the processes postulated to occur in the formation of phosphine- or carbene-stabilized Pn^I salts (see Chapters 2, 3 and 6).[8,12,14-17] In the case of α-diimines, a further intermolecular RedOx process involving oxidation of Pn^I to Pn^{III} and reduction of the ligand to its doubly-reduced form has been suggested to generate the observed pnictogenium cations.[18,21] Finally, the β-diketiminate ligand does not appear to chelate to putative Pn^I centres under conditions analogous to those employed for the other imine-containing ligands.[48]

Computational Investigations

In an attempt to understand the clearly different chelating behaviour of the various diimine ligands and Pn^{I} centres, we performed a series of DFT calculations and NBO analyses on the model compounds of the Pn-containing compounds chelated by the ligands DAB, NacNac, Dimpy and Bipy. Models of the free ligands and their doubly-reduced forms are also presented for comparative purposes. Additional calculations were undertaken on the dications $[(NacNac)Pn]^{+2}$ to assess the viability of β-diketiminate chelate of Pn^{III} cations. In each model, all substituents have been replaced with hydrogen atoms and the highest-reasonable point symmetry was enforced; important computational results are compiled in Table 5-5.

Table 5-5 - Selected Computed Energies for the Model Ligands and Pnictogen Complexes.

Models	Sym[a]	# *i*[b]	Corrected Energy[c], Etotal (au)	Rel. E (kJ mol^{-1})	HOMO (eV)	LUMO (eV)	HOMO–LUMO (eV)
Ligands							
Oxidized							
DAB	C_{2h}	0	-188.00875	0	-7.82	-2.18	5.64
	C_{2h}	0	-188.00532	8.99	-7.65	-2.42	5.23
	C_{2v}	1	-187.99769	29.04	-7.70	-2.35	5.36
$[NacNac]^{-}$	C_{2v}	0	-226.72162		0.02	3.80	3.78
Dimpy	C_{2v}	0	-435.00098		-7.32	-2.17	5.15
Bipy	C_{2h}	0	-495.18458	0	-6.74	-1.79	4.95
	C_{2v}	1	-495.17350	29.09	-6.78	-1.81	4.97
Reduced							
$[DAB]^{-2}$	C_{2v}	0	-187.81280		7.09	7.45	0.36
$[NacNac]^{-3}$	C_{2v}	0	-226.28566		8.34	8.77	0.43
$[Dimpy]^{-2}$	C_{2v}	2	-434.88185		5.48	5.90	0.42
$[Bipy]^{-2}$	C_{2v}	3	-495.05336		5.16	5.74	0.58
Complexes							
P species							
$[(DAB)P]^{+}$	C_{2v}	0	-529.15437		-12.33	-7.51	4.82
(NacNac)P	C_{2v}	1	-568.00279	25.31	-3.50	-1.96	1.53
	C_s	0	-568.01243	0	-3.95	-1.87	2.08

$[(Dimpy)P]^+$	C_{2v}	1	-776.16392		-10.28	-6.93	3.35
	C_s	0	-776.16388		-10.28	-6.87	3.41
$[(Bipy)P]^+$	C_{2v}	0	-836.30040		-9.65	-6.30	3.36
As species							
$[(DAB)As]^+$	C_{2v}	0	-2423.67771		-11.90	-7.56	4.35
(NacNac)As	C_{2v}	1	-2462.54314	15.67	-3.55	-1.87	1.68
	C_s	0	-2462.54911	0	-3.91	-1.81	2.10
$[(Dimpy)As]^+$	C_{2v}	0	-2670.69820		-10.01	-6.77	3.24
$[(Bipy)As]^+$	C_{2v}	0	-2730.82791		-9.43	-6.31	3.12
Dications							
$[(NacNac)P]^{+2}$	C_{2v}	0	-567.36234		-19.12	-14.08	5.04
$[(NacNac)As]^{+2}$	C_{2v}	0	-2461.89521		-18.58	-14.03	4.55

[a] Point group symmetry. [b] Number of imaginary vibrational frequencies. [c] $E_{total} = E_{calculated} + ZPVE$.

The C_{2v} symmetry optimized geometries of the phosphorus- and arsenic-containing model compounds are depicted in Figure 5.8 and Figure 5.9, respectively, and the computed values of important metrical parameters are provided. The only phosphorus compound for which analogues have been structurally characterized experimentally (with substituents other than hydrogen) is the cation $[(DAB)P]^+$; given the simplicity of the model used, the agreement between the metrical parameters of the calculated and experimental structures (*vide supra*) is excellent and attests to the suitability of the computational method employed herein. Furthermore, the calculated structure of $[(DAB)P]^+$ is consistent with those computed previously using different theoretical methods.[54] Similarly, there is good agreement between the computed metrical parameters of the models $[(DAB)As]^+$ and $[(Dimpy)As]^+$ and those reported for their corresponding crystallographically-characterized analogues.[21,52]

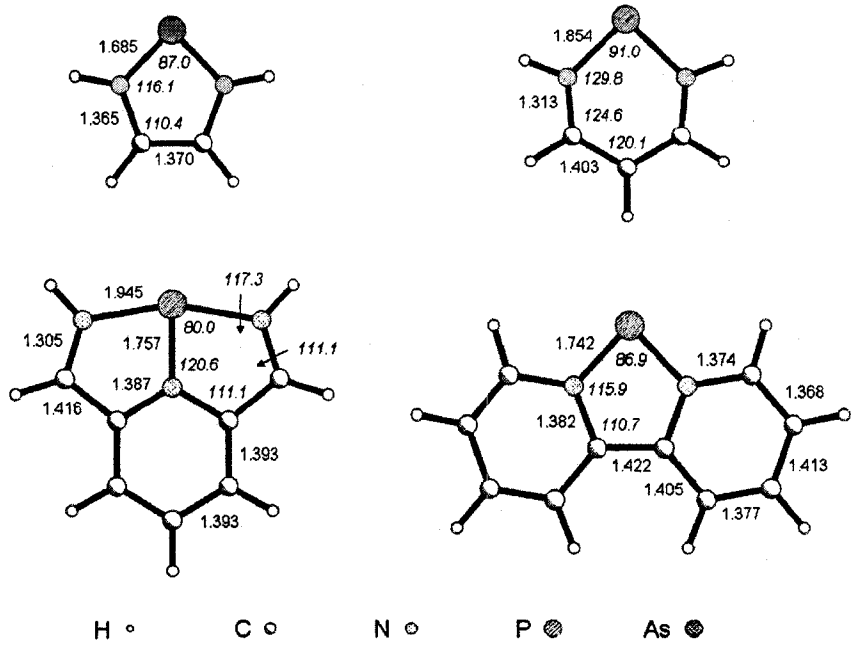

Figure 5.8 - Optimized structures (C_{2v} symmetry) of the phosphorus-containing species $[(DAB)P]^+$, (NacNac)P, $[(Dimpy)P]^+$, and $[(Bipy)P]^+$. Selected bond distances (Å) and angles (°) are indicated.

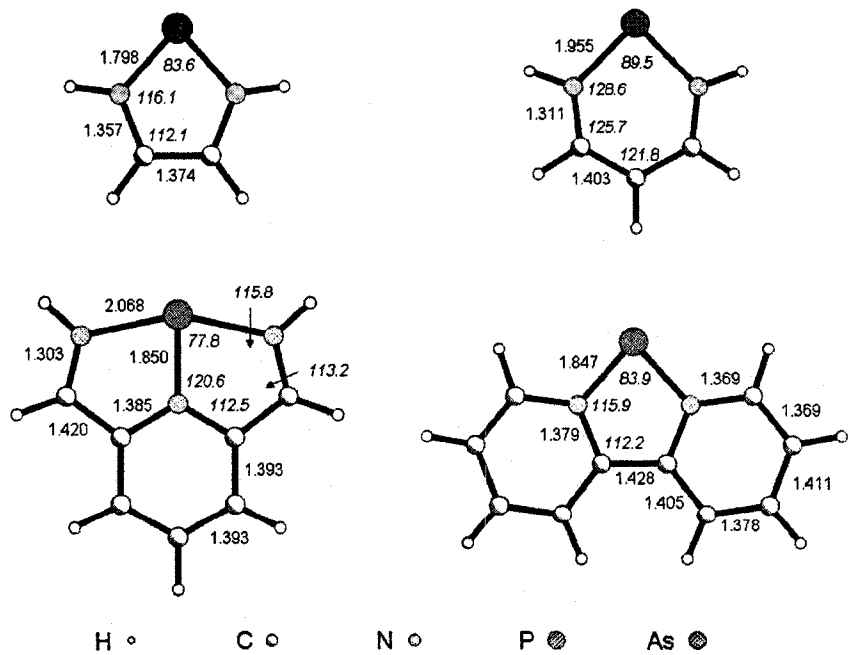

Figure 5.9 - Optimized structures (C_{2v} symmetry) of the arsenic-containing species $[(DAB)As]^+$, (NacNac)As, $[(Dimpy)As]^+$, and $[(Bipy)As]^+$. Selected bond distances (Å) and angles (°) are indicated.

There are several noteworthy findings with regard to the structures presented in Figure 5.8 and Figure 5.9. Most importantly, the optimized structures of (NacNac)P, $[(Dimpy)P]^+$ and (NacNac)As are not minima on the potential energy hypersurface when they are constrained to C_{2v} symmetry. True minima are observed for these model compounds when they are optimized in C_s-symmetry; the structures thus obtained are depicted in Figure 5.10 and will be discussed below. In regard to the C_{2v} structures, one important feature distinguishes the models containing DAB, Dimpy and Bipy ligands from the models including the NacNac ligand. Whereas the relatively short Pn-N distances (P: 1.685 to 1.757 Å; As: 1.798 to 1.850 Å) in the cationic α-diimine systems suggest the presence partial multiple-bonding, the Pn-N distances in the putative neutral (NacNac)Pn are extremely long (P: 1.854 Å; As: 1.955 Å) and are beyond the values typically observed for single bonds. The contrast between the P-N bond distances suggests significant differences in the nature of the bonding between the ligands and the Group 15 element. The contrasting behaviour is highlighted by the C_s-symmetry optimized structures of (NacNac)Pn which, while retaining very long Pn-N bonds, adopt boat-like conformations with a clearly pyramidal carbon environment.

Whereas the difference between the planar and non-planar (NacNac)Pn structures are drastic, the planar C_s-symmetry structure of the $[(Dimpy)P]^+$ model is distorted only slightly away from C_{2v}-symmetry, as illustrated in Figure 5.10, and the imaginary frequency corresponding to this deformation is only -75cm^{-1}. The metrical parameters of this cation suggest that it is probably best understood as being composed of an intermolecularly imine-coordinated phosphenium cation, as particularly evidenced by the

dramatically different N-C_{imine} bond distances of 1.320 Å and 1.291 Å and the corresponding C_{imine}-C_{α} distances of 1.403 Å and 1.430 Å, respectively.

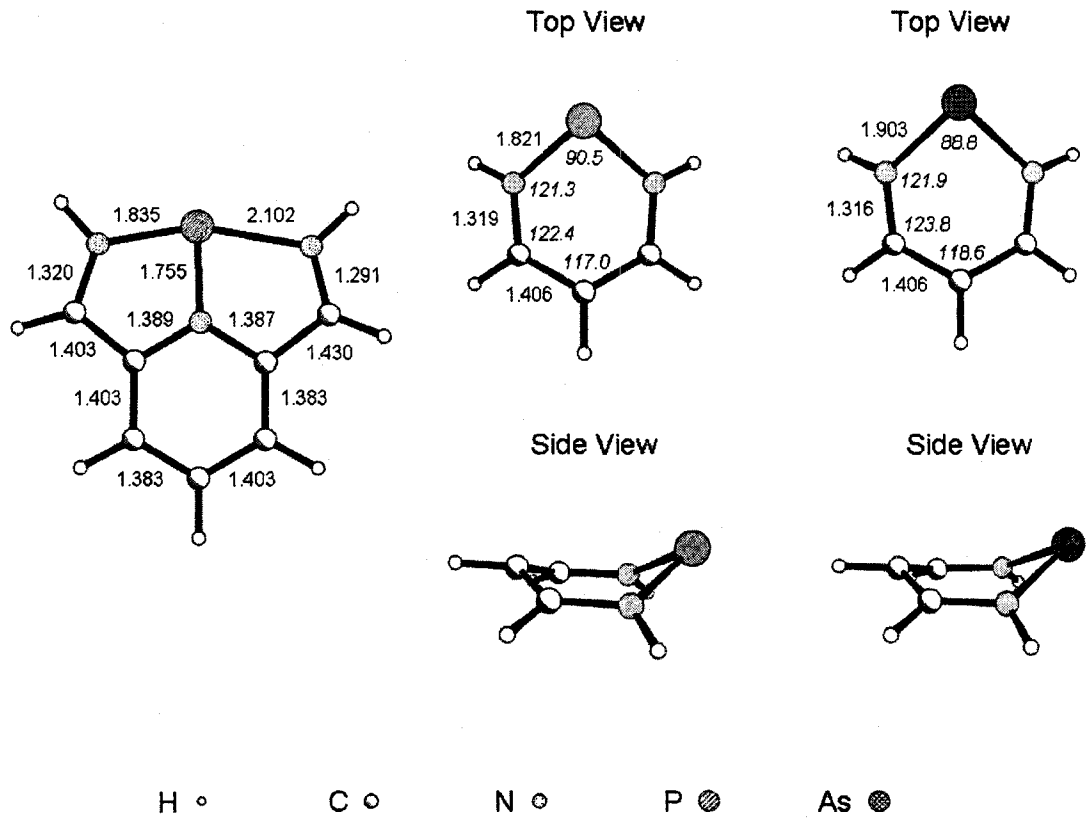

Figure 5.10 - Optimized structures (C_s symmetry) of the phosphorus- and arsenic-containing species [(Dimpy)P]$^+$, (NacNac)P, (NacNac)As. Selected bond distances (Å) and angles (°) are indicated.

To assess the structural changes that occur to the ligands upon coordination to the pnictogen centres and to evaluate the postulate that the ligands become doubly-reduced in certain instances, we have determined the optimized geometries of the free ligands (Figure 5.11) and their doubly-reduced forms (Figure 5.12). In both figures, only the C_{2v}-symmetry structures are presented because they are the most appropriate models for comparison to the pnictogen-containing heterocycles. It should be noted that for DAB and Bipy, the C_{2v}-symmetry structures are first-order transition states; the true minimum

optimized structures of $[Bipy]^{-2}$ and $[Dimpy]^{-2}$ were not determined as these are not likely to exist as isolated dianions.

As large changes in the angles within the ligands in their uncomplexed and complexed forms are unavoidable, the examination of such metrical parameters is not as helpful as is the comparison of bond distances. Several important observations are gleaned from the comparison of the bond distances of the ligands and those of their Group 15 complexes. Perhaps the most noteworthy is that the imine-like N-C distances in the complexes involving the neutral ligands (DAB, Dimpy, and Bipy) are longer than those observed for the free ligands. In stark contrast, the N-C distances in the putative (NacNac)Pn complexes (for both the C_{2v} and C_s models) are almost identical to that found in the free anion $[NacNac]^-$. Similarly, while there are obvious and significant contractions of the C_{imine}-C_α bonds for each of the complexes of the neutral ligands, there is only a slight contraction observed for the complexes of $[NacNac]^-$. Thus, once again, the metrical parameters highlight the considerably different behaviour of the β-diketiminate ligand.

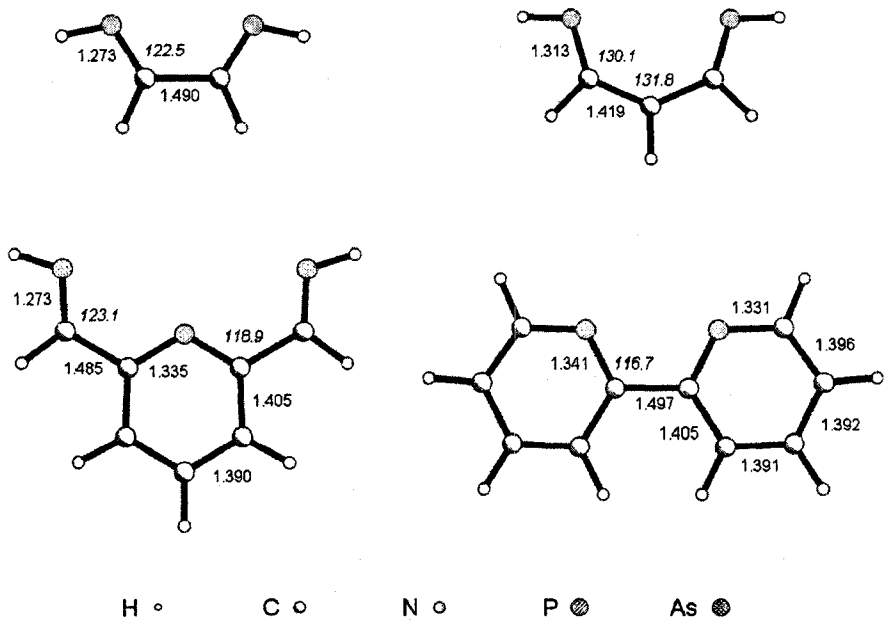

Figure 5.11 - Optimized structures (C_{2v} symmetry) of the free ligands DAB, [NacNac]$^-$, Dimpy, and Bipy. Selected bond distances (Å) and angles (°) are indicated.

In regard to the metrical parameters calculated for the species containing DAB, Dimpy and Bipy ligands, it is also noteworthy that the distances observed for the $[(DAB)Pn]^+$ models are more similar to those calculated for the doubly-reduced $[DAB]^{-2}$ dianion than those for the free ligand. For the Dimpy and Bipy complexes, many of the metrical parameters appear to fall between those found in the neutral and doubly-reduced ligands, with the $[(Dimpy)Pn]^+$ complexes having parameters closer to those of the doubly-reduced ligand than are the corresponding parameters in the $[(Bipy)Pn]^+$ complexes. For example, while the imine N-C_{imine} distance of 1.303 Å in $[(Dimpy)As]^+$ is between the values of 1.273 Å in Dimpy and 1.331 Å in $[Dimpy]^{-2}$, the N-$C_{pyridyl}$ distance of 1.385 Å in $[(Dimpy)As]^+$ is identical to that predicted for the $[Dimpy]^{-2}$ model. Overall, the examination of the metrical parameters in each of these models

suggests that the DAB ligand is the most completely reduced upon complexation to a putative Pn^{I} centre, followed by Dimpy and then Bipy. In sharp contrast, the bond distances in the $[NacNac]^{-}$ anion appear to be largely unaffected by complexation to the electron-rich Group 15 centre.

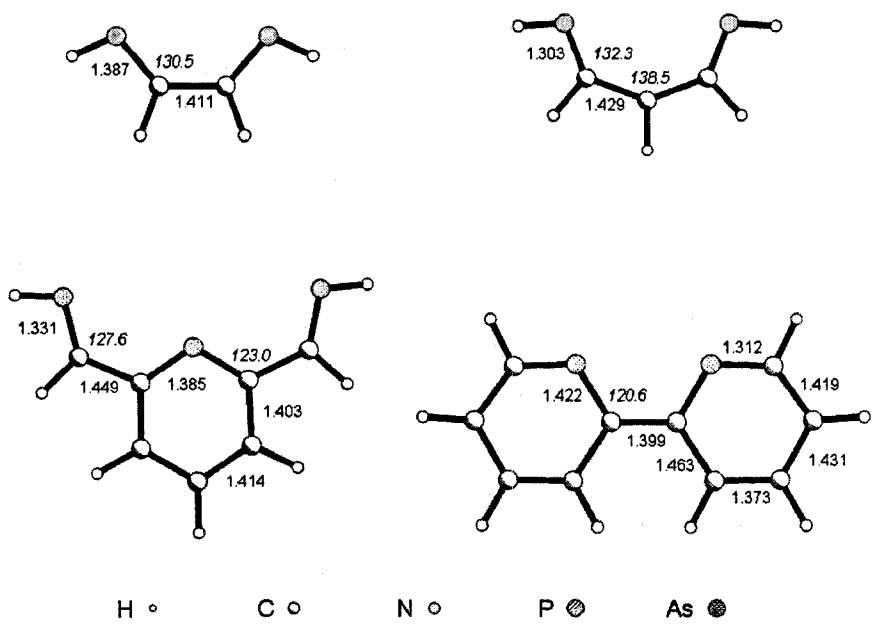

Figure 5.12 - Optimized structures (C_{2v} symmetry) of the doubly-reduced ligands $[DAB]^{-2}$, $[NacNac]^{-3}$, $[Dimpy]^{-2}$, and $[Bipy]^{-2}$. Selected bond distances (Å) and angles (°) are indicated.

In order to quantify the nature of the interaction between the various ligands and the pnictogen atoms, we performed NBO population analyses of each of the model compounds and pertinent results are compiled in Table 5-6 and Table 5-7. With regard to the discussion of the metrical parameters described above, it is noteworthy that the NBO Wiberg bond indices (WBI) mirror the trends suggested by the analysis of the bond distances. For example, whereas the Wiberg bond indices for the N-C bonds and the C-C bonds in $[(DAB)Pn]^{+}$ are almost identical to those in the $[DAB]^{-2}$ dianion, the

corresponding values for the neutral (NacNac)Pn models are much closer to those observed in the free $[(NacNac)]^-$ anion. While the indices for the $[(Bipy)Pn]^+$ models fall between those of the neutral and doubly-reduced ligands, as anticipated on the basis of the metrical parameters, it is somewhat surprising that the indices for the N-C and C-C bonds in the $[(Dimpy)Pn]^+$ are remarkably similar to those in the doubly-reduced $[Dimpy]^{-2}$ dianion.

The Wiberg bond indices of the Pn-N bonds provide some initial insight into the magnitude of the interactions between the various ligand and the Group 15 element. Most notably, the WBIs for the Pn-N bonds are greatest for the $[(DAB)Pn]^+$ models, which exhibit the shortest bonds between those elements. The next highest indices are observed for the bonds between the pnictogen atoms and the pyridyl nitrogen atoms in the Dimpy ligands; the values for these indices are very similar to those calculated for the $[(Bipy)Pn]^+$ models and suggest that such cations may be reasonable synthetic targets. The Pn-N bond indices for the (NacNac)Pn models are considerably smaller than those of the cationic α-diimine models and suggest that the long P-N bonds may be considerably weaker than those in the other models.

Table 5-6 - Selected Computed Data for the Model Ligands.

Model	Sym[a]	q(N)[b]	N-C_{imine} WBI[c]	C_{imine}-C_α WBI[c]	π HOMO[d] (eV)	π LUMO[d] (eV)	π HOMO-LUMO (eV)
Oxidized							
DAB	C_{2h}	-0.62	1.9256	1.0487	-8.19	-2.18	6.01
	C_{2h}	-0.59	1.9433	1.0512	-8.97	-2.42	6.55
	C_{2v}	-0.58	1.9506	1.0276	-8.60	-2.35	6.25
$[NacNac]^-$	C_{2v}	-0.81	1.6575	1.315	0.02	4.47	4.45
Dimpy	C_{2v}	-0.58 (-0.36)[e]	1.9377	1.0366	-7.37	-2.17	5.20

Bipy	C_{2h}	-0.46	1.3802	1.0402	-6.74	-1.79	4.95
	C_{2v}	-0.41	1.3863	1.0343	-6.78	-1.81	4.98
Reduced							
$[DAB]^{-2}$	C_{2v}	-1.14	1.2941	1.5346	7.09	9.51	2.42
$[NacNac]^{-3}$	C_{2v}	-1.02	1.8007	1.339	6.74	10.82	4.08
$[Dimpy]^{-2}$	C_{2v}	-0.85 (-0.69)[e]	1.5374	1.1819	5.48	6.58	1.10
$[Bipy]^{-2}$	C_{2v}	-0.54	1.0989	1.4436	5.16	7.13	1.97

[a] Point group symmetry. [b] NBO charge on the dicoordinate imine N atoms. [c] NBO Wiberg bond indices for the specified bonds. [d] Frontier orbitals involving only the π-system in the ligands. [e] NBO charge of the $N_{pyridyl}$ atom.

Table 5-7 - Selected Electron Population Analysis Data for the Model Pnictogen Complexes.

Model	Sym[a]	Occ Pn p(π)[b]	q(Pn)[c]	q(N)[c]	Pn-N WBI[d]	N-C_{imine} WBI[d]	C_{imine}-C_{α} WBI[d]
P species							
$[(DAB)P]^{+}$	C_{2v}	0.893	1.18	-0.86	1.0496	1.2281	1.5450
(NacNac)P	C_{2v}	1.905	0.24	-0.79	0.6690	1.4854	1.3278
	C_s	1.408	0.27	-0.81	0.6900	1.4579	1.3489
$[(Dimpy)P]^{+}$	C_{2v}	1.046	0.98	-0.76	0.6129	1.5475	1.2318
				-0.62[e]	0.8738[e]		
	C_s	1.040	0.99	-0.79	0.7498	1.4377	1.2945
				-0.72	0.4560	1.6682	1.1714
				-0.62[e]	0.8786[e]		
$[(Bipy)P]^{+}$	C_{2v}	1.278	0.87	-0.59	0.8559	1.1486	1.2079
As species							
$[(DAB)As]^{+}$	C_{2v}	0.916	1.22	-0.87	0.9995	1.2614	1.5085
(NacNac)As	C_{2v}	1.924	0.28	-0.80	0.6316	1.4955	1.3352
	C_s	1.473	0.30	-0.81	0.6486	1.4751	1.3472
$[(Dimpy)As]^{+}$	C_{2v}	1.076	1.04	-0.76	0.5624	1.5763	1.2179
				-0.62[e]	0.8411[e]		
$[(Bipy)As]^{+}$	C_{2v}	1.318	0.90	-0.60	0.8011	1.1649	1.3083
Dications							
$(NacNac)P^{+2}$	C_{2v}	0.592	1.52	-0.86	1.0119	1.2979	1.4200
$(NacNac)As^{+2}$	C_{2v}	0.565	1.61	-0.88	0.9499	1.3286	1.4131

[a] Point group symmetry. [b] NBO population of the valence p orbital on the Pn atom of suitable symmetry to interact with the π-system of the ligand. [c] NBO charge on the dicoordinate P atom. [d] NBO Wiberg bond indices for the specified bonds. [e] NBO charges and Wiberg bond indices involving the $N_{pyridyl}$ atom.

Two other quantities obtained from the NBO analyses may provide insight into the nature of the ligand-Pn interaction and are worthy of discussion. Firstly, the almost negligible positive charges (0.24-0.3) on the Pn atoms in the (NacNac)Pn models (Table 5-7) demonstrate that the pnictogen centres in these compounds are considerably more electron-rich than are the Pn atoms in any of the other model compounds (q(Pn) > 0.87 in each case). Such an observation is consistent with the trends observed for the metrical parameters, which suggest that the NacNac ligand does not become reduced significantly.

More importantly in the context of intermolecular ligand reduction, the population of one of the valence p orbitals on the Pn centre can be used to gauge (admittedly in a rough manner) the amount of electron density transferred from the pnictogen to the ligand. Using the assumption for such a analysis that a singlet Pn^{I} cation suitable for ligation should have a population of 2.0 electrons in two valence orbitals and that the interaction of the ligands will generate the σ-framework of the molecule (with one of the filled valence orbitals becoming a "lone pair" of electrons), the most obvious transfer of electron density should be manifested in the population of the valence p orbital of π-type symmetry (p(π)). In this light, several observations are noteworthy. Perhaps most obviously, the occupancy of the valence p(π) for both the $[(DAB)Pn]^{+}$ and $[(Dimpy)Pn]^{+}$ models are considerably lower than 2.0 (ranging from 0.893 to 1.076 electrons) and are consistent with significant transfer of electron density from the Pn atom to the ligand. While the $[(Bipy)Pn]^{+}$ models are consistent with somewhat less transfer of electron density (P: 1.278, As: 1.318), the magnitudes of the transferred electron density is significantly larger than those calculated for phosphine-stabilized Pn^{I} centres (Chapter 2). Probably the most important observation is that the occupancy of the Pn p(π) orbitals in

the C_{2v}-symmetry (NacNac)Pn models (P: 1.905, As: 1.924) suggest that virtually no electron density is transferred to the π-system of the ligand. The adoption of the non-planar structure allows reduces the occupancy of the corresponding orbitals in the C_s-symmetry (NacNac)Pn models and suggest one reason for the adoption of the non-planar structure.

For phosphine-stabilized Pn^I cations, the transfer of electron density was considered in terms of hyperconjugation (or back-bonding) between the p(π) orbital and the ligand π-system. For the systems in this work, the greater magnitude of the donation suggests that it may be more appropriate to call the interaction Pn-ligand electron transfer in the case of the DAB ligand, however the underlying concept is the same in both instances (it is just much more difficult to reduce a phosphine than a diimine). To understand how the ligands do or do not remove electron density from the putative Pn^I cations, one must examine the shape and composition of important molecular orbitals on the ligands. Given the discussion regarding the population of the Pn p(π) orbital, the composition of the vacant orbitals involving the π-system on each uncoordinated ligand are presumably the most relevant. The lowest unoccupied molecular orbitals involving the π-system are depicted in Figure 5.13 and illustrate an important difference between the neutral ligands and the $[NacNac]^-$ chelate. Whereas the LUMO in each of the neutral ligands is of the correct symmetry (b_1 in C_{2v}) to interact with a filled p(π) orbital on the Pn^I centre, the lowest vacant orbital involving the π-system on the $[NacNac]^-$ model does not have the appropriate symmetry (a_2 in C_{2v}) to interact in the same way. In that system, the first vacant orbital of b_1 symmetry is the LUMO+6 orbital, which is significantly

higher in energy than the LUMO (5.67 eV vs. 4.47 eV) and which is based primarily on the unique α-carbon atom in the ligand.

In regard to the composition of the orbitals of the neutral ligands depicted in Figure 5.13, one other point should be noted. Due to its relatively localized nature, population of the LUMO in the DAB model will have a dramatic and obvious effect on the metrical parameters of the resultant structure. In contrast the LUMOs of the Bipy and Dimpy are considerably more delocalized and thus the changes in individual bond distances in the ligands upon population of the LUMO are anticipated to be more subtle. For this reason, population analyses of the type presented herein are a valuable tool for the examination of such systems.

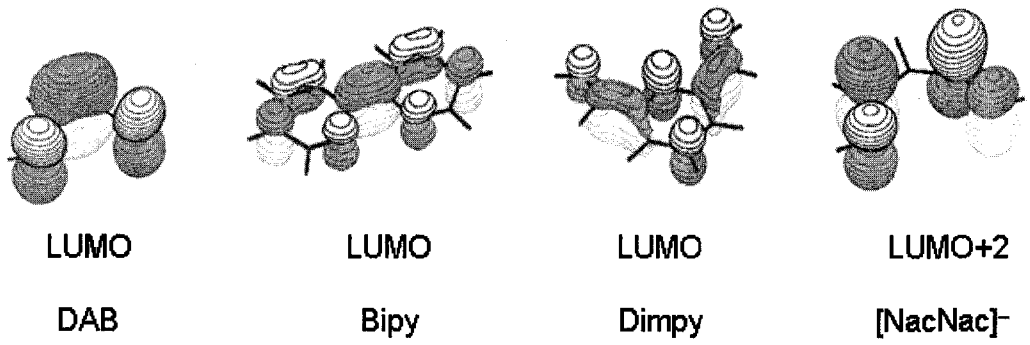

Figure 5.13 - Lowest unoccupied molecular orbitals involving the π-systems on the model ligands DAB, Bipy, Dimpy and [NacNac]⁻ in C_{2v} symmetry.

While it appears that the differing nature of the vacant orbitals explains the contrasting behaviour of the neutral ligands there does not appear to be any obvious correlation between the apparent "amount" of reduction observed for the various ligands and the HOMO-LUMO energy differences (Table 5-5) or the energy differences between the highest occupied and lowest unoccupied orbitals of π-type symmetry (Table 5-6). It may be important, however, to note that the overall energy of the LUMO in DAB is the

lowest, followed by that of Dimpy, then Bipy and finally $[NacNac]^-$. The apparent magnitude of ligand reduction may be related to the energy of the LUMO. This correlation also fits with the anticipated behaviours of the ligands: it should be easier to reduce the neutral 4 π-electron system in DAB than to reduce the conjugated aromatic systems in the Dimpy and Bipy. All of these should be much easier to reduce than the anionic ligand that already contains 6 electrons in its π-system.

The composition of the filled molecular orbitals on the ligands can also provide insight into the differing nature of the interaction between Pn and the neutral and anionic ligands. Whereas the HOMOs for each of the neutral ligands correspond to "lone pair" orbitals in the σ-systems of the molecules, the HOMO for the $[NacNac]^-$ model involves the π-system and the largest lobe is situated on the α-carbon atom (this atom also has a relatively large negative charge of –0.559). In this light, the observed monodentate ligation to phosphorus centres through the C_α atom should not be considered surprising or unexpected. Furthermore, given that the HOMO of the $[NacNac]^-$ ligand is of b_1 symmetry, it is more reasonably suited to donate electron density into vacant p(π) orbitals – the shape of this occupied orbital explains why this ligand is able to interact successfully through the nitrogen atoms with electron-poor centres from Group 13 and Group 14.

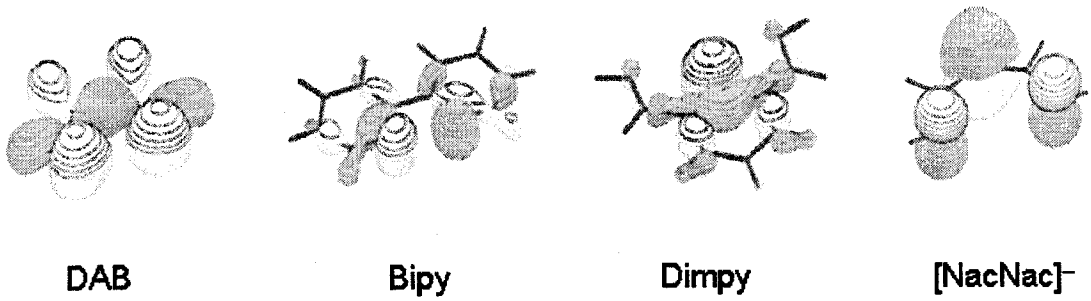

Figure 5.14 - Highest occupied molecular orbitals (HOMOs) for the model ligands DAB, Bipy, Dimpy and [NacNac]⁻ in C_{2v} symmetry.

Finally, an examination of some of the orbitals in the pnictogen complexes provides further insight into the electronic structure of these species. Because the orbitals for both the phosphorus-and arsenic-containing models are virtually identical in every case, only those of the arsenic-containing species are presented. For example, selected frontier orbitals of $[(DAB)As]^+$ are presented in Figure 5.15. The appearances of these orbitals, in particular the "lone pair" of HOMO–2 and the π-systems in the HOMO and HOMO–1 orbitals, are entirely consistent with those calculated previously for Group 15[54-56] and Group 14 *N*-heterocyclic carbenoids,[57,58] and the results suggest that the description of cations of the form $[(DAB)Pn]^+$ as containing Pn^{III} centres is not unreasonable.

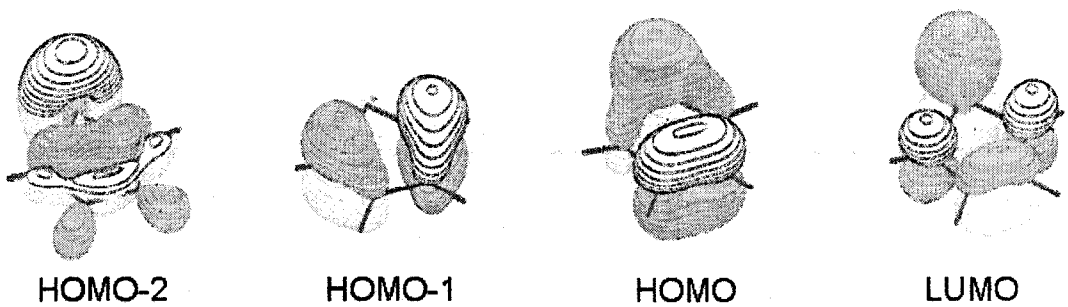

Figure 5.15 - Selected frontier orbitals for the model $[(DAB)As]^+$.

Selected frontier orbitals of the model $[(Dimpy)As]^+$ are depicted in Figure 5.16. These orbitals are particularly informative in that they show quite clearly the σ-type "lone pair" on As in HOMO–1 and, while there is some delocalization in the HOMO, the largest lobe is obviously located on the As centre and the orbital is most consistent with it being a π-type "lone pair" on As. Such "lone pairs" are exactly consistent with the orbitals found for Arduengo's "10-Pn-3" low-coordinate, hypervalent pseudo-trigonalbipyramidal systems.[24] In this light, the description of this cation as containing As^I is likely the most appropriate in spite of the transfer of some electron density from the Pn centre to the ligand.

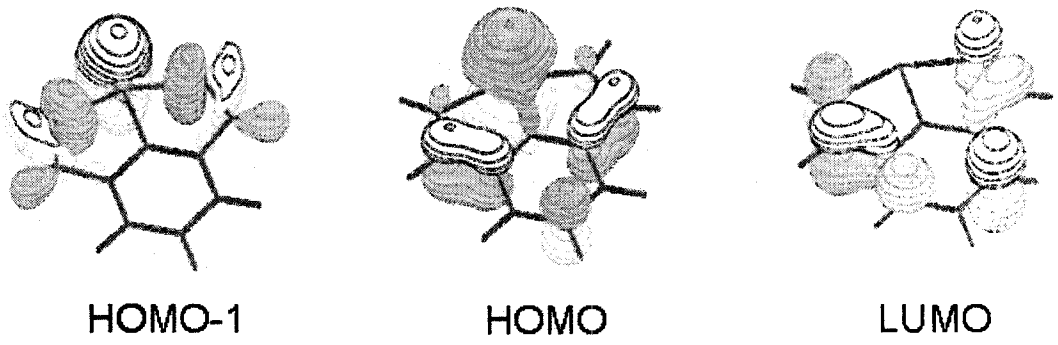

Figure 5.16 - Selected frontier orbitals for the model $[(Dimpy)As]^+$.

Not surprisingly, although the situation is similar to that in $[(Dimpy)As]^+$, the orbitals are somewhat more complicated for the $[(Bipy)As]^+$ system, shown in Figure 5.17. Many of the orbitals are attributable to the more extensive π-system in Bipy however the HOMO appears to be consistent with a π-type "lone pair" on As and HOMO–5 is clearly a σ-type "lone pair" on As. While some Pn-N π-delocalization is apparent in HOMO–4, it is considerably less than that observed, for example, in the HOMO of $[(DAB)As]^+$. Overall, the orbitals in $[(Bipy)As]^+$ are most consistent with the

presence of an As^{I} centre in the molecule. Such an interpretation is also in keeping with the "trapped singlet carbon" analogue [(Bipy)C] reported by Weiss and co-workers.[59] It is also worthy of note that and the energy difference between the HOMO and LUMO in the $[(Bipy)As]^{+}$ models (see Table 5-5) suggests that such compounds may have enough stability for their experimental isolation.

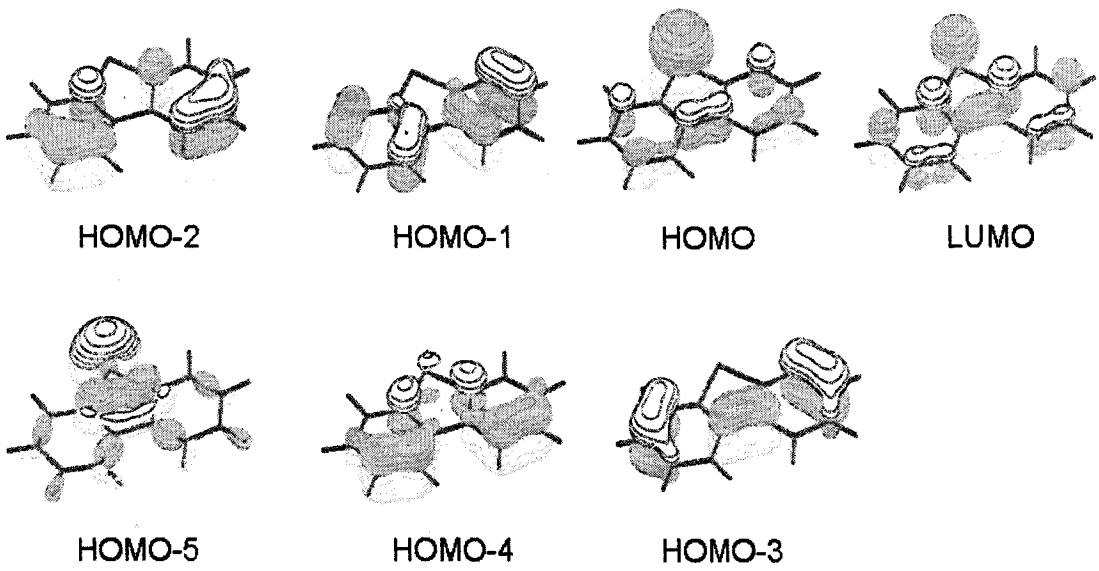

Figure 5.17 - Selected frontier orbitals for the model $[(Bipy)As]^{+}$.

For the model (NacNac)As, it is instructive to examine the orbitals of both the unfavourable C_{2v} form in addition to those of the C_s form. The orbitals for the putative C_{2v}-symmetry compound are presented in Figure 5.18. Several interesting features are observed upon examination of these orbitals. While the HOMO–2 orbital is similar in appearance to the other σ-type "lone pair" orbitals found in the other models, the HOMO is actually quite different in detail than those of any of the complexes described above. In particular, the HOMO in (NacNac)As is clearly anti-bonding in regard to the pnictogen and nitrogen atoms whereas the corresponding orbitals are either bonding (in $[(DAB)As]^{+}$

and [(Dimpy)As]$^+$) or non-bonding ([(Bipy)As]$^+$) in the other models. Perhaps more importantly, the HOMO–5 also shows that the π-system in this model is not completely delocalized and; this is likely a consequence of having a non-Hückel aromatic total of 8 electrons in the π-system (HOMO–5, HOMO–4, HOMO–1 and HOMO are all filled). In this context, the unfavourability of the planar (NacNac)Pn models is not surprising.

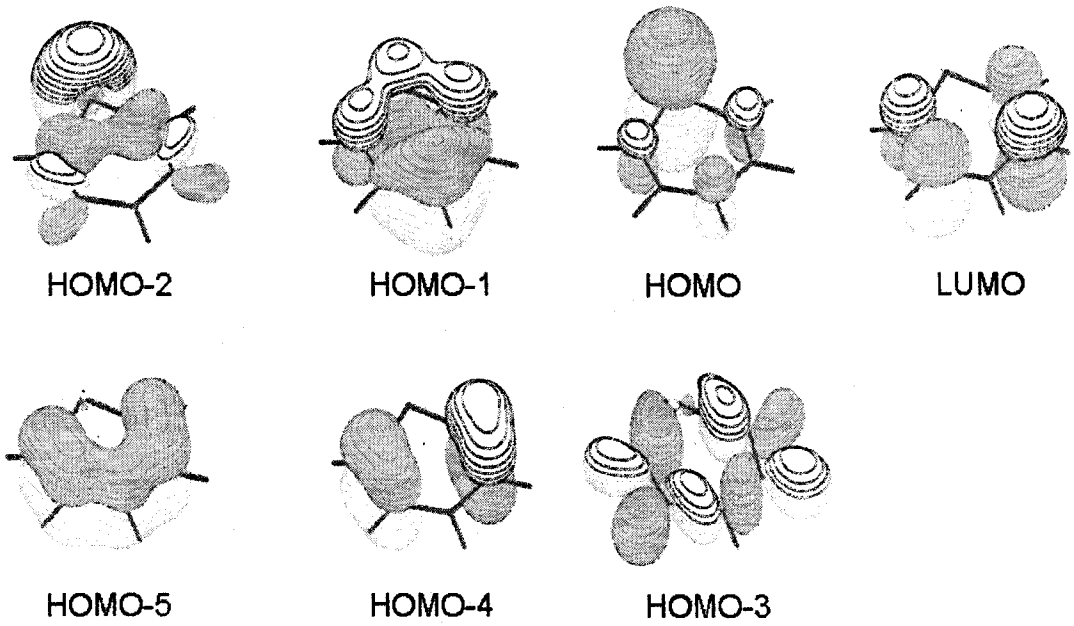

Figure 5.18 - Selected frontier orbitals for the C_{2v}-symmetry model (NacNac)As.

Distortion of the (NacNac)As model from planarity to the C_s-symmetry boat conformation changes the appearances (and energies – see Table 5-5) of the frontier orbitals, as shown in Figure 5.19. While the appearance of the σ-type "lone pair" orbitals in HOMO–2 does not change drastically, the appearance of the HOMO is instructive. The bending of the As atom and the C_α atom toward each other allows for the in-phase overlap of the lobes on these atoms. To some extent, such overlap (and those in the other distorted orbitals) explains the dramatically lower p(π) population in the C_s-symmetry model. In any event, it must still be emphasized that the energy difference between the

HOMO and LUMO are still considerably smaller for this model than for any of the other models described above and such molecules may be so reactive as to continue to elude experimental isolation.

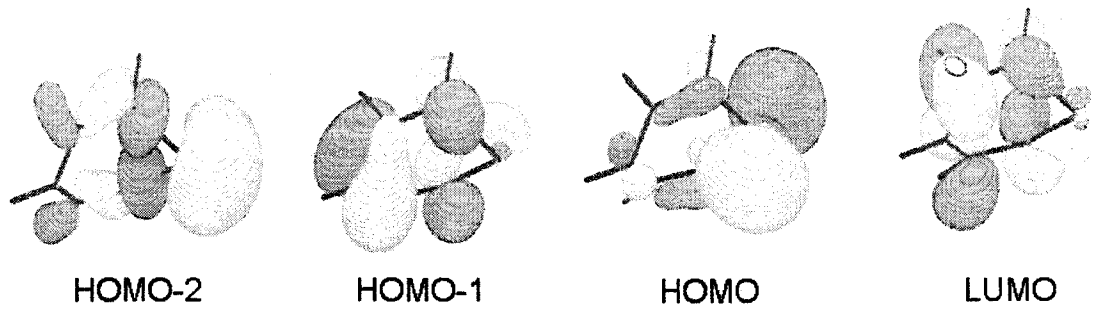

Figure 5.19 - Selected frontier orbitals for the C_s-symmetry model (NacNac)As.

Since the most obvious problems with the (NacNac)Pn species are clearly associated with the presence of 8 potential π-electrons in the 6-membered ring generated by the chelation of the 6 π-electron $[NacNac]^-$ fragment with the 2 π-electron Pn^I cation, we reasoned that the $[NacNac]^-$ ligand would likely produce a more stable complex if it chelates to a Pn^{III} cation bearing no π-electrons. As illustrated by the data in Tables 2 and 4, the resultant dications of the form $[(NacNac)Pn]^{+2}$ should be considerably more stable than their neutral analogues. The optimized structures for the cations are shown in Figure 5.20 and the metrical parameters are clearly indicative of ligand-Pn bonding that is very different from that in (NacNac)Pn. For example, the Pn-N distances in $[(NacNac)Pn]^{+2}$ are almost identical to those in the $[(DAB)Pn]^+$ models and the N-C and C-C distances are consistent with *removal* of electron density from the HOMO of the $[NacNac]^-$ ligand.

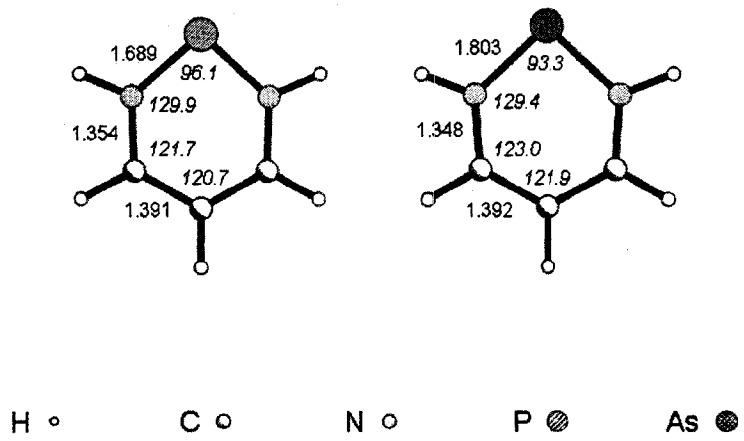

Figure 5.20 - Optimized structures (C_{2v}-symmetry) of $[(NacNac)P]^{+2}$ and $[(NacNac)As]^{+2}$. Selected bond distances (Å) and angles (°) are indicated.

In a similar vein, selected frontier orbitals for $[(NacNac)As]^{+2}$ are depicted in Figure 5.21 and these are much more similar to those of the $[(DAB)As]^{+}$ model in Figure 5.15 than to those of either of the neutral models for (NacNac)As. It is clear that the HOMO is bonding in terms of the Pn-N interaction, which looks very similar to that of the $[(DAB)As]^{+}$ model and, perhaps more importantly, the appearance of HOMO–5 demonstrates that the π-system is completely delocalized in this case. The difference in HOMO and LUMO energies is quite large for these dications and the preponderance of the data suggest that salts of $[(NacNac)Pn]^{+2}$ are viable synthetic targets that should be obtainable through judicious choice of counter anions. Cowley and co-workers' recent report of the isolation of salts of the form $[(R\text{-}NacNac)P\text{-}Cl][SO_3CF_3]$ lend credence to these predictions because the cations in their isolated systems are the mono chloride adducts of these putative $[(R\text{-}NacNac)P]^{+2}$ dications.[48]

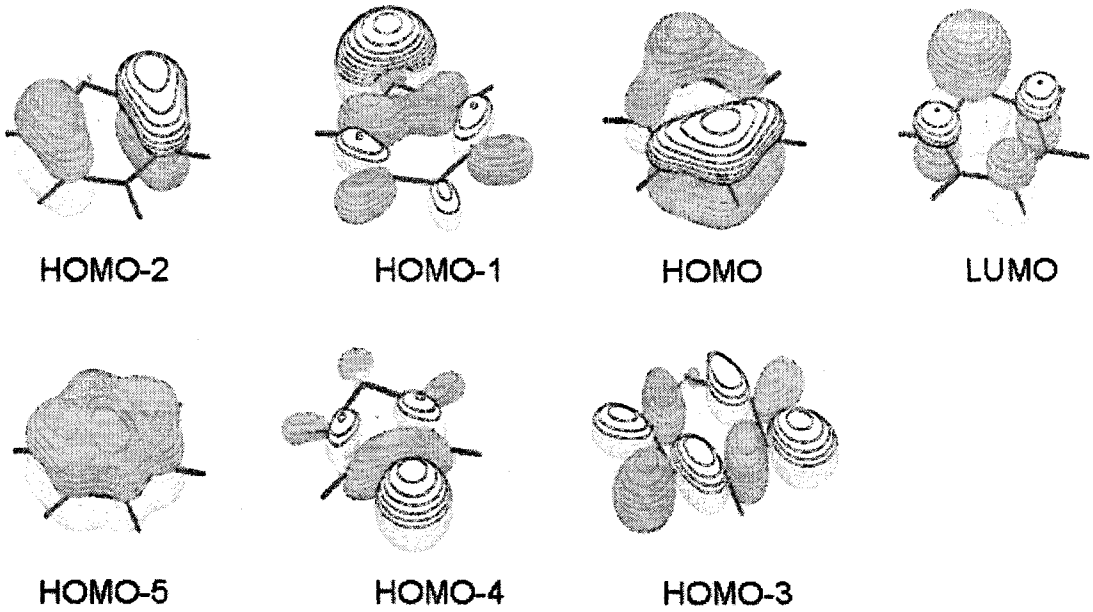

Figure 5.21 - Selected frontier orbitals for the C_{2v}-symmetry model $[(NacNac)As]^{+2}$.

5.4 Conclusions

Experimental investigations in this work and those of other groups have demonstrated that the chelation of putative Pn^{I} centres by diimines is a viable and very clean method for the synthesis of Pn-containing heterocycles. In the case of the reaction of 1,4-diaryl-2,3-dimethyl-1,4-diazabutadiene with either PI_3 or a mixture of PCl_3 and $SnCl_2$, the products are salts of phosphenium cations, which contain P^{III} centres, as one would expect on the basis of the reported behaviour of related systems. In contrast, when the analogous reactions using the related β-diketiminate ligand are attempted, many products appear to be formed and the reactions are certainly not clean or quantitative.

The computational investigations reveal that whereas ligands containing α-diimine-like fragments (DAB, Dimpy, Bipy) are predicted to chelate effectively with Pn^{I}

cations to produce planar complexes, the β-diketiminate anion $[NacNac]^-$ form relatively unstable complexes which adopt boat-like conformations. The nature of the interactions between the ligands and the pnictogen atoms are also clearly dependent on the nature of the ligand and, in particular, on the symmetry and composition of the LUMO associated with the π-system on the ligands. For $[(DAB)Pn]^+$, the metrical parameters and population analyses are consistent with the presence of the ligand in its dianionic form and implies the oxidation of Pn^I to Pn^{III}. The metrical parameters for the models containing pyridyl groups, namely $[(Dimpy)Pn]^+$ and $[(Bipy)Pn]^+$ are more consistent with a smaller transfer of electron density to the ligand and can still be considered most appropriately as containing Pn^I centres. This conforms to the understanding that imines should be easier to reduce than pyridyl groups and suggests that many ligands containing these fragments may be employed for analogous heterocycle synthesis.

In contrast, the interaction of the 6 π-electron system on $[NacNac]^-$ with the 2 π-electrons on a Pn^I cation produces unstable complexes and it is proposed that such anionic ligands can be more successfully employed in the stabilization of Pn^{III} centres. The large HOMO–LUMO energy difference and orbital structure consistent with known pnictogenium species suggest that the correct selection of counter anion should allow for the isolation of the dicationic $[(NacNac)Pn]^{+2}$ salts.

5.5 Prospective Developments

The chemistry developed for the synthesis of pnictogenium cations with diimines should be general to easily reduced ligands. Although, thus far, the generation of cations with a saturated carbon-backbone using mono-imines has been unsuccessful, preliminary

work has begun on the use of appropriate diketones and dienes to trap and oxidize Pn^I cations generated through both the $PnCl_3/SnCl_2$ and PnI_3 methodologies descried above (Equation 5.8). The development of this chemistry will lead to the facile synthesis of numerous small heterocycles and help to further expand the growing chemistry of pnictogen(I) cations. The inconsistencies in the anions generated as a result of the interaction of AsI_3 with various diimines should be further investigated to better control the products of the reactions in terms of solvent, reagent concentrations and temperature.

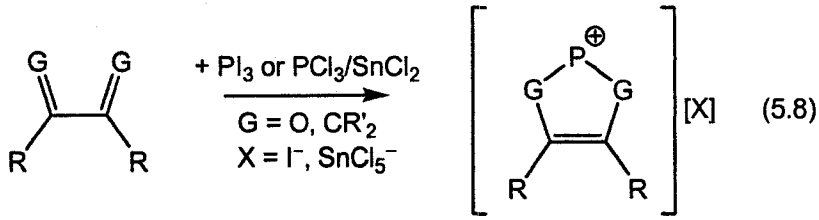

(5.8)

5.6 References

1. Macdonald, C.L.B. and Ellis, B.D. in *Encyclopedia of Inorganic Chemistry, 2nd Edition*, 2005, R. B. King (Ed), Hoboken, NJ: John Wiley & Sons, Inc., Low Oxidation State Main Group, pp. 6696.
2. Ellis, B.D. and Macdonald, C.L.B., *ACS Symp. Ser.*, **2006**, *917*, 108-121.
3. Mathey, F., *Angew. Chem., Int. Ed. Engl.*, **1987**, *26*, 275-286.
4. Lammertsma, K. and Vlaar, M.J.M., *Eur. J. Org. Chem.*, **2002**, 1127-1138.
5. Lammertsma, K., *Top. Curr. Chem.*, **2003**, *229*, 95-119.
6. Schmidpeter, A., *Heteroat. Chem.*, **1999**, *10*, 529-537.
7. Gamper, S.F. and Schmidbaur, H., *Chem. Ber.*, **1993**, *126*, 601-604.

8. Barnham, R.J., Deng, R.M.K., Dillon, K.B., Goeta, A.E., Howard, J.A.K. and Puschmann, H., *Heteroat. Chem.*, **2001**, *12*, 501-510.

9. Driess, M., Ackermann, H., Aust, J., Merz, K. and Von Wullen, C., *Angew. Chem. Int. Ed.*, **2002**, *41*, 450-453.

10. Ackermann, H., Aust, J., Driess, M., Merz, K., Monse, C. and Van Wullen, C., *Phosphorus, Sulfur Silicon Relat. Elem.*, **2002**, *177*, 1613-1616.

11. Ellis, B.D. and Macdonald, C.L.B., *Phosphorus, Sulfur Silicon Relat. Elem.*, **2004**, *179*, 775-778.

12. Boon, J.A., Byers, H.L., Dillon, K.B., Goeta, A.E. and Longbottom, D.A., *Heteroat. Chem.*, **2000**, *11*, 226-231.

13. Kilian, P., Slawin, A.M.Z. and Woollins, J.D., *Dalton Trans.*, **2006**, 2175-2183.

14. Ellis, B.D., Carlesimo, M. and Macdonald, C.L.B., *Chem. Commun.*, **2003**, 1946-1947.

15. Ellis, B.D. and Macdonald, C.L.B., *Inorg. Chem.*, **2006**, *45*, 6864-6874.

16. Ellis, B.D. and Macdonald, C.L.B., *Inorg. Chem.*, **2004**, *43*, 5981-5986.

17. Ellis, B.D., Dyker, C.A., Decken, A. and Macdonald, C.L.B., *Chem. Commun.*, **2005**, 1965-1967.

18. Reeske, G., Hoberg, C.R., Hill, N.J. and Cowley, A.H., *J. Am. Chem. Soc.*, **2006**, *128*, 2800-2801.

19. Cowley, A.H. and Kemp, R.A., *Chem. Rev.*, **1985**, *85*, 367-382.

20. Mathey, F. in *Multiple Bonds and Low Coordination in Phosphorus Chemistry*, 1990, M. Regitz and O. J. Scherer (Ed), Stuttgart: Georg Thieme Verlag, *In Situ* Generated Phosphinidenes, pp. 33-47.

21. Reeske, G. and Cowley, A.H., *Chem. Commun.*, **2006**, 1784-1786.

22. Gudat, D., Haghverdi, A., Hupfer, H. and Nieger, M., *Chem.--Eur. J.*, **2000**, *6*, 3414-3425.

23. Arduengo, A.J., III, Stewart, C.A., Davidson, F., Dixon, D.A., Becker, J.Y., Culley, S.A. and Mizen, M.B., *J. Am. Chem. Soc.*, **1987**, *109*, 627-647.

24. Arduengo, A.J., III and Stewart, C.A., *Chem. Rev.*, **1994**, *94*, 1215-1237.

25. Bourget-Merle, L., Lappert, M.F. and Severn, J.R., *Chem. Rev.*, **2002**, *102*, 3031-3066.

26. Bourget-Merle, L., Cheng, Y., Doyle, D.J., Hitchcock, P.B., Khvostov, A.V., Lappert, M.F., Protchenko, A.V. and Wei, X.-h., *ACS Symp. Ser.*, **2006**, *917*, 192-207.

27. Roesky, H.W. and Kumar, S.S., *Chem. Commun.*, **2005**, 4027-4038.

28. Roesky, H.W., *ACS Symp. Ser.*, **2006**, *917*, 20-31.

29. Hitchcock, P.B., Lappert, M.F. and Nycz, J.E., *Chem. Commun.*, **2003**, 1142-1143.

30. Ragogna, P.J., Burford, N., D'Eon, M. and McDonald, R., *Chem. Commun.*, **2003**, 1052-1053.

31. Burford, N., D'Eon, M., Ragogna, P.J., McDonald, R. and Ferguson, M.J., *Inorg. Chem.*, **2004**, *43*, 734-738.

32. Pangborn, A.B., Giardello, M.A., Grubbs, R.H., Rosen, R.K. and Timmers, F.J., *Organometallics*, **1996**, *15*, 1518-1520.

33. Tom Dieck, H., Svoboda, M. and Greiser, T., *Z. Naturforsch., B: Anorg. Chem., Org. Chem.*, **1981**, *36B*, 823-832.

34. Feldman, J., McLain, S.J., Parthasarathy, A., Marshall, W.J., Calabrese, J.C. and Arthur, S.D., *Organometallics*, **1997**, *16*, 1514-1516.

35. Frisch, M.J., Trucks, G.W., Schlegel, H.B., Scuseria, G.E., Robb, M.A., Cheeseman, J.R., Zakrzewski, V.G., Montgomery, V.G., Jr., Stratmann, R.E., Burant, J.C., Dapprich, S., Millam, J.M., Daniels, A.D., Kudin, K.N., Strain, M.C., Farkas, O., Tomasi, J., Barone, V., Cossi, M., Cammi, R., Mennucci, B., Pomelli, C., Adamo, C., Clifford, S., Ochterski, J., Petersson, G.A., Ayala, P.Y., Cui, Q., Morokuma, K., Salvador, P., Dannenberg, J.J., Malick, D.K., Rabuck, A.D., Raghavachari, K., Foresman, J.B., Cioslowski, J., Ortiz, J.V., Baboul, A.G., Stefanov, B.B., Liu, G., Liashenko, A., Piskorz, P., Komaromi, I., Gomperts, R., Martin, R.L., Fox, D.J., Keith, T., Al-Laham, M.A., Peng, C.Y., Nanayakkara, A., Challacombe, M., Gill, P.M.W., Johnson, B., Chen, W., Wong, M.W., Andres, J.L., Gonzalez, C., Head-Gordon, M., Replogle, E.S. and Pople, J.A., *Gaussian98*, Revision A.11.1, 2001, Pittsburgh, PA: Gaussian, Inc.

36. Becke, A.D., *J. Chem. Phys.*, **1993**, *98*, 5648-5652.

37. Perdew, J.P. and Wang, Y., *Phys. Rev. B: Condens. Matter*, **1992**, *45*, 13244-13249.

38. Reed, A.E., Curtiss, L.A. and Weinhold, F., *Chem. Rev.*, **1988**, *88*, 899-926.

39. Sheldrick, G.M., *SHELXTL*, 2001, Madison, WI: Bruker AXS, Inc.

40. Schaftenaar, G. and Noordik, J.H., *J. Comput.-Aided Mol. Des.*, **2000**, *14*, 123-134.

41. *SMART, Molecular Analysis Research Tool*, 2001, Madison, WI: Bruker AXS, Inc.

42. *SAINTPlus, Data Reduction and Correction Program*, 2001, Madison, WI: Bruker AXS, Inc.

43. *SADABS, An Empirical Absorption Correction Program*, 2001, Madison, WI: Bruker AXS, Inc.

44. Sheldrick, G.M., *SHELXS-97*, 1997, Gottingen: Universitat Gottingen.

45. Altomare, A., Burla, M.C., Camalli, M., Cascarano, G.L., Giacovazzo, C., Guagliardi, A., Moliterni, A.G.G., Polidori, G. and Spagna, R., *J. Appl. Crystallogr.*, **1999**, *32*, 115-119.

46. Farrugia, L.J., *J. Appl. Crystallogr.*, **1999**, *32*, 837-838.

47. Sheldrick, G.M., *SHELXL-97*, 1997, Gottingen: Universitat Gottingen.

48. Vidovic, D., Lu, Z., Reeske, G., Moore, J.A. and Cowley, A.H., *Chem. Commun.*, **2006**, 3501-3503.

49. Allen, F.H., *Acta Crystallogr., Sect. B: Struct. Sci.*, **2002**, *B58*, 380-388.

50. Litvinov, I.A., Naumov, V.A., Gryaznova, T.V., Pudovik, A.N. and Kibardin, A.M., *Dokl. Akad. Nauk SSSR*, **1990**, *312*, 623-625.

51. Denk, M.K., Gupta, S. and Lough, A.J., *Eur. J. Inorg. Chem.*, **1999**, 41-49.

52. Carmalt, C.J., Lomeli, V., McBurnett, B.G. and Cowley, A.H., *Chem. Commun.*, **1997**, 2095-2096.

53. Kirsanov, A.V., Gorbatenko, Z.K. and Feshchenko, N.G., *Pure Appl. Chem.*, **1975**, *44*, 125-139.

54. Gudat, D., *Eur. J. Inorg. Chem.*, **1998**, 1087-1094.

55. Sauers, R.R., *Tetrahedron*, **1997**, *53*, 2357-2364.

56. Boyd, R.J., Burford, N. and Macdonald, C.L.B., *Organometallics*, **1998**, *17*, 4014-4029.

57. Boehme, C. and Frenking, G., *J. Am. Chem. Soc.*, **1996**, *118*, 2039-2046.

58. Heinemann, C., Mueller, T., Apeloig, Y. and Schwarz, H., *J. Am. Chem. Soc.*, **1996**, *118*, 2023-2038.

59. Weiss, R., Reichel, S., Handke, M. and Hampel, F., *Angew. Chem. Int. Ed.*, **1998**, *37*, 344-347.

Chapter 6 – Low Oxidation State As^I Compounds

6.1 Introduction

The chemistry of Group 15 elements (pnictogens, Pn) in low-coordinate or multiple-bonded environments has been an active area of research during the last 30 years. The results of such investigations have provided for numerous insights into the rules governing the chemistry of the Main Group elements in general.[1,2] Research in this area has primarily concentrated on compounds containing pnictogen atoms in either of their typical oxidation states (+3 or +5), while the chemistry of compounds containing pnictogens in lower oxidation states has largely been ignored.

While the majority of the research into the chemistry of compounds containing Group 15 elements in the +1 oxidation state has focused on P^I, there has been limited development of As^I chemistry. The first As^I cation was reported by Gamper and Schmidbauer in 1993, which was prepared by the reduction of $AsCl_3$ with $SnCl_2$ in the presence of a chelating phosphine;[3] this approach is analogous to the method used by Schmidpeter to isolate his first P^I cation.[4] Dillon and co-workers have also recently used $SnCl_2$ to reduce $AsCl_3$ with various chelating phosphines, which were identified by their ^{31}P NMR shifts and, for two compounds, by X-ray crystallography.[5] A related approach to the synthesis of As^I cations is the reduction of $AsCl_3$ by an additional equivalent of phosphine, *i.e.* $P(NMe_2)_3$,[6,7] which generates the arsenic analogues of the acyclic P^I cation isolated by Schmidpeter.[8] Another related, but perhaps surprising approach to As^I–containing molecules involves the reaction of $AsCl_3$ with lithium salts,

either $LiC(PPh_2)(SiMe_3)$ or $LiN(PPh_2)$, which act as both metathesis and reducing agents to produce cyclic As^I compounds.[9,10]

We have undertaken an investigation of the low oxidation state chemistry of the p-block elements and herein we report some of our results concerning our new source for As^I and we demonstrate that our precursor is an effective reagent for the controlled production of As-I fragments.

6.2 Experimental

Reagents and General Procedures. All manipulations were carried out using standard inert-atmosphere techniques. Arsenic(III) chloride, arsenic(III) iodide, tin(II) chloride and 1,2-bis-(diphenylphosphino)ethane (dppe) were purchased from Strem, Me_3NO was obtained from Aldrich and $[PPh_4][I]$ was procured from Fluka. Arsenic(III) chloride was distilled prior to use and all reagents were used without further purification. CD_2Cl_2 was dried over calcium hydride and all other solvents were dried on a series of Grubbs' type columns[11] and were degassed prior to use. **Arsenic compounds are toxic and should be handled with care.** Please note that the yields reported are after the salt had been washed several times; unfortunately, some of the by-products appear to have similar solubility characteristics as the products and efforts to obtain satisfactory elemental analyses have been unsuccessful. It must also be noted that the reactions appear to be quantitative according to all spectroscopic data recorded.

Instrumentation. NMR spectra were recorded at room temperature in CD_2Cl_2 solutions on a Bruker Avance 300 MHz spectrometer. Chemical shifts are reported in ppm, relative to external standards ($SiMe_4$ for ^1H and ^{13}C, 85% aq. H_3PO_4 for ^{31}P).

Coupling constant magnitudes, $|J|$, are given in Hz. FT-IR spectra were recorded as Nujol mulls on KBr plates using a Bruker Vector 22 spectrometer and are presented as wavenumber (cm^{-1}) maxima. Melting points (mp) or decomposition points (dp) were obtained on samples sealed in glass capillaries under dry nitrogen using an Electrothermal® Melting Point Apparatus. Elemental analysis was performed in-house using a PerkinElmer 2400 C, H, N analyzer in the Centre for Catalysis and Materials Research, Department of Chemistry and Biochemistry, University of Windsor.

X-ray Crystallography. Crystals were coated in Nujol, mounted on a glass fibre and placed in the 173 K N_2 boil-off stream of the Kryoflex low-temperature apparatus. Reflection data were integrated from frame data obtained using hemisphere scans with the SMART[12] software on a Bruker APEX CCD diffractometer using a graphite monochromator with MoKα radiation (λ = 0.71073Å). Diffraction data and unit-cell parameters were consistent with assigned space groups. Lorentz and polarization corrections and empirical absorption corrections, based on redundant data at varying effective azimuthal angles, were applied to the data sets using SAINTPlus[13] and SADABS[14] software. The structures were solved by direct methods using SHELXS[15] or Sir97[16] (as implemented in the WinGX software package[17]), completed by subsequent Fourier syntheses and refined with full-matrix least-squares methods against F^2 data using SHELXL.[18] All non-hydrogen atoms were refined anisotropically and all hydrogen atoms were placed in appropriate geometrically-calculated positions or refined isotropically when bound to a phosphorus atom. Thermal ellipsoid plots of the molecular structures were generated using SHELXTL.[19] The experimental details for each of the diffraction experiments are listed in Table 6-1 and Table 6-2.

Powder X-ray diffraction experiments were performed with a Bruker D8 Discover diffractometer equipped with a Hi-Star area detector using Cu Kα radiation (λ = 1.54186 Å).

Preparation of $[(dppe)As]_2[SnCl_6]$

A colourless solution of dppe (1.673 g, 4.200 mmol) in CH_2Cl_2 (20 mL) was added to a white slurry of $SnCl_2$ (0.531 g, 2.800 mmol) in CH_2Cl_2 (10 mL) and white precipitate slowly formed. A colourless solution of $AsCl_3$ (0.508 g, 2.800 mmol) in CH_2Cl_2 (10 mL) was added to the mixture and the precipitate rapidly dissolved to give a yellow solution. The solution was left to stir for 15 minutes. Volatile components were removed under reduced pressure. Following redissolution in CH_2Cl_2 and slow evaporation of the solvent, yellow crystalline material was obtained. Yield: 63% (2.248 g, 1.759 mmol). $^{31}P\{^1H\}$ NMR: 61.7 (s). $^{13}C\{^1H\}$ NMR: 31.2 (d, $^1J_{CP}$ = 38), 126.2 (d, $^1J_{CP}$ = 60), 130.0 (s), 133.1 (s), 133.7 (s). ^1H NMR: 3.51 (d, $^2J_{HP}$ = 19, 4H), 7.53 (m, 12H), 7.80 (m, 8H). mp: 122-123 °C. Anal. Calcd. For $C_{52}H_{48}As_2Cl_6P_4Sn$ (1278.102): C 48.87, H 3.79. Found: C 48.49, H 3.63%.

Preparation of [(dppe)As][I]

A colourless solution of dppe (0.336 g, 0.843 mmol) in CH_2Cl_2 (10 mL) was added to a yellow solution of AsI_3 (0.380 g, 0.834 mmol) in CH_2Cl_2 (15 mL), which resulted in the formation of an orange solution. The solution was left to stir for 2 hours. A yellow precipitate had formed, which was removed by filtration through Celite. Volatile components were removed under reduced pressure and the crude residue was

washed with ether, then with pentane and dried *in vacuo* to produce a tan solid. Yield: 55% (0.279 g, 0.465 mmol). $^{31}P\{^{1}H\}$ NMR: 61.3 (s). $^{13}C\{^{1}H\}$ NMR: 30.0 (d, $^{1}J_{CP}$ = 39), 126.8 (d, $^{1}J_{CP}$ = 60), 129.9 (s), 133.4 (s), 133.6 (s). ^{1}H NMR: 3.68 (m, 4H), 7.57 (m, 12H), 7.79 (m, 8H). dp: 142-143 °C. Anal. Calcd. For $C_{26}H_{24}AsIP_2$ (600.242): C 52.00, H 4.03. Found: C 53.98, H 4.46%.

Preparation of [(dppe)As][(dppe)As$_2$I$_7$]

A colourless solution of dppe (0.307 g; 0.771 mmol) in CH_2Cl_2 (15 mL) was added to a yellow solution of AsI_3 (0.527 g; 1.157 mmol) in CH_2Cl_2 (15 mL). The solution was left to stir for 2 hours. A yellow precipitate had formed in the orange solution. The precipitate was removed by filtration through Celite. Volatiles components were removed under reduced pressure to produce a yellow crystalline solid. Yield: 61% (0.452 g; 0.237 mmol). $^{31}P\{^{1}H\}$ NMR: 60.4 (s), –13.6 (s, br). $^{13}C\{^{1}H\}$ NMR: 27.2 (s, br), 127.0 (s, br), 130.2 (s), 130.4 (s), 133.2 (s), 133.3 (s), 133.4 (s), 133.5 (s). ^{1}H NMR: 2.97 (s, br, 8H), 7.59 (m, 40H). IR: 1584.1 (w), 1568.9 (w), 1434.8 (m), 1094.9 (w), 737.0 (w), 686.2 (m), 529.2 (w), 513.4 (w). mp: 116-118 °C.

Preparation of [PPh$_4$]$_2$[As$_6$I$_8$]

A colourless solution of [PPh_4][I] (0.070 g; 0.150 mmol) in CH_2Cl_2 (5 mL) was added to an orange solution of [(dppe)As][I] (0.270 g; 0.450 mmol) in CH_2Cl_2 (15 mL). A solution of Me_3NO (0.068 g; 0.900 mmol) in CH_2Cl_2 (5 mL) was then added and the clear orange solution became cloudy yellow. The mixture was left to stir for 1 hour. The white precipitate that formed was removed by filtration through Celite to afford a clear

yellow filtrate. Volatile components were removed under reduced pressure. The crude yellow solid was washed with toluene (5 mL) and Et_2O (5 mL) to remove $dppeO_2$. The yellow solid was dissolved in a minimal amount of CH_2Cl_2 and upon slow evaporation yellow crystalline solid was produced. Yield: 52% (0.083 g; 0.0387 mmol). $^{31}P\{^1H\}$ NMR: 23.5 (s). $^{13}C\{^1H\}$ NMR: 118.0 (d, $^1J_{CP}$ = 89), 131.2 (s), 135.0 (s), 136.2 (s). ^1H NMR: 7.62 (m, 8H), 7.79 (m, 8H), 7.93 (m, 4H). IR: 1584.3 (w), 1435.6 (m), 1186.6 (m), 1175.3 (m), 1122.8 (m), 1107.1 (m), 996.2 (w), 763.07 (w), 753.28 (m), 740.83 (m), 730.13 (m), 694.17 (m), 531.84 (m), 512.21(w). mp: 204-205 °C.

Table 6-1 - Summary of X-ray Crystallographic Data for Compounds $6.1_2[SnCl_6]$, $6.1[(dppe)As_2I_7]$ and $[Ph_2P(O)(CH_2)_2P(OH)Ph_2]_2$6.2.

Compound	$6.1_2[SnCl_6]$	$6.1[(dppe)As_2I_7]$	$[Ph_2P(O)(CH_2)_2P(OH)Ph_2]_2$6.2
Empirical formula	$C_{54}H_{52}As_2Cl_{10}P_4Sn$	$C_{52}H_{48}As_3I_7P_4$	$C_{54}H_{54}As_6Cl_4I_8O_4P_4$
Formula weight	1447.89	1909.84	2497.37
Crystal system	Triclinic	Monoclinic	Triclinic
Space group	*P-1*	$P2_1/c$	*P-1*
Unit cell dimensions:			
a (Å)	10.8800(7)	19.1484(15)	11.7825(7)
b (Å)	11.6466(7)	18.8443(15)	12.4177(7)
c (Å)	12.9541(8)	16.6084(13)	13.1465(7)
α (°)	69.1440(10)	90	79.6010(10)
β (°)	79.8270(10)	91.508(2)	88.6590(10)
γ (°)	81.8680(10)	90	74.8660(10)
Volume (Å^3)	1504.29(16)	5990.9(8)	1825.71(18)
Z	1	4	1
Density (calc'd) (g cm^{-3})	1.598	2.118	2.272
Abs. coef. (mm^{-1})	2.102	5.411	6.370
F(000)	722	3560	1160
θ range for data collection (°)	1.88 to 27.49	1.06 to 27.50	1.73 to 27.49
Limiting indices	$-14 \le h \le 14$ $-15 \le k \le 15$ $-16 \le l \le 16$	$-24 \le h \le 24$ $-24 \le k \le 24$ $-21 \le l \le 21$	$-15 \le h \le 15$ $-16 \le k \le 16$ $-17 \le l \le 17$
Reflections collected	13129	56694	17934
Independent reflections	6552	13757	8326
R_{int}	0.0286	0.0489	0.0239
Data / restraints / parameters	6552 / 0 / 322	13757 / 0 / 595	8326 / 0 / 360
Goodness-of-fit on F^2	1.285	1.045	1.070
Final *R* indices[a] [I>2s(I)]	*R*1 = 0.0520 *wR*2 = 0.1023	*R*1 = 0.0435 *wR*2 = 0.0893	*R*1 = 0.0326 *wR*2 = 0.0805
R indices (all data)	*R*1 = 0.0570 *wR*2 = 0.1088	*R*1 = 0.0674 *wR*2 = 0.0988	*R*1 = 0.0406 *wR*2 = 0.0839
Largest difference map peak and hole (e Å^{-3})	1.366 and -1.211	1.611 and -0.675	1.207 and -1.172

Table 6-2 - Summary of X-ray Crystallographic Data for Compounds $[PPh_4]_2$6.2, dppe/2$SbCl_3$ and 3dppe/2SbI_3.

Compound	$[PPh_4]_2$6.2	dppe/2$SbCl_3$	3dppe/2SbI_3
Empirical formula	$C_{48}H_{40}As_6I_8P_2$	$C_{28}H_{28}Cl_{10}P_2Sb_2$	$C_{78}H_{72}I_6P_6Sb_2$
Formula weight	2143.46	1024.46	2200.10
Crystal system	Triclinic	Triclinic	Rhombohedral
Space group	*P-1*	*P-1*	*R-3c*
Unit cell dimensions:			
a (Å)	11.7453(6)	9.1707(15)	14.7670(15)
b (Å)	11.9257(6)	12.674(2)	14.7670(15)
c (Å)	12.0263(6)	16.796(3)	59.932(8)
α (°)	75.2730(10)	90.820(3)	90
β (°)	77.4120(10)	92.816(3)	90
γ (°)	65.1890(10)	95.689(3)	120
Volume (Å^3)	1466.89(13)	1939.9(6)	11318(2)
Z	1	2	6
Density (calc'd) (g cm^{-3})	2.426	1.754	1.937
Abs. coef. (mm^{-1})	7.673	2.184	3.341
F(000)	980	996	6300
θ range for data collection (°)	1.77 to 27.50	1.21 to 27.50	1.73 to 27.49
Limiting indices	$-15 \le h \le 15$	$-11 \le h \le 11$	$-19 \le h \le 19$
	$-15 \le k \le 15$	$-16 \le k \le 16$	$-19 \le k \le 19$
	$-15 \le l \le 15$	$-21 \le l \le 21$	$-77 \le l \le 77$
Reflections collected	14442	14078	33801
Independent reflections	6708	7615	2897
R_{int}	0.0294	0.0633	0.0816
Data / restraints / parameters	6708 / 0 / 289	7615 / 12 / 234	2897 / 0 / 139
Goodness-of-fit on F^2	1.204	1.241	1.058
Final *R* indices[a] [I>2s(I)]	*R*1 = 0.0317	*R*1 = 0.2407	*R*1 = 0.0318
	*wR*2 = 0.0668	*wR*2 = 0.4918	*wR*2 = 0.0670
R indices (all data)	*R*1 = 0.0487	*R*1 = 0.2485	*R*1 = 0.0519
	*wR*2 = 0.0832	*wR*2 = 0.4958	*wR*2 = 0.0749
Largest difference map Peak and hole (e Å^{-3})	1.437 and -1.255	7.574 and -6.266	1.178 and -0.521

Table 6-3 - Selected Metrical Parameters for compounds $6.1_2[SnCl_6]$ and $6.1[(dppe)As_2I_7]$.

Parameter	$6.1_2[SnCl_6]$	$6.1[(dppe)As_2I_7]$	
		Cation	Anion
	Distances (Å)		
As(2)-P(1)	2.2519(12)	2.2559(17)	2.5383(15)
As(2)-P(3)	2.2509(12)	2.2542(18)	2.5275(14)
P(1)-C(5)	1.816(4)	1.852(6)	1.810(5)
P(3)-C(4)	1.819(4)	1.851(6)	1.821(5)
C(4)-C(5)	1.533(6)	1.391(9)	1.520(8)
As(7)-I(2)			2.7838(7)
As(7)-I(1)			2.8636(7)
As(7)-I(3)			3.1641(7)
As(7)-I(4)			3.1307(6)
As(9)-I(1)			3.3229(7)
As(9)-I(3)			3.3749(8)
As(9)-I(4)			3.1182(7)
As(9)-I(5)			2.6741(7)
As(9)-I(6)			2.6442(7)
As(9)-I(7)			2.6373(7)
	Angles (°)		
P(1)-As(2)-P(3)	85.63(4)	85.44(6)	82.60(5)
As(2)-P(1)-C(5)	106.42(14)	106.0(2)	103.02(18)
As(2)-P(3)-C(4)	107.88(14)	105.6(2)	103.95(18)
P(1)-C(5)-C(4)	107.5(3)	109.3(4)	112.4(4)
P(3)-C(4)-C(5)	107.4(3)	108.9(4)	112.0(4)

Table 6-4 - Selected Metrical Parameters for compounds $[Ph_2P(O)(CH_2)_2P(OH)Ph_2]_26.2$ and $[PPh_4]_26.2$.

Parameter	$[Ph_2P(O)(CH_2)_2P(OH)Ph_2]_26.2$	$[PPh_4]_26.2$
	Distances (Å)	
O(1)-P(1)	1.533(3)	
O(2)-P(2)	1.521(3)	
P(1)-C(1)	1.804(4)	
P(2)-C(2)	1.803(4)	
C(1)-C(2)	1.539(5)	
As(1)-I(1)	2.7136(5)	2.6951(7)
As(2)-I(2)	2.6862(5)	2.6608(7)
As(3)-I(3)	2.6367(6)	2.6911(6)
As(1)-I(4)	4.1676(5)	4.1033(6)
As(2)-I(4)	3.1472(6)	3.1578(7)
As(3)-I(4)	4.0500(5)	3.9981(6)
As(1)-As(2)	2.4656(6)	2.4709(7)
As(1)-As(3)	2.4599(6)	2.4563(8)
As(3)-As(2a)	2.4563(6)	2.4708(8)
	Angles (°)	
As(2)-As(1)-As(3)	96.46(2)	100.90(3)
As(1)-As(3)-As(2a)	98.73(2)	101.62(3)
As(3)-As(2a)-As(1a)	97.47(2)	97.68(3)
average As-As-I (terminal)	89.74	89.29

6.3 Results and Discussion

Synthesis Employing $SnCl_2$ Protocol

The addition of $AsCl_3$ to one or two equivalents of many phosphines or arsines results only in the formation of adducts.[20] Although in the presence of tin(II) chloride and a chelating diphosphine, such as dppe, the arsenic centre is reduced from As^{III} to As^{I} and stabilized by the chelate.

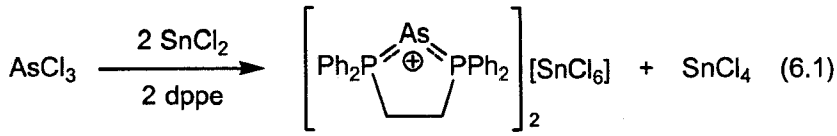

6.1$_2$[$SnCl_6$]

Although the compound [(dppe)P]$_2$[$SnCl_6$] **6.1**$_2$[$SnCl_6$] has been previously identified by its ^{31}P NMR chemical shift, it was not isolated from the reaction mixture or structurally characterized.[5] There are only five previous examples of such As^I phosphine-stabilized cyclic compounds comprised of either four-,[9,10] five-,[5] six-,[3] or seven-membered rings,[21] and one acyclic cation[7] that have been structurally characterized. The salt **6.1**$_2$[$SnCl_6$] crystallizes in the space group *P-1* with one molecule of CH_2Cl_2 in the asymmetric unit. The molecular structure is depicted in Figure 6.1 and selected metrical parameters are listed in Table 6-3. The cation **6.1** has As-P bond lengths of 2.2508(12) and 2.2518(12) Å in the solid state, which are consistent with the As-P distances in the cyclic examples (2.244 to 2.273 Å) and are intermediate between average As-P single bonds (2.331 Å) and double bonds (2.129 Å) found in the Cambridge Structural Database (CSD).[22] The P-As-P angle of 85.63(4) lies between those found in the four-membered rings (average angle of 69.68°) and that found in the six-membered ring (93.04°).

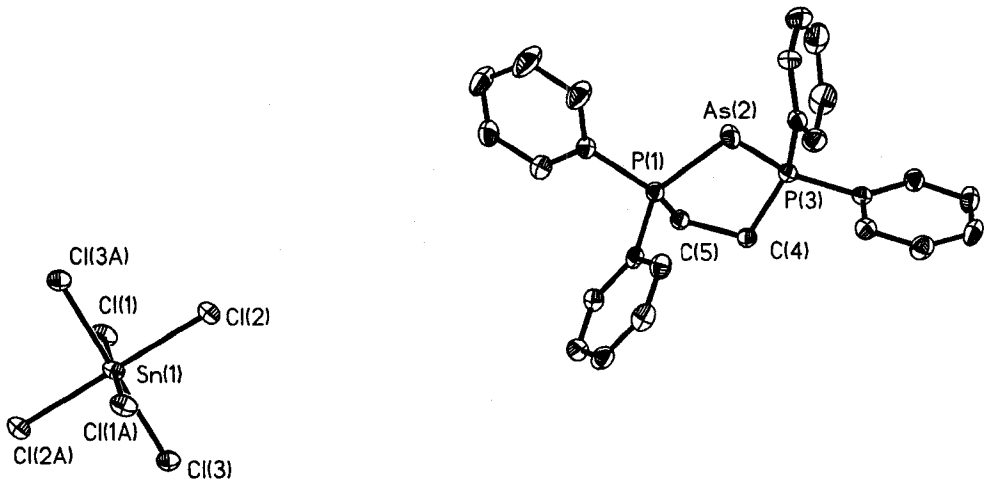

Figure 6.1 - Thermal ellipsoid plot (30% probability surface) of a $6.1_2[SnCl_6]$. Hydrogen atoms and a molecule of dichloromethane are omitted for clarity.

Synthesis Employing Disproportionation

In the course of our investigations into the chemistry of low oxidation state Group 15 elements, we required a readily accessible As^{I} cation with a less problematic counter anion. Analogous to the reactions involving phosphorus(III) iodide (Chapter 2), the room temperature reaction of equimolar amounts of AsI_3 with dppe results in the formation of [(dppe)As][I] **6.1**[I] with the concomitant release of iodine (Equation 6.2). We postulate that a similar RedOx couple is occurring where in solution disproportionation of the arsenic(III) iodide into I_2 and "As-I" fragments is facilitated by the chelating diphosphine and ultimately stabilized by the chelating ligand.

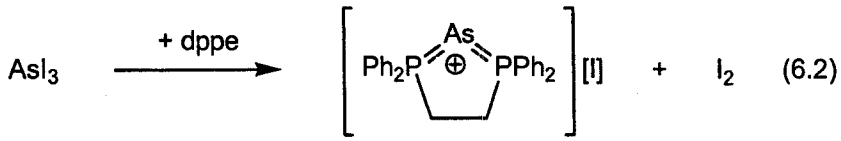

6.1[I]

While the purity of **6.1**[I] has been confirmed by both spectroscopic and micro-analytical methods, we have yet to obtain crystalline material of the salt suitable for a single-crystal diffraction experiment. The powder X-ray diffraction spectrum of "as prepared" pure **1** did not exhibit any peaks and suggests that it is non-crystalline.

In an attempt to obtain X-ray quality single crystals of **6.1**[I], the reaction mixture of dppe and AsI_3 was allowed to stir overnight before removal of the volatile substances. ^{31}P NMR spectra of the solid thus obtained exhibited two peaks that are attributable to coordinated dppe fragments: the peak at 60.4 ppm was consistent with the expected chemical shift for the cation **6.1**, however identity of the component that gives rise the much broader peak at -13.6 ppm was unclear. Fortunately, concentration of such reaction mixtures consistently results in the deposition of orange prism-shaped crystals amenable to crystallographic study. The results of such diffraction experiments allow for the identification of both peaks in the ^{31}P NMR spectrum and reveal that the salt obtained under these reaction conditions is [(dppe)As][(dppe)As_2I_7] **6.1**[(dppe)As_2I_7] (Equation 6.3).

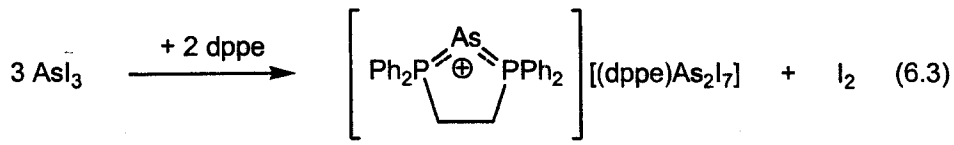

6.1[(dppe)As_2I_7]

The mixed valence salt **6.1**[(dppe)As_2I_7] crystallizes in the space group $P2_1/c$ and exhibits no unusually short cation-anion contacts. The asymmetric unit of **6.1**[(dppe)As_2I_7], depicted in Figure 6.2, consists of a single As^I cation, $[(dppe)As]^+$, and an unprecedented dinuclear As^{III} monoanion, $[(dppe)As_2I_7]^-$. The metrical parameters of the "(dppe)As" fragments in each of the ions, listed in Table 6-3, are distinct and

emphasize the differences in the bonding between the diphosphines and the As^{I} and As^{III} centres. In particular, the P-As distances in the cation (2.2559(17) Å and 2.2542(18) Å) are considerably shorter than the corresponding distances in the anion (2.5383(15) Å and 2.5275(14) Å). This observation is contrary to what one would predict based on the ionic radii of As^{I} and As^{III} and is indicative of the presence of π back-bonding between the As^{I} cation and the dppe ligand. The larger P-As-P angle in the cation (85.44(6)° vs. 82.60(5)° in the anion) is consistent with the shorter P-As distances and the constraints of the dppe ligand. Overall, the structure of the cation is identical to that found in the salt **6.1**$_2$[$SnCl_6$].

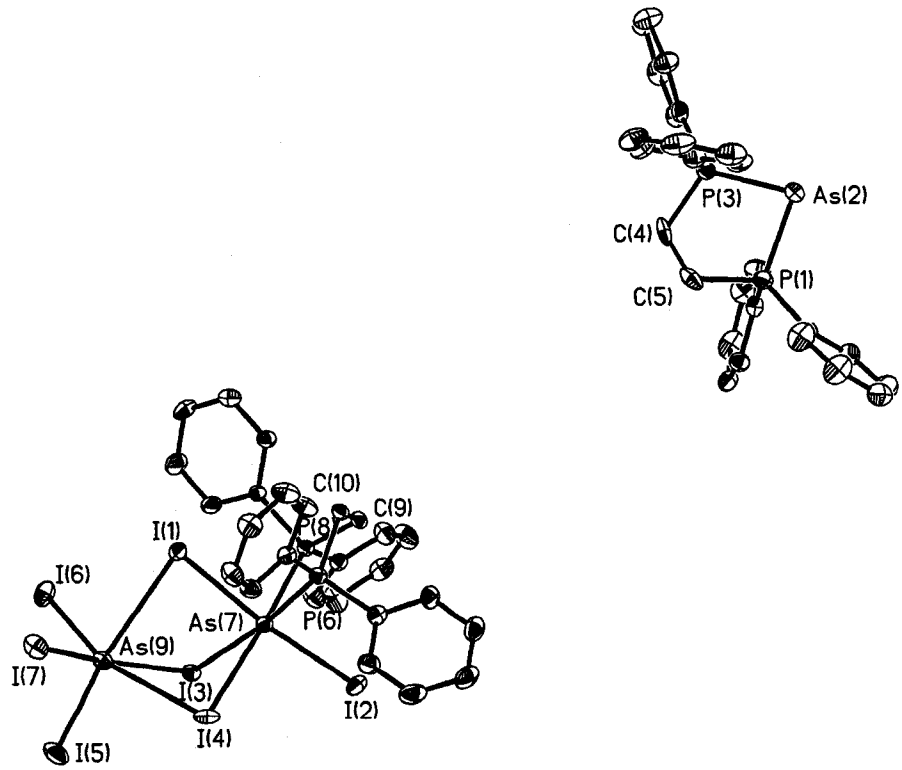

Figure 6.2 - Thermal ellipsoid plot (30% probability surface) of 6.2[(dppe)As_2I_7]. Hydrogen atoms are omitted for clarity.

The structure of the anion, while unique, is clearly related to those of polyanions of the type $[As_2X_8]^{-2}$ and $[As_2X_9]^{-3}$.[23,24] Each arsenic atom in the anion exhibits a distorted octahedral coordination environment composed of 3 terminal ligands and 3 bridging iodide anions; the lone pairs of electrons on these As^{III} cations are not stereochemically active. The framework of the anion is depicted in Figure 6.3. The presence of three bridging ligands allows the overall structure of the anion to be described as a being composed of two face-sharing AsL_6 octahedra. Predictably, the distances to the terminal iodide anions (As(7)-I(2): 2.7838(7)Å; range for As(9) terminal I atoms: 2.6373(7)-2.6741(7)Å) are significantly shorter than are those to the bridging ligands (range for As(7) to μ-I: 2.8636(7)-3.1641(7)Å; range for As(9) to μ-I: 3.1182(7)-3.3749(8)Å). Overall, the metrical parameters of the anion $[(dppe)As_2I_7]^-$ are consistent with the analogous values reported for $[As_2I_8]^{-2}$ [25] (unfortunately $[As_2I_9]^{-3}$ has not yet been reported) and do not require further comment.

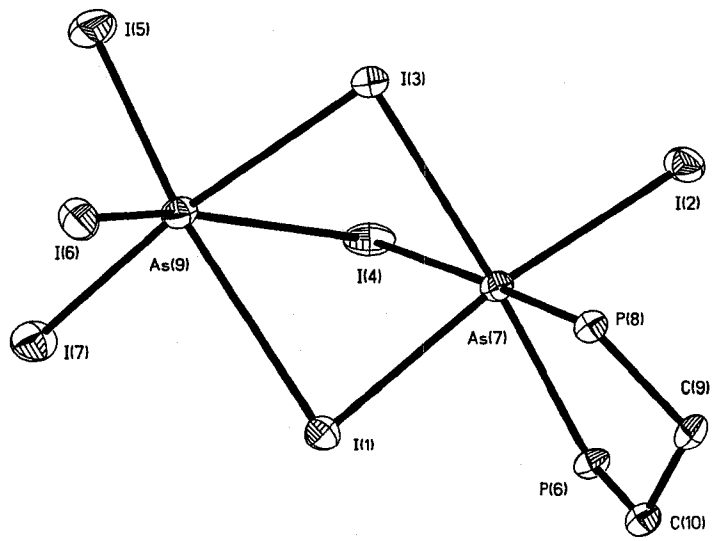

Figure 6.3 - Thermal ellipsoid plot (30% probability surface) of the framework of the anionic component from 6.2[(dppe)As_2I_7]

It should be noted that the production of **6.1**[I] or **6.1**[(dppe)As_2I_7] in such reactions appears to be highly-dependent on the concentration of the reagents in solution. Obviously, if a stoichiometry of 3 AsI_3 to 2 dppe is used in a dilute reaction, the reaction produces **6.1**[(dppe)As_2I_7] in high yield, however, when equimolar amounts of AsI_3 and dppe are mixed, the proportion of **6.1**[I] and **6.1**[(dppe)As_2I_7] obtained is determined by the concentration of the solution. If the solution is adequately dilute, such that the AsI_3 is completely dissolved, only **6.1**[I] is formed. The formation of **6.1**[I] over **6.1**[(dppe)As_2I_7] can also be accomplished by using donor solvents such as thf or MeCN, although the purity of the product is compromised by the concomitant generation of $dppeI_4$ with similar solubility to **6.1**[I] (see Chapter 2). While the actual process involved in the formation of the anion is unclear, the composition of the ion suggests that two equivalents of AsI_3 interact with an iodide anion and one dppe ligand to produce the dinuclear anion, as depicted in Figure 6.4.

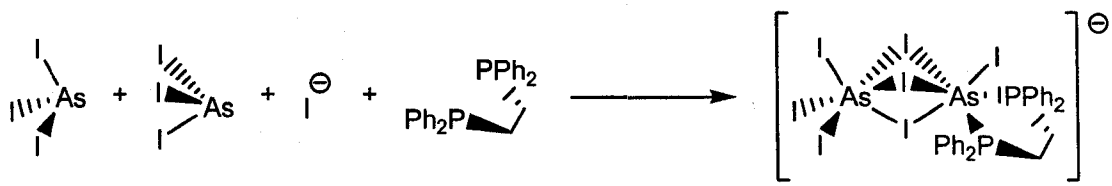

Figure 6.4 - Constituents of the anion in $[(dppe)As_2I_7]^-$.

Oxidative Release Chemistry

Whereas the salt **6.1**$_2$[$SnCl_6$] appears to be relatively stable when exposed to the atmosphere, **6.1**[I] is air-sensitive. Although such sensitivity is predictable, the actual product of the decomposition is unexpected and suggests a new and unique use for such molecules. When a solution of **6.1**[I] in dichloromethane was exposed to the atmosphere, large prism-shaped crystals formed after 7 days. The ^{31}P NMR spectrum of this solid

exhibited a single signal at 32 ppm, indicative of the oxidation of dppe, however the composition of the solid remained unclear.

A single crystal X-ray diffraction experiment revealed that the solid obtained is the new salt $[Ph_2P(O)(CH_2)_2P(OH)Ph_2]_2[As_6I_8]$, $[Ph_2P(O)(CH_2)_2P(OH)Ph_2]_2$**6.2**. The salt is composed of oxidized and mono-protonated dppe cations and the hetero-cubane dianion $[As_6I_8]^{-2}$. The molecular structures of the cations and anion are shown in Figure 3. Two cations form a centro-symmetric dimer by way of intermolecular hydrogen bonding interactions (the H atom was found in the Fourier difference map and refined isotropically; the O(1)-O(2a) distance is 2.416(4)Å) and have no unusually close interactions with the dianion. While such hydroxyphosphonium-phosphine oxide cations are quite rare, the metrical parameters and overall structure are as one would expect.[26]

The dianion is composed of an As_6I_6 ring arranged in a chair conformation (with each terminal iodine ligand in an equatorial position) and is rendered dianionic by the μ_3-iodide anions that cap each face of the ring. The metrical parameters for the centro-symmetric dianion, compiled in Table 6-4, are essentially identical to those reported for the only other examples of such anions.[27,28] For example, the As-As distances range from 2.4599(11)Å to 2.4657(11)Å the As-I distances to the terminal I atoms range from 2.6367(6)Å to 2.7136(5)Å. The As-I distances to the bridging iodide anions are longer and range from 3.1472(6)Å to 4.1676(5)Å, and attest to the distorted arrangement of the hetero-cubane core.

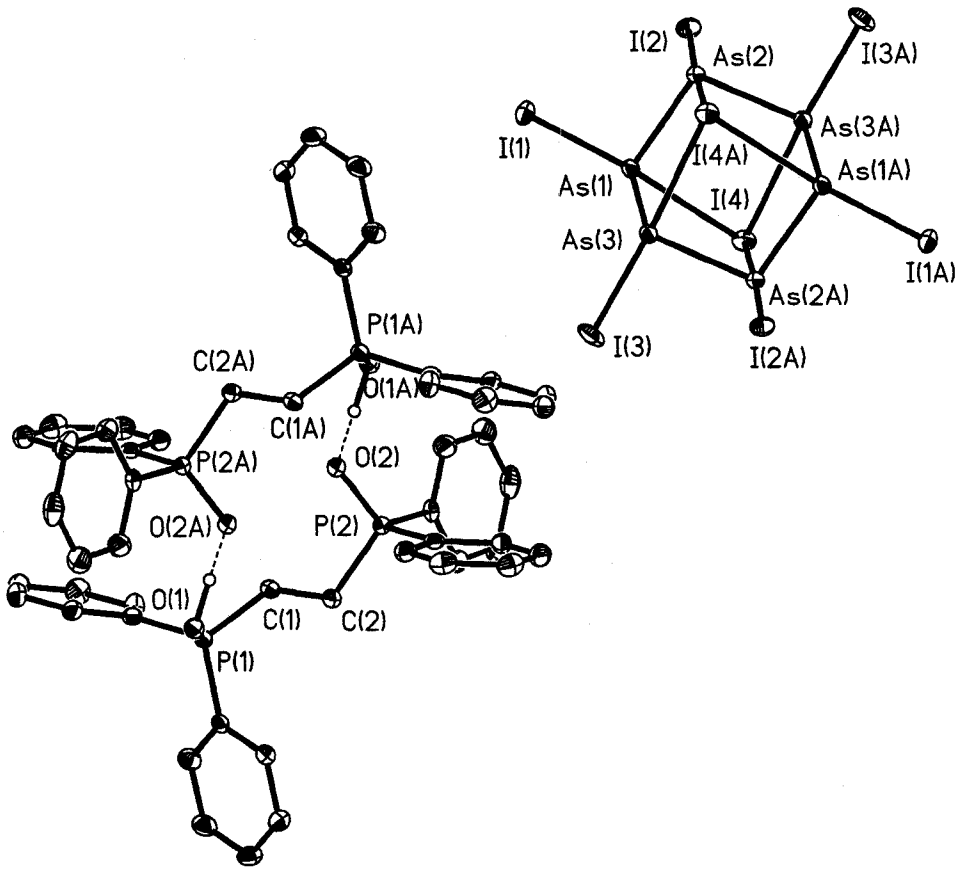

Figure 6.5 - Thermal ellipsoid plot (30% probability surface) of a cation and anion of $[Ph_2P(O)(CH_2)_2P(OH)Ph_2]_2$6.2 · 2 CH_2Cl_2. Most of the hydrogen atoms and a molecule of dichloromethane have been removed for clarity.

While the mechanism of the formation of $[Ph_2P(O)(CH_2)_2P(OH)Ph_2]_2$**6.2** remains unclear, the nature of the salt components are important for the insight that they provide into the reactivity, and potential utility, of compounds such as **6.1**[I]. Most importantly, the dianion is composed of six As^I cations, which are clearly not oxidized in the process. Consequently, the oxidation appears to happen exclusively at the dppe ligand. Together, the results suggest that the oxidation of the dppe ligand releases intact As^I-I fragments; these fragments can then cyclize to produce the As_6I_6 ring (c.f. As_6Ph_6 or the other

organoarsenic analogues[29]). Overall, the components of the decomposition product suggested to us that selective oxidation of the stabilizing ligand may be used to effect the controlled release of arsinidene fragments.

To test our hypothesis, we undertook a more rational synthesis of a salt of the heterocubane dianion. In this vein, the reaction of six equivalents of **6.1**[I] with twelve equivalents of trimethylamine-*N*-oxide in the presence of two equivalents of tetraphenylphosphonium iodide results in the formation of $[PPh_4]_2[As_6I_8]$, $[PPh_4]_2$**6.2**, in high yield (Equation 6.4). It should be noted that the only other reported syntheses of such anions resulted from the unintended reduction of $[As_2SBr_5]^{-1}$ or AsI_3 by transition metal complexes, making the method described herein the only rational synthesis of such a cluster.

$$\underset{\textbf{6.1}[I]}{6\ [(dppe)As][I]} + 12\ Me_3NO + 2\ [PPh_4][I] \xrightarrow[-\ 6\ dppeO_2]{} \underset{[PPh_4]_2\textbf{6.2}}{[PPh_4]_2[As_6I_8]} \quad (6.4)$$

Recrystallization of the salt from dichloromethane produced yellow crystals of $[PPh_4]_2$**6.2** that were suitable for X-ray diffraction. The structure of the salt is depicted in Figure 3 and there are no unusually short cation-anion contacts. As evidenced by the metrical parameters listed in Table 6-4, the geometry of the tetraphenylphosphonium cation is typical of the type and the structure of the $[As_6I_8]^{-2}$ dianion is identical to that described for $[Ph_2P(O)(CH_2)_2P(OH)Ph_2]_2$**6.2**.

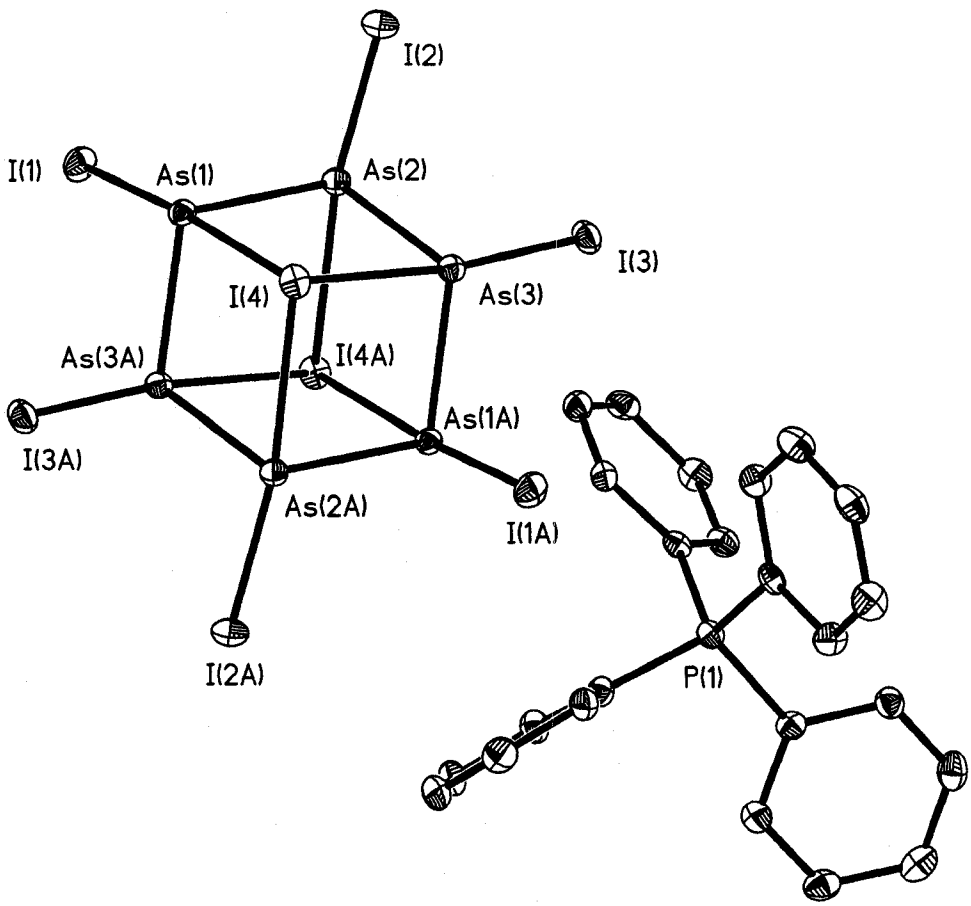

Figure 6.6 - Thermal ellipsoid plot (30% probability surface) of a $[PPh_4]_2$6.2. Hydrogen atoms are omitted for clarity.

It should be noted that the oxidation of the dppe ligand is in stark contrast to the results observed in the oxidation reactions performed initially by Schmidpeter et al.[30] and more recently by Dillon *et al.*[31] for analogous P^I compounds. The oxidation of triphosphenium cations with $[H][AlCl_4]$, alkylhalides and methyl triflate sometimes results in the oxidation of the dicoordinate P^I atom to give a P^{III} compound (Equation 6.5), while the reactions reported herein clearly involve the oxidation of the dppe ligand.

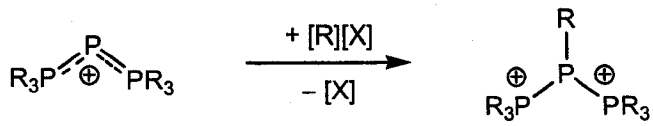

(6.5)

R = proton or alkyl cation
X = halide, tetrachloroaluminate or triflate

A simplistic rationale for this differing reactivity is suggested by the electronic structures of both the cation and the particular oxidizing agent used in each reaction. As illustrated in Figure 6.7, density functional theory (DFT) calculations on the model compound $[(Me_2P(CH_2)_2PMe_2)As]^+$ reveal that whereas the highest occupied molecular orbital (HOMO) is based primarily on the dicoordinate As atom, the lowest unoccupied molecular orbital (LUMO) of the cation is based primarily on the stabilizing ligand as is observed for phosphorus (Chapter 2). In this light, lone-pair bearing ("nucleophilic") oxidizing agents such as Me_3NO, oxygen or other elemental chalcogens may tend to attack the stabilizing ligand, as observed in the reactions producing $[Ph_2P(O)(CH_2)_2P(OH)Ph_2]_2$**6.2** and $[PPh_4]_2$**6.2**. In contrast, non lone-pair bearing ("electrophilic") oxidizing agents, such as a proton or a methyl cation tend to react with the univalent dicoordinate pnictogen atom. While this additional work is required to prove this hypothesis, such a reactivity model suggests that a high level of control over the nature of the products obtained in such reactions may be attainable.

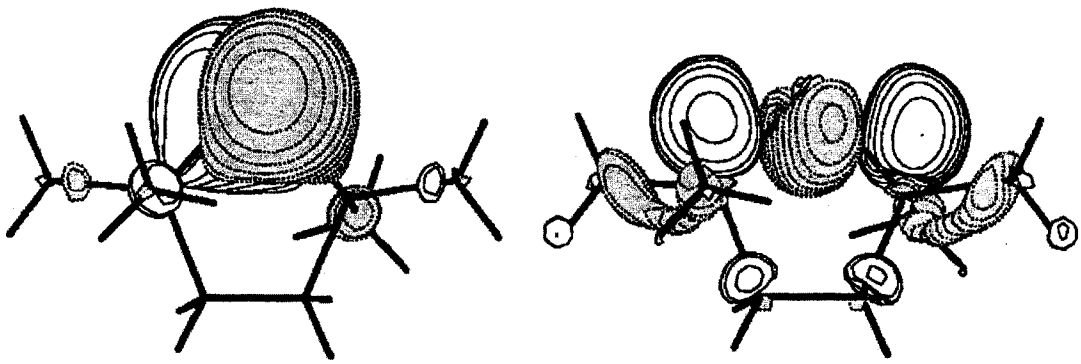

Figure 6.7 - MOLDEN[32] depictions of the highest-occupied and lowest-unoccupied molecular orbitals for the model cation $[(Me_2P(CH_2)_2PMe_2)As]^+$ calculated at the B3PW91/6-311+G(3df,2p)//B3PW91/6-31G(d) level of theory using the Gaussian98 suite of programs.

Furthermore, we believe that the "release" chemistry (oxidative or otherwise) described above may well be relatively general for compounds such as **6.1**[I]. For example, the planar phosphonium and arsonium cations reported by Driess and co-workers definitely result from a similar cleavage of the ligands and liberation of "free" P^I or As^I cations.[7,34] It should be noted that for arsenic, salts containing the cation found in **1** with robust anions appear to be stable indefinitely in inert atmospheres. As such, these salts are potentially more practical As^I precursors than salts containing the relatively short-lived $[((Me_2N)_3P)_2As]^+$ cations.

Attempted Synthesis of Sb^I and Bi^I Cations

We sought to determine if it was possible to generate thus far unknown Sb^I or Bi^I cations using either the $SnCl_2$ reduction of $PnCl_3$ or PnI_3 disproportionation procedures that have been developed for phosphorus and arsenic. In this vein, a solution of $SbCl_3$

was added to a slurry of dppe and $SnCl_2$. Initially a clear yellow solution is generated, consistent with the PCl_3 and $AsCl_3$ reactions, however within fifteen minutes dark brown solid begins to precipitate from solution, which is likely Sb^0. Following filtration and slow concentration of filtrate crystalline material suitable for single crystal X-ray diffraction was obtained. The molecular structure of the product, which crystallizes in the space group *P-1*, is depicted in Figure 6.8. There are two molecules of $SbCl_3$ with two halves of dppe molecules and two molecules of the dichloromethane solvent per asymmetric unit. There are no close contacts between $SbCl_3$ and either the phosphorus atoms or phenyl rings, as observed in Menshutkin complexes,[35] in the dppe molecules; the closest contacts to Sb atoms are to other chlorines on adjacent $SbCl_3$ molecules as the $SbCl_3$ molecules stack on top of each other. A diagram showing the packing of the $SbCl_3$ and dppe molecules is presented in Figure 6.9. Similar reaction conditions were applied to $BiCl_3$, which rapidly (within fifteen minutes) deposited copious amounts of brown solid. The identity of any products was not able to be determined.

As an alternative route, Pn^I cations were also sought through the disproportionation of either SbI_3 or BiI_3 in the presence of a chelating diphosphine. A dichloromethane solution of dppe was added to a slurry of SbI_3 in the same solvent. Immediately upon addition of the diphosphine, orange precipitate was generated. Following filtration, a yellow solution was obtained, which upon slow concentration yielded crystals amenable to X-ray diffraction study. Again, the desired Sb^I salt was not isolated, but instead a coordination complex of SbI_3 and dppe was obtained. The mixture crystallizes in the space group *R-3c* with half of a dppe molecule and a third of a SbI_3 molecule per asymmetric unit giving an overall ratio of 3 dppe to 2 SbI_3 molecules; the

molecular structure is depicted in Figure 6.10. In contrast to the $SbCl_3$ structure, the closest contacts to the Sb centre are to P centres in the dppe at a distance of 3.315(1) Å, although the distance is still significantly longer than Sb-P bonds in other examples of chelating diphosphines coordinating to SbI_3 fragments such as in $(Me_2P(CH_2)_2PMe_2)SbI_4^-$ (2.6658(14) and 2.6437(14) Å)[36] or $(Me_3P\text{-}SbI_3)_2$ (2.633(6) and 2.627(5) Å).[37] Attempted generation of Bi^I cation from BiI_3 and dppe resulted in the rapid deposition of a brown solid upon addition of the diphosphine and no products are able to be identified.

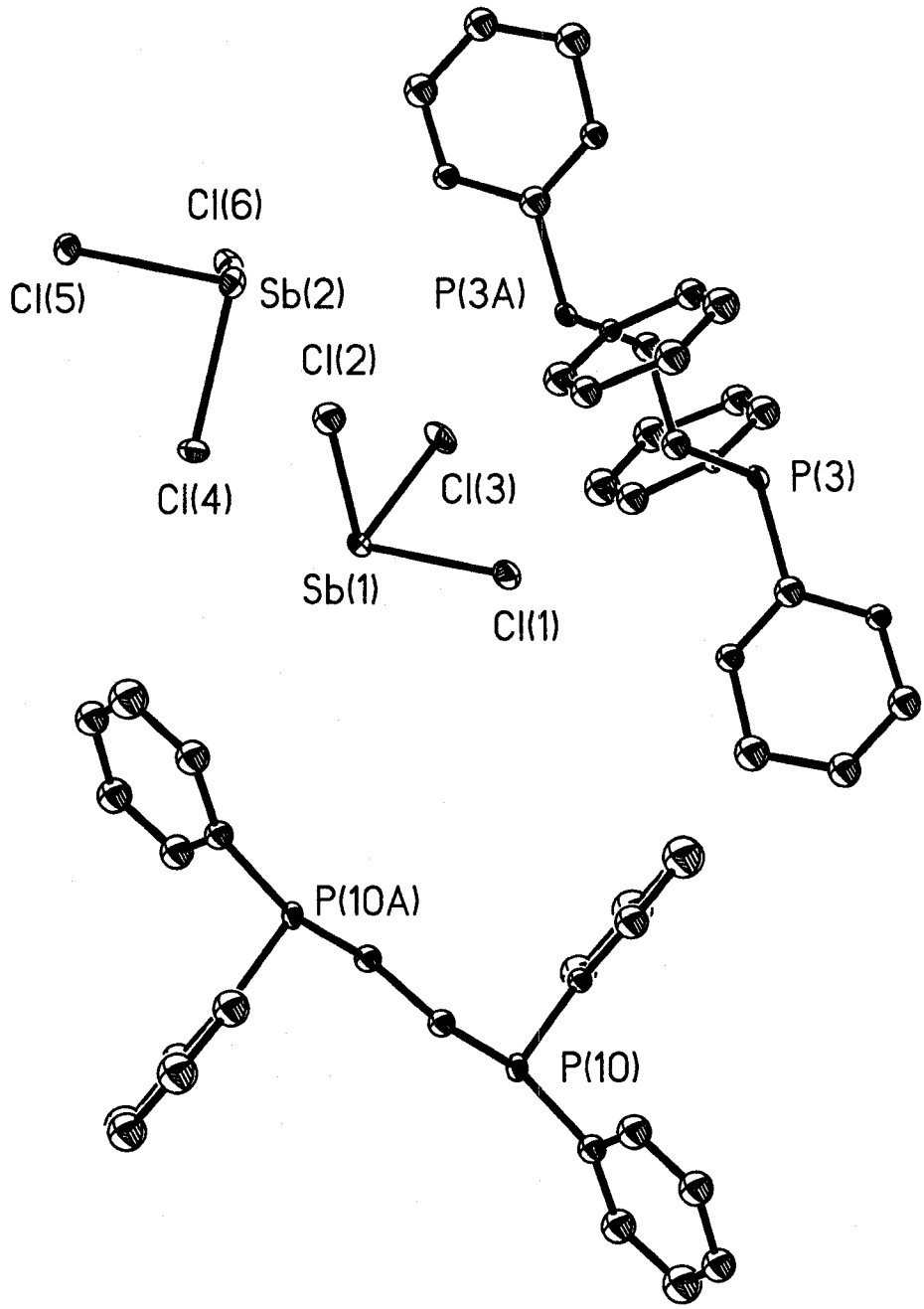

Figure 6.8 - Thermal ellipsoid plot (30% probability surface) of a dppe/2$SbCl_3$. Hydrogen atoms and two molecules of dichloromethane are omitted for clarity.

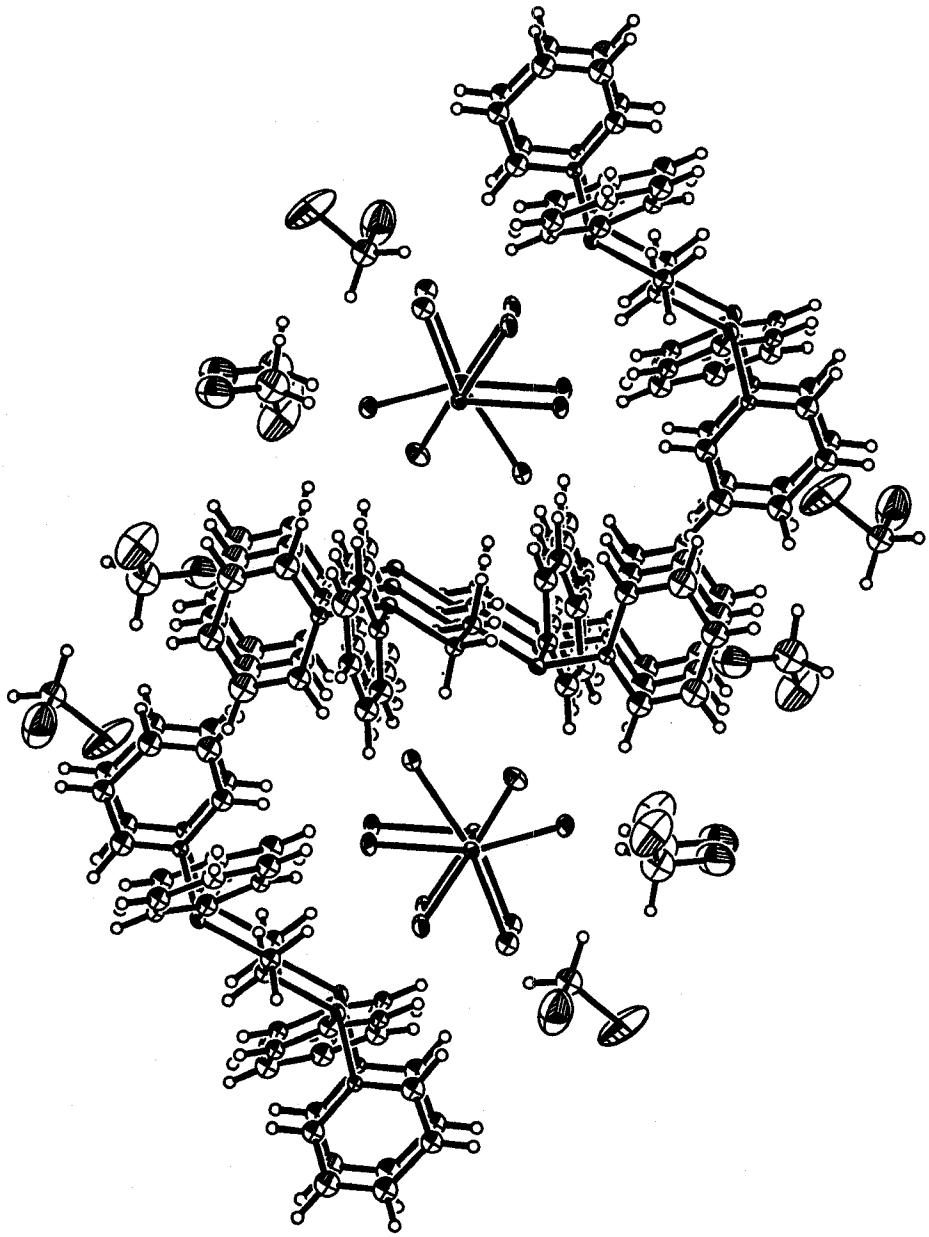

Figure 6.9 - Packing diagram of dppe/2$SbCl_3$.

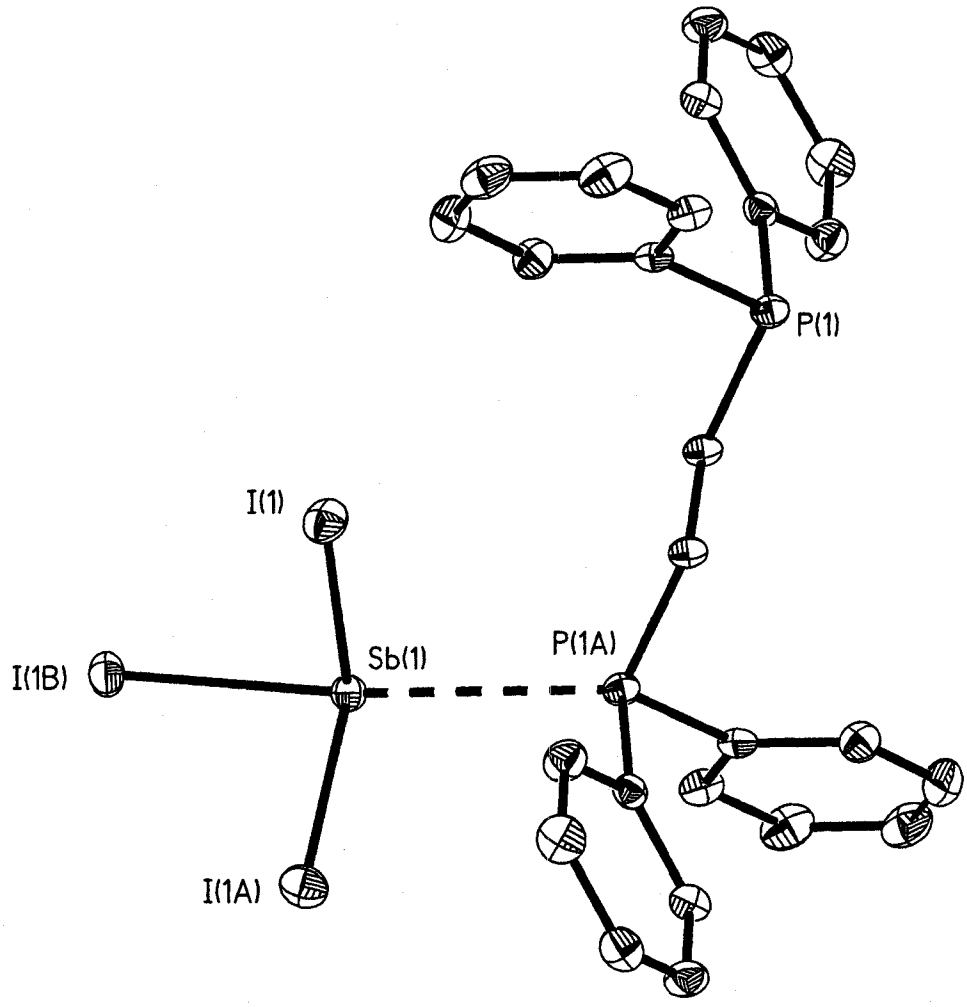

Figure 6.10 - Thermal ellipsoid plot (30% probability surface) of a 3dppe/2SbI_3. Hydrogen atoms are omitted for clarity.

6.4 Conclusions

We have discovered convenient and mild methods for the preparation, stabilization and delivery of As^I cations and related arsinidenes. While the solid state structure of **6.1**[I] remains unavailable, the structure of the mixed valence salt **6.1**[(dppe)As_2I_7] confirms the structure of the cation and highlights the differences in the

bonding of dppe ligands to As^{I} and As^{III} centers. More importantly, initial observations and experiments indicate that compounds such as **6.1**[I] may be used as sources of As^{I} species. In particular, the reaction of our improved As^{I} source **6.1**[I] with Me_3NO results in the formation of clusters composed of As^{I}-I fragments.

6.5 Prospective Developments

Although the As^{I} salt **6.1**[I] has been synthesized cleanly by ^{31}P NMR experiments and micro-analysis, it's solid-state structure remains elusive. The acquisition of a molecular structure of this type may be accessible through judicious choice of the stabilizing diphosphine. In addition, following the anion metathesis procedures outlined in Chapter 2 will lead to new As^{I} cations that may be more amenable to crystallographic study. The release of "As-I" fragments using Me_3NO is also achievable through the treatment of reagents such as **6.1**[I] with elemental chalcogens (S_8, Se) and needs to be further explored as an effective delivery mechanism for such fragments. A detailed study should be undertaken to determine if such chemistry is also amenable to phosphorus, for which preliminary results show similar reactivity.

6.6 References

1. Power, P.P., *Chem. Rev.*, **1999**, *99*, 3463-3503.
2. Driess, M. and Gruetzmacher, H., *Angew. Chem., Int. Ed. Engl.*, **1996**, *35*, 828-856.
3. Gamper, S.F. and Schmidbaur, H., *Chem. Ber.*, **1993**, *126*, 601-604.

4. Schmidpeter, A., Lochschmidt, S. and Sheldrick, W.S., *Angew. Chem., Int. Ed. Engl.*, **1982**, *21*, 63-64.

5. Barnham, R.J., Deng, R.M.K., Dillon, K.B., Goeta, A.E., Howard, J.A.K. and Puschmann, H., *Heteroat. Chem.*, **2001**, *12*, 501-510.

6. Ackermann, H., Aust, J., Driess, M., Merz, K., Monse, C. and Van Wullen, C., *Phosphorus, Sulfur Silicon Relat. Elem.*, **2002**, *177*, 1613-1616.

7. Driess, M., Ackermann, H., Aust, J., Merz, K. and Von Wullen, C., *Angew. Chem. Int. Ed.*, **2002**, *41*, 450-453.

8. Schmidpeter, A. and Lochschmidt, S., *Angew. Chem., Int. Ed. Engl.*, **1986**, *25*, 253-254.

9. Karsch, H.H., Witt, E. and Hahn, F.E., *Angew. Chem., Int. Ed. Engl.*, **1996**, *35*, 2242-2244.

10. Karsch, H.H. and Witt, E., *J. Organomet. Chem.*, **1997**, *529*, 151-169.

11. Pangborn, A.B., Giardello, M.A., Grubbs, R.H., Rosen, R.K. and Timmers, F.J., *Organometallics*, **1996**, *15*, 1518-1520.

12. *SMART, Molecular Analysis Research Tool*, 2001, Madison, WI: Bruker AXS, Inc.

13. *SAINTPlus, Data Reduction and Correction Program*, 2001, Madison, WI: Bruker AXS, Inc.

14. *SADABS, An Empirical Absorption Correction Program*, 2001, Madison, WI: Bruker AXS, Inc.

15. Sheldrick, G.M., *SHELXS-97*, 1997, Gottingen: Universitat Gottingen.

16. Altomare, A., Burla, M.C., Camalli, M., Cascarano, G.L., Giacovazzo, C., Guagliardi, A., Moliterni, A.G.G., Polidori, G. and Spagna, R., *J. Appl. Crystallogr.*, **1999**, *32*, 115-119.

17. Farrugia, L.J., *J. Appl. Crystallogr.*, **1999**, *32*, 837-838.

18. Sheldrick, G.M., *SHELXL-97*, 1997, Gottingen: Universitat Gottingen.

19. Sheldrick, G.M., *SHELXTL*, 2001, Madison, WI: Bruker AXS, Inc.

20. Hill, N.J., Levason, W. and Reid, G., *J. Chem. Soc., Dalton Trans.*, **2002**, 1188-1192.

21. Dotzler, M., Schmidt, A., Ellermann, J., Knoch, F.A., Moll, M. and Bauer, W., *Polyhedron*, **1996**, *15*, 4425-4433.

22. Allen, F.H., *Acta Crystallogr., Sect. B: Struct. Sci.*, **2002**, *B58*, 380-388.

23. Kaub, J. and Sheldrick, W.S., *Z. Naturforsch., B: Anorg. Chem., Org. Chem.*, **1984**, *39B*, 1257-1261.

24. Kaub, J. and Sheldrick, W.S., *Z. Naturforsch., B: Anorg. Chem., Org. Chem.*, **1984**, *39B*, 1252-1256.

25. Sheldrick, W.S. and Kiefer, J., *Z. Naturforsch., B: Chem. Sci.*, **1992**, *47*, 1079-1084.

26. Matsukawa, S. and Imamoto, T., *J. Am. Chem. Soc.*, **2000**, *122*, 12659-12662.

27. Ghilardi, C.A., Midollini, S., Moneti, S. and Orlandini, A., *J. Chem. Soc., Chem. Commun.*, **1988**, 1241-1242.

28. Mueller, U. and Sinning, H., *Angew. Chem., Int. Ed. Engl.*, **1989**, *28*, 185-186.

29. Rheingold, A.L. and Sullivan, P.J., *Organometallics*, **1983**, *2*, 327-331.

30. Schmidpeter, A., Lochschmidt, S., Karaghiosoff, K. and Sheldrick, W.S., *J. Chem. Soc., Chem. Commun.*, **1985**, 1447-1448.

31. Dillon, K.B. and Olivey, R.J., *Heteroat. Chem.*, **2004**, *15*, 150-154.

32. Schaftenaar, G. and Noordik, J.H., *J. Comput.-Aided Mol. Des.*, **2000**, *14*, 123-134.

33. Frisch, M.J., Trucks, G.W., Schlegel, H.B., Scuseria, G.E., Robb, M.A., Cheeseman, J.R., Zakrzewski, V.G., Montgomery, V.G., Jr., Stratmann, R.E., Burant, J.C., Dapprich, S., Millam, J.M., Daniels, A.D., Kudin, K.N., Strain, M.C., Farkas, O., Tomasi, J., Barone, V., Cossi, M., Cammi, R., Mennucci, B., Pomelli, C., Adamo, C., Clifford, S., Ochterski, J., Petersson, G.A., Ayala, P.Y., Cui, Q., Morokuma, K., Salvador, P., Dannenberg, J.J., Malick, D.K., Rabuck, A.D., Raghavachari, K., Foresman, J.B., Cioslowski, J., Ortiz, J.V., Baboul, A.G., Stefanov, B.B., Liu, G., Liashenko, A., Piskorz, P., Komaromi, I., Gomperts, R., Martin, R.L., Fox, D.J., Keith, T., Al-Laham, M.A., Peng, C.Y., Nanayakkara, A., Challacombe, M., Gill, P.M.W., Johnson, B., Chen, W., Wong, M.W., Andres, J.L., Gonzalez, C., Head-Gordon, M., Replogle, E.S. and Pople, J.A., *Gaussian98*, Revision A.11.1, 2001, Pittsburgh, PA: Gaussian, Inc.

34. Driess, M., Aust, J., Merz, K. and Van Wullen, C., *Angew. Chem. Int. Ed.*, **1999**, *38*, 3677-3680.

35. Menshutkin, B., *Zh. Russ. Fiz. Khim. Ova.*, **1911**, *43*, 1298-1308.

36. Clegg, W., Elsegood, M.R.J., Graham, V., Norman, N.C. and Pickett, N.L., *J. Chem. Soc., Dalton Trans.*, **1993**, 997-998.

37. Clegg, W., Elsegood, M.R.J., Graham, V., Norman, N.C., Pickett, N.L. and Tavakkoli, K., *J. Chem. Soc., Dalton Trans.*, **1994**, 1743-1751.

Chapter 7 – Dissertation Summary

7.1 Summary

Pnictogen atoms are typically found in either of their common oxidation states: +3 or +5. Over the past few decades, there has been increasing interest in compounds containing pnictogens in the lower oxidation state +1.[1-3]

In the early 1980's, Schmidpeter and co-workers began working on a new series of phosphorus compounds, which they called triphosphenium cations.[4-7] Although numerous cations were synthesized, their characterization was based almost entirely on the, albeit convincing, ^{31}P NMR coupling pattern exhibited by these types of species. Surprisingly, little attention seemed to be directed towards the chemistry of these electron rich species, with the notable exception of ligand substitution to generate new cations.[6] Fifteen years later, interest in triphosphenium cations was renewed, particularly through the work of Dillon and co-workers who synthesized numerous new cyclic cations.[8-10] The results of their studies had similar difficulties to that of Schmidpeter's in that their reactions generate difficult to separate by-products due to comparable solubility characteristics. The presence of unwanted by-products poses a potential problem for those who wish to study and potentially exploit the chemistry of these fascinating low oxidation state phosphorus species.

Our initial work in this area focused on the synthesis of phosphorus(I) triphosphenium cations that can be isolated in the absence of by-products.[11] This was achieved through the disproportionation of phosphorus(III) iodide in the presence of chelating diphosphines, which results in the generation of cyclic triphosphenium cations

with easily removed iodine as the only soluble by-product. These P^I iodide salts are ideal for anion metathesis reactions to generate salts with non-reactive anions. Furthermore, we also employed computational chemistry to better understand the electronic structure of such cations and guide future reactivity studies (Chapter 2).[12]

Schmidpeter had shown that acyclic triphosphenium cations undergo sequential substitution by increasingly basic phosphines.[6] Cyclic analogues are more resistant to substitution by phosphines, however we showed that new low oxidation state phosphorus compounds can be synthesized through ligand exchange with the stronger electron donating *N*-heterocyclic carbene class of compounds. In addition, we demonstrated that the same carbene-stabilized phosphorus(I) compounds are also accessible through reduction of phosphorus(III) halides, with excess carbenes as the reducing agent (Chapter 3).[13]

Triphosphenium cations can act as Lewis bases through their two available sets of "lone pairs" of electrons. While Schmidpeter demonstrated that acyclic cations can coordinate to aluminum(III) chloride,[14] we have begun a more thorough examination of the coordination chemistry of cyclic triphosphenium cations with both Main Group and Transition Metal electron acceptors. Although we have shown that coordination does occur on the basis of ^{31}P NMR data, the complexes are unstable with respect to decomplexation and we have used computational investigations to rationalize the observed behaviour (Chapter 4).

Recently, Cowley and co-workers have shown that both phosphorus(I) and arsenic(I) cations, generated either by Schmidpeter's original synthetic protocol of reduction using tin(II) chloride or our pnictogen(III) iodide disproportionation approach,

can be "trapped" by diimines.[15,16] The nature of the diimine dictates the oxidation state of the pnictogen atom in the final product. We have synthesized more cations implementing both procedures and have explained the behaviour of such systems and predicted some potential new compounds with the aid of computational chemistry (Chapter 5).[17]

Very little attention has been directed towards synthesizing heavier pnictogen(I) compounds. In 1993, Schmidbaur and co-workers isolated the first As^{I} cation using the tin(II) chloride reduction protocol.[18] Dillon has identified some phosphine-stabilized arsenic(I) cations by their ^{31}P NMR spectra,[9] and Driess and co-workers successfully synthesized the arsenic analogue of one of Schmidpeter's original acyclic cations.[19] We have extended the procedures developed for phosphorus to isolate arsenic(I) cations and we have undertaken an initial investigation into their oxidation chemistry. This has resulted in the discovery of the arsenic(I) cation as a source of arsenic-iodide fragments that may be used to build clusters (Chapter 6).[11,20]

The chemistry of phosphorus(I) and arsenic(I) cations is only now beginning to be developed and should lead to interesting and unique advances as we better understand their structure, bonding and reactivity of this remarkable family of electron-rich compounds. We have only seen the "tip of the iceberg" in this promising area of chemistry.

7.2 References

1. Ellis, B.D. and Macdonald, C.L.B., *ACS Symp. Ser.*, **2006**, *917*, 108-121.

2. Macdonald, C.L.B. and Ellis, B.D. in *Encyclopedia of Inorganic Chemistry, 2nd Edition*, 2005, R. B. King (Ed), Hoboken, NJ: John Wiley & Sons, Inc., Low Oxidation State Main Group, pp. 6696.

3. Ellis, B.D. and Macdonald, C.L.B., *Coord. Chem. Rev.*, **2006**, in press.

4. Schmidpeter, A., Lochschmidt, S. and Sheldrick, W.S., *Angew. Chem., Int. Ed. Engl.*, **1982**, *21*, 63-64.

5. Schmidpeter, A., Lochschmidt, S., Burget, G. and Sheldrick, W.S., *Phosphorus Sulfur Relat. Elem.*, **1983**, *18*, 23-26.

6. Schmidpeter, A., Lochschmidt, S. and Sheldrick, W.S., *Angew. Chem., Int. Ed. Engl.*, **1985**, *24*, 226-227.

7. Schmidpeter, A. and Lochschmidt, S., *Angew. Chem., Int. Ed. Engl.*, **1986**, *25*, 253-254.

8. Boon, J.A., Byers, H.L., Dillon, K.B., Goeta, A.E. and Longbottom, D.A., *Heteroat. Chem.*, **2000**, *11*, 226-231.

9. Barnham, R.J., Deng, R.M.K., Dillon, K.B., Goeta, A.E., Howard, J.A.K. and Puschmann, H., *Heteroat. Chem.*, **2001**, *12*, 501-510.

10. Dillon, K.B., Monks, P.K., Olivey, R.J. and Karsch, H.H., *Heteroat. Chem.*, **2004**, *15*, 464-467.

11. Ellis, B.D., Carlesimo, M. and Macdonald, C.L.B., *Chem. Commun.*, **2003**, 1946-1947.

12. Ellis, B.D. and Macdonald, C.L.B., *Inorg. Chem.*, **2006**, *45*, 6864-6874.

13. Ellis, B.D., Dyker, C.A., Decken, A. and Macdonald, C.L.B., *Chem. Commun.*, **2005**, 1965-1967.

14. Lochschmidt, S., Mueller, G., Huber, B. and Schmidpeter, A., *Z. Naturforsch., B: Anorg. Chem., Org. Chem.*, **1986**, *41B*, 444-454.

15. Reeske, G., Hoberg, C.R., Hill, N.J. and Cowley, A.H., *J. Am. Chem. Soc.*, **2006**, *128*, 2800-2801.

16. Reeske, G. and Cowley, A.H., *Chem. Commun.*, **2006**, 1784-1786.

17. Ellis, B.D. and Macdonald, C.L.B., *Inorg. Chim. Acta*, **2006**, in press.

18. Gamper, S.F. and Schmidbaur, H., *Chem. Ber.*, **1993**, *126*, 601-604.

19. Driess, M., Ackermann, H., Aust, J., Merz, K. and Von Wullen, C., *Angew. Chem. Int. Ed.*, **2002**, *41*, 450-453.

20. Ellis, B.D. and Macdonald, C.L.B., *Inorg. Chem.*, **2004**, *43*, 5981-5986.

VITA AUCTORIS

Name:	Bobby Dean Ellis
Place of Birth:	Yarmouth, Nova Scotia, Canada
Date of Birth:	July, 13, 1979
Education:	University of Windsor, Windsor, Ontario 2001-2006, Ph.D. (Chemistry)
	Dalhousie University, Halifax, Nova Scotia 1997-2001, B.Sc. Honours (Chemistry)
	Yarmouth Consolidated Memorial High School, Yarmouth, N.S. 1994-1997